

# **Laser Surface Texturing To Create Biomimetic Surface Topographies For Marine Antifouling Efficacy Testing**

A thesis submitted in partial fulfilment of the requirements of Liverpool John Moores  
University for the degree of Doctor of Philosophy.

**Rosie Julia Horner**

**November 2019**

## Acknowledgements

The completion of this work would not have been possible without the help and support from family, friends and supervisors throughout the PhD process. First of all, I would like to thank my supervisors Dr Martin Sharp and Dr Paul French for their guidance on the engineering aspects of the project, and Dr Simone Durr for her guidance on the marine biology aspects of the project. I would also like to thank advisors Dr Sheelagh Conlan and external advisor Dr Geraldine Reed for their guidance. I would also like to thank Beverly McGrath, Alan Simms, Jerry Bird, Jeff Cullen, Andy Goudie, Julian Todd, and Sensor City staff for helping in various ways throughout the project. I would also like to extend my thanks to staff and students at LJMU for their support and assistance in making this experience an enjoyable one. This work could not have been complete without funding from Liverpool John Moores University. I am grateful for all the opportunities I have had at here at LJMU such funding to present my work at an international conference.

I am forever grateful for the support of my mum, dad, brother, sister, and grandma who always believed in me and encouraged me to undertake this work. I am also very thankful for all my friends who have supported me throughout this process. Particularly, Liverpool University Sub Aqua Club who have enabled me to explore an underwater world, and provided a happy distraction to rest my mind outside of my research.

## Declaration

No portion of the work referred to in the thesis has been submitted in support of an application for another degree or qualification of this or any other university or other institute of learning.

Signed \_\_\_\_\_

Date \_\_\_\_\_

## Abstract

Biofouling is the unwanted colonisation of organisms on a living or artificial surface. Convergent evolution has led to the development of antifouling textures on many marine species. This thesis provides novel investigation into creating biomimetic antifouling surface directly onto marine grade stainless steel using laser micro machining. The investigation was split into three main research questions: (1) can laser surface texturing be used to create antifouling surfaces, and their effects on surface parameters (roughness / contact angle); (2) can biomimetic antifouling surfaces be created using laser surface texturing?; (3) can features of those successful surfaces be combined to create enhanced biomimetic antifouling surface?. All three experiments had similar methods, as laser processing was used to transfer the selected biomimetic micro-topography patterns onto marine grade stainless steel (316L). Samples were deployed in the field (Liverpool South Docks, UK) for 7 days. Abundance of biofilm was assessed using random systematic sampling. For the biomimetic surfaces, a fringe projection microscope (GFM) was used to investigate 3D scans of the surface topography of shells of bivalve and crab species, to provide bio-inspiration for the design of the surfaces created in this research. It was found that the micro-topography pattern limits the attachment of the biofilm to the surface. This thesis shows that (1) laser surface texturing can be used to create antifouling surfaces; (2) biomimetic antifouling surfaces can be created and enhance antifouling efficacy, and (3) that combining biomimetic features into multi-scale and multi-feature patterns have enhanced antifouling effects. This reinforces that biomimetic surfaces have the potential to be a non-toxic, eco-friendly antifouling technology that work directly on marine metal structures without the need for further coatings or chemicals.

Table of Contents	
Acknowledgements.....	i
Declaration.....	i
Abstract.....	ii
Table of Contents.....	iii
List of Figures.....	vii
List of Tables.....	xiv
List of Abbreviation.....	xvi
Chapter 1 Literature Review.....	17
1.1 Introduction to Biofouling.....	17
1.1.1 Biochemical Phase.....	18
1.1.2 Biofilm Phase.....	18
1.1.3 Macrofoulers Phase.....	24
1.2 Problems caused by biofouling.....	26
1.2.1 Problems caused by Biofilm.....	26
1.2.2 Problems caused by macrofouling.....	27
1.2.3 Costs of biofouling.....	29
1.3 Previously used antifouling (AF) techniques.....	30
1.3.1 Tributyltin.....	30
1.3.2 Alternatives to Tributyltin.....	31
1.4 Evolutionary response to biofouling.....	34
1.4.1 Negative effects of fouling on fitness of marine organisms.....	35
1.4.2 Convergent evolutionary response to fouling.....	39
1.5 The diatom attachment theory.....	43
1.6 Biomimicry.....	46
1.7 Multi-scale Multi-feature surfaces.....	48
1.8 Lasers.....	49
1.8.1 Laser micro-machining.....	50
1.8.2 Laser surface texturing.....	51
1.8.3 Effect of Laser surface texturing on roughness and contact angle.....	52
1.8.4 Effect of Roughness and contact angle on settlement.....	53
1.8.5 Laser surface texturing and Biomimicry.....	55
1.9 Table of studies.....	56
Chapter 2 Aims.....	58
2.1 Objectives.....	58
2.2 Justification.....	58

2.3 Novelty.....	59
Chapter 3 Methods .....	60
3.1 Equipment used .....	60
3.2 Creating surfaces.....	60
3.3 Laser set up .....	62
3.4 Testing of surfaces for antifouling potential.....	63
3.4.1 Field site .....	63
3.4.2 Experimental set up .....	66
3.5 Data collection .....	68
3.5.1 Biofilm settlement .....	69
3.5.2 Biofilm position on patterns .....	69
3.5.3 Statistical analysis .....	70
Chapter 4 : An Investigation Into The Use Of Nanosecond Laser Surface Texturing Of Stainless Steel (316L) As A Method To Reduce The Settlement Of Marine Biofilm. ....	72
4.1 Introduction .....	72
4.2 Materials and methods.....	74
4.2.1 Laser surface texturing.....	74
4.2.2 Contact angle measurement.....	75
4.2.3 Roughness (Sa) measurement .....	75
4.2.4 In-situ testing for marine biofilm .....	76
4.2.5 Data collection .....	76
4.2.7 Statistical analysis .....	76
4.3 Results.....	77
4.3.1 Effect of Laser Parameters on Surface.....	77
4.3.2 Effect of surface on biofilm settlement .....	85
4.4 Discussion.....	91
4.4.1 Effect of the laser parameter on surface .....	91
4.4.2 Effect of surface on biofilm settlement .....	96
4.5 Conclusions .....	100
Chapter 5 Biomimicry: Investigating single feature biomimetic patterns for their antifouling effect .....	101
5.1 Introduction .....	101
5.2 Methods.....	103
5.2.1 Creating biomimetic patterns on marine grade steel.....	103
5.2.1.1 Sampled species for pattern reproduction .....	103
5.2.1.2 Reproduction of biological patterns using laser surface texturing.....	107
5.2.1.3 Surface characterization .....	109
5.2.2 Antifouling efficacy testing of surfaces.....	109

5.3 Results .....	110
5.3.1 Surface topography.....	110
5.3.2 Biofilm settlement .....	115
5.3.3 Position .....	117
5.3.4 Position per pattern .....	121
5.4 Discussion.....	124
5.4.1 Surface topography.....	124
5.4.2 Biofilm settlement .....	125
Chapter 6 Biomimicry: Investigating multi-scale multi-feature biomimetic patterns for their antifouling effect.....	133
6.1 Introduction .....	133
6.2 Methods.....	136
6.2.1 Laser set up of combined patterns .....	136
6.2.1a Base micro-topography.....	136
6.2.1b Overlay micro-texture.....	137
6.2.1c Multi-feature micro-texture.....	137
6.2.2 Pattern design .....	137
6.2.1 <i>Experiment 1: Multi-scale circles (M1)</i> .....	137
6.2.2 <i>Experiment 2: Shell base and Crab overlay combination (Multi-feature 2)</i> .....	140
6.2.3 <i>Experiment 3: Crab base and shell overlay combination (Multi-feature 3)</i> .....	142
6.2.4 <i>Experiment 4: Crab based and Crab overlay combination (multi-feature 4)</i> .....	145
6.2.5 <i>Experiment 5: Circular crab pattern and shell combination (Multi-feature 5)</i> .....	147
6.2.3 Antifouling efficacy .....	149
6.2.3.1 Statistical analysis .....	149
6.2.3.2 Biofilm species identification (G. Reid, World Museum Liverpool) .....	149
6.3 Results.....	151
6.3.1 Surface Topography .....	151
6.3.2 Biofilm Settlement .....	157
6.3.3 Position of Biofilm.....	160
6.3.4 Position per pattern .....	165
6.4 Discussion.....	168
6.4.1 Surface topography.....	168
6.4.2.1 Multi scale pattern.....	169
6.4.2.2 Multi-feature pattern.....	170
Chapter 7 Overall Discussion .....	176
7.1 Laser surface texturing to develop bio-inspired surfaces.....	178
7.2 Single scale surfaces (crab and shell).....	181
7.2.1 Diatom attachment theory .....	181

7.2.2 Air entrapment theory .....	186
7.3 Multi- scale, Multi-feature patterns .....	189
7.4 Longevity of textures .....	192
7.5 Lab vs. Field based studies .....	206
7.6 Antifouling textures without additional chemicals.....	207
7.7 Limitations of this study.....	208
7.8 Conclusion.....	212
Chapter 8 Future work.....	215
References .....	219

List of Figures

*Figure 1.1 Biofouling process where (1) biochemical conditioning of the surface takes place within seconds to minutes, then (2) the biofilm layer develops within minutes to days where bacteria, diatoms, ascidians and other algal spores are attaching to the surface, which leads to (3) a complex climax fouling community made up of multicellular macrofoulers. The nature of the process switches from physical to biological (modified from (Wahl, 1989; Kirschner and Brennan, 2012)).....17*

*Figure 1.2 A schematic illustration of biofilm development reproduced from Chambers et al, (2006).....18*

*Figure 1.3 The ‘mother cell’ model for diatom reproduction where (a) the cell settles on surface and secretes a permanent adhesive, (b) the cell undergoes division and (c) the mother cell remains attached while the daughter cell is free to glide away [source: Horner R] .....21*

*Figure 1.4 Three different attachment types of diatoms to a surface where (a) is erect attachment (b) motile attachment and (c) adnate attachment .....22*

*Figure 1.5 A schematic illustration of theoretical attachment points of a diatom; (a) attachment on a flat surface; (b) attachment where micro-topography that is larger than organism (micro-refuge) (c) attachment where micro-topography is smaller than the diatom therefore a reduction in attachment points (Adapted from Scardino et al, 2006).....45*

*Figure 1.6 Images from (a) a scanning electron micrograph of the skin of the spinner shark scales and (b) White-light optical profilometry magnification of the of the Sharklet AF™ pattern raised on a surface (Kirschner and Brennan, 2012)... .....47*

*Figure 1.7 A schematic diagram of (a) Cassie-Baxter model and (b) Wenzel model.....53*

*Figure 1.8 A Schematic diagram demonstrating the effects of air pocket size on diatom attachment where (a) the air pocket is much larger than the diatom, (b) the air pocket is similar size to the diatom and (c) the air pocket is smaller than the diatom.....55*

*Figure 3.1 An example of how peaks are formed using cross hatch laser parameters.....62*

<i>Figure 3.2 Schematic diagram of a laser set-up for direct laser patterning moveable focussed laser beam controlled by a mirror galvanometer (Tzu Goh, 2014).</i>	<b>63</b>
<i>Figure 3.3 Field site [source: google maps]</i>	<b>65</b>
<i>Figure 3.4 Experimental set-up shown as (a) frame set up, (b) block set up and (c) deployment of the frame. The total length of the frame is 188cm. Blue squares: PVC panel (20x20 cm) attached using cable ties (black lines), thick brown line: ABS piping plus 90° bends and T-pieces pieces [Source: Dr S. Dürr]</i>	<b>67</b>
<i>Figure 3.5 A schematic illustration of the photo taking process for data collection</i>	<b>68</b>
<i>Figure 3.6 (a) real microscope images and (b) schematic illustration of the position of marine fouling organisms according to three different categories used for data collection</i>	<b>70</b>
<i>Figure 4.1 Scans of laser textures surfaces for number of passes treatment using (A) White light interferometer scans before submersion and (B) Zeiss AX10 microscope image after submersion</i>	<b>78</b>
<i>Figure 4.2 The relationship between the number of passes of the laser and (a) depth of the surface topography and (b) peaks of the surface topography</i>	<b>81</b>
<i>Figure 4.3 Scans of laser textures surfaces for hatch spacing treatment using (A) White light interferometer scans before submersion and (B) Zeiss AX10 microscope image after submersion</i>	<b>81</b>
<i>Figure 4.4 Relationships between; roughness (Sa) and (a) number of passes of the laser (b) hatch spacing; contact angle and (c) number of passes of the laser and (d) hatch spacing; and contact angle and roughness for (e) number of passes treatment and (f) hatch spacing treatment</i>	<b>84</b>

<i>Figure 4.5 The number of individual marine organisms settled across laser processed surfaces with a varying number of passes.....</i>	<b>86</b>
<i>Figure 4.6 The number of individual marine organisms settled across laser processed surfaces with a hatch spacing of 250, 500 and 750 <math>\mu\text{m}</math>.....</i>	<b>87</b>
<i>Figure 4.7 Relationships between settlement of marine biofilm and surface parameters; (a) contact angle (b) roughness and (c) topography for the number of passes experiment.....</i>	<b>89</b>
<i>Figure 4.8 Relationships between settlement of marine biofilm and surface parameters; (a) contact angle (b) roughness and (c) topography for the hatch spacing experiment.....</i>	<b>90</b>
<i>Figure 4.9 A schematic illustration of laser pulses in relation to the number of passes of the laser on a single hatch line .....</i>	<b>92</b>
<i>Figure 4.10 Flow chart of key findings of this study.....</i>	<b>92</b>
<i>Figure 5.1 A Schematic diagram showing how laser surface texturing can be used to create “peaks” and “valleys” on surfaces .....</i>	<b>109</b>
<i>Figure 5.2 The settlement of biofilm [median <math>\pm</math> quartiles] settled across biomimetic micro-textured patterns where (a) is experiment 1, (b) is experiment 2, (c) is experiment 3 and (d) is experiment 4. <b>A, B and C</b> represent significant differences between groups.....</i>	<b>116</b>
<i>Figure 5.3 (i) Principal Component Ordination for the settlement of biofilm settled in relation to position 1 (v1) position 2 (v2) and position 3 (v3) where (a) is experiment 1, (b) is experiment 2, (c) is experiment 3 and (d) is experiment 4 (ii) The number of individuals [median <math>\pm</math> quartiles] settled in all three positions on bio-inspired micro-textured patterns where (a) is experiment 1, (b) is experiment 2, (c) is experiment 3 and (d) is experiment 4.....</i>	<b>119</b>
<i>Figure 5.4 The number of individuals [median <math>\pm</math> quartiles] settled in the most important position on bio-inspired micro-textured patterns where (a) experiment 1, (b) experiment 2, and (c) experiment 3 are position 1, and (d) experiment and are position 2.....</i>	<b>123</b>

<i>Figure 5.5 Flow chart of this study’s findings.....</i>	<b>131</b>
<i>Figure 6.1 Multi-scale textures of (a) Sharklet™ pattern (Schumacher et al., 2007), and (b) and (c) where both are uHWST textures at different part of the same sample showing the difference in scale of wrinkles (Efimenko et al., 2009).....</i>	<b>134</b>
<i>Figure 6.2 Multi-scale and multi-feature textures from (a) Schumacher et al., (2007) and (b-e) (Sullivan and Regan (2017). All surfaces were created on PDMSe using photolithography techniques.....</i>	<b>135</b>
<i>Figure 6.3 3D micro-topographical scan of shore crab carapace .....</i>	<b>138</b>
<i>Figure 6.4 Draft sight design for experiment 1, where (a) diameter of circles was changeable for 230 μm for pattern 1, 280 μm for pattern 2 and 360 μm for pattern 3 and (b) where all three sizes were combined to create a combined pattern for pattern 4.....</i>	<b>139</b>
<i>Figure 6.5 A white light interferometer scan of the circular “cut out” feature created by laser texturing of an inverted circular pattern drawn on draftsight and imported into samlight laser software.....</i>	<b>139</b>
<i>Figure 6.6 Flow chart of how combined pattern was reach for experiment 1 from patterns tested in chapter 4.....</i>	<b>141</b>
<i>Figure 6.7 Example of pattern scaled up to 50x50mm.....</i>	<b>142</b>
<i>Figure 6.8 A flow diagram of how the combined pattern came to be, inspired from previously tested patterns (experiment 4 pattern 1 and experiment 6 pattern 1).....</i>	<b>144</b>
<i>Figure 6.9 A flow chart diagram from crab and shell organism, to topographical scans, to patterns tested in chapter 5, to draftsight designs then to the final pattern tested.....</i>	<b>146</b>
<i>Figure 6.10 A flow chart diagram from crab and shell organism, to topographical scans, to patterns tested in chapter 5, to draft sight designs then to the final pattern tested.....</i>	<b>148</b>

<i>Figure 6.11 Draft sight designs of patterns where (a) is the base pattern inspired by shore crab, (b) is the overlay pattern inspired by cockle shell ridges and (c) is the combined pattern of both of them together.....</i>	<b>149</b>
<i>Figure 6.12 Abundance of Biofilm [Median ± Quartiles] per cm<sup>2</sup> across the control, base, overlay and multi-feature patterns tested in this chapter where (a) is experiment 1 (b) is experiment 2 (c) is experiment 3 (d) is experiment 4 and (e) is experiment 5. ABCD show significant differences....</i>	<b>153</b>
<i>Figure 6.13 A reminder of the definition of positions outlined in methods section 3.5.2.....</i>	<b>160</b>
<i>Figure 6.14 Principal Component Ordination for the abundance of biofilm settled in relation to position 1 (v1) position 2 (v2) and position 3 (v3) where (a) is experiment 1, (b) is experiment 2, (c) is experiment 3 and (d) is experiment 4 and (e) is experiment 5.....</i>	<b>162-164</b>
<i>Figure 6.15 The number of individuals [median ± quartiles] settled in the most important position on bio-inspired micro-textured patterns where (a) experiment 1 is position 1, and (b) experiment 2 (c) experiment 3 and (d) experiment and (e) is experiment 5 are position 2.....</i>	<b>167</b>
<i>Figure 6.16 Flow chart of this study's key findings.....</i>	<b>174</b>
<i>Figure 7.1 Biomimetic surfaces where (a-c) are from previous studies on polymer substrates and (d-f) are replicates created using laser surface texturing. Where, a is a white crab ( Chen et al., 2010) ; b is crab inspired (Brzozowska et al., 2014); c is Sharklet™ pattern inspired by spinner shark (Magin, Cooper and Brennan, 2010); d and e are laser textured crab pattern (this thesis) and f laser textured shark pattern.....</i>	<b>179</b>
<i>Figure 7.2 A schematic illustration of theoretical attachment points of a diatom; (a) before attachment; (b) attachment on a flat surface; (c) attachment where micro-topography that is larger than organism (micro-refuge) (d) attachment where micro-topography is smaller than the diatom with three points of attachment and (e) attachment where micro-topography is smaller than the diatom with three points of attachment adapted from (Adapted from Scardino et al, 2006).....</i>	<b>182</b>

<i>Figure 7.3 A schematic diagram showing the reduction of EPS use as a “glue” for aiding diatom settlement.....</i>	<b>184</b>
<i>Figure 7.4 A Schematic diagram of laser textured surfaces showing potential effects of hydrostatic forces on diatom settlement .....</i>	<b>185</b>
<i>Figure 7.5 A Schematic diagram demonstrating the effects of air pocket size on diatom attachment where (a) the air pocket is much larger than the diatom, (b) the air pocket is similar size to the diatom and (c) the air pocket is smaller than the diatom (adapted from (Wu et al., 2013) .....</i>	<b>187</b>
<i>Figure 7.6 The relationship between roughness (Ra, nm) of stainless steel and settlement of viable cells (CFU/mL) for two bacteria species; (a) S. aureus and (b) P. aeruginosa (adapted from Wu (2018).....</i>	<b>182</b>
<i>Figure 7.7 Schematic diagram showing possible interactions between (a) base an (b) combined patterns on difference sizes diatoms, where based and combined pattern both limit the attachment points of fouling organism.....</i>	<b>189</b>
<i>Figure 7.8 Schematic diagram showing possible effects of (a) base an (b) combined patterns on difference sizes diatoms, where base and combined pattern may not limit the attachment points of smaller fouling organisms.....</i>	<b>191</b>
<i>Figure 7.9 Dominant species Synedra fasciculata of various sizes found on multi-scale and multi-feature surfaces throughout this study [Source: R Horner].....</i>	<b>197</b>
<i>Figure 7.10 Schematic diagram showing possible species richness, diversity and interaction when the dominant species is (a) non-chain building and (b) chain building diatoms [Source Horner R].....</i>	<b>199</b>
<i>Figure 7.11 Schematic diagram showing attachment strategies of (a) non-chain forming diatoms and (b) chain forming diatoms.....</i>	<b>201</b>

*Figure 7.12 Schematic diagram showing chain forming diatoms in a positive feedback loop where (a) they settle on the micro textured surface and produce chains, (b) sections of the chain are dislodged and land on other areas of the micro-texture, and (c) settlement and chain building of dispersed chain forming diatoms, as feedback loop starts again.....***201**

*Figure 7.13 The cycle of a biofilm; attachment, growth, detachment (Lewandowski, 2000)...***203**

*Figure 7.14 Schematic diagram showing settlement mechanisms of (a) single diatoms of different sizes and (b) mucilage aggregates.....***204**

*Figure 7.15 Evolution of experimental chapters to meet overall aim of thesis.....***213**

*Figure 7.16 Interlinking relationships between multi-feature and multi-scale topography, roughness and contact angle, and aspect ratio of fouling organisms that lead to the optimum antifouling potential of a surface.....***215**

*Figure 8.1 Spinner shark inspired laser surface textured pattern directly onto marine grade steel using processes outlined in methods section and chapter 6 where (a) is at x100 magnification, (b) at x1000 magnification and (c) a 3D scan of the surface at x1000 magnification.....***218**

List of Tables

<i>Table 1.1 Biofouling problems caused by macro-fouling organisms</i> .....	<b>28</b>
<i>Table 1.2 Antifouling methods and their problems and benefits</i> .....	<b>33</b>
<i>Table 1.3 Examples of epibiosis in the marine environment and the problems that it causes</i> .....	<b>37</b>
<i>Table 1.4 Micro-topographies patterns displayed in from a range of species</i> .....	<b>40-42</b>
<i>Table 1.5 Table of studies</i> .....	<b>57</b>
<i>Table 3.1 Key equipment</i> .....	<b>60</b>
<i>Table 3.2 Laser parameters</i> .....	<b>61</b>
<i>Table 4.1 Exact dates of experiments</i> .....	<b>76</b>
<i>Table 5.1 Images and features from topographical scans of crab species (lines on images are where cross-sections have been drawn for measuring purposes)</i> .....	<b>104</b>
<i>Table 5.2 Images and features from topographical scans of shell species (lines on images are where cross-sections have been drawn for measuring purposes)</i> .....	<b>106</b>
<i>Table 5.3 Laser parameters for the patterns created and tested in this chapters experiments</i> .....	<b>108</b>
<i>Table 5.4 Exact dates of experiments</i> .....	<b>110</b>
<i>Table 5.5 Crab and inverse crab based biomimetic patterns created by laser surface texturing</i> .....	<b>111</b>
<i>Table 5.6 Shell based biomimetic patterns created by laser surface texturing</i> .....	<b>113</b>
<i>Table 5.7 Depth and width of laser processed features of surfaces in this chapter</i> .....	<b>115</b>
<i>Table 6.1 Topographical and microscope images of surfaces in experiment 1</i> .....	<b>152</b>

<i>Table 6.2 Topographical and microscope images of surfaces in experiment 2 ....</i>	<b>153</b>
<i>Table 6.3 Topographical and microscope images of surfaces in experiment 3 .....</i>	<b>154</b>
<i>Table 6.4 Topographical and microscope images of surfaces in experiment 4 .....</i>	<b>155</b>
<i>Table 6.5 Topographical and microscope images of surfaces in experiment 5.....</i>	<b>156</b>
<i>Table 7.1 Previous studies on the development of micro-textures for antifouling purposes with addition of this study .....</i>	<b>177</b>
<i>Table 7.2a Species list of diatoms found on surfaces .....</i>	<b>194</b>
<i>Table 7.2b Species list of diatoms found on surfaces .....</i>	<b>195</b>

## List of Abbreviations

AF antifouling

CA contact angle

EPS extracellular polymeric substances

GFM fringe projection microscope

TBT Tributyltin

WHO World Health Organisation

PDMS Poly (dimethylsiloxane)

SiO<sub>2</sub> Silicone dioxide

IMO International Maritime Organisation

OLN-93 Oligodendroglia cell line

MIC Microbial Induced Corrosion

EU European Union

## Chapter 1 Literature Review

### 1.1 Introduction to Biofouling

Biofouling is described by Wahl (1989) as a colonization process of a solid surface that is either living or dead. The classical view of biofouling of surfaces follows a basic sequence that was described 3 phases (Figure 1.1), which are (1) biochemical conditioning, (2) biofilm development and (3) multicellular colonisation (Figure 1.1) (Wahl, 1989).

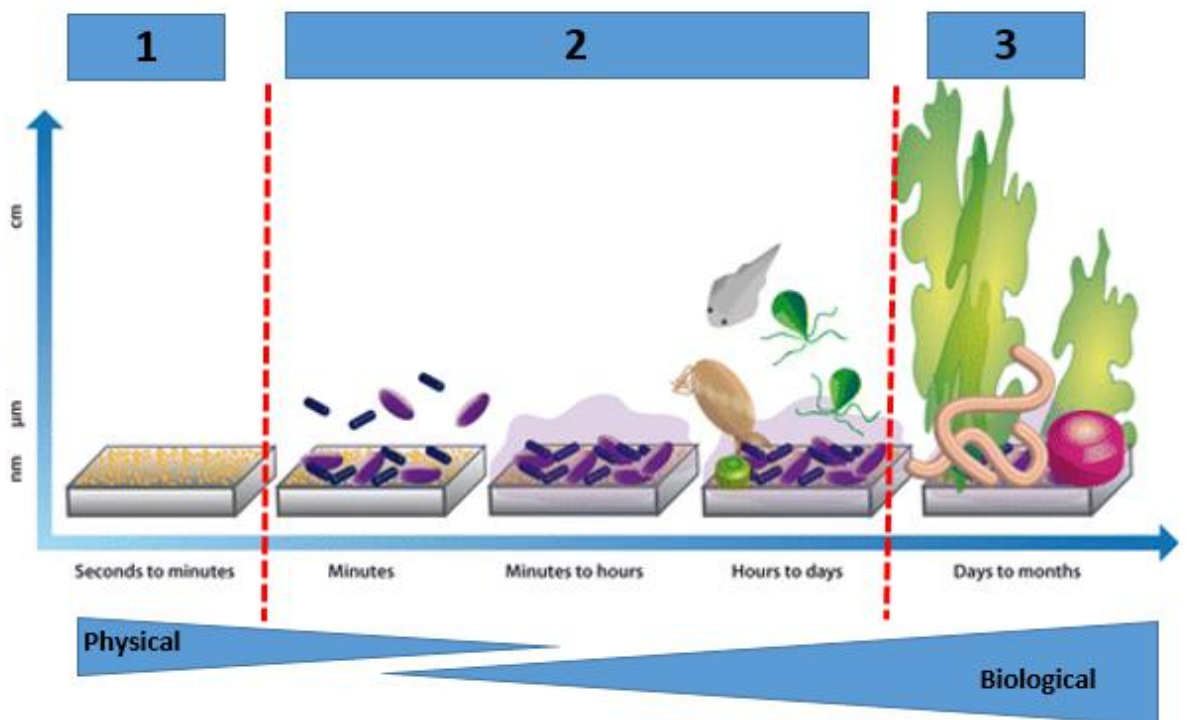


Figure 1.1 Biofouling process where (1) biochemical conditioning of the surface takes place within seconds to minutes, then (2) the biofilm layer develops within minutes to days where bacteria, diatoms, ascidians and other algal spores are attaching to the surface, which leads to (3) a complex climax fouling community made up of multicellular macrofoulers. The nature of the process switches from physical to biological (modified from (Wahl, 1989; Kirschner and Brennan, 2012).

Biofouling is a process in which both settlement and recruitment occur. Settlement is the initial contact between a new individual that comes into contact with a substratum (Hadfield, 1986; Caley *et al.*, 1996). However, recruitment often measured once individuals have metamorphosed, or have grown in size, or the time of reproduction (Hadfield, 1986).

### 1.1.1 Biochemical Phase

The first stage of fouling is governed by physical processes and these occur instantly on immersion of the inert substratum (Wahl, 1989). During the biochemical conditioning stage electrostatic interactions and Van der Waal's forces promote the adsorption of dissolved chemical compounds (mostly macromolecules such as carbon residuals and organic materials), which are freely available from the surrounding water column (Chambers *et al*,2006).

### 1.1.2 Biofilm Phase

Primary succession occurs on hard substrata that is introduced into the marine environment, that has never been previously colonised. The primary colonizers within the marine environment are bacteria and diatoms. Diatoms are unicellular algae that possess a cell wall composed of silicon dioxide (SiO<sub>2</sub>) and are living in nearly every body of water (Round *et al*,. 1990). Therefore, this results in a biofilm in which diatoms and bacteria are the dominant microorganisms. Colonisation can occur within 24 hours to a week, with full biofilm growth occurring within 2 weeks to one month (Figure 1.2; Chambers *et al*, 2006).

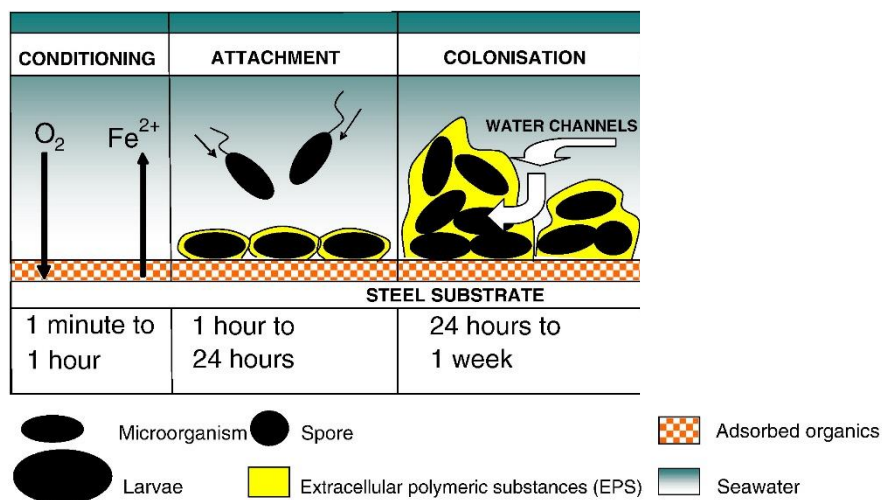


Figure 1.2 Biofilm development between initial submersion to one week time scale (modified from Chambers *et al*, (2006).

Diatom and bacteria are commonly found in all water bodies and are suspended in the water column. They move through the water column in various ways, one of these ways is Brownian motion. Brownian motion is random motion of lots of suspended particles in a fluid bumping into each other and changing course (Chambers et al., 2006). Diatoms and bacteria also move via sedimentation which is rising and falling movements within the water due to heating and cooling (Chambers et al., 2006). Currents and turbulence within the water column are also responsible for passively connecting diatoms and bacteria within the water column to substratum (Wahl, 1989). Biofilm species such as algal spores of *Ulva sp.* are able to actively seek out substratum and travel towards them using propulsion from flagella. *Ulva sp.* changes from a random swimming pattern to a searching pattern when in close contact with the substratum as a means of exploration (Callow et al., 2002).

Once bacteria and diatoms are at the substratum they can attach and settle onto it by secreting extracellular polymeric substances (EPS). It was originally assumed that diatoms could not attach without the presence of bacteria (Marszalek, Gerchakov and Udey, 1979), however, it has since been proved that diatoms can attach to a clean surface in a laboratory setting (Cooksey, 1981) although in a natural environment diatoms and bacteria will attach simultaneously. Extracellular polymeric substances are secreted from both diatoms and bacteria and they are defined as biosynthetic polymers that participate in the formation of microbial aggregates (Geesey, 1982). Acidic polysaccharides are the main components of the EPS (Chambers et al., 2006), it also contains lipopolysaccharides, proteins and nucleic acids (Flemming et al., 2000).

The way in which diatoms settle is dependent on which group of diatoms they belong. There are two major groups of diatoms that are divided by their symmetry; pennate and centric diatoms. Pennate diatoms have bilateral symmetry and are often

benthic, whereas centric diatoms are mainly planktonic and radially symmetrical (Wetherbee *et al.*, 1998). Another main difference in distinguishing diatoms is the presence or absence of a raphe. Pennate diatoms generally have a raphe, which is an elongate slit in one of the frustules (Wetherbee *et al.*, 1998). In pennate diatoms, the raphe is responsible in secreting the EPS for diatom settlement. Strands of EPS from the raphe act as a glue to attach the diatom to the substrata, however the EPS are also important in mobility of raphid diatoms (Rosowski, 1980; Cooksey, 1981; Edgar, 1983; Edgar and Pickett-Heaps, 1983; Edgar and Zavortink, 1983; Edgar and Pickett-Heaps, 1984). It has been proposed that the release of actin/myosin strands from the raphe within the EPS act as a motor which generates the gliding movement (Edgar and Zavortink, 1983; Edgar and Pickett-Heaps, 1984). An alternative in EPS involvement in diatom mobility has been suggested, in that when the EPS hydrated with sea water upon secretion, a force is generated that pushes the diatom forward (Gordon, 1987). Overall, EPS was not only crucial to attachment of diatoms, but it also enable motility across the substrata.

Settlement and mobility mechanisms of araphid and centric diatoms differ to pennate due to the lack of raphe. Some studies have investigated the alternative view that specific sites in the cell frustule secrete mucilage on adhesion to the substrata, and it is this that hydrates and swells to thrust the cell forwards (Pickett-Heaps, Hill and Blaze, 1991; Hoagland *et al.*, 1993). Although centric diatoms are mainly planktonic, there have been several reports of motility across surfaces within the literature (Medlin, Crawford and Andersen, 1986; Pickett-Heaps, Hill and Wetherbee, 1986). Although centric diatoms do not have a raphe, they have been found to be able to secrete mucilaginous material from two deep grooves located at each end of the frustule which enables multi-directional movement of the cell (Pickett-Heaps, Hill and Blaze, 1991).

Diatoms settle passively and are subsequently motile, actively choosing preferred settlement sites (Scardino *et al.*, 2006). Once attached and secreting EPS, bacteria and diatoms can multiply to colonise a substratum and form a functioning biofilm. Diatoms glide across the surface using an actin-myosin motility system (Poulsen *et al.*, 1999) and using EPS as lubricant. It has been found that diatom motility is variable and velocity of movement varied significantly at different times of day (Poulsen *et al.*, 1999). Once in a preferred space they settle and start to divide (Figure 1.3).

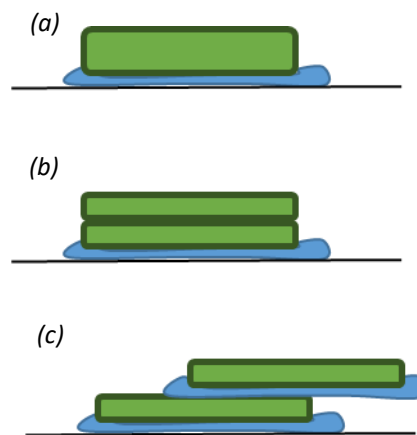


Figure 1.3 The 'mother cell' model for diatom reproduction where (a) the cell settles on surface and secretes a permanent adhesive, (b) the cell undergoes division and (c) the mother cell remains attached while the daughter cell is free to glide away.

In many studies, biofilm is not identified down to species level, the biofilm is referred to as bacteria and diatoms rather than individual species (Efimenko *et al.*, 2009). However, diatoms are easily identifiable using light microscopy due to their silica shells. Diatoms have a wide range in dimensions and adhesion strategies, both of which will be affecting the way settlement occurs on the micro-textured surface, and therefore should not be grouped together, as different species settle in different ways. There are three main adhesion strategies found in benthic diatom communities (Round *et al.*, 1990; Majewska *et al.*, 2013a; Majewska *et al.*, 2013b; Sullivan and Regan, 2017): 1) erect attachment, where diatoms attach to the surface using mucilage stalks, pads or peduncles (Figure 1.4a); 2) motile attachment, where diatoms with valve face adherent to the substratum secrete EPS

to attach and move within the horizontal boundaries of a surface (Figure 1.4b); 3) adnate attachment, where diatoms can attach and grow together in clusters or chains and settle both horizontally and vertically on the surface (Figure 1.4c).

Understanding which diatoms are present on the surface, and their dimensions and adhesion strategies enables a deeper understanding of the interactions at the interface of the surface; therefore an understanding of diatom species assemblages may help understand how the biofilm grow and change.

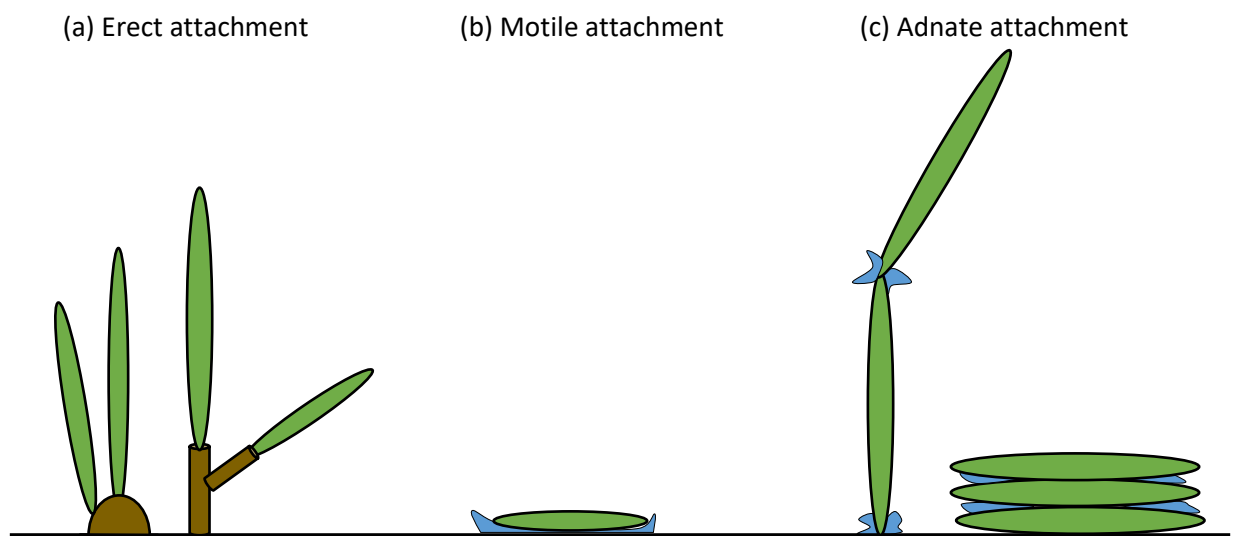


Figure 1.4 Three different attachment types of diatoms to a surface where (a) is erect attachment (b) motile attachment and (c) adnate attachment.

Biofilms are an important diverse community within the marine environment. The early species compositions depend on the presence of the colonising species, and the physical and chemical conditions of the surface and surrounding environmental factors (Dobretsov, 2010). Changes in the abiotic (e.g. season, depth) and biotic (e.g. predation, grazing) environmental conditions effects the species composition within a biofilm (Qian *et al.*, 2007) as adhered organisms can attract or repel the co-adhesion of other micro-organisms (Marshall *et al.*, 1971; Vandevivere and Kirchman, 1993).

Changes in abiotic and biotic environmental factors may also lead to changes within the biofilm density, productivity and architecture of biofilms (Qian *et al.*, 2007). As biofilms mature they develop a three dimensional structure (O'Toole *et al.*, 2000). The shape of this structure is highly dependent on the species function and diversity, physical factors (hydrodynamic forces, flow rate), chemical factors (EPS production, nutrient availability) and biological factors (competition, predation). However, the general structure of a biofilm is mushroom like colonies with voids between them to allow water to flow (Costerton *et al.*, 1995). Streamers, which are elongated strands of the micro-colonies, are produced in mature biofilms which detach from the biofilm and spread to colonise other areas. Detachment can also occur due to erosion or corrosion of substrata (Videla and Characklis, 1992).

Biofilm mass, growth and structure are under constant dynamic change as they are affected by disturbance. Disturbance is defined as any discrete event in time or space that changes the structure of populations, communities or ecosystems, and changes the resources available or the physical environment (Pickett and White, 2013). The first pioneering studies on disturbance of fouling have shown that disturbances such as wave action pushing logs into the intertidal shore line have provided new space in which new colonisation can begin (Dayton, 1971). Disturbance can be small or large scale, and is the result of physical action such as earthquakes, storms, extreme wave action, ice scouring or land slides, or biological as a result of grazing and predation. Large physical disturbances are rarer, although when they do occur they have a larger influence on biofouling than smaller disturbances (McCook and Chapman, 1997; Turner *et al.*, 1998; Underwood, 1998). Smaller disturbances are more common within a marine fouling community, and when they occur they may only remove part of the community (Platt and Connell, 2003), creating a patch work like effect. Once a small patch has been removed due to a disturbance, there is free space to be colonised. It has been found that disturbance regimes reduced the average

total cover of the biofilm assemblage (Atalah *et al.*, 2007). If the whole fouling community is removed, there is the chance of completely new species colonising the free space (Airoldi, 1998). However, if only part of the community has been removed, in instances like abrasion, the free space was quickly utilised by the surrounding species.

Examples of disturbances that affect marine biofilm are: (1) increased nutrient run off from fertilizer used on land which decreased density and connectivity within biofilms (Lawes *et al.*, 2016), , and (2) increased acidification of the ocean which has changed the biofilm community composition, although the biofilm was able to undergo rapid change to adapt to new biotic conditions to maintain functions such as oxygen production (Witt *et al.*, 2011) (3) graziers which can composition of the biofilm community (Sabater *et al.*, 2002). Disturbance events are critical to increasing the diversity of species within a fouling community (Hastings, 1980).

Diatom species are specific to the habitats in which they grow (Smol and Stoermer, 2010). Seasonal changes such as light, depth and climate also have an effect on variation of species as some species are present all year round but some are only present in particular seasons (Forrest and Atalah, 2017). Some diatom species bloom in winter months (Kiss and Genkal, 1993) whereas others bloom in spring / summer.

### 1.1.3 Macrofoulers Phase

The final phase of biofouling happens when macrofoulers colonise the surface and species such as mussels, barnacles, seaweed, or tube worms become dominant. This occurs between days to months on a surface.

As described in the opening paragraph, the classical view of fouling is that it is linear, and follows a pattern of a conditioning layer forming within seconds, then a biofilm within a couple of hours to days, and then within days to weeks larger fouling organisms (Wahl, 1989). However, in reality this classical view may be an over simplification. In this

classical view, the community progresses from a low diversity pioneer stage (biofilm), to a high diversity intermediate stage, to a low diversity climax stage (macro-fouling). However, it is rare in nature that a low diversity macro-fouling climax community is reached, as disturbance events such as storms cause a fragmented habitat, and some patches of the community are reverted to earlier levels of succession (Menge & Sutherland, 1987). Biological disturbance events can also occur such as predation, which can also lead to this patchy fragmented habitat, therefore, fouling can have an impact on these predator-prey relationships, and plays a role in the community development (Menge & Sutherland, 1987). It has been previously found that epibionts have the potential to dramatically increase or decrease the mortality of their hosts (Wahl *et al.*, 1997). It was found that barnacle *Balanus* enhanced predation on mussels *Mytilus*, this scenario is known as shared doom (Wahl *et al.*, 1997). Whereas, the hydrozoan *Laomedea* reduced predation on mussels *Mytilus*, this scenario is known as associational resistance (Wahl *et al.*, 1997). Therefore, fouling can influence the predator-prey dynamics within a community at the macro-fouling level.

The presence and activity of marine biofilm is known to influence higher order processes such as invertebrate settlement (Qian *et al.*, 2007). However, it has been well established over many studies that barnacle *Balanus amphitrite* settles without biofilm present, and in fact biofilms show an inhibiting effect on barnacle settlement (Olivier *et al.*, 2000, Maki *et al.*, 1990, Neal and Yule, 1994, Keough and Raimondi, 1995). Algal species, *Ulva*, have motile spores which are able to settle on a clean surface within minutes (Callow *et al.*, 1997).

The presence of a biofilm has also been known to effect the predator / prey relationship other fouling organisms (Flemming *et al.*, 2007). Another study has shown that the age of the biofilm increased the inhibiting effect on predator / prey relationships (Faimali *et al.*, 2004). However, this effect is mainly for barnacles, as other fouling species

have shown that they need a biofilm present to be able to settle. A study on the tube worm, *Hydroides elegans*, found that a minimum density of bacteria is required before settlement, and that settlement does not occur in the absence of biofilm (Huggett *et al.*, 2009). Studies on different species of mussels have shown that biofilm promotes settlement of *Mytilus galloprovincialis* (Bao *et al.*, 2007), *Mytilus edulis* (Toupoint *et al.*, 2012) and *Mytilus coruscus* (Wang *et al.*, 2012) showing the trend that mussels prefer the presence of a biofilm for settlement. It has also been found that the presence of biofilm promotes settlement in oysters (Campbell *et al.*, 2011). Therefore, there is evidence that biofilms promote the settlement of fouling species, and if the biofilm density is limited, or absent, the settlement of macrofoulers may not occur.

## 1.2 Problems caused by biofouling

### 1.2.1 Problems caused by Biofilm

Biofilms are known to increase corrosion of surfaces by microbial induced corrosion (MIC). This occurs for two reasons, one as the EPS secreted by micro-organisms present in the biofilm have the capacity to bind to metal ions (Kinzler *et al.*, 2003; Rohwerder *et al.*, 2003; Sand, 2003). The interaction occurs between the metal ions and the negatively charged (anionic) functional groups that are common on the carbohydrate and protein molecules within the EPS (Beech and Sunner, 2004). The interaction that occurs is a redox reaction which causes increased corrosion and visible rust on the surface (Beech and Sunner, 2004).

Another sources of increased corrosion within the biofilm layer is the presence of anaerobic niches. It is generally accepted that anaerobic niches can occur within biofilms developed in oxygenated systems. Within these anaerobic niches sulphate reducing bacteria (SRB) thrive. Electrons are transported from the metallic surface through the bacterial sulphate reduction pathway through the use of hydrogenase enzymes (De

Romero *et al.*, 2002; Beech, 2003; De Romero *et al.*, 2003). It is this reduction that leads to the increase in corrosion under anaerobic conditions (Beech and Sunner, 2004).

Biofilms within water cooling systems allow bacteria to grow and thrive as temperatures are raised to between 25° and 35°, therefore, proliferation occurs rapidly (Di Pippo *et al.*, 2018). Under these conditions, it is not just MIC that can be an issue, it is also the effect the bacteria can have on humans that can be a problem. Water cooling systems are known to pose health problems associated with the presence of pathogens like *Legionella pneumophila* so much so that the World Health Organisation (WHO) have issued guidelines on preventing and controlling the risk of Legionella proliferation in cooling towers (Mouchtouri *et al.*, 2010).

Biofilms have been found increase risk of human infection in drinking water systems (Bachmann and Edyvean, 2005; Fish, Osborn and Boxall, 2017). This problem also exists in dental chairs units, as water systems are used in dental practises and it has been found that water is often contaminated with high densities of micro-organisms including Legionella and Pseudomonas species which can cause pneumonia within humans (Coleman *et al.*, 2009).

### 1.2.2 Problems caused by macrofouling

Macrofouling species attach to the substrata after the biofilm has formed. Macrofouling species are larger, and often hard shelled organisms and therefore can cause more damage through biofouling than the biofilm alone (Table 1.1).

Table 1.1 Biofouling problems caused by macrofouling organisms

Industry	Problem(s)	References
Aquaculture	<ul style="list-style-type: none"> <li>• Biofouling of infrastructure</li> <li>• Fouling of stock species causing damage and reducing sale price.</li> <li>• Reduction in food supply to farmed species therefore slower growth of farmed species</li> <li>• Introduction of diseases/ toxins / parasites</li> <li>• Reduced water flow and oxygen influx leading to death or reduced growth in finfish</li> </ul>	(De Nys and Guenther, 2009) Hidu <i>et al</i> , 1981 Lodeiros and Garcia, 2004 Atalah <i>et al.</i> , 2016, Forrest and Atalah, 2017; Dürr and Watson, 2010)
Water and Power	<ul style="list-style-type: none"> <li>• Blockages of pipelines in cooling systems</li> <li>• Corrosion causing weakening and breakage leading to leaks</li> </ul>	(Venugopalan, 2018) (Feeley <i>et al.</i> , 2005)
Shipping	<ul style="list-style-type: none"> <li>• Increasing drag on ships hull</li> <li>• More fuel usage</li> <li>• More CO<sub>2</sub> outputs from fuel</li> <li>• Introduction of invasive species</li> <li>• Motor damage</li> </ul>	(Schultz, 2007; Schultz <i>et al.</i> , 2011)

Macrofouling organisms such as mussels, barnacles, tubeworms and ascidians cause various problems for industry, shown in Table 1.1. The most common problems are blockages of pipelines in water cooling systems and therefore reduction of water flows leading to overheating. One of the main problems that effects all of these industries, and is and the interest to national conservation efforts is the invasion of non-native species. An example an invasive species being introduced to UK waters is the invasion of the freshwater Zebra Mussel *Dreissena polymorpha* to UK (Aldridge *et al*, 2004). It was first recorded in Britain in Surrey Docks (London) and at Cambridgeshire in 1824, and within 10 years, they had spread to Scotland (Coughlan., 1998). Studies have repeatedly shown that

once the zebra mussel is present in a water body, the native mussel species populations decrease and become vulnerable to extinction (Aldridge, 1998; Mclvor, 1999). Biofouling is responsible for the invasion of the zebra mussel as increased shipping trade resulting from the nineteenth century Industrial Revolution facilitated the spread of the zebra mussel (Morton, 1993) from Baltic region to England. This spread of the zebra mussel was further increased by Zebra mussels arrived in Ireland, probably in 1994 or earlier, attached to the hulls of used pleasure craft imported from either England or the Netherlands (Minchin and Moriarty 1998; 1999).

### 1.2.3 Costs of biofouling

Within industry, the problems biofouling causes often equates to a loss of money. In aquaculture it is estimated € 120000 to replace nets and it is estimated that mussel farmers in Scotland spend € 450000-750000 a year on biofouling related costs (Willemsen, 2005). Conservative estimates of the costs of biofouling are equivalent to 5-10% of the industry value (Lane and Willemsen, 2004). For salmon farming in Norway, the cost of fouling has been estimated at between €0.02 and €0.09 Kg<sup>-1</sup> of salmon produced (Dürr and Watson, 2010).

In water and power industries, the blockages of pipelines by zebra mussels is estimated to cost industry in the United States US\$5billion each year (Khalanski, 1997). The cost of fouling on naval ships is primarily driven by hull fouling, increasing costs due to increased fuel consumption due to increased friction drag (Schultz *et al.*, 2011). The overall cost associated with hull fouling for the American Navy's fleet is estimated to be \$56M per year or \$1B over 15 years (Schultz *et al.*, 2011).

### 1.3 Previously used antifouling (AF) techniques

The problems associated with biofouling have been affecting shipping throughout history, therefore there has always been a demand for antifouling (AF) technologies. The earliest record of the use of antifouling technology comes from the ancient Phoenicians and Carthaginians who used lead and copper sheets to cover the ship's hull (Yebra *et al.*, 2004; Howel and Behrends, 2010).

#### 1.3.1 Tributyltin

Since this time, AF technologies have developed and AF coating become the standard way to protect ships hulls from biofouling. Self-polishing copolymer coatings containing Tributyltin (TBT) were most popular as they had self-polishing properties as well as AF properties which help improve the hydrodynamics and increased the length of service (Howel and Behrends, 2010). However, TBT had negative effects on the marine environment. Tributyltin leached from the hull of ships into the water column and disrupted the endocrine functions of marine organisms such as causing masculinisation and irreversible sperm damage in zebrafish (*Danio rerio*; McAllister and Kime, 2003) and cause imposex in gastropod species such as *Nucella lapillus* (Oehlmann *et al.*, 1998), *Hexaplex trunculus* (Terlizzi *et al.*, 1999) and *Thais clavigera* (Blackmore, 2000). Tributyltin has also been found to affect molluscs, crustaceans and ascidians (Rees *et al.* 2001; Smith *et al.* 2008). Other research has shown that TBT directly impairs mitochondrial function (Nishikimi *et al.*, 2001) which means it is not targeting marine biofouling species, but has the potential to affect all species within the marine environment. Overall, TBT had negative effects on the ocean and since its ban studies have shown that affected populations have started to improve (Smith *et al.*, 2008).

Consequently, TBT was banned from small vessels in the UK in 1987 under the Food and Environment Protection Act 1985 (Great Britain-Parliament 1985), and by 1<sup>st</sup>

January 2008, The International Maritime Organization (IMO, 2002) announced a complete prohibition of TBT globally. Countries have followed recommendations and phased out TBT over a ten year period (Christen, 1999). New Zealand and Japan had already banned TBT use on most vessels before the recommendation was issued (Champ, 2000). Around the time of the ban, TBT based antifouling products made up more than 80% of the global antifouling market (Scott, 1999), therefore, this ban opened up the antifouling market to the potential of new antifouling technologies.

### 1.3.2 Alternatives to Tributyltin

Since the ban on TBT, copper based paints are used as the principle biocide (Voulvoulis *et al*, 2002, Trentin *et al.*, 2001; Cima and Ballarin, 2012). These paints have less negative effects on the ocean than TBT (Hall and Anderson, 1999), however, copper-based compounds are limited as it seems to have good antifouling properties against macrofouling, but micro fouling is more resistant to the antifouling effects (Perez *et al*, 2015). A study by Chen *et al*, (2013) found a high diversity of bacteria on copper based anti-fouling paints, similar to the diversity found within the general biofilm. This reinforces that copper based paints have limited effects on the biofilm. To overcome this problem, booster biocides can be used to enhance the effect of the antifouling paint (Voulvoulis *et al*, 2002). Nine booster biocides have been registered under the European Union's (EU) Biocidal Products Directive 98/8/EC (European Commission, 1998). and are able to be used in the UK as active ingredients in antifouling coatings (Voulvolis *et al*, 2002). However, there is concern that TBT could be substituted for a biocide that is equally or as damaging to marine environments (Voulvolis *et al*, 2002), as there is uncertainty over the safety of 3 of the 9 biocides as TCMS pryride, TCMTB and Dichlofluanid as they are similar to TBT for aquatic toxicity and could end up having similar detrimental effects on the marine environment. Studies on these booster biocides have shown that they can inhibit algae growth, (Okamura *et al.*, 2003), have negative effects on ascidians (Gallo and Tosti, 2015)

corals (Owen *et al.*, 2002) and macrophytes (Scarlett *et al.*, 1997; Scarlett *et al.*, 1999).

Therefore, although the booster biocides are 'healthier' for the oceans than TBT, there is concern over the environmental impacts, especially long term as they have only been used for a couple of years and are already having negative effects.

Another popular antifouling method on the market are foul release coatings. Foul release coatings are silicone elastomeric materials which produce a low surface energy "non-stick" effect (Anderson *et al.*, 2003). It is this low surface energy that gives the antifouling effect (Ekin and Webster, 2007; Sommer *et al.*, 2010). Foul release coatings are popular as they can be applied by airless spray, and work well on macrofouling organisms such as barnacles (Aldred and Clare, 2008). Accumulated fouling is released from the surface through the action of hydrodynamic forces generated as a vessel moves through water (Buskens *et al.*, 2013). Foul release coatings may not be appropriate for static conditions as it is claimed that vessels should be operating at or above 10 kts (1 kt = 1.85 km per hour) to benefit from foul release coatings (Buskens *et al.*, 2013).. It has also been found that foul release silicones have little effect on diatom settlement (Holland *et al.*, 2004), therefore a biofilm persists on foul release silicones. Although foul release coatings can be effective under hydrostatic forces, coatings are relatively soft and easily damaged.

Although antifouling paints are the most common method for the maritime industry, there are a range of other methods outlined in Table 1.2.

Table 1.2 Antifouling methods and their problems and benefits.

Type	How it works	Problems	Benefits	Safe	Reference
Tributyltin (TBT)	Inhibits energy transfer in respiration	-Affects none target organisms causing localised extinctions.	Easily available and dominated the market (before ban)	No	Callow and Callow, 2002
Silicone foul release coating	Minimising adhesion strength of organisms	-Only works at high speeds, and has little effect on biofilm layer	Effective on hard foulers such as barnacles	Yes	Callow and Callow, 2002
Natural Marine Product (NMP) antifoulants	Extracted compounds and secondary metabolite production from marine bacteria, plants, sea weeds such as <i>red algae Laurencia</i> (Masuda <i>et al.</i> , 1997)	-Organisms can overcome the effect - Bioaccumulation - often difficulties in obtaining enough pure compounds to use within a paint (Bobzin and Faulkner, 1992; Barbosa <i>et al.</i> , 2007)	-Lots of choice of compounds, more than 300 from one species (Masuda <i>et al.</i> , 1997) -compounds can be mixed to increase antifouling potential (Hellio <i>et al.</i> , 2009)	Yes	Terlezzi, 2000 Steinberg <i>et al.</i> , 1997 Armstrong <i>et al.</i> , 2000 Flemming, (Hellio <i>et al.</i> , 2009)
Biological control	Natural predators/ grazers of fouling organisms are introduced	Limited to aquaculture where bio-fouling occurs in a confined space	Positive results; biological control using sea urchins and hermit crabs has proved effective for controlling fouling of suspended shellfish systems (Hasse, 1974) and for fin fish systems by co-culturing (Kuwa, 1984).  No harmful chemicals added to systems	Yes	Willemsen 2005; (De Nys and Guenther, 2009)

Micro-topographical surfaces	Limits cell settlement in biofilm development stage	Early stages of development, more research needed	Universal, No leaching into environment, no harmful chemicals,	Yes	Carman <i>et al</i> , 2006
------------------------------	---	---	--	-----	----------------------------

Overall, past antifouling methods have had negative effects on the wider ocean ecosystem as chemicals have leached away from the surface, and into the water column. Today, regulations are stricter in regards to what chemicals can be used in the ocean, as protecting species diversity is of importance. Some alternative methods such as foul release show promising results for macrofoulers, however, biofilm is persistent and difficult to target. This section highlights that there is an increasing demand for a cheap, eco-friendly, non-toxic antifouling solution. With the recent global ban of TBT opening up the antifouling market there is potential for new antifouling technologies to emerge and compete within this market.

#### 1.4 Evolutionary response to biofouling

Convergent evolution is the evolution of phenotypic similarities (e.g. micro-textured surfaces) by unrelated species in response to environmental challenges (Stern, 2013). One of the most common example of convergent evolution is the missile shaped body that has evolved across various unrelated species, over millions of years as a response to the functional constrains of locomotion in water (McGhee *et al.*, 2011). The fusiform morphology is a direct response to limiting the drag when swimming in the dense medium of water (McGhee *et al.*, 2011). This streamlined shape of bony fish and cartilage fish appeared in the Silurian, and then 230 million years later land dwelling reptiles rediscovered the same morphology on their evolutionary journey back to the sea. This shape appeared again when mammals returned to the sea 175 million years later. This results in today's animals such as the great white shark, and the bottle nose dolphin having

a similar streamlined shape, although the evolution of both animals do not share a distant common ancestor, as one is a bony fish and one is a mammal. This example shows that convergent evolution brings about morphological traits in response to the environmental conditions. The development of micro-textures on the outermost surface of marine organisms that are not closely related, such as pilot whales and shore crabs, is an example of convergent evolution. Micro-textures have evolved as a response to environmental conditions.

#### 1.4.1 Negative effects of fouling on fitness of marine organisms

Biofouling occurs on living surfaces within marine and freshwater habitats, this is known as epibiosis (Wahl, 1989). The living organism that is being fouled is known as the basibiont and the organism that is doing the fouling is known as the epibiont (Wahl, 1989); for example, a sponge would be the epibiont as it attaches and lives on a periwinkle which is the basibiont (Table 1.3). A well-known example of epibiosis is barnacles attaching and living on a humpback whale *Megaptera novaeangliae* (Fertl, 2002). They are fouled by the acorn barnacles, *Coronula diadema* and *Coronula reginae*, and these barnacles are in turn fouled by the stalked barnacles, *Conchoderma auritum* and *Conchoderma virgatum* (Clarke 1966, Dawbin 1988, Fertl 2002). Although the barnacles are epibionts, and are attaching too and living on the whale, they are not parasitic, they do not feed on body fluids of the whale. However, they can cause problems by increasing drag and affecting hydrodynamics if they become abundant (Felix *et al*, 2006). Although small amounts of barnacles are unlikely to affect a humpback whale, there has been a reported case where a humpback whale had more than 1000 lb of barnacles attached to its body (Slijper, 1979).

Although biofouling seems trivial for a humpback whale, as the sheer size of their body mass means that biofouling does not have much effect on their general wellbeing and they are able to live as long even though they are fouled. This is not the case for smaller

marine organisms such as periwinkles and crabs. A study on periwinkle *Littorina littorea* found that fouled snails crawled at over 13 times slower than unfouled snails (Buschbaum and Reise, 1998). This slow crawling speed would affect their ability to flee from predators and forage for food in mussel beds as their agility is reduced. Both of these factors would lead to a higher risk of mortality. Mortality was studied in the same experiment and significantly more fouled periwinkles died than unfouled periwinkles; 43 fouled snails died, whereas only 15 unfouled snails died. They suggest that this is because a cold period caused stress on both fouled and unfouled tanks, but the unfouled snails are able to cope with a less than optimum environment better than unfouled snails (Buschbaum and Reise, 1998).

Fouling of living organisms can cause many problems (shown in Table 1.3) which can be detrimental to the basibiont organism and can result in reduced growth, higher predation, and eventually death.

Table 1.3 Examples of epibiosis in the marine environment and the problems that it causes

Epibiont (Biofouling organism)	Basibiont (organism being fouled)	Problem fouling organism causes	Reference
Sponges / Barnacles <i>Cliona sp.</i> <i>Polydora ciliate</i>	Periwinkle <i>Littorina littorea</i>	Weakens shell making periwinkle prone to predation  Increases drag making crawling speed slower, and therefore easier to be caught by predators.	Stefaniak <i>et al</i> , 2005  Thieltges and Buschbaum, 2007
Bryozoans	Sea weed <i>Gelidium rex</i>	Reduces rates of photosynthesis which lowers growth rate and reproduction.	Cancino <i>et al</i> , 1987
Mussels	Crab <i>Limulus polyphemus</i>	Reduced aeration of gills	Patil & Anil, 2000
Protozoa <i>Colacium vesiculosum</i>	Zooplankton <i>Daphnia</i>	Increased risk of predation as fouling organism increases the visibility.	Chiavelli <i>et al</i> , 1993
Hardfoulers Barnacles platyhelminth worms, annelid worms mussels	Sea Turtle	Increase drag by disrupting the laminar flow  Increase energy expenditure on long distance migrations causing exhaustion/ drowning  Burrowing foulers can increase vulnerability to pathogens.	Logan and Morreale, 1994  Alfaro, 2008 Frick & Pfaller, 2013;

The main problems with epibiosis that are seen throughout the literature is that drag is increased on the basibiont therefore, this makes movement harder and uses more energy. This in turn, increases the risk of predation, reduced growth, reduced food intake, reduced reproduction and eventually death for the basibiont. It has been found that there is a preference for settlement on areas of the shell where the periostracum (outermost layer) is abraded or absent (Kaehler, 1999). The end result for the majority of heavily

fouled organisms is death of the host organism (the basibiont) (Che *et al.*, 1996; Kaehler and McQuaid, 1999).

Biofilms containing micro-fouling species such as diatoms and bacteria are also prone to fouling other marine organisms. In fact, the vast majority of marine organisms are fouled with epibiotic biofilms, which may vary in species composition and density (Lachnit *et al.*, 2009; Grossart, 2010). This may be because many soft bodies species do not have insulating coatings such as hair, fur and wax or mechanical features such as spines or shells, therefore no defence to biofilm fouling. These species are able to survive without insulating or mechanical coatings as the ocean is a benign environment for most species (Wahl *et al.*, 2012)(REF), and they may rely on escape, hiding or poor palatability as a defences from predators. However, they are threatened by biofouling, as this interface is often very delicate, and it acts as a major physiological interface between the organism and the environment as physiological functions such as respiration, exudation of wastes and the uptake of nutrients occur. Therefore, micro-fouling is a threat to this interface and can have negative consequences on the host species such as: increased weight and friction, impeded epidermal exchanges, loss of buoyancy, mobility issues (e.g., Prescott, 1990; Dougherty and Russell, 2005; Wahl, 2008b).

Usually the biofilm composition on the surface of marine organisms is composed of bacteria, diatoms, fungi, and protozoa (Bodammer and Sawyer, 1981; Höller *et al.*, 2000; Burja and Hill, 2001; Hentschel *et al.*, 2003; Webster and Taylor, 2012). The abundance level in which fouling occurs widely varies between species, as some species such as the decorator crabs are heavily fouled (Hultgren and Stachowicz, 2011), whereas other species such as didemnid tunicates are very lightly fouled (Wahl and Lafargue, 1990).

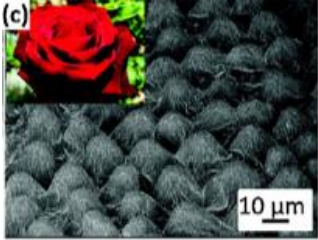
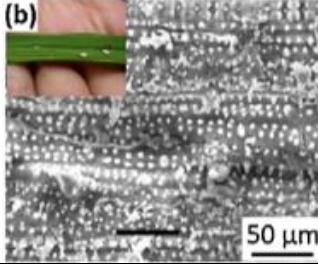
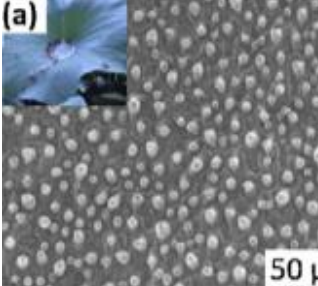
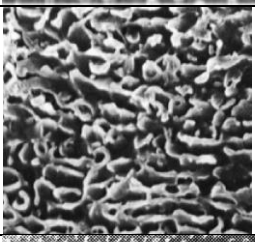
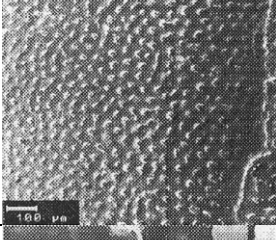
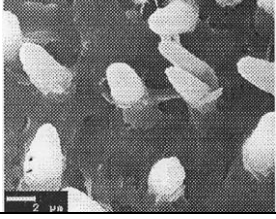
Although fouling can have many negative effects, as discussed in the Table 1.3, there are instances in the natural world in where fouling can be beneficial to the marine organisms being fouled. An example of this comes from the bryozoan larvae *Bugula*

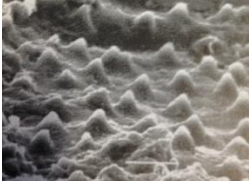
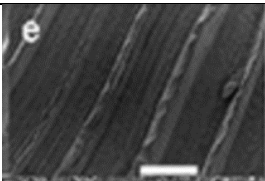
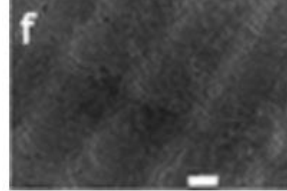
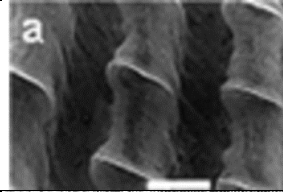
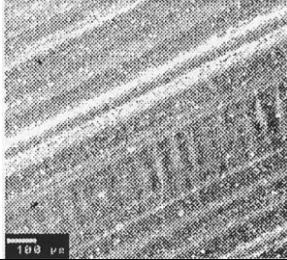
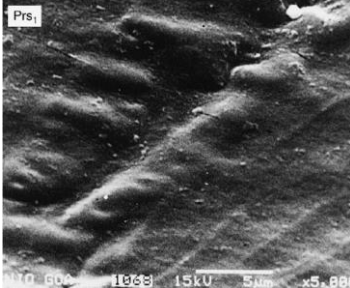
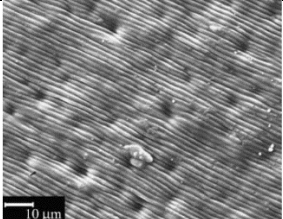
*neritina*, which is specifically fouled by bacteria *Candidatus Endobugula sertula*. This symbiotic relationship is beneficial for both the bryozoan larvae and the bacteria, as the microenvironment of the larvae host supports growth of the bacteria (Woollacott, 1981; Haygood and Davidson, 1997) and in return, the bryostatin produced by the bacteria protects the larvae from predatory fishes (Thakur et al., 2004; Sharp et al., 2007; Sharp et al., 2007 in Wahl 2012). Some fouling species offer the host associational resistance, for example the hydrozoan *Laomedea* reduced predation on mussels *Mytilus*, and therefore fouling can offer protection for the host species.

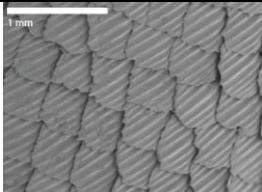
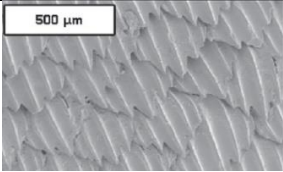
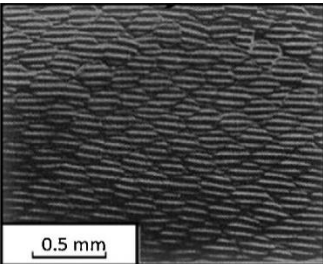
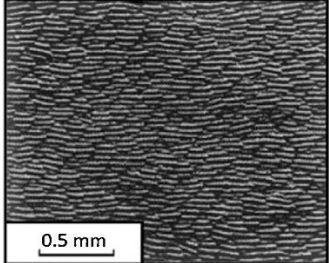
#### 1.4.2 Convergent evolutionary response to fouling

As biofouling can lead to increased mortality rates within species, it has been a driving force of evolution, and individuals which had evolved antifouling defence mechanisms would thrive and survive within a population to reproduce, whereas individuals that do not have antifouling mechanisms would die. This driving force has led to the presence of natural antifouling mechanisms in species today. There are multiple antifouling defence mechanisms that have evolved such as: chemical defence mechanisms (Teo and Ryland, 1995), mucus release (Hellio *et al.*, 2002), moulting (Russell and Veltkamp, 1984; Becker and Wahl, 1996). One of the natural defence mechanisms is the production of micro-topography surfaces on the outermost surface. The production of micro-topographies across a whole range of species is an example of convergent evolution as organisms that are not closely related (eg. Shore crabs and pilot whales), independently evolve similar traits as a result of having to adapt to being fouled. This type of protection has evolved independently across many species (Table 1.4).

Table 1.4 Micro-topographies patterns displayed in from a range of species

Micro topography Type	Image	Species	Size (μm)	Reference
Nodules		Rose petal	10	(Feng <i>et al.</i> , 2008)
Nodules		Rice leaf	10	(Guo and Liu, 2007)
Nodules		Lotus leaf	10	(Liu and Jiang, 2011)
Pores		Pilot whale <i>Globicephala melas</i>	0.1-1.2	(Baum <i>et al.</i> , 2001)
Pores		Brittle Starfish <i>Ophiura texturata</i>	10	(Bers & Wahl, 2004)
Pyramids		Crab <i>Cancer pagurus</i>	2-2.5	(Bers & Wahl, 2004)

Pyramids		Bivalve <i>Tellina plicata</i>	5	(Scardino <i>et al.</i> , 2006)
Ridges		Blue mussel <i>Mytilus galloprovincialis</i>	1.8-1.9	(Scardino <i>et al.</i> , 2009)
Ridges		Bivalve <i>Pinctada margaritifera</i>	<10	(Liu <i>et al.</i> , 1999).
Ridges		Bivalve <i>Acrotergima reeveanum</i>	500	(Scardino <i>et al.</i> , 2009)
Ridges		Bivalve <i>Septifer bilocularis</i>	200	(Scardino <i>et al.</i> , 2009)
Ridges		Bivalve <i>Dosinia juvenilis</i>	400-500	(Scardino <i>et al.</i> , 2009)
Ridges		Catshark egg case <i>Scyliorhinus canicula</i>	15-115	(Bers & Wahl, 2004)
Ridges		Horseshoe crab <i>Limulidae Sp.</i>		(Patil and Anil, 2000)
Ripples		Blue mussel <i>Mytilus edulis</i>	1-2	(Bers <i>et al.</i> , 2006)

Ripples		Penguin's wing oyster <i>Pteria penguin</i>	0.8	(Gunther and Nys, 2006)
Ripples		Winged oyster <i>Pteria perna</i>	1.5-2	(Bers <i>et al</i> , 2006)
Ripples		Winged oyster <i>Pteria chinensis</i>	0.65	(Gunther and Nys, 2006)
Scales		Spinner shark <i>Carcharhinus brevipinna</i>	<30	(Kirschner and Brennan, 2012)
Scales		Galapagos shark <i>Carcharhinus galapagensis</i>	<30	(Kirschner and Brennan, 2012)
Scales		Shortfin mako shark Mako <i>Isurus oxyrinchus</i>	<10	(Bechert, <i>et al.</i> , 2000)
Scales		Smooth Hammerhead <i>Sphyrna zygena</i>	<10	(Bechert <i>et al.</i> , 2000)

The use of micro-textures as a way to alter surface properties is reported throughout the natural world (Feng *et al.*, 2008; Guo and Liu, 2007; Liu and Jiang, 2011; Baum *et al*, 2001; Bers & Wahl, 2004; Scardino *et al*, 2006; Scardino *et al*, 2003; Scardino and de Nys, 2003; Liu *et al.*, 1999; Scardino *et al*, 2009; Patil and Anil, 2000; Bers *et al*, 2006; Gunther and Nys, 2006; Kirschner and Brennan, 2012; Bechert *et al.*, 2000). Rosebud, rice leaf micro topographies are taken from land plants (Feng *et al.*, 2008; Guo and Liu, 2007; Liu and Jiang, 2011), therefore it is unlikely that they have evolved for the purpose of antifouling. However, lotus and rice plants grow in aquatic conditions therefore it may be

possible that these topographies have developed on rice leave to limit the settlement of diatoms, which may be inhibiting the photosynthesis process.

The rest of the surfaces in the table are from marine organisms, therefore it is plausible to say that these micro-textures may have developed as a natural defence mechanism by marine organisms is reported across a wide range of species within the literature (Table 1.4). A study by Liu *et al.*, (1999) found that the grooved micro-topography of the mollusc *Pinctada margaritifera* was an example of iridescent photonic structures and used to diffract light. However, on reflection of this, there is also the possibility that these ridges have an antifouling effect, as they are not too dissimilar to grooves found on mussel or cockle shells.

Imprints and moulds taken from Bers and Wahl (2004) study were tested in field trials and there were mixed results. The micro-topography of *C. pagurus* and *M. edulis* limited the settlement of macrofoulers such as barnacles. Whereas, *O. texturata* had deterrent effects on microfoulers (*Z. commune*, *Vorticella* sp.) and the *S. canicula* eggcase had deterred settlement of both micro and macrofouling.

### 1.5 The diatom attachment theory

The diatom attachment theory has been suggested as a reason to explain why these micro textures may be working to reduce settlement of marine biofilm (Scardino *et al.*, 2006). Diatoms are a primary fouling organism and may often be the first species to settle and colonise a submerged surface. When a surface is flat, diatoms can settle easily on the surface and form multiple attachment points (Figure 1.5a). However, when a surface has a micro-texture, one of two things may occur to the diatom. If the surface topography is larger than the scale of the diatom, the diatom may settle comfortably within the crevices, form multiple attachment points, and be protected from hydrostatic forces (Granhag *et al.*, 2004) and abrasion (Figure 1.5b). However, if the surface topography is smaller than the diatom, the diatom may settle on top of the surface features, and have

less surface area of its silica shell in contact with the surface, therefore reducing the amount of attachment points that it can form, leading to weak attachment (Figure 1.5c).

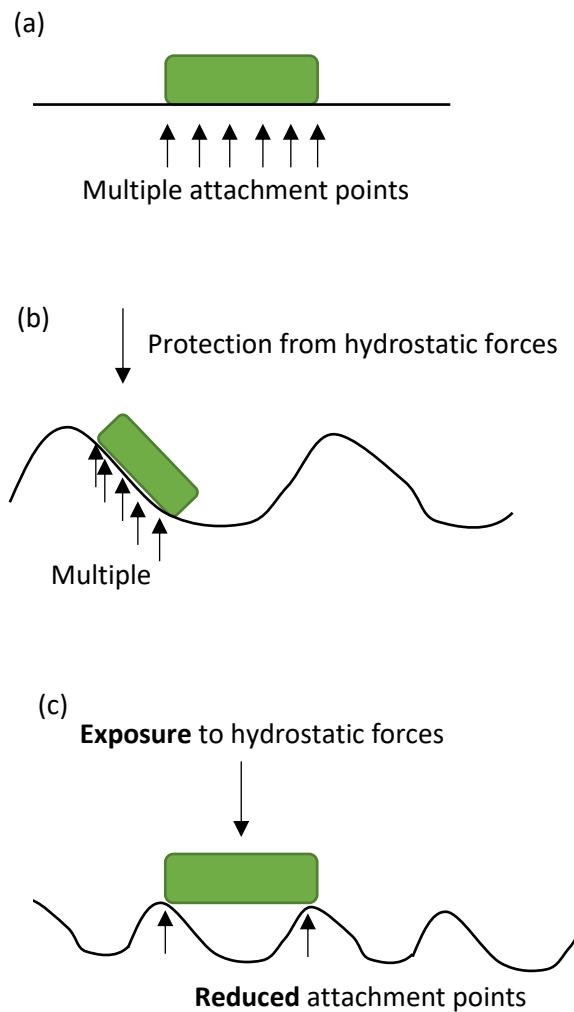


Figure 1.5 A schematic illustration of theoretical attachment points of a diatom; (a) attachment on a flat surface; (b) attachment where micro-topography that is larger than organism (micro-refuge) (c) attachment where micro-topography is smaller than the diatom therefore a reduction in attachment points (Adapted from Scardino *et al.*, 2006).

This is known as diatom attachment theory (Scardino *et al.*, 2006), and it has been demonstrated with a range of species such as *Ulva linza* (Callow *et al.*, 2002; Hoipkemeier-Wilson *et al.*, 2004; Carman *et al.*, 2006) multiple species of diatom (Scardino *et al.*, 2006) and for larger fouling species such as barnacle cyprids (Aldred *et al.*, 2010) bryozoan *Buluganeritina* and tube worm *Hydroides elegans* (Scardino *et al.*, 2008).

The micro-topographies that have arisen throughout nature (Table 1.4) and manufactured (eg. Sharklet) could be utilizing the diatom attachment theory and therefore this is why they have antifouling properties. Although this is sometimes contested, it is thought that the species of diatoms and bacteria present in biofilm can influence the settlement of macrofouling species further along the biofouling process. The attachment of spores and larvae can be influenced by bacterial biofilms via bacterial quorum sensing signals, both encouraging (Callow and Callow, 2006; Huggett *et al.*, 2006) or discouraging settlement of macrofouling species (Dobretsov *et al.*, 2006). An example of this occurring in the field is the settlement of larvae of the common Australian sea urchin *Heliocidaris erythrogramma* on the surface of coralline algae in response to the chemical compounds produced by bacteria biofilm on the surface of coralline algae (Huggett *et al.*, 2006). Therefore, reducing the settlement of diatoms and bacteria will limit the process of biofouling and limit settlement of macrofouling communities.

## 1.6 Biomimicry

Biomimicry is an innovative approach to solving human challenges by taking inspiration from patterns and strategies that have developed in nature over long time periods. The term biomimicry was first described by Otto Schmitt in 1957.

The most successful example biomimicry in the antifouling field to date is Sharklet™ developed by Carmen *et al.* (2006; Figure 1.6b). Sharklet™ is a novel microscopic physical surface modification which is inspired by *Carcharhinus brevipinna* (Figure 1.6a). The Sharklet™ micro-topography consists of rectangular ribs 2 µm wide and of varying length from 4-16 µm with a spacing of 2 µm and height of 3 µm. The ridges form a diamond like shape mimicking the scales of the spinner shark (note similarity between figure 1.6a and 1.6b).

Figure 1.6 Images from (a) a scanning electron micrograph of the skin of the spinner shark scales and (b) White-light optical profilometry magnification of the of the Sharklet AF™ pattern raised on a surface (Kirschner and Brennan, 2012).

The Sharklet™ pattern has been tested using both microfouling and macrofouling organisms and it has been found to reduce the attachment of of the green algae *Ulva sp.* (by 86% ; Carman *et al*, 2006; Schumacher *et al*, 2008 ); bacterium *Cobetia marina* (Magin *et al*, 2010); diatom *Navicula incerta* (Long,2009) and cyrpid of the barnacle *Balanus amphitrite* (Schumacher *et al*, 2010). However, all of these experiments have been done in a lab environment; there is no significant reports of it working in the field.

Not only has Sharklet™ been tested using algae species, it has also been tested for use in medicine as an antifouling mechanism for bacterial biofilms. Sharklet™ has been tested for use in catheters as a way of reducing catheter related urinary tract infections and catheter-related blood stream infection (Reddy *et al*, , 2011; May *et al*, 2015) and has showed a significant reduction in the coverage of *Staphylococcus aureus* bacteria compared to a smooth surface (Chung *et al*, 2007).

Sharklet, and other tested surfaces are created on polymer substratum using a technique called photolithography, (Carman *et al*, 2006). When used in the marine environment, micro-abrasion may chip off parts of the polymer pattern, hence adding to

the micro plastics problem in the ocean and lending the pattern ineffective towards fouling.

### 1.7 Multi-scale Multi-feature surfaces

The majority of biomimetic surfaces for the marine antifouling studies have focused on the use of a single feature or a single scale of pattern (Cunha *et al*, 2016; Schumacher *et al*, 2008; Brzozowska *et al*, 2014). However, in recent years the investigation into multi feature, multi scale surfaces has grown in application to the medical field. Multiscale texturing of surfaces using laser surface texturing has been utilised for the medical field, as it has been used on the surface of hip implants to enhance implant longevity (Ratner *et al.*, 2004). The multiscale laser textured surfaces modify the behaviour of osteoblast cells and other cells increasing their attachment to the implanted surface and therefore increasing the chances of successful implant (Wong *et al.*, 1995; Anselme, 2000; Bronzino and Park, 2002; Ratner *et al.*, 2004). There are four different interactions occurring during this process, that are happening on different scales: atomic scale, nanoscale, microscale and macroscale. At the atomic scale, the surface energy of implanted surface can be modified by chemical processing has been shown to improve bonding of proteins and cells (Van Kooten *et al.*, 1992). At the nanoscale, surface features can affect microfilaments and microtubules, which form the protein complex that attaches osteoblast cells to the surface (Brunette, 1988; Curtis and Wilkinson, 1997; Flemming *et al.*, 1999). This would be similar to affecting the EPS that marine cells secrete. Nanoscale features can also effect cell signalling, encouraging more cells to settle (Brown and Arnold, 2010). Micron-sized features such as grooves, ridges, craters provide more opportunities for osteoblast cells attachment, and macroscale features can physically interlock the implant with the bone, therefore increasing longevity, which was the overall aim of the multiscale surface (Wang *et al.*, 1993; Ward and Hammer, 1993; Den Braber *et al.*, 1998; Kurella and Dahotre, 2005).

Although the multiscale example is not antifouling based, it is actually the opposite as it is encouraging settlement of osteoblast cells, it highlights that settlement of cells is a multiscale issue. It shows that different interactions at multiple scales are happening to increase cell settlement, therefore, it could also be argued that the reverse effect could be achieved, by using multiscale textures to limit settlement.

Another multi-scale study using nano and micro texturing found that by having the ability to alter the texture at various scales with precision enabled the surface to create the desired cellular responses (Tan and Saltzman, 2004). It has also been found that surfaces that have multiple length scales bear a closer resemblance to biological matrices than those with single scale features (Tan and Saltzman, 2004), therefore multi-scale and multi-feature surfaces may enable a more precise biomimicry and be more advantageous than single scale and single feature patterns. This hierarchical approach of overlaying textures of both micro, and nano- scales to create multi-feature, multi-scale surfaces has had the most attention within the medical field, although it may be applicable for marine antifouling applications.

## 1.8 Lasers

The first time laser pulsed were used was in 1960 when Theodore Maiman constructed a laser from a Ruby rod excited by the light of a flashlamp (Maiman, 1960). A laser produces light that is unique in several ways. First it is monochromatic – its wavelength is very well defined, and it is coherent – the electromagnetic waves that form the beam of light travel almost perfectly in phase. This allows the laser light to travel as a well-defined beam with little divergence over large distances, and for that light to be focussed by a lens or similar optic to a small spot size, i.e. less than 100 $\mu$ m for many lasers. In particular it is the ability to concentrate the power of the laser light into such a small spot that has enabled the laser to be considered as a tool for processing materials. Since 1960 many different types of lasers have been developed such as Carbon Dioxide (CO<sub>2</sub>), Nd-

YAG (Neodymium doped Yttrium Aluminium Garnet) lasers, and fibre lasers. These lasers have found applications in many areas including welding, scientific analysis, metrology, communications, entertainment and materials processing.

#### 1.8.1 Laser micro-machining

Laser micromachining can be used either to remove materials or to change a material's properties (Gattass and Mazur, 2008). Well defined laser tracks, “vectors”, are used to machine the surface. These laser tracks are often straight line hatches and are the width of the laser beam. A computer controlled X-Y stage moves the laser beam precise distances to follow the vectors. As the laser spot hits the surface, ablation of the substratum at the centre of the laser spot occurs by direct absorption of laser energy (Brown and Arnold, 2010). The material is vaporized and a highly directed plume of solid and liquid clusters of material forms at the radiated site. Towards the outside of the laser spot the energy is less, therefore all of the material cannot be ablated, and it is melted. The plume is ejected from the radiated zone, and can cause the surrounding molten surface to move in liquid form and re-solidify to create ripples and ridge like structures (Brown and Arnold, 2010) . Re-solidification of the material from the vapour plume can create clusters of nano-particles which further alter the roughness of the substratum at the ablated region (Semaltianos *et al.*, 2008; Brown and Arnold, 2010).

Depth and surface finish will be determined by pulse energy, pulse length, spot size and traverse speed. These parameters are the top-level parameters, often programmed directly into a micromachining system. Areas are machined by filling the area with hatch vectors. These can be simple parallel tracks suitably spaced (“hatch spacing”), cross hatch or other parameters. Laser micro-machining can be used on larger areas, to create laser surface texturing.

An advantage of laser micro-machining is that there is not direct contact with the surface, unlike in moulding or other surface modification techniques, therefore, less risk of imperfections. However, a disadvantage of this laser micro-machining process is that excess heat from the beam may cause melt, and re-melt to harden into random, unpredictable structures, therefore causing imperfections on the surface pattern (Duncan *et al.*, 2002). Laser ablation may also cause possible alterations to surface chemistry which may influence fouling (Scardino, 2009). However, there are a some disadvantages with the laser micro-machining process in that is it energy intensive, and can be costly when done on a large scale (Gower, 2000). In many application this can be overcome by creating a master using the laser processing, and then casting material off the master to produce high volumes of replica parts to be manufactured at low unit costs (Gower, 2000).

#### 1.8.2 Laser surface texturing

The process outlined for micromachining can lead to areas of the surface becoming textured, especially if a coarse hatch spacing (greater than spot size) is used. Textures with a spatial feature sizes of  $\mu\text{m}$ 's can be produced. Laser surface texturing enables a well defined and reproducible pattern to be etched onto a surface at the micron scale. Surfaces are at the interface between two different environments, whether that be between two different components within an engine or between marine and terrestrial environments. Surfaces are the area where interactions occur, for example, surfaces of moving components within an engine rubbing together and creating friction. The surface of these components can be altered at the microscale by laser surface texturing to reduce friction (Braun *et al.*, 2014). The altering of surfaces by laser surface texturing within industry has had many useful application such as increasing fuel efficacy of engines (Etsion and Sher, 2009), increasing the light trapping efficacy of silicon wafers within solar cells (Nayak *et al.*, 2011) and increase solar absorbance of tantalum carbide pellets for solar energy applications (Sciti *et al.*, 2017).

### 1.8.3 Effect of Laser surface texturing on roughness and contact angle

Laser surface texturing has shown to have effects on the surface characteristics of materials. Laser surface texturing can alter the roughness and the contact angle (CA) of surfaces (Bizi-Bandoki *et al.*, 2011). Some studies showing that laser surface texturing decreases contact angle creating hydrophilic properties (Cunha *et al.*, 2013), whereas others have found that laser surface texturing has increased the contact angle, creating hydrophobic and even super hydrophobic surfaces (Dunn *et al.*, 2016). It is now generally agreed that laser surface texturing can both increase and decrease the wettability of the surface, depending on factors such as type of laser, laser parameters, substratum surface and the time exposed to air after laser irradiation (Li *et al.*, 2016). The ability to change the wettability of surfaces has many applications for industry such as enhanced boiling in heat transfer applications (Zupančič *et al.*, 2017) and reducing corrosion of surfaces (Trdan, Hočevár and Gregorčič, 2017). The ability to control wettability may be useful in creating an antifouling surface as wettability studies on marine organisms have shown that some species prefer to settle on hydrophobic surfaces (Rittschof and Costlow 1989; Gerhart *et al.* 1992; Holm *et al.* 1997), whereas others prefer to settle on hydrophilic surfaces (Dahlström *et al.*, 2004).

Roughness and wettability are interlinked (Kubiak *et al.*, 2011). The contact angle of a surface may be explained by two models, the Cassie-Baxter model (Cassie, 1948) and the Wenzel model (Wenzel, 1936). In the Cassie-Baxter model, the droplet sits on top of the textured surface, with air trapped underneath (Figure 1.7a), and can be used to explain hydrophobic and super hydrophobic surfaces, where contact angle (CA) is above 150° (Cassie, 1948; Ma and Hill, 2006; Bormashenko, 2008; Erbil and Cansoy, 2009). In the Wenzel model, there is no trapped air, and the droplet spreads out among the surface (Figure 1.7b), and can be used to explain hydrophilic surfaces where the contact angle is

less than  $90^\circ$ . The main difference between the two is the surface of exposed air that is under the droplet in the Cassie-Baxter system.

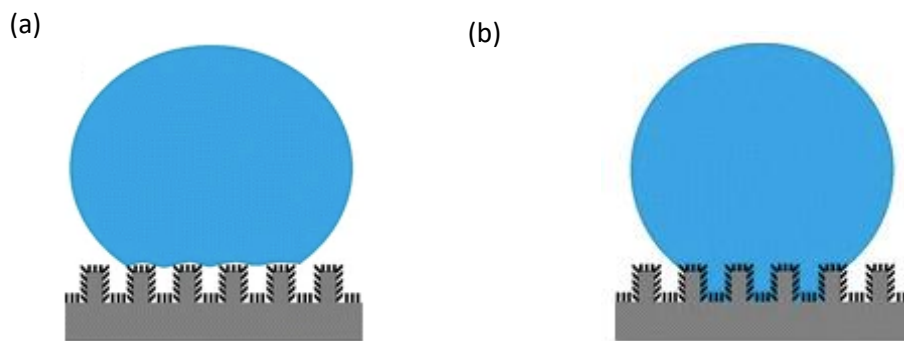


Figure 1.7 A schematic diagram of (a) Cassie-Baxter model and (b) Wenzel model ( modified from Liu and Choi, 2013)

#### 1.8.4 Effect of Roughness and contact angle on settlement

Laser surface texturing alters the roughness and the wettability of surfaces.

Altering the roughness of a surface can change the wettability, as both are interlinked (Kubiak *et al.*, 2011). The entrapped air bubbles that are discussed in the Cassie-Baxter model, are also thought to have antifouling properties as they act as a barrier between the fouling organism and the surface (Wu *et al.*, 2013; Figure 1.8). The air bubble acts as barrier in which reduces the attachment point of the fouling organism, in a way similar to the diatom attachment theory.

However, this air entrapment theory may not be completely accepted by some authors due to the likelihood of entrapped air when submerged. In Wu *et al* (2013) investigation in-situ small-angle x-ray scattering was used to measure the percentage interface that remains dry on superhydrophobic surfaces immersed in diatom culture

media. It was found that surfaces exhibited a degree of resilience against wetting as the small-angle x-ray scattering profiles obtained from the submerged surfaces suggest that the super-hydrophobic surface virtually remains dry after initial immersion (Wu *et al*, 2003). The surfaces were immersed for a 6 hour period, and the results remained constant suggesting that no further wetting occurred on the super-hydrophobic surfaces (Wu *et al*, 2003), therefore, providing evidence that air entrapment is occurring on these surfaces, which may be leading to the antifouling effects.

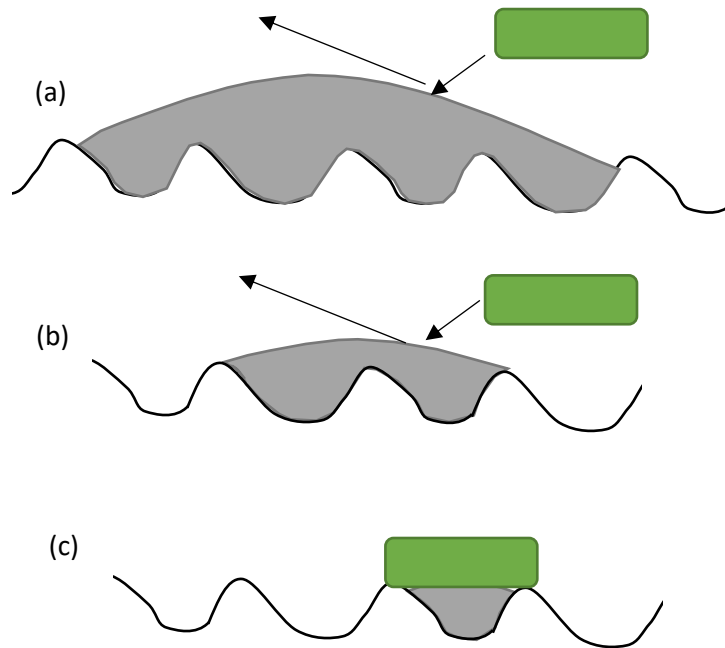


Figure 1.8 A Schematic diagram demonstrating the effects of air pocket size on diatom attachment where (a) the air pocket is much larger than the diatom, (b) the air pocket is similar size to the diatom and (c) the air pocket is smaller than the diatom (adapted from (Wu *et al.*, 2013).

It has been suggested that roughness is a key factor in the stability of the air pockets in which determine the contact angle regime (Wu *et al.*, 2013), therefore roughness, contact angle and antifouling potential may all be interlinked. This reinforces marine fouling species may be repelled by surface wettability, and therefore laser surface texturing will be a useful tool in creating this change in surface wettability.

#### 1.8.5 Laser surface texturing and Biomimicry

For the majority of biomimetic antifouling studies so far, photolithography techniques have been used. There has been one study using laser surface texturing to recreate Sharklet™ type structures (Bixler and Bhushan, 2013) but this study was aimed at drag reduction rather than investigating antifouling properties. A laser surface texturing for biomimetic surfaces is a study by (Greiner and Schäfer, 2015) who investigated laser-

created textures inspired by the scales found on the skin of snakes and certain lizards. However, this study was aimed at using biomimetic surfaces to reduce friction of components. Snakes were chosen as their natural behaviour involves friction with the ground as they move, therefore it was thought that snake scales may have developed to reduce the friction, as this is a benefit to the snake as less energy is required to move (Greiner and Schäfer, 2015). It was found that snake scale biomimicry patterns reduced friction forces by more than 40% in an unlubricated contact (Greiner and Schäfer, 2015). However, when lubricated, the friction increased by a factor of 3. However, it is argued that snakes travel over the ground in unlubricated conditions, so the mimicked surface will also work best under unlubricated conditions. They predict that even higher friction reduction will be possible once the exact contact mechanical mechanisms are known (Greiner and Schäfer, 2015). Although this study is not an antifouling study, it directly shows that laser surface texturing can be used for biomimicry purposes.

A study by Scardino *et al* (2006) used laser surface texturing to create biomimetic surfaces on polyimide film substratum based on the natural surfaces of the mussels *Mytilus galloprovincialis* and *Tellina plicata*. In this study the biomimetic surfaces reduced the settlement of *Ulva sp.* This study is rare in that it is one of the few that use lasers to (a) create biomimetic surfaces and (b) test these surfaces for antifouling resistance. However, this study (Scardino, Harvey and De Nys, 2006) dissimilar to our study as surfaces were created on polyimide film, and not laser etched directly onto marine grade steel.

## 1.9 Table of studies

Micro-textured surfaces have been recently emerging as a protection against fouling. These studies have been categorised and reported in Table 1.5. There are many factors such as substratum type, texturing method, and fouling organism which cause differences between these studies, however, all show the general trend that micro-textures can be used to reduce fouling.

Table 1.5 Table of micro-textured antifouling studies

Substratum	Method of texturing	Fouling organism	Species	Micro-textures reduce biofouling	Lab or Field	Bio-mimetic	Based on	Features	Reference
PDMS	photolithographic techniques	Zoospores	<i>Ulva linza</i>	Yes	Lab	No	straight lines	single	Hoipkemeier-Wilson <i>et al.</i> , (2004)
PDMS	photolithographic techniques	Cyprid	<i>B. amphitrite</i>	Yes	Lab	Yes	Sharklet	single	Schumacher <i>et al.</i> , (2007)
PDMS	photolithographic techniques	Bacteria	<i>Staphylococcus aureus</i>	Yes	Lab	Yes	Sharklet	single	Chung <i>et al.</i> , (2007)
PDMS	photolithographic techniques	Zoospores	<i>Ulva</i>	Yes	Lab	Yes	Sharklet and others	Multi	Schumacher <i>et al.</i> , (2007)
PDMS	photolithographic techniques	Zoospores	<i>Ulva linza</i>	Yes*	Lab	Yes	Sharklet	Single	Carman <i>et al.</i> , (2006)
PDMS	photolithographic techniques	Diatom	<i>Amphora coffeaeformis</i>	Yes	Lab	Yes	Crab	single	Brzozowska <i>et al.</i> , (2014)
		Cyprid	<i>Amphibalanus amphitrite</i>	Yes	Lab	Yes	Crab	single	Brzozowska <i>et al.</i> , (2014)
PDMS	photolithographic techniques	Tube Worms	Unknown	Yes	Field	Yes	<b>Crab</b>	single	Brzozowska <i>et al.</i> , (2014)
PDMS	photolithographic techniques	Diatoms	Mixture	No	Field	No	targeted to diatoms	Multi	Sullivan <i>et al.</i> , (2017)
PDMS	photolithographic techniques	Zoospores	<i>Ulva linza</i>	Yes	Lab	Yes	Sharklet	single	Schumacher <i>et al.</i> , (2008)
PDMS	photolithographic techniques	Zoospores	<i>Ulva</i>	Yes	Lab	Yes	Sharklet	single	Schumacher <i>et al.</i> , (2007)
PDMS	photolithographic techniques	Bacteria	<i>C. marina</i>	Yes	Lab	Yes	Sharklet triangles and pillars	multi	Magin <i>et al.</i> , (2010)
PDMS	photolithographic techniques	Diatoms	<i>Navicular incerta</i>	Yes	Lab	Yes	Sharklet	Single	Long (2009)
PDMS	wrinkled surface topographies	Zoospores	<i>Ulva linza</i>	Yes*	Lab	No		Multi	Efimenko <i>et al.</i> , (2009)
PDMS	wrinkled surface topographies	Diatoms	unknown	Yes	Field	No		Multi	Efimenko <i>et al.</i> , (2009)
Epoxy resin	Cast directly off marine organism	Range of species**	Range of species**	Yes	Field	Yes	Range of species	single	Bers and Wahl (2004)
Epoxy resin	Cast directly off marine organism	Range of species		Yes	Field	Yes	Mussel	single	Scardino and R. de Nys (2004)
PDMS	Cast directly off marine organism	Diatoms	<i>Closterium</i> and <i>Navicula</i>	Yes	Lab	Yes	lotus leaf, crab shell	Single	Chen <i>et al.</i> , (2015)
Stainless Steel (4N)	Electro-polishing	Bacteria	<i>S. aureus</i> and <i>P. aeruginosa</i>	Yes	Lab	No		Single	Wu <i>et al.</i> , (2018)
PDMS	Laser ablation	Diatoms	<i>N. paleacea</i> , <i>N. jeffreyi</i> , <i>Amphora sp. F. carpentariae</i>	Yes	Lab	Yes	Mussel	single	Scardino <i>et al.</i> , (2006)
PET	Laser ablation	Osteoprogenitor cells		Yes	Lab	No		single	Duncan <i>et al.</i> , (2002)
Polycarbonate	Laser ablation	Diatoms, algae	<i>Amphora sp.</i> , <i>Ulva rigida</i> , <i>Hydroides elegans</i>	Yes	Lab	No		Single	Scardino <i>et al.</i> , (2006)
		Tube Worm	<i>Centroceras clavulatum</i> , <i>Bugula neritina</i>						
		Tube Worm							
		Bryozoa							
Titanium alloy	Laser ablation	Bacteria	<i>S. aureus</i>	Yes	Lab	No		Single	Cunha <i>et al.</i> , (2016)
Chitosan	Laser ablation	OLN 93 cell line	oligodendroglia cell	Yes	Lab	Yes	Sponge	Single	Rusen <i>et al.</i> , (2014)
Stainless Steel	Laser ablation and coating	Unknown		Yes	Field	No		Single	Sun <i>et al.</i> , (2018)

## Chapter 2 Aims

The aim of this study is to develop a biomimetic pattern using laser surface texturing directly onto marine grade steel that has antifouling properties. The biomimetic pattern will be inspired by investigating the marine surfaces found in the natural world such as on crab and shell surfaces. The topography will combine features found on natural surfaces that protect against fouling in the natural marine environments.

### 2.1 Objectives

- Evaluate if laser surface texturing can be used as a potential antifouling method [Chapter 4].
- Evaluate micro-topographical structures found in nature [Chapter 5].
- Artificially mimic these patterns using lasers on metal surfaces to create single feature biomimetic surfaces [Chapter 5].
- Test single feature surfaces in field experiments and statistically evaluate results to find the best pattern(s) [Chapter 5].
- Combine features of best patterns to increase antifouling potential to create new multi- feature and multi-scale antifouling surface textures [Chapter 6].
- Test these new multi- feature and multi-scale antifouling surfaces in field experiments and statistically evaluate results to find the best pattern(s) [Chapter 6].

### 2.2 Justification

As outlined in the literature review, biofouling is a costly problem for the maritime industries, and previous antifouling methods have had negative effects on marine life, and the health of our oceans. With ongoing bans of toxic chemicals, there is high demand in the antifouling industry for a non-toxic, eco-friendly, antifouling method. This project has the potential to fill the gap in the antifouling market.

Previous studies on laser textured surfaces have shown that the surface topography has the ability to alter the settlement of cells (Rusen *et al.*, 2014; Cunha *et al.*, 2016; Sun *et al.*, 2018). It is shown in the literature review, that the biofilm layer which is made up of individual algae cells and bacteria is important in the succession of fouling (Wahl, 1989. Chambers *et al.*, 2006). This study is to determine if laser textured micro-topographies are able to have an antifouling effect in the marine environment. Other research has shown that micro-topographies created on polymer substratums have limited settlement of marine fouling species under lab conditions (Hoipkemeier-Wilson *et al.*, 2004; Schumacher *et al.*, 2007; Carman *et al.*, 2006; see Table 1.5). This study is taking a real world approach and is testing the steel directly in the marine environment rather than in a lab setting.

This study is building upon knowledge of laser surface texturing, the interactions between surface characteristic and cells, and exploiting the ever growing demand in the anti-fouling market for a eco-friendly solution to fouling.

### 2.3 Novelty

The novelty within this study lies within various parts:

- (1) Fabrication of surfaces: laser surface texturing has been widely used, but not for testing for antifouling potential directly in the marine environment.
- (2) The marine species investigated for biomimetic purposes
- (3) The laser textured patterns produced are novel
- (4) Field testing – very few biomimetic surfaces were tested in the field and not limited to one species.

## Chapter 3 Methods

### 3.1 Equipment used

Throughout this project, there are key pieces of equipment used regularly. This equipment is detailed in this section.

Table 3.1 Key equipment

Equipment	Function
White light interferometer (BRUKER Contour GT)	<ul style="list-style-type: none"><li>• Creates 3D scans of surfaces</li><li>• Has smaller field of view than topographical microscope</li><li>• Finer detail than topographical microscope</li><li>• Best used for flat surfaces</li></ul>
Fringe projection Topographical Microscope (GFM MikroCAD Premium 1.6x1.2 (now LMI Technologies Inc.))	<ul style="list-style-type: none"><li>• Creates 3D scans of surfaces.</li><li>• Has a larger field of view than White light interferometer, therefore easier to use when scanning shells and curved objects.</li></ul>
Laser System	<ul style="list-style-type: none"><li>• SPI G3 ns pulsed infra-red fibre laser<ul style="list-style-type: none"><li>○ 20W average power</li><li>○ 1064nm wavelength</li></ul></li><li>• Lino Beam Expanding Telescope</li><li>• GSI Lightning Galvanometer scanning head with Linos 100mm focal length f-theta lens giving a 60x60 mm working area</li></ul>
ZEISS microscope (for surface photos)	<ul style="list-style-type: none"><li>• Zeiss x200 lenses</li><li>• With camera.</li></ul>
Keyence microscope (for surface photos)	<ul style="list-style-type: none"><li>• VHX-5000</li></ul>
ZEISS microscope (for diatom species analysis)	<ul style="list-style-type: none"><li>• Zeiss Axio Imager. A2</li><li>• With DIC (Differential Interference Contrast) and plan apochromat lenses</li></ul>

### 3.2 Creating surfaces

Micro-textured surfaces were created by laser texturing 50x50 mm marine grade stainless steel coupons (316L) using the SPI Fibre laser. There are a number of parameters that control the laser texturing parameters. These parameters are set both in the laser control and the galvanometer scanning software:

Table 3.2 Laser parameters

Parameter	Units	Function
Hatch spacing (Galvo)	μm	The space between the parallel laser tracks that are used to fill an area. This parallel hatch spacing can be used to create texture patterns
Hatch Angle (Galvo)	°	The angle of the hatch lines to the X axis of the galvanometer system
Speed (Galvo)	mm/s	The speed of the focussed laser spot across the surface. This controls how the individual pulsed laser spots are spread out along the track. Faster speeds allow for individual laser spots to not overlap.
% Power (Laser)	%	The laser is a 20W average laser maximum, and the percentage power controls the overall average power produced. When used at 100% 20W are delivered, and at 50% 10W.
Frequency (Laser)	kHz	The repetition rate of the laser pulses generated. Normally 25kHz or higher
Pulse length (Waveform) (Laser)	ns	The temporal length of each laser pulse, measured in ns. The SPI laser have a set menu of “waveforms” giving different pulse lengths, e.g. Waveform 0 has a nominal pulse length of 200ns. This is the longest pulse length delivered by the SPI laser used.
Passes (Galvo)	n/a	The number of passes of the laser over the surface

Various different parameters can be altered to create different micro-textured patterns. Overall, the micro-textured are created by the laser moving across the surface on a programmed route, an example is shown in Figure 3.1.

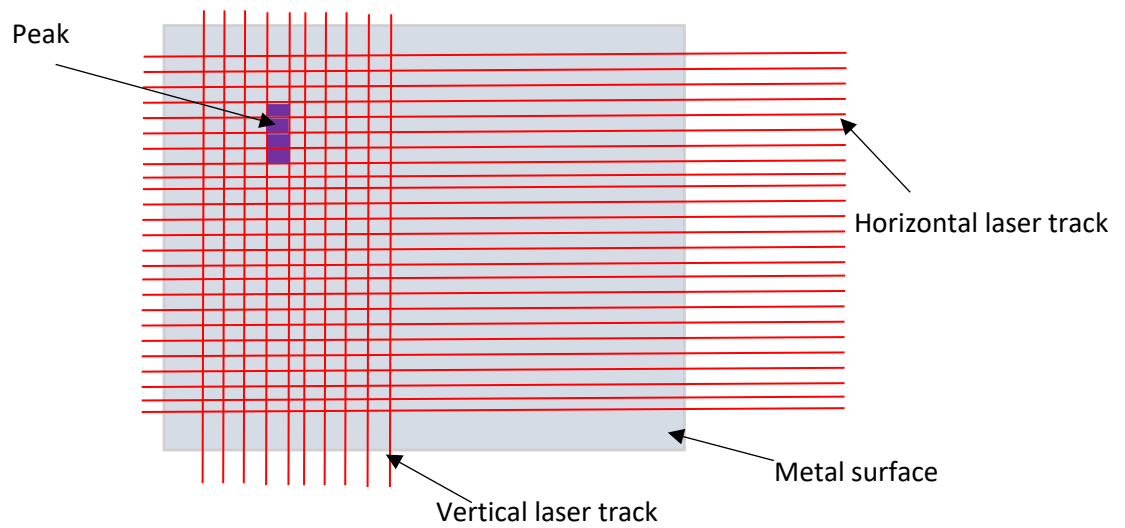


Figure 3.1 An example of how peaks are formed using cross hatch laser parameters.

To create different patterns the different laser parameters indicated in table 3.2 were altered. All of these parameters are recorded for each pattern and are shown within the individual methods chapters.

### 3.3 Laser set up

The laser source employed for the laser texturing is a SPI Lasers G3 20W nS pulsed fibre laser operating at a wavelength of 1064nm. The laser beam is delivered by fibre optic to a beam expanding telescope (LINOS) where the beam is collimated to fill the 10mm diameter input aperture of a GSI LDS-10 Lightning galvanometer scanning head fitted with a Qioptiq (Linos) Ronar 100mm f-theta focussing lens. This gives a 25 $\mu$ m focal spot diameter in the focal plane and a working field of 60mm x 60mm. The galvanometer scanning head is controlled using SCAPS Samlight software. The laser texturing is performed by tracing the laser beam along a programmed vector paths, typically a hatched square of size to match the sample coupons. The software controls the laser spot traverse speed (mm/s) and the spacing of the hatch lines ( $\mu$ m) and the number of overall passes applied to the surface. The SPI Laser parameters are controlled from a PC using a USB serial

link. Parameters set are the % average power (W), the pulse repetition frequency (kHz) and the nominal pulse length (nS). They were created using a pulsed laser beam controlled by a galvanometer which used a X-Y axis mirrors to reflect the laser beam (Figure 3.2).

*Figure 3.2 Schematic diagram of a laser set-up for direct laser patterning moveable focussed laser beam controlled by a mirror galvanometer (Tzu Goh, 2014).*

### 3.4 Testing of surfaces for antifouling potential

Once the 50x50mm textured surface was created, they were tested in the field for antifouling properties. The surfaces were submerged for 7 days (actual dates in chapter methods).

#### 3.4.1 Field site

The field site used for testing the surfaces is based in the Albert Dock, Liverpool (53°24'1.08" N -2°59'33.72" W; Figure 3.3). The field site was a semi-enclosed marine water body, that had previous been restored as it is no longer used for commercial shipping (Geist and Hawkins, 2016). Lake and reservoir restoration techniques were successfully used in deeper dock basins, such as the use of Helixor air lift pumps which pumps de-stratified the dock and prevented build up of an anoxic layer (Russell *et al.*, 1983; Allen *et*

*al.*, 1992; Allen and Hawkins, 1993a, 1993b; Wilkinson *et al.*, 1996). Prior to the restoration, the water body had suffered with eutrophication, and therefore an anoxic zone which was caused by dense phytoplankton blooms in the nutrient-rich surface layer (Geist and Hawkins, 2016). The water body is 27ppm, and this environment enabled a dense settlement of filter feeders such as mussels to natural settle in the dock (Hawkins *et al.*, 1992). To the present day, the mussels provide an ecosystem service for the Royal Albert Docks as they act as a bio-filtration system, as it has been estimated that the whole water body volume is filtered through mussels every 12 days (Geist and Hawkins, 2016). This has led to a thriving marine assemblage present in the docks, and the water body is now safe under EU bathing regulations (Geist and Hawkins, 2016). Migratory sea trout, *Salmo trutta*, have returned to the Dock areas, due to the cleaner waters and thriving ecosystem (Hawkins *et al.*, 1999b).

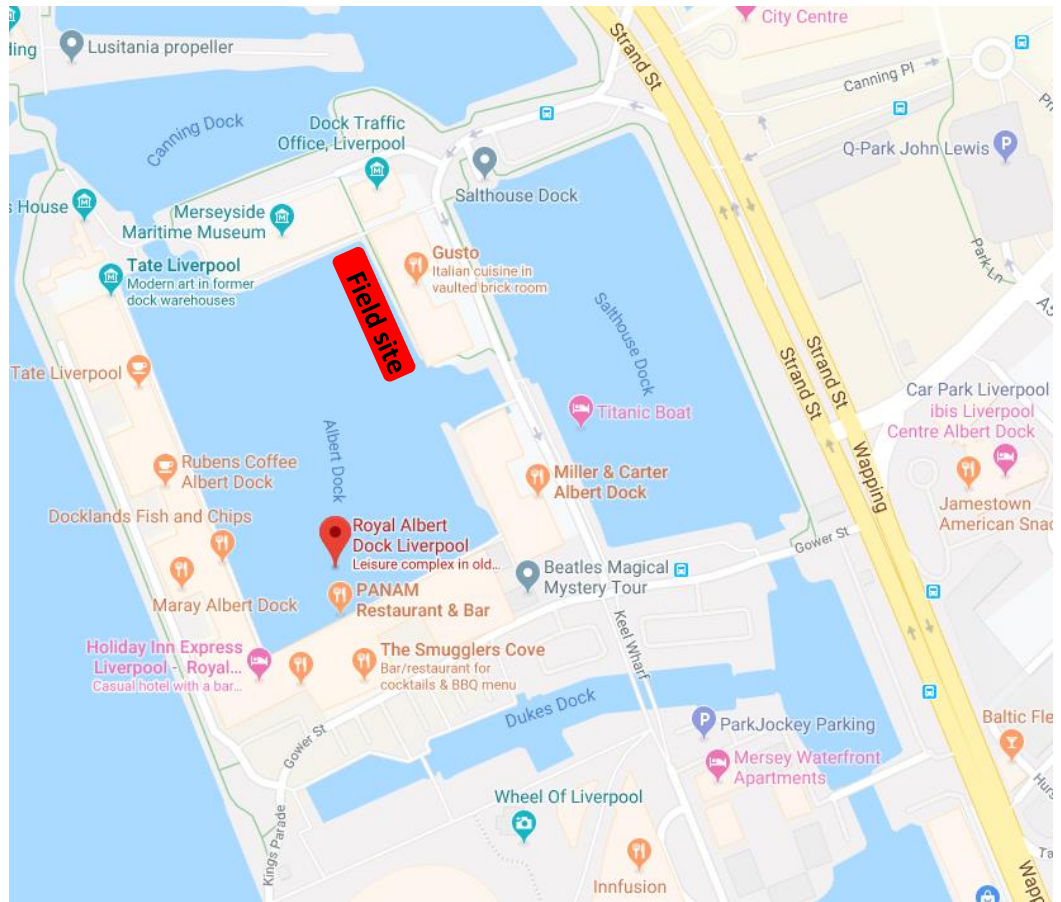


Figure 3.3 Field site

### 3.4.2 Experimental set up

Each micro-textured pattern has 5 replicates, and the control with 5 replicates were submerged using a randomised block design method (Hurlbert, 1984). Each pattern was attached to a larger 20x20 PVC panel (block) using Velcro™. Each block contained one replicate of each pattern and one replicate of the control (figure 3.4). The positioning of each pattern within the block was randomised. The blocks were part of a larger frame which was made out of ABS piping (RS). The frame was immersed at a depth of 1 metre at the study site for approximately one week (exact dates, see experimental chapters). Biofilm growth rate is highest in the euphotic zone as abiotic factors such as light availability, and temperature effect the growth and presence of biofilm species (Patrick, 1971; Pyne, Fletcher and Jones, 1986b; Munda, 2005; Yang *et al.*, 2015).

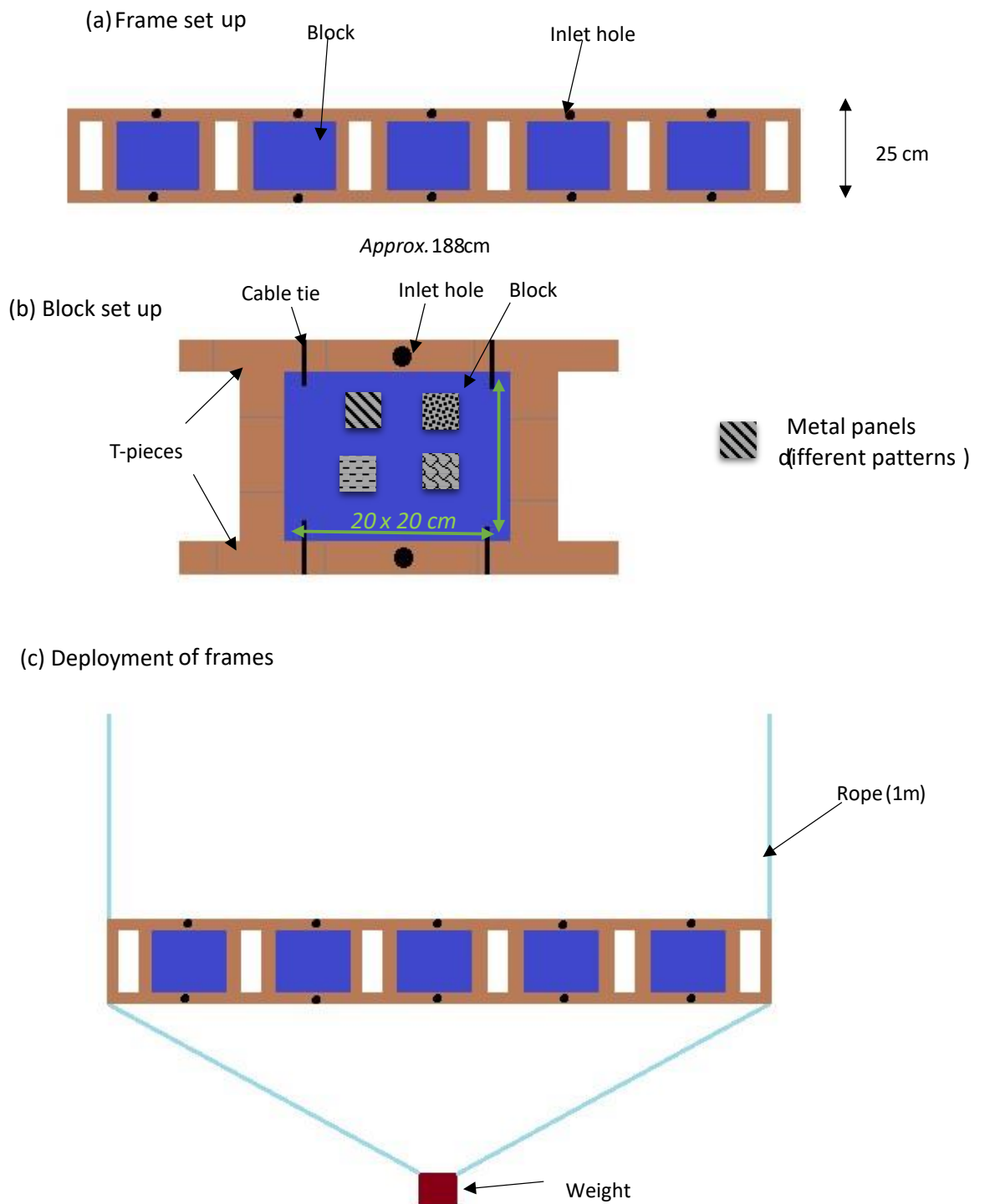


Figure 3.4 Experimental set-up shown as (a) frame set up, (b) block set up and (c) deployment of the frame. The total length of the frame is 188cm. Blue squares: PVC panel (20x20 cm) attached using cable ties (black lines), thick brown line: ABS piping plus 90° bends and T-pieces pieces [Source: Dr S. Dürr].

### 3.5 Data collection

Once removed from the field site and preserved in 70% ethanol, surfaces were analysed using microscope techniques. A Zeiss AX10 microscope at x50 magnification was used on the single pass experiments, a Zeiss / Keyence microscope was used on the combined pass experiments; however, methods are the same.

Firstly, the surface was transferred into a petri dish lid with low sides so that the surface can still be fully submerged but can fit under the microscope.

Due to changes in species' distributions near habitat edges (Ries and Sisk, 2004), photographs are taken of the inner 20x20mm square (Figure 2.5). The field of view of both cameras was 1600  $\mu\text{m}$  by 1300  $\mu\text{m}$ .

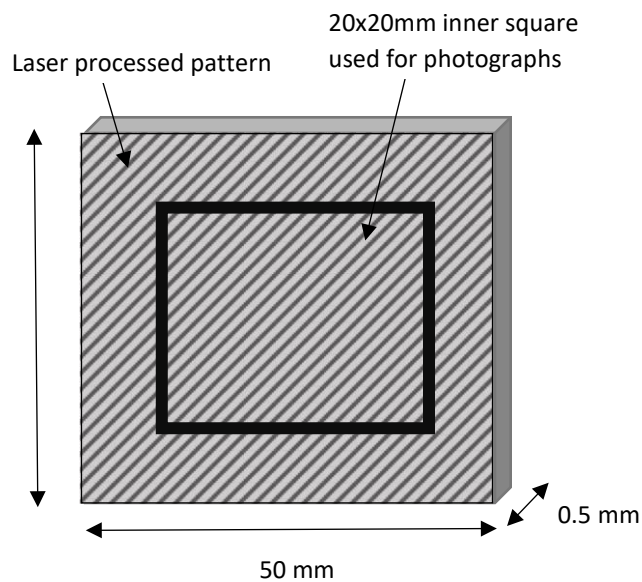


*Figure 3.5 A schematic illustration of the photo taking process for data collection.*

The 20 x 20mm inner square was broken down into 195 consecutive photos. The 15mm border surrounding the 20 x 20mm inner square was not

used in the image capture process and was there to buffer any edge effects that may occur, so that edge effects are not included in the analysis.

### 3.5.1 Biofilm settlement

For every panel there are 195 photographs, numbered 1 to 195 (.JPEG for chapter 5, .TIF for chapter 6 files). Random number tables (RAND, 2001) were used to select 50 photos randomly from the 195 (method is based on (Butler *et al.*, 2010)). Images were analysed in imageJ (Rasband, 2007) where the number of individuals settled on the surface were counted manually. An individual is defined as a biological structured shape, this could include colonies of bacteria. However, amorphous shapes were not counted.

### 3.5.2 Biofilm position on patterns

Where the pattern permits, the total number of individuals counted was separated into three categories depending on their position within the pattern. Position 1 is recorded when the individual settled solely on the laser feature, position 2 is recorded when the individual settled on the unprocessed area between the laser features and position 3 was recorded when the individual is settling next too but not on top of a laser processed feature (Figure 3.6).

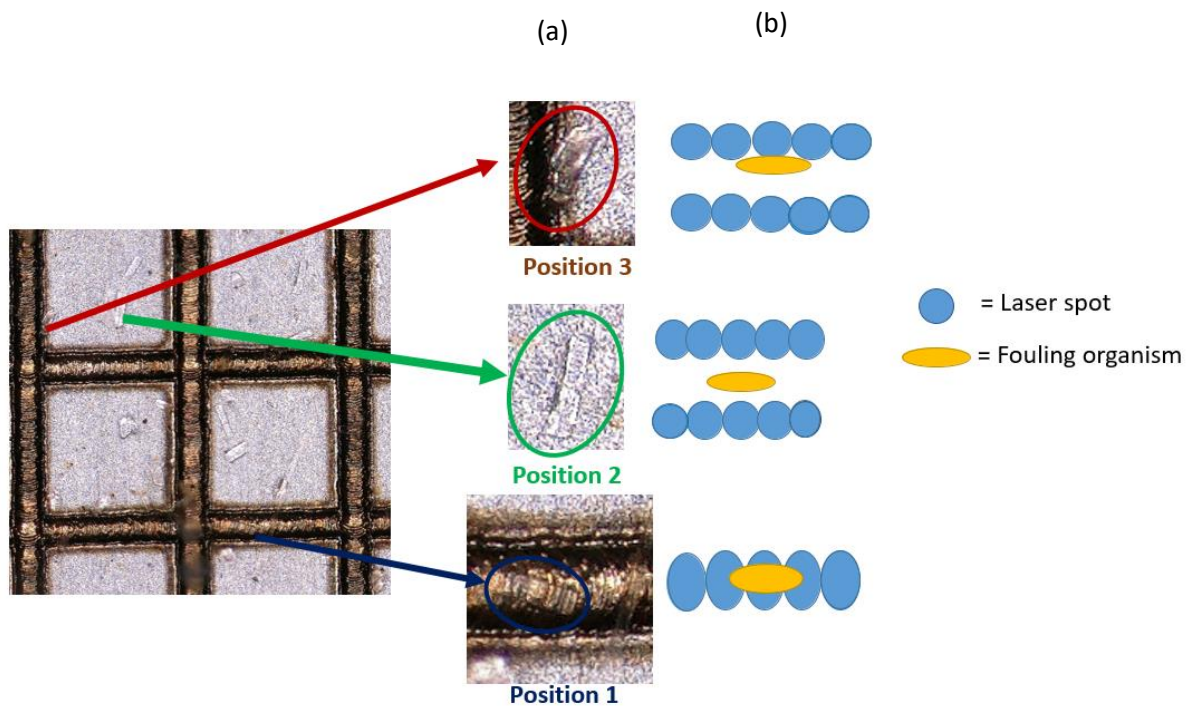


Figure 3.6 (a) real microscope images and (b) schematic illustration of the position of marine fouling organisms according to three different categories used for data collection.

### 3.5.3 Statistical analysis

A one factor ANOVA (Field, 2013) was carried out in SPSS (Version 26, IBM) to determine if block design was having an effect on the settlement results. No significant differences in settlement between blocks was found for any of the experiments within this thesis ( $p > 0.05$ ; full test reported in results section for each chapter), so blocks were ignored in further statistical analysis. Data was tested for normality using Shapiro-Wilk test (Field, 2013) and homogeneity using Levene's test (Field, 2013). Depending on the outcome of those tests, a one factor ANOVA (Field, 2013) or Kruskal Wallis (Field, 2013) test was carried out in SPSS (Version 26, IBM) on the number of individuals settled on each pattern to determine their antifouling potential. This was followed by a post hoc Dunnett's test to determine if certain patterns worked better than others. Level of significance was always

5%. Dunnett's t (2 sided) was also used when no significant differences were found post hoc, but there was a clear difference between control and all other patterns ( $p < 0.05$ ).

PRIMER-e (Quest Research Limited) one factor PERMANOVA (Anderson and Walsh, 2013) was used to analyse the three positions within the settlement data to determine if there was a significant difference in the position of settlement between patterns. Post hoc pairwise tests were used to compare between patterns. Level of significance was 5%. Analysis of similarity (SIMPER; Clarke 1993) was also performed on the position data to identify the position that is most responsible for the dissimilarity in settlement between patterns. Kruskal Wallis (Field, 2013) test was carried out in SPSS (Version 26, IBM) on the position data to determine if significantly more settlement occurred in a given position on a pattern. This was followed by a post hoc Dunnett's test to determine if certain patterns had more settlement in one position than other patterns.

## Chapter 4 : An Investigation Into The Use Of Nanosecond Laser Surface Texturing Of Stainless Steel (316L) As A Method To Reduce The Settlement Of Marine Biofilm.

### 4.1 Introduction

The concerns with traditional antifouling methods have led to a search for alternative solutions. Recently there has been focus on the use of micro-textures to control cell settlement (Cunha *et al.*, 2016b; Scardino *et al.*, 2008). Micro-textures have been found to reduce settlement of bacteria and it has shown potential for antifouling applications within the medical field was a way to eliminate the use of extra chemicals used on implants to combat bacterial biofouling (Cunha *et al.*, 2016b). Micro-textured silicone polydimethylsiloxane elastomer (PDMSe) by photolithography techniques has also been tested for antifouling of marine biofilm species in lab based assays (Section 1.9, table 1.5; Schumacher *et al.*, 2007; Hoipkemeier-Wilson *et al.*, 2004; Carman *et al.*, 2006; Brzozowska *et al.*, 2014). It has been found that micro-textures reduce settlement of a range of marine species such as marine alga *Ulva* (Schumacher *et al.*, 2007b), marine bacterium *Cobetia marina* (Magin *et al.*, 2010) marine diatom *Amphora* (Vucko *et al.*, 2014) and cyprids of barnacle *Amphibalanus reticulatus* (Vucko *et al.*, 2014). Mostly, the testing of micro-textured PDMSe and other micro-textured substrates has been limited to lab based assays, however, two studies have report a successful trial of micro-textured PDMSe for antifouling properties when static testing in-situ (Sullivan and Regan, 2017, Vucko *et al.*, 2014).

The creation of micro textures have been done in lots of different way, such as photolithography (Schumacher *et al.*, 2007), laser surface texturing (Cunha *et al.*, 2016b), hot embossing (Bixler *et al.*, 2014), sand blasting (Arnold and Bailey, 2000), sanding and electro-polishing (Wu *et al.*, 2018). The substrate being used will help determine which

micro-texturing method is used, as process such as photolithography are limited by substrate type.

The use of lasers in surface texturing allow for controllability and reproducibility of surface topography by allowing for precise control of parameters such as the number of times the laser passes the surface, and the hatch spacing between the laser tracks. For metal substrates, laser surface texturing has shown to have antifouling effects on biofilm using substrates such as titanium (Cunha *et al.*, 2016). Laser surface texturing has also been shown to have antifouling effects on graphene (Singh *et al.*, 2017). However, the marine studies tend to focus on the use of PDMS as a substrate, as it is known to have foul release properties (Chaudhury *et al.*, 2005, Brady Jr and Singer, 2000). However, there is emerging concern around using silicone based antifouling methods as it has been found that unbound silicone oils may leach out and have negative impacts on the marine environment, as they can be fatal to a range of marine organisms (Nendza, 2007). Surprisingly, there has been little interest in the direct texturing of metal for the marine environment, although this could be useful for maritime industry as are many places where exposed metal could be fouled such as infrastructure associated with aquaculture (De Nys and Guenther, 2009), water pipelines from desalination and power plants (Henderson, 2010) and oil and gas platforms (Page *et al.*, 2010). Direct texturing of metal surface for antifouling may be useful is within marine research as science installation features such as moorings and optical sensors have exposed metal surface prone to fouling. In fact, biofouling is one of the main limiting factor in deployment of short term monitoring equipment in oceanographic studies as the fouling effects measurement accuracy of devices (Manov *et al.*, 2004).

Therefore, the aim of this study was to determine the effect of laser surface micro-texturing of metal as anti-fouling on biofilm settlement under alteration of surface properties (contact angle, roughness, laser passes and hatching).

## 4.2 Materials and methods

### 4.2.1 Laser surface texturing

The laser source employed for the laser texturing is a SPI Lasers G3 20W nS pulsed fibre laser operating at a wavelength of 1064nm (as described in section 3.3).

Based on this experimental setup the following treatments were undertaken:

#### *(a) Number of passes treatment*

For this treatment, a simple one dimensional hatch path was programmed to cover the coupon. The spacing between the hatch lines were fixed at 100  $\mu\text{m}$ . The speed was fixed at 3200mm/s, the power was fixed at 75% power (15 Watts), the pulse repetition frequency was 25 kHz and the pulselengths fixed at 200nS. The experiment was designed to test the effect of applying different numbers of passes of the laser path on the coupon surfaces on the resulting antifouling effect. All the other parameters for the laser processing were held constant, except the different number of passes that were altered to 1 pass, 10 passes, 50 passes and 100 passes of the laser path.

#### *(b) Hatch spacing treatment*

For this treatment, a simple cross hatch path was programmed to cover the coupon. The spacing between the hatch lines was altered as this experiment was designed to test the effect of differing hatch distances of the laser path on production of surfaces for an antifouling effect. All the parameters for the laser processing were constant, except the difference between hatch line spacing. A single pass was used. The speed was fixed at 500mm/s, the power was fixed at 70% power (14 Watts) and the frequency and

pulselength were fixed at 25khz and 200ns, respectively. Three different hatch line spacing were produced at 250 $\mu\text{m}$  , 500 $\mu\text{m}$  and 750 $\mu\text{m}$  spacing. These were repeated at a 90° angle to create a cross hatch laser path.

#### 4.2.2 Contact angle measurement

To determine the contact angle for each surface, a static sessile drop approach is used with an KSV CAM101 contact angle goniometer was used to measure advancing contact angles. The sessile drop method is a standard approach in measuring contact angle (Drelich, 2013) and has been used on various metal materials (Schuster *et al.*, 2015, Prajitno *et al.*, 2016). The surfaces in this study were placed on a flat platform where a light source and a camera are focused, then the drop was released and the camera took several hundred images of the projected surface as a droplet was placed upon it. Replicates were taken on clean un-wetted sections of the surface (typically 3-5 measurements). The sessile drop method was used with a constant droplet volume of distilled water (RS PRO 5 L Jerrycan Deionized Water).

#### 4.2.3 Roughness (Sa) measurement

Roughness may be an important factor influencing marine biofouling, therefore each laser processed sample were evaluated using white light interferometric microscopy (Bruker Contour-GT white light interferometer with lateral resolution of 0.26 $\mu\text{m}$  and RMS repeatability of 0.02nm). The areal roughness (Sa) was calculated using Bruker Contour-GT software from 3D scans of the surface at x2.5 magnification (for hatch spacing) and x10 (for number of passes). The Sa is the extension of Ra (arithmetical mean height of a line) to a surface, which has been used in previous antifouling studies (Scardino *et al.*, 2009). Ra has been a traditional measure of surface and was generally measured using a stylus devised

that would travel over a short straight line on the surface, whereas an instrument like the Bruker is making using the topography measured over a surface area.

#### 4.2.4 In-situ testing for marine biofilm

These were immersed in the test site at the Royal Albert Dock, Liverpool as described in section 3.4.1. For further details on antifouling testing see section 3.4 (3.4.1 for study site and 3.4.2 for experimental set up).

*Table 4.1 Exact dates of experiments*

Experiment	Date submerged	Date removed
Passes treatment	05.07.2017	23.10.2017
Hatch Treatment	23.10.2017	30.10.2017

#### 4.2.5 Data collection

Data was collected as outlined in section 3.5 (3.5.1 biofilm settlement, 3.5.2 Biofilm position on patterns).

#### 4.2.7 Statistical analysis

Data were analysed as outlined in section 3.5.2 . Statistical analysis of the data collected was carried out in IBM SPSS Software. Regressions of various curve shapes were used to find the best fit for the roughness, contact angle and settlement data. For the hatch treatment, zero hatch control data was omitted from the regression as a hatch of zero would just create a single line, rather than no laser processing at all (i.e. a control panel). For the topography data, a Kruskal Wallis test was carried used to test for significant difference between marine biofilm settlement on hatch spacing patterns. A one-way ANOVA was used to test for significant difference between marine biofilm settlement on the topographies produced by the number of passes treatment. Post hoc Dunnett's T3 test was also used on all experiments.

### 4.3 Results

There was not a significant difference in settlement between blocks for both the number of passes experiment ( $F_{(4,23)}=0.295$ ,  $p=0.878$ ), and the hatch spacing experiment ( $F_{(4,23)}=0.142$ ,  $p=0.972$ ), therefore blocks were ignored in further statistical testing.

#### 4.3.1 Effect of Laser Parameters on Surface

##### 4.3.1.1 Topography

3D topographic scans were taken of the laser-processed surfaces using white light interferometry (Bruker) for the number of passes treatment (Figure 4.1) and the hatch spacing treatment (Figure 4.3). Measurements for maximum depth (the lowest point of a surface below original surface) and maximum peak (the highest point of a surface below original surface) were taken for each pattern from the 3D topographic scans.

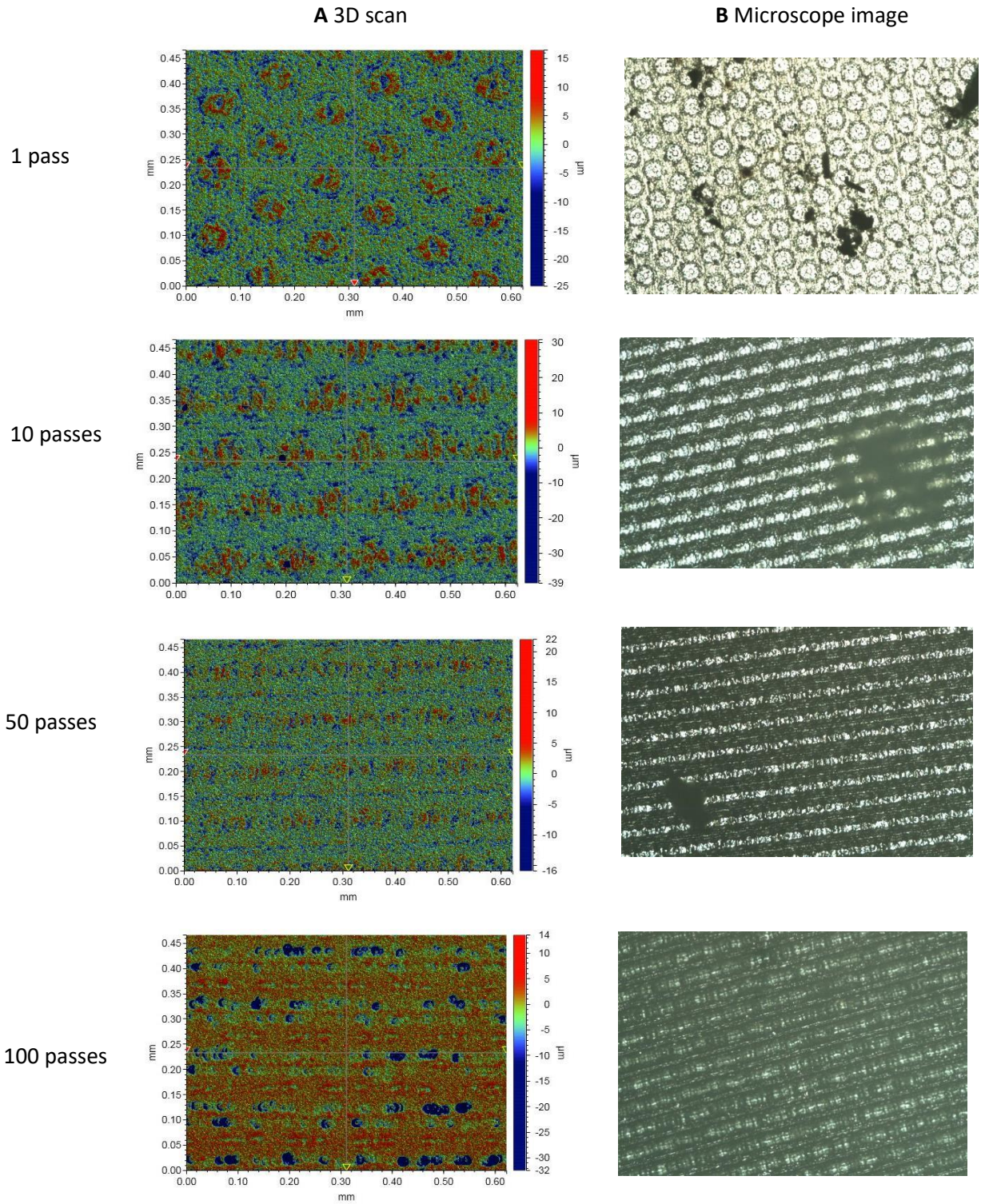


Figure 4.1 Scans of laser textures surfaces for number of passes treatment using (A) White light interferometer scans before submersion and (B) Zeiss AX10 microscope image after submersion.

As the number of passes increases the clarity of the pits seen in Figure 4. 1 was reduced. The circular peaks pattern created by 1 pass, becomes less clear at 10 passes, and then by 100 passes the distinct pattern is no longer visible.

There was a significant relationship between the number of laser passes and depth of pattern ( $F_{(1,12)}=5.505$ ,  $p=0.039$ ). The  $R^2$  value was 0.334 therefore, about 33.4% of the variation in the depth data is explained by number of passes. There was a positive but mild relationship between number of laser passes and depth of pattern (Figure 4.2a).

There was not significant relationship between the number of laser passes and peaks of pattern ( $F_{(1,12)}=0.125$ ,  $p=0.73$ ; Figure 4.2b). This was also not significant when tested without the control (0 passes of the laser,  $F_{(1,8)}=4.26$ ,  $p=0.79$ ).

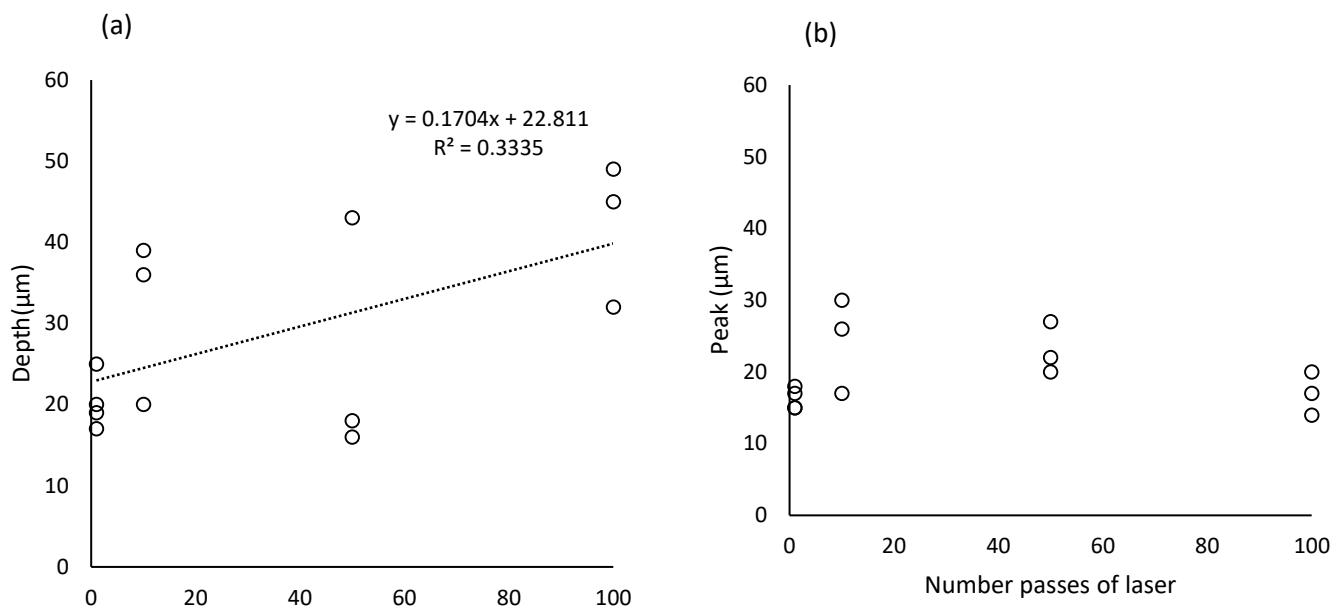


Figure 4. 2 The relationship between the number of passes of the laser and (a) depth of the surface topography and (b) peaks of the surface topography.

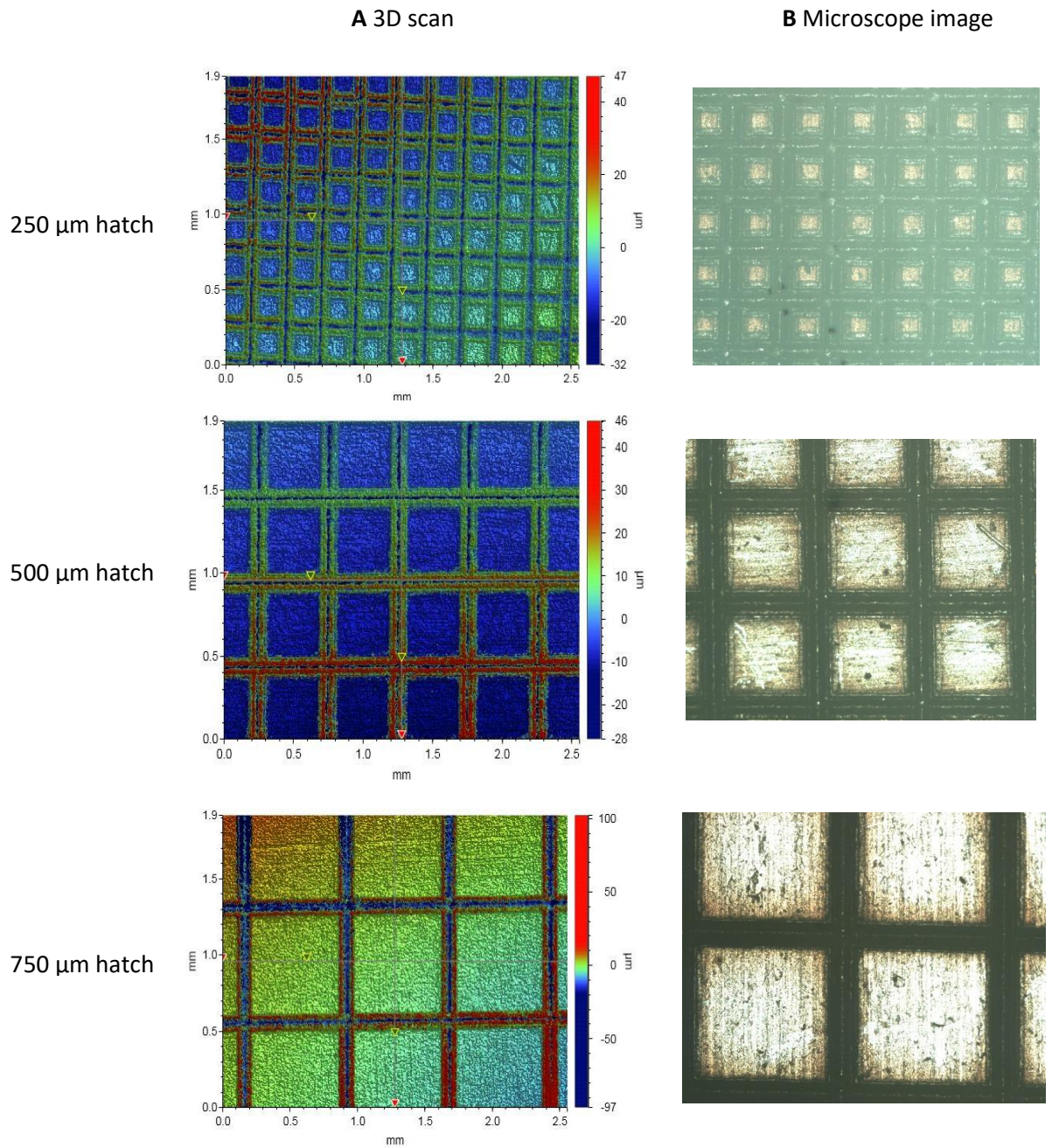


Figure 4.3 Scans of laser textures surfaces for hatch spacing treatment using (A) White light interferometer scans before submersion and (B) Zeiss AX10 microscope image after submersion.

As the hatch spacing increases there is more free space and unprocessed metal material in between the hatch lines (Figure 4.3).

#### 4.3.1.2 Contact angle and Roughness

There was a significant relationship between the number of laser passes and roughness ( $F_{(2,22)}=20.791$ ,  $p < 0.001$ ). The  $R^2$  value was 0.634 therefore, 63.4 % of the variation in the roughness data is explained by number of passes. There is a strong positive relationship between number of laser passes and roughness (Figure 4.4a). The regression equation may not be useful for making predictions since the value of  $r^2$  is mid range.

There was a significant relationship between the hatch spacing and roughness ( $F_{(2,22)}=14.62$ ,  $p=0.001$ ). The  $R^2$  value was 0.709 therefore, about 71% of the variation in the contact roughness data is explained by hatch spacing. There is a positive strong relationship between hatch spacing and roughness until around 500um and then the relationship peaks and becomes a strong negative relationship between hatch spacing and roughness (Figure 4.4b). The regression equation may be useful for making predictions since the value of  $r^2$  is close to 1.

There was a significant relationship between the number of laser passes and contact angle ( $F_{(2,22)}=9.676$ ,  $p=0.001$ ). The  $R^2$  value was 0.468 therefore, about 46.8% of the variation in the contact angle data is explained by number of passes. There was a positive but mild relationship between number of laser passes and contact angle (Figure 4.4c). The regression equation may not be useful for making predictions since the value of  $r^2$  is mid range.

There was a significant relationship between hatch spacing and contact angle ( $F_{(1,14)}= 42.076$ ,  $p<0.001$ ; Figure 4.4d). The  $R^2$  value was 0.808 therefore, 80.8 % of the variation in the contact angle data is explained by hatch spacing. There is a positive and strongly increasing relationship between hatch spacing and contact angle.

There was a significant relationship between the roughness and contact angle for the number of passes treatment ( $F_{(1,23)}=51.038$ ,  $p<0.001$ ). The  $R^2$  value was 0.699 therefore, 69.9% of the variation in the contact angle data by roughness. There is a positive strong relationship between contact angle and roughness (Figure 4.4e). The regression equation may be useful for making predictions since the value of  $r^2$  is close to 1.

There was not a significant relationship between the roughness and contact angle for the hatch spacing treatment ( $F_{(1,11)}=3.845$ ,  $p=0.078$ ; Figure 4.4f).

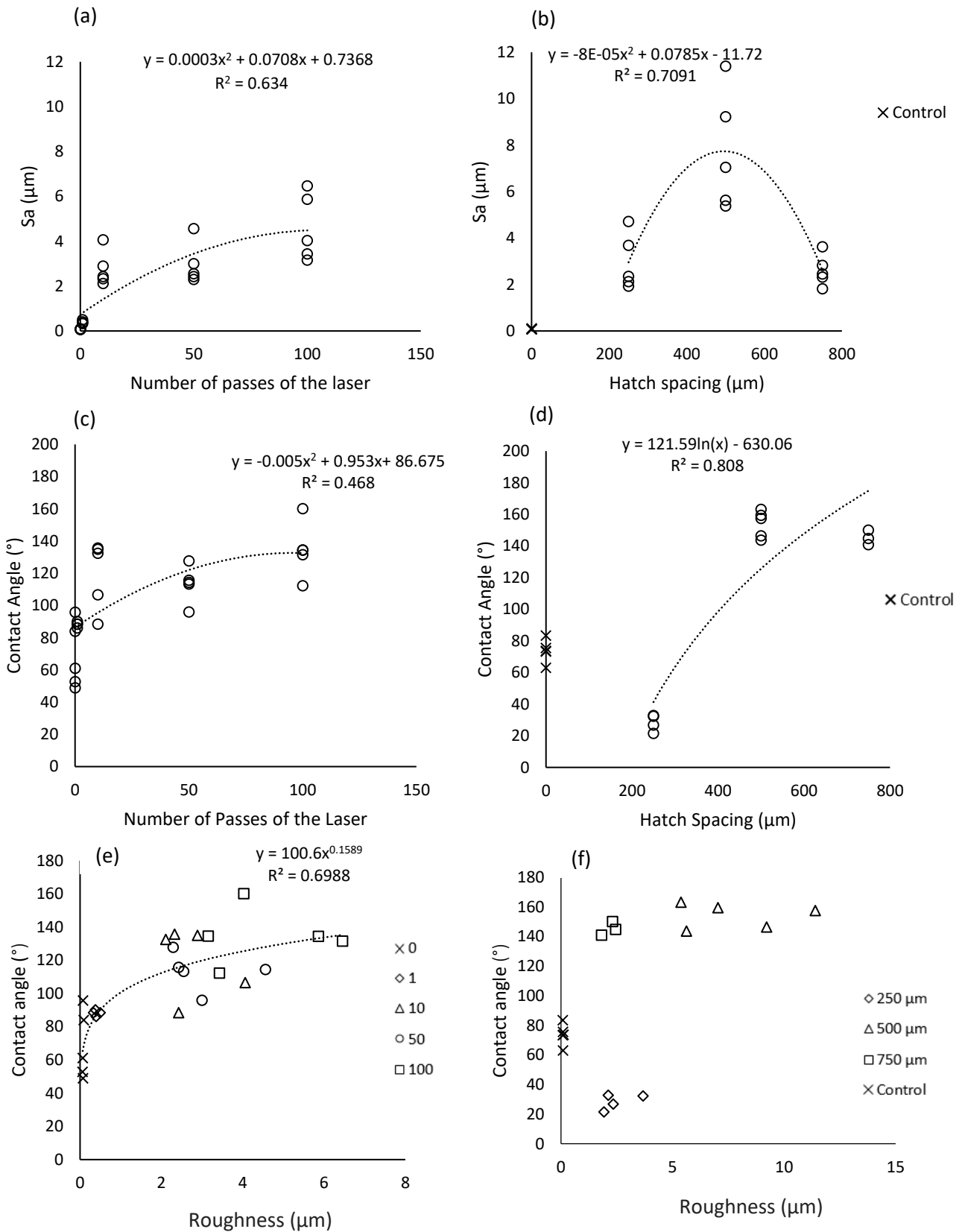


Figure 4.4 Relationships between; roughness ( $S_a$ ) and (a) number of passes of the laser (b) hatch spacing; contact angle and (c) number of passes of the laser and (d) hatch spacing; and contact angle and roughness for (e) number of passes treatment and (f) hatch spacing treatment.

### 4.3.2 Effect of surface on biofilm settlement

#### 4.3.2.1 Topography

A one-way ANOVA test showed that there was a statistically significant difference in biofilm settlement between the different passes treatments ( $F_{(4)} = 197.5$ ,  $p < 0.01$ ; Figure 4.5). Dunnett's T3 post hoc test revealed that all laser processed micro-topographies (from 1 pass to 100 passes) had significantly less settlement than the control ( $P < 0.001$ ). Control samples which had no passes of the laser had significantly higher settlement of biofilm (mean = 1650.6, SE= 182.5) than laser textured patterns (1 pass: mean = 593.2.6, SE= 81.7; 10 passes: mean = 165.8, SE= 16.28; 50 passes: mean = 49.8, SE= 10.63; 100 passes: mean = 92, SE= 15.4; Figure 4.5). There was not a significant difference between 50 and 100 passes (50 passes: mean = 49.8, SE= 10.63; 100 passes: mean = 92, SE= 15.4;  $p=0.348$ ).

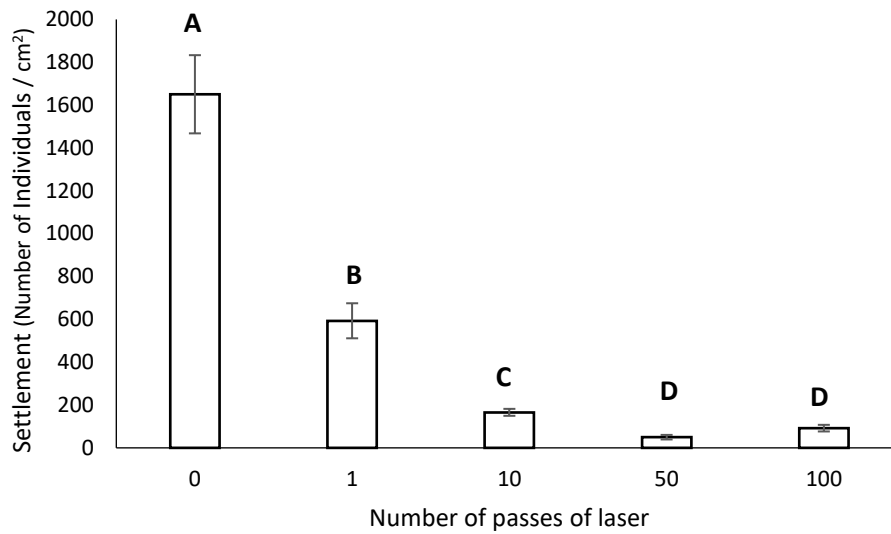


Figure 4.5 The number of individual marine organisms settled across laser processed surfaces with a varying number of passes; none (control), 1 pass, 10 passes, 50 passes and 100 passes. **A**, **B** and **C** represent significant differences between groups.

There was a statistically significant difference in settlement of marine organisms between the different hatch treatments ( $\chi^2_{(3)} = 14.143$ ,  $p = 0.003$ ; Figure 4.6). Dunnetts T3 post hoc test revealed 250 $\mu$ m hatch spacing (median = 88, LQ = 84, UQ = 252) had significantly less settlement than all of the other micro-topographies (control: median = 840, LQ = 748, UQ = 848; 500  $\mu$ m: median = 656, LQ = 616, UQ = 772; 750  $\mu$ m: median = 672, LQ = 596, UQ = 732;  $p < 0.001$ ). There was no difference in settlement between control (median = 840, LQ = 748, UQ = 848) and 500  $\mu$ m hatch spacing (median = 656, LQ = 616, UQ = 772,  $p = 0.127$ ), control and 750 $\mu$ m (median = 672, LQ = 596, UQ = 732;  $p = 0.171$ ) and between 500  $\mu$ m hatch spacing (median = 656, LQ = 616, UQ = 772) and 750  $\mu$ m hatch spacing (median = 672, LQ = 596, UQ = 732;  $p = 1$ ).

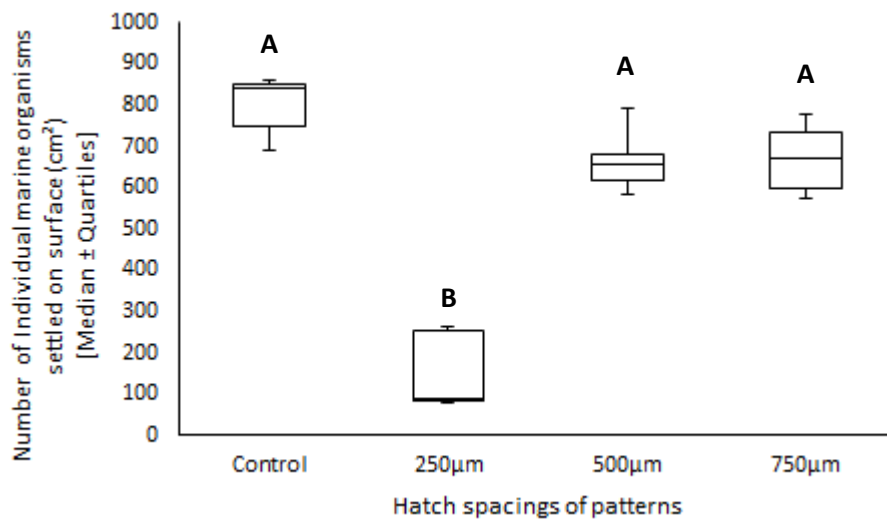


Figure 4.6 The number of individual marine organisms settled across laser processed surfaces with a hatch spacing of 250, 500 and 750 µm. The control surface is not laser processed. Solid horizontal bars = statistically different groups. A, B and C represent significant differences between groups.

#### 4.3.2.2 Contact angle, roughness and laser parameters

There was a significant relationship between the contact angle and settlement for number of laser passes treatment ( $F_{(2,22)}=29.9$ ,  $p < 0.001$ ). The  $R^2$  value was 0.7311 therefore, 73.11% of the variation in the settlement data is explained by contact angle. There was a strong negative relationship between settlement and contact angle (Figure 4.7a). The regression equation may be useful for making predictions since the value of  $r^2$  is close to 1.

There was a significant relationship between the contact angle and settlement for hatch spacing treatment ( $F_{(1,10)}=80.1$ ,  $p < 0.001$ ). The  $R^2$  value was 0.889 therefore, 88.9% of the variation in the settlement data is explained by contact angle. There was a strong positive relationship between contact angle and settlement (Figure 4.8a). The regression

equation may be useful for making predictions since the value of  $r^2$  is close to 1. The control for this regression was omitted as a hatch spacing of 0 is a straight line, therefore there cannot be a hatch spacing 0 measurement.

There was a significant relationship between the roughness and marine biofilm settlement for the number of passes laser treatment ( $F_{(1,22)}=117.8$ ,  $p<0.001$ ). The  $R^2$  value was 0.843 therefore, 84.3 % of the variation in the settlement data is explained by roughness. There was an exponentially decreasing relationship between number of roughness and biofilm settlement for the number of passes treatment (Figure 4.7b). The regression equation may not be useful for making predictions since the value of  $r^2$  is close to 1.

There was not a significant relationship between the roughness and marine biofilm settlement for the hatch spacing treatment ( $F_{(1,13)}=1.521$ ,  $p=0.239$ ; Figure 4.8b).

There was a significant relationship between the number of laser passes and marine biofilm settlement ( $F_{(2,23)}=19.833$ ,  $p<0.001$ ). The  $R^2$  value was 0.474 therefore, 47.4% of the variation in the settlement data is explained by number of passes. There is a mild exponentially decreasing relationship between number of laser passes and settlement (Figure 4.7c). The regression equation may not be useful for making predictions since the value of  $r^2$  is close to mid range.

There was a significant relationship between hatch spacing and marine biofilm settlement ( $F_{(1,14)}=49.058$ ,  $p<0.001$ ). The  $R^2$  value was 0.7905 therefore, 79.05% of the variation in the settlement data is explained by hatch spacing. There is positive increasing relationship between hatch spacing and settlement (Figure 4.8c). The regression equation may be useful for making predictions since the value of  $r^2$  is close to 1. The control for this regression was omitted as a hatch spacing of 0 is a straight line, therefore there cannot be a hatch spacing 0 measurement.

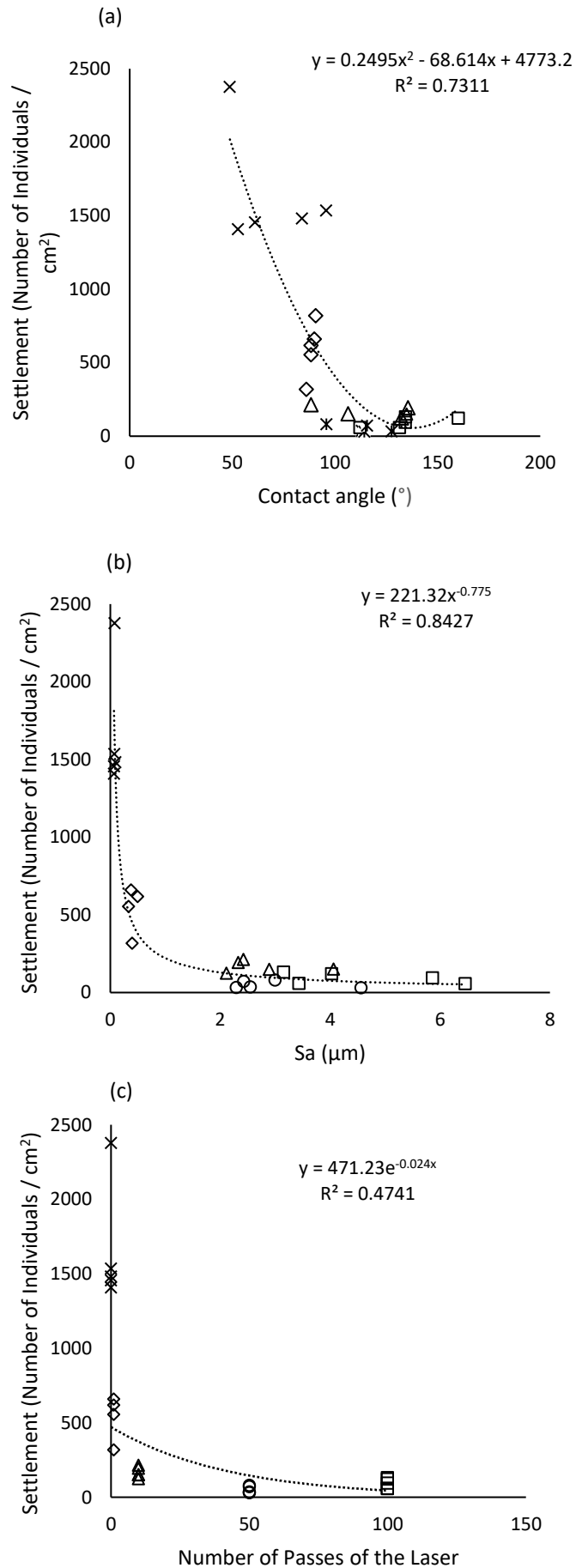


Figure 4.7 Relationships between settlement of marine biofilm and surface parameters; (a) contact angle (b) roughness and (c) topography for the number of passes experiment.

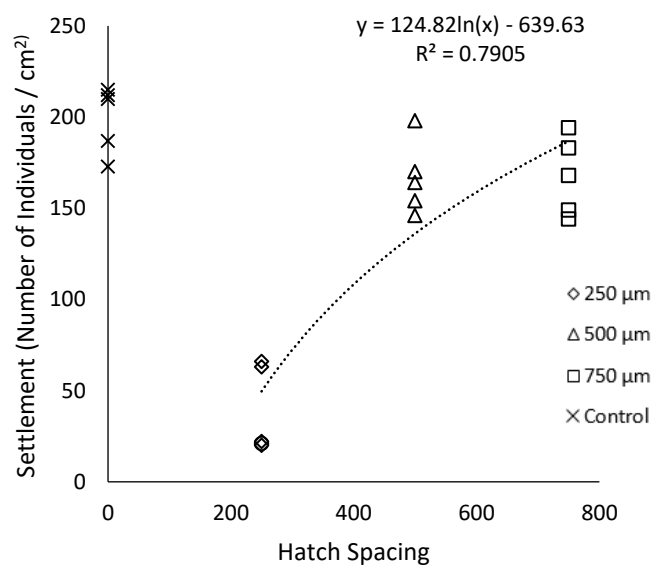
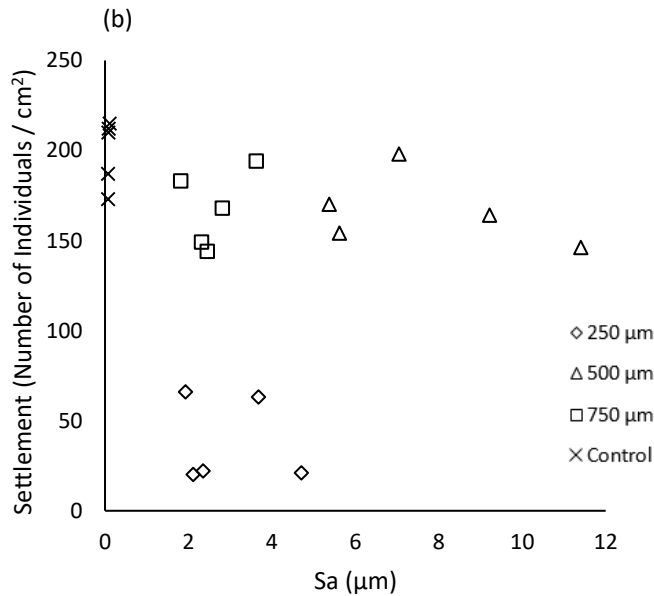
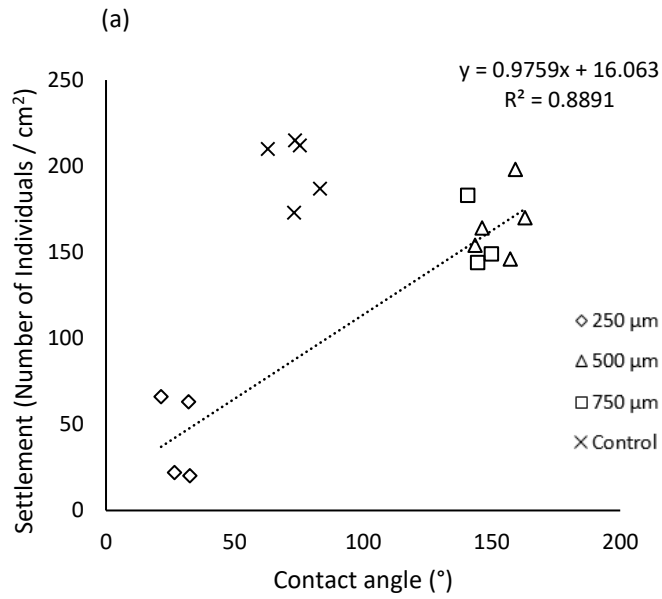


Figure 4.8 Relationships between settlement of marine biofilm and surface parameters; (a) contact angle (b) roughness and (c) topography for the hatch spacing experiment.

#### 4.4 Discussion

The aim of the study was to determine the effect of laser surface micro-texturing of metal as antifouling on biofilm settlement under alteration of surface properties (contact angle, roughness, laser passes and hatching). It was found that the number of passes treatment, and the hatch spacing treatment alter the surface of the metal in different ways, as the number of passes had strong links with the roughness and contact angle and the hatch spacing treatment with topography. In turn, it is these parameters in which have been contributing to the antifouling properties found on the laser textured surfaces.

##### 4.4.1 Effect of the laser parameter on surface

Two different laser parameters were used throughout this study, the number of passes treatment and the hatch spacing treatment.

##### 4.4.1.1 Topography

For number of passes treatment, it was found that the depth of the resulting topography increased with the number of passes of the laser. Other studies have found that depth does not increase at a proportionate rate to the number of passes (Li and Ananthasuresh, 2001). This study found that there was a relationship between depth and the number of passes, however after a certain amount of passes depth will not increase anymore. This may be because it reaches a constant depth where by increasing the number of passes will have no effect on depth. This trend has been found in previous studies (Li and Ananthasuresh, 2001) and can be explained by the lack of focus of the laser beam at different depths. The laser set up in this study did not allow for the variation in focus at varying depths, to increase depth further the focus of the beam would need to be reset along the Z axis.

Although the depth of the topography increased with the number of passes of the laser the preciseness of the features on topographical pattern faded. For other surface modification techniques the preciseness of the surface features have been altered to specifically target biofouling species *Ulva* (2µm) and barnacle cyprid (20µm) (Schumacher *et al.*, 2007a, Estes, 2005). However, this would not be possible for a surface using laser surface texturing, as the distinct features faded with increased number of passes. As the number of passes increased, the depth of the topography increased, but the surface features went from a distinct, reproducible micro-topography surface (1 pass) to random and not clearly defined (50 and 100 passes). This may be because the laser spot did not hit the same position with each pass, as there was not a direct synchronisation between the beam scanner and the pulsing of the laser (Figure 4.9). Therefore, the laser spots spread out resulting in non-distinct irregular micro-topographies for 50 and 100 passes, rather than deeper, regular topographies as anticipated.

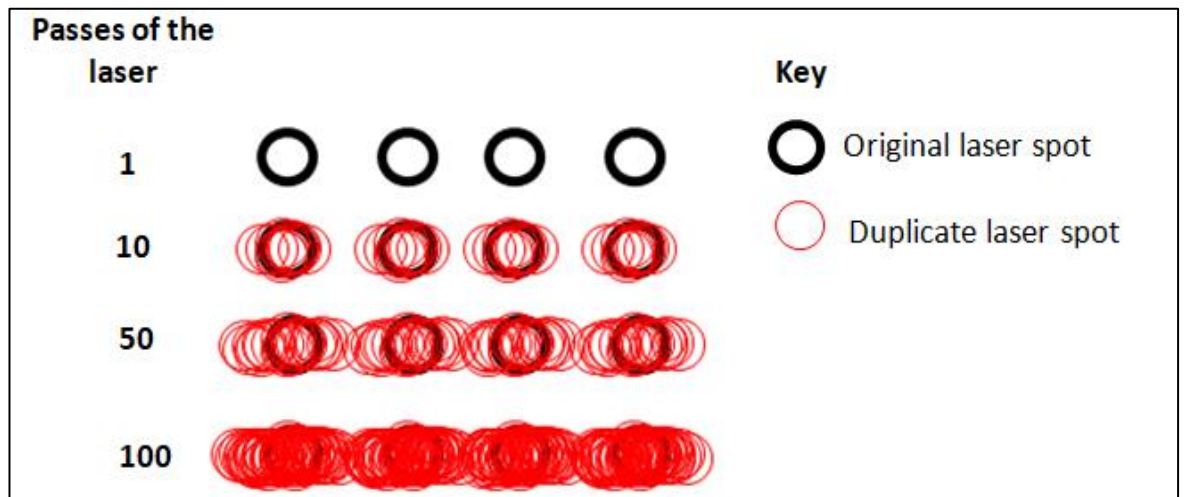


Figure 4.9 A schematic illustration of laser pulses in relation to the number of passes of the laser on a single hatch line.

For the hatch spacing treatment, the resulting topographies were in line with the laser parameter setting. This is because the width of micro-topography is easily controlled

using hatch spacing function and can be accurate down to 0.01 mm. Therefore, this was easily programmable into the laser software, and resulted in distinct crosshatch micro-topographies. Although width can be controlled, and the number of passes of the laser can act as a proxy for depth, the resulting topographies of different aspect ratios may not be similar as the synchronisation of the beam alters the reproducibility of creating the same pattern at different scales.

#### 4.1.1.2 Roughness and contact angle

Increasing the number of passes of the laser increased the roughness of the surface. This trend has also been found in previous studies (Lee *et al.*, 2008). This trend may be occurring because the number of passes increases the melt and re-solidification that produces fine ridges and random structures, as there is little control over the behaviour of the re-solidified material. When a laser spot hits the surface, ablation of the substrate at the centre of the laser spot occurs by direct absorption of laser energy (Brown and Arnold, 2010). The material is vaporized and a highly directed plume of solid and liquid clusters of material forms at the radiated site. Towards the outside of the laser spot the energy is less, therefore all of the material cannot be ablated, and it is melted. The plume is ejected from the radiated zone, and can cause the surrounding molten surface to move in liquid form and re-solidify to create ripples and ridge like structures (Brown and Arnold, 2010). Re-solidification of the material from the vapour plume can create clusters of nanoparticles which further alter the roughness of the substrate at the ablated region (Brown and Arnold, 2010, Semaltianos *et al.*, 2008). This has also been observed by Razi *et al.*, (2016) where the central regions of the irradiated spot had significant ablation, and deposited particles were observed in the periphery of the laser spot. The re-solidification leads to higher roughness values of the surface. With more laser passes comes more ablation, melt and random re-solidification opportunities for the material, therefore this

explains why the roughness is increased with the number of passes of the laser. This has also been found for other studies as the surface becomes rougher due to the thicker re-solidified material and debris re-deposition (Lee *et al.*, 2008).

Increasing the number of passes of the laser also increased the contact angle of the surface. It is known that laser texturing can have an effect on the wettability of the surface, previous studies show nanosecond laser texturing can create super-hydrophobic surfaces on copper and brass (Ta *et al.*, 2015). The results of this study are in agreement a study found the contact angle increased with increasing laser passes creating a hydrophobic surface (Bizi-Bandoki *et al.*, 2011). Another study using laser pulses on silicone substrate found that laser texturing can increase the contact angle by over half, changing it from a hydrophilic to a hydrophobic surface (Wang *et al.*, 2009). This increase in contact angle by increasing the number of passes may be due to the increase in roughness of the surface. The contact angle of roughened surfaces have been studied extensively and are thought to be intertwined (Bhushan *et al.*, 2007, Marmur, 2003, Lafuma and Quéré, 2003, Bico *et al.*, 2002, Gao and McCarthy, 2006). The Cassie-Baxter model predicts that air pockets form between the roughness peaks of the surface, and become trapped below the droplet of water, therefore the water droplet beads up and has hydrophobic properties as it is sitting on an interface of solid, liquid and air (Cassie and Baxter, 1944, Reyssat *et al.*, 2006, Choi *et al.*, 2009, Bormashenko, 2008). This type of behaviour is found across a range of micro-textures found in nature such as lotus leaf (Ensikat *et al.*, 2011, Cheng and Rodak, 2005). This is what may be happening at the interface of the surfaces in the number of passes treatment. The increasing number of passes cause a larger re-melt and re-deposition of the material, which increases the roughness of the surface, which in turn increases the air entrapment, which leads to increases contact angles.

The increase in hatch spacing treatment found an increasing relationship with roughness, to when hatch spacing was 500 $\mu\text{m}$ , then roughness decreases with further increases to hatch spacing. The roughness of the surface may have increased with smaller hatches, as areas of the surface will have been ablated, re-solidified and debris re-deposition may have occurred leading to increase in roughness (Razi *et al.*, 2016; Lee *et al.*, 2008). However, once the hatch spacing was above 500 $\mu\text{m}$ , the amount of “free space” that had not been laser processed may have been larger than the laser processed areas, leading to smoother Sa values. Therefore, the roughness decreased as hatch spacing became larger past 500  $\mu\text{m}$ , as the amount of unprocessed area increased.

The relationship between hatch spacing and CA is increasing, and does not follow the relationship between roughness and hatch spacing. This may be because although CA and roughness are thought to be interlinked, it may not always be the case as other studies have also found that surface roughness was found not to influence measured contact angles (Busscher *et al.*, 1984). In this study, the 250 $\mu\text{m}$  micro-topography had a low roughness value and had hydrophilic contact angles of  $<50^\circ$ . Roughness may not fully explain the contact angle results for hatch spacing as the hatch 250 $\mu\text{m}$  and 750 $\mu\text{m}$  have similar roughness values but different contact angles. This may be explained by the Wenzel model (Wenzel, 1936), in which there are no trapped air pockets, and the liquid spread out amongst the small gaps caused by roughness, and therefore the contact angle is lower. Although 250 $\mu\text{m}$  and 750 $\mu\text{m}$  have similar roughness values, one surface may be exhibiting the Cassie-Baxter effect and the other the Wenzel effect therefore this may be causing the difference in contact angle. The topography may also play a role in the contact angle measurements.

Overall, the process parameters (number of passes and hatch spacing) have varying relationships with depth, roughness, contact angle and topography. Depth, the surface

roughness and contact angle have strong relations with the number of passes parameter, whereas the hatch spacing treatment has a more complex relationship with contact angle and roughness. However, both treatments highlight the interlinking between contact angle, roughness and topography.

#### 4.4.2 Effect of surface on biofilm settlement

##### 4.4.2.1 Passes of the laser treatment

Increasing the number of passes of the laser reduced the settlement of marine biofilm. The relationship between number of passes and biofilm settlement became constant at 50 passes, as increasing the passes to 100 did not further reduce biofilm settlement. This trend found between the passes of the laser and settlement occurred because increasing the number of passes of the laser, also increased the roughness and the contact angle of the laser, and therefore these parameters effected the settlement of marine biofilm.

Increasing the number of passes of the laser, increased the roughness of the surface, and this had an effect on the settlement of marine biofouling. A similar study on marine biofouling organism *Ulva* also found a decreasing linear relationship between engineered roughness index and the settlement of *Ulva* spores (Schumacher *et al.*, 2007). A decreasing exponential relationship between biofilm settlement roughness has also been found when analysing data roughness and settlement data from electro-polished stainless steel when tested with two different bacteria species (Wu *et al.*, 2018). Roughness may not be the sole parameter that is causing the reduction of settlement in this study, as previously discussed; roughness and contact angle are interlinked. In this study increasing the number of passes of the laser is increasing the roughness of the surface, which is then increasing the contact angle of the surface, and combined, this is reducing the settlement of marine biofilm. This can be explained by air entrapment theory (Wu *et al.*, 2013) which suggests that the trapped air bubbles, that cause the higher contact angles seen in the

Cassie-Baxter model (Cassie, 1948) may also be limiting the settlement of marine biofouling (Wu *et al.*, 2013). They limit the settlement of marine biofouling by reducing the surface area interaction between the biofouling organism and the substrata (Wu *et al.*, 2013). If the size of the air bubbles are larger than the biofouling organism, the organism cannot settle, as surface area contact is limited (Wu *et al.*, 2013). This may not be in agreement with all authors as there may be disagreements over the wettability of a fully submerged surface, however, Wu *et al.* (2013) showed that their surface were immersed for a 6 hour period and still had micro-scale air pockets where no further wetting occurred. Therefore, Wu *et al.*, (2003) study was evidence that air entrapment is occurring on these surfaces, which may be leading to the antifouling effects.

#### 4.2.2.2 Hatch spacing treatment

As the hatch spacing increased from 250µm to 500 and 750µm the settlement of marine biofilm increased. It was found that only one topographical pattern 250µm hatch reduced marine biofilm. As 250µm was the only topography found to reduce biofouling compared to the control, it may have been reasonable to suggest that the air entrapment theory may be happening on this topography also, however, this is unlikely as 250µm had low contact angle values therefore air bubbles may not have been present. For the hatch spacing treatment, roughness and contact angle do not appear to be closely interlinked. Similar results have been found for previous studies in that surfaces with the same roughness value have exhibited contact angles that differ by 30° (Jopp *et al.*, 2004). Therefore, roughness and contact angle do not explain the antifouling results seen on 250µm pattern.

The reduction in biofouling on the 250µm may have been a direct result of the topographical features (peaks, dips and flat areas) and can be explained by diatom attachment theory (Scardino *et al.*, 2006, Scardino *et al.*, 2008). As the 250µm pattern has smallest hatches, the amount of “free space” in which marine biofouling can settle without

the disruption of their attachment points was limited (Scardino *et al.*, 2006, Scardino *et al.*, 2008). The topographical features of the 250 $\mu$ m pattern was limiting the attachment points of biofouling organisms, therefore leading to reduced marine settlement (Scardino *et al.*, 2006, Scardino *et al.*, 2008). On the 500 $\mu$ m and 750 $\mu$ m patterns, the amount of “free space” in which marine organisms can attach with multiple, undisrupted attachment points was greater, leading to increased settlement of marine biofouling. Therefore, unlike the passes treatment where the antifouling effects were a result of roughness and contact angle alternations to the surface, the antifouling effects seen on hatch spacing treatment 250 $\mu$ m may have been largely influenced topographical features. This study highlights that roughness, topography, and contact angle are all interlinked, and are all be contributing to the overall antifouling effect (figure 4.10).

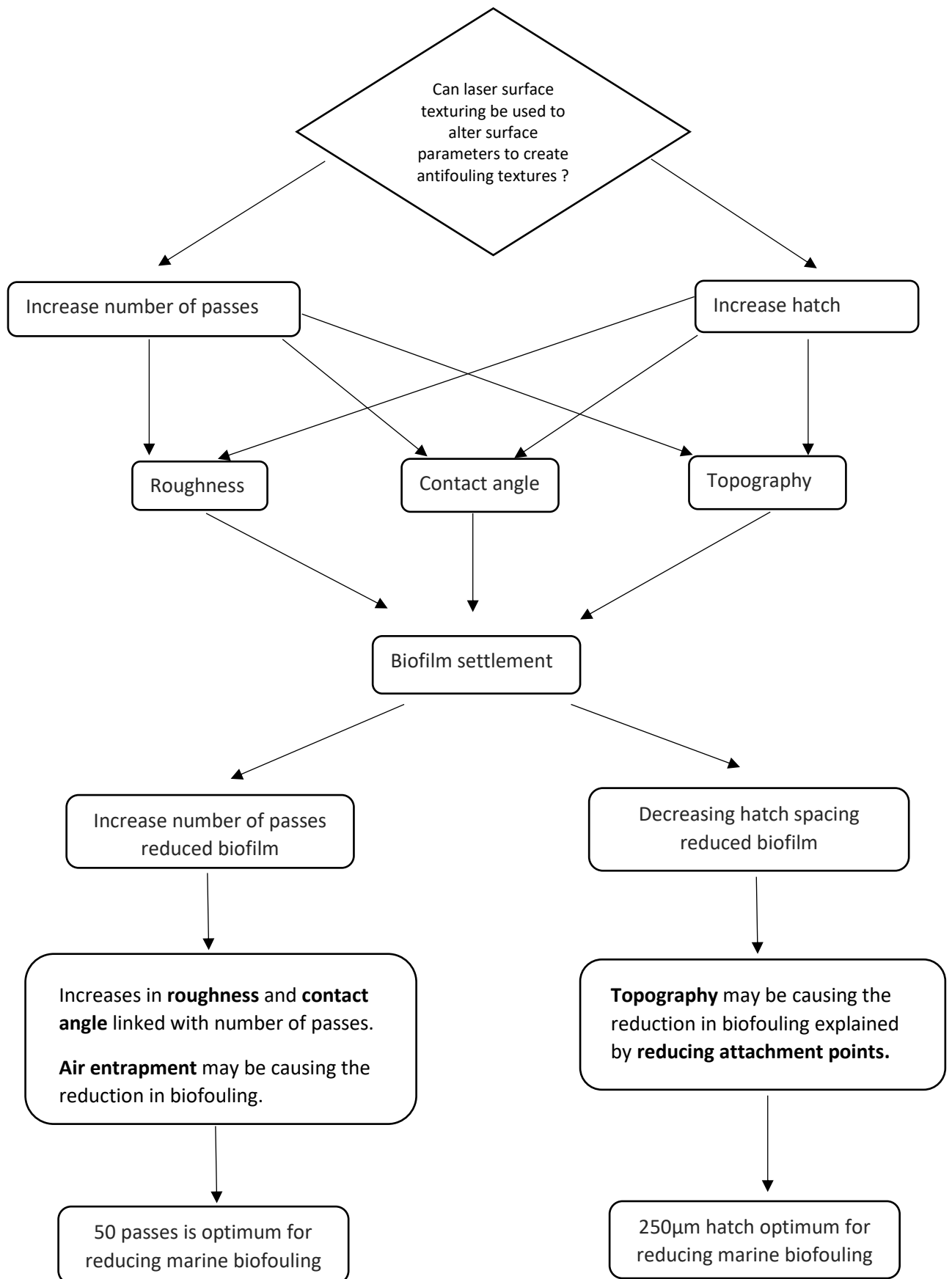


Figure 4.10 Flow chart of key findings of this study

#### 4.5 Conclusions

Overall, this study demonstrates that it is possible to produce laser-processed micro topographies onto stainless steel (316L) that have marine antifouling properties. The number of passes of the laser and the hatch spacing's are key variables that can be controlled in the production of the micro-topographies. Hatch spacing around 250  $\mu\text{m}$  had an effect on the settlement; however, larger hatch spacing did not provide any antifouling properties. Increasing the number of passes reduced settlement, until an asymptote was reached at 50 passes where further increasing passes had no further effect on the settlement. A combination of surface topography, roughness, and wettability may play intertwining roles in the antifouling properties of a surface. Laser surface texturing was successful as a tool to create antifouling surfaces against marine biofilm. Laser processed antifouling topographies are not species specific and therefore may be the best approach for a widely effecting antifouling surfaces.

## Chapter 5 Biomimicry: Investigating single feature biomimetic patterns for their antifouling effect

### 5.1 Introduction

Biomimicry (bio- meaning life in Greek, and -mimesis, meaning to copy) is a modern scientific discipline in which biological systems are studied and concepts are mimicked and adapted to solve human based problems (Benyus, 1997, Lurie-Luke, 2014).

Material development has become the largest area of biomimicry research, with approximately 50% of all reviewed references about the topic (Lurie-Luke, 2014). In the context of marine biofouling, biological surfaces within the marine environment have been studied for bio-inspiration in their response to biofouling (e.g. Pilot whale *Globicephala melas* (Baum *et al.*, 2002) and sea stars *Cryptasterina pentagona* and *Archaster typicus* (Guenther and de Nys 2007). The most commonly studied biological surface for antifouling potential is that of the spinner shark, which lead to the production of Sharklet™ surface topography that has now become commercial as it is used on catheter tubes to reduce biofilm (May *et al.*, 2015, Reddy *et al.*, 2011).

However, it has also been found that structures on shell surfaces also have anti-fouling effects. A study on *Mytilus galloprovincialis* and *Pinctada imbricate* found that shells were largely unfouled despite strong fouling pressure (Scardino *et al.*, 2003). They also found that there was a strong correlation between low level of fouling and the presence of an intact periostracum (outer layer) of the shell. This leads to the conclusion that the micro-topography on the periostracum of the shell is playing a role in that natural defence of biofouling (Scardino *et al.*, 2003). The use of micro-topographies as antifouling method on shells is highly probable as they are hard surfaces that do not have obvious chemical or mechanical defences against fouling (Bers *et al.*, 2010). A study has been performed investigating algae and barnacle fouling on a shell micro-topography of the

mussel *M. edulis*, where fouling was compared on the micro-topography area of the shell and on a smooth area where the micro-topography pattern was physically removed. It was found that fouling was significantly greater on areas of shell where the micro-topography had been physically removed (Wahl *et al.*, 1998).

Similarly to shells, many crabs are little fouled in nature. It has been found that the natural micro-topography of the crab *Cancer pagurus* is repellent to macrofoulers (Bers and Wahl, 2004), showing that crabs may be a suitable marine organism to mimic for their antifouling effects. Fouling on the horseshoe crab (*Limulidae sp.*) is low considering their life span, therefore the natural defence mechanism of a micro topographical surface is working on by keeping the horseshoe crab fouling low (Patil and Anil, 2000).

The creation of biomimetic surfaces for antifouling potential have already been undertaken in various surface modification methods such as photolithographic techniques (Schumacher *et al.*, 2007b), hierarchically wrinkled surface topographies (Efimenko *et al.*, 2009), casting directly off marine organisms (Bers and Wahl, 2004), laser surface texturing (Rusen *et al.*, 2014, Scardino *et al.*, 2006b) and laser surface texturing with added coatings (Sun *et al.*, 2018). The methods of photolithography, wrinkled surfaces, and casting directly off marine organisms are limited in that they are only able to be used on polymer substrates such as Polydimethylsiloxane elastomer (PDMS) and epoxy resin. Whereas, laser surface texturing enables micro-textures to be created on both polymer (PMDS) substrate (Scardino *et al.*, 2006b) and on metal substrates (Rusen *et al.*, 2014) for antifouling potential. Therefore, creating a topography using laser surface texturing allows for a more universal approach, as the substrate material is not limited, and may have a wider industrial application.

The majority of the previous studies investigating biofilm settlement on biomimetic surfaces are lab based (Hoipkemeier-Wilson *et al.*, 2004, Schumacher *et al.*, 2007a,

Schumacher *et al.*, 2007b, Chung *et al.*, 2007, Carman *et al.*, 2006, Schumacher *et al.*, 2008, Chen *et al.*, 2015, Scardino *et al.*, 2006b, Rusen *et al.*, 2014) and report a reduction in settlement of fouling after conducting fouling assays using one or two individual species compared to a smooth control. However, the present study is the first to test laser produced biomimetic antifouling surfaces on marine grade steel directly in the marine environment. This is important, as there is no known control of the species present in the water column, as it is a fully natural environment, therefore will produce a real world results rather than lab based (within the limitation of the field site discussed in section 3.4.1). This study aims to (a) use laser surface texturing to create biomimetic crab and shell surfaces on marine grade steel and (b) to determine the efficacy of these surfaces for their antifouling potential in the marine environment.

## 5.2 Methods

The methods of the chapter are broken up into two sections with 5.2.1 creating the natural patterns and with 5.2.2 antifouling efficacy testing the natural patterns.

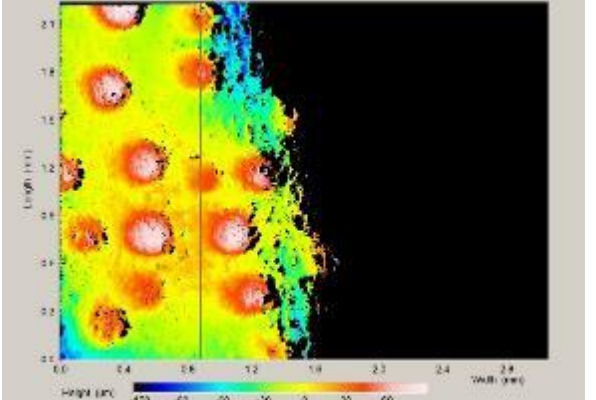
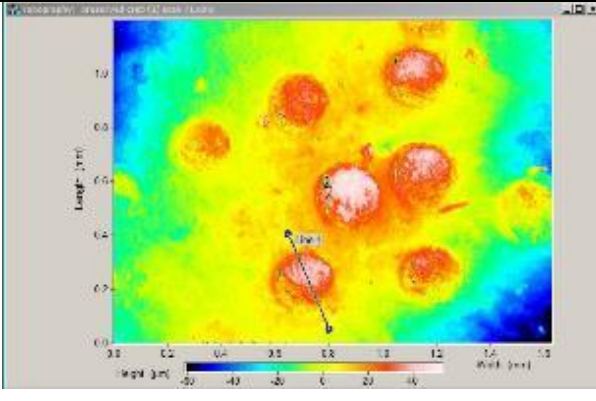
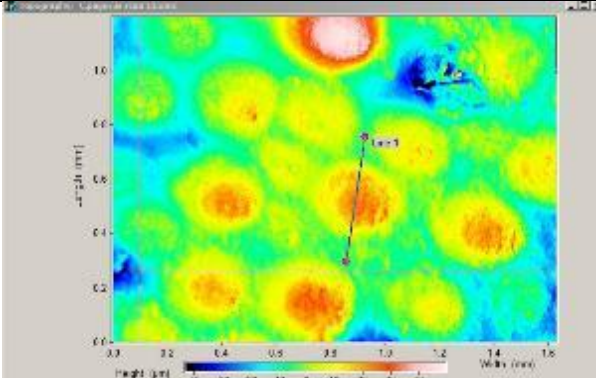
### 5.2.1 Creating biomimetic patterns on marine grade steel

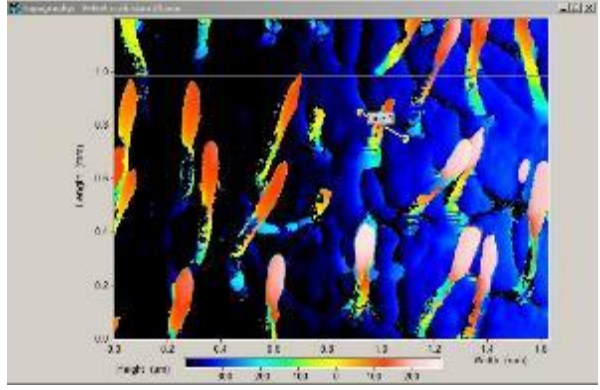
#### 5.2.1.1 Sampled species for pattern reproduction

Various natural surfaces were investigated during this study, shown in Table 5.1 (crabs) and Table 5.2 (shells). A 3D topographical microscope was used to scan natural surfaces directly. Preserved crabs were taken from LJMU storage for scanning, and juvenile shells were collected from Thurstaston Beach, Wirral, UK. In total 3 crab species were used; Shore Crab *Carcinus maenas*, Edible Crab *Cancer pagurus* and Velvet swimming crab *Necora puber* and one bivalve species common cockle *Cerastoderma edule*. The scans were taken from randomly selected areas of the carapace of the crab and from randomly selected areas of the shells. Preserved carapace of shore crab was compared with freshly deceased carapace of shore crab (Table 5.1) and similar measurements were gained from

both freshly deceased and preserved specimens, therefore, for other species, preserved carapace were chosen.

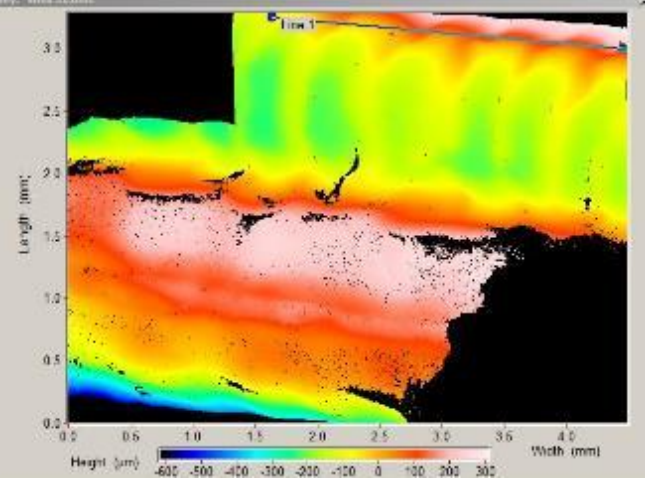
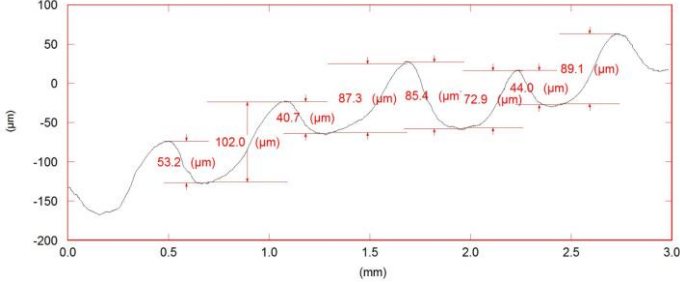
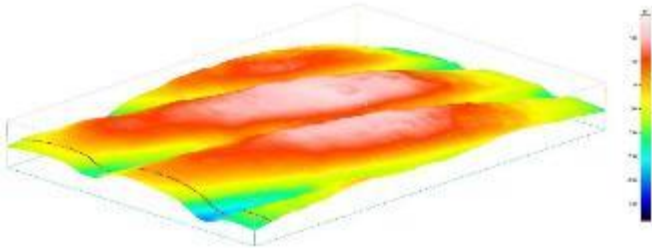
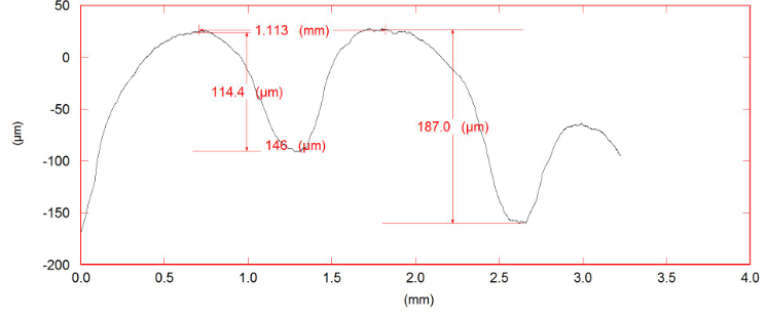
Table 5.1 Images and features from topographical scans of crab species (lines on images are where cross-sections have been drawn for measuring purposes).

Crab	3D topographical microscope scan image	Features
Shore crab <i>Carcinus maenas</i> (alive)		<ul style="list-style-type: none"> <li>• Raised hills (<b>peaks</b>) approximately 30 <math>\mu\text{m}</math></li> <li>• Lower valley between peaks (<b>pits</b>).</li> <li>• Randomly arranged</li> <li>• Likely to be able to be replicated using laser surface texturing.</li> </ul>
Shore crab <i>Carcinus maenas</i> (preserved)		<ul style="list-style-type: none"> <li>• Raised hills (<b>peaks</b>) approximately 20 <math>\mu\text{m}</math>.</li> <li>• Lower valley between peaks (<b>pits</b>).</li> <li>• Randomly arranged</li> <li>• Likely to be able to be replicated using laser surface texturing.</li> </ul>
Edible crab <i>Cancer pagurus</i>		<ul style="list-style-type: none"> <li>• Raised hills (<b>peaks</b>) approximately 30 <math>\mu\text{m}</math>.</li> <li>• Lower valley between peaks (<b>pits</b>).</li> <li>• Randomly arranged</li> <li>• Likely to be able to be replicated using laser surface texturing.</li> </ul>

<p>Velvet swimming crab <i>Necora puber</i></p>		<ul style="list-style-type: none"> <li>• Raised thin hair like structures approximately 100<math>\mu</math>m.</li> <li>• Randomly arranged</li> <li>• Linearly arranged, seem to be in rows.</li> <li>• Unlikely to be able to be replicated using laser surface texturing.</li> </ul>
---	--	--

The edible crab *C. pagurus* and shore crab *C. maenas* have similar topographies (see table 5.1) which can be replicated using laser processing. The velvet swimming crab *N. puber* has an interesting hair like structure on the top of the surface, however these are unlikely to be able to be replicated using laser processing due to the length and fineness of the structure. The common features that can be drawn from the table are peaks, between 20-30 $\mu$ m which are common to the surface of both shore and edible crab. These peaks are accompanied by pits either side where the topography becomes lower and valley like. It is these peaks and pits that can be mimicked using laser processing.

Table 5.2 Images and features from topographical scans using bivalve species *Cerastoderma edule* (lines on images are where cross-sections have been drawn for measuring purposes).

Species	Image	Features
Cockle <i>Cerastoderma edule</i>		<ul style="list-style-type: none"> <li>• Focus on the top right hand side. Rest of image not in focus due to curvature of the shell.</li> <li>• Focus in this image is on the small ridges within the larger ridge.</li> </ul>
Cockle <i>Cerastoderma edule</i>		<ul style="list-style-type: none"> <li>• Cross section of line drawn on image above (small ridges).</li> <li>• Measurement of peaks where they can be smallest of 41um and largest of 102um</li> </ul>
Cockle <i>Cerastoderma edule</i>		<ul style="list-style-type: none"> <li>• 3D of larger ridges.</li> </ul>
Cockle <i>Cerastoderma edule</i>		<ul style="list-style-type: none"> <li>• Cross-sectional scan of larger ridges.</li> <li>• Measurement of peaks can range from 114um to 187um.</li> <li>• Valley width (centre of</li> </ul>

		peak to peak) is over 1mm.
--	--	-------------------------------

The cockle shell has both small and larger ridge topographies (see table 5.2) which can be replicated using laser processing. The common features that can be drawn from the table are peaks, between 40-100µm which are common to the surface of the cockle shell. These peaks are accompanied by pits either side where the topography becomes lower. The topographies found in both crabs (table 5.1) and shells (table 5.2) were the bio-inspiration for the patterns created in this study.

#### 5.2.1.2 Reproduction of biological patterns using laser surface texturing

The main methods of this experiment follow the methods outlined in the methods (section 3). Laser surface texturing was used to attempt to mimic the surfaces of shore crab *Carcinus maenas* and Cockle shells *Cerastoderma edule* at the micro-scale.

Table 5.3 Laser parameters for the patterns created and tested

Exp	Pattern	Speed	Hatch 1 (mm)	Angle	Hatch 2	Angle	Passes	kHz	ns	%power
1	Crab 1	3125	0.1	135	0.1	45	20	125	30	100
1	Shell 1	3125	0.05	135	0.05	45	20	125	30	100
1	Crab 2	3125	0.15	65	0.02	140	5	125	30	100
1	Crab 3	5000	0.08	135	0.08	45	10	125	30	100
2	Crab 4	625	0.05	135	0.05	45	5	25	200	50
2	Shell 2	625	0.15	65	0.02	140	5	25	200	50
2	Crab 5	800	0.05	135	0.05	45	5	25	200	75
3	Shell 3	1200	0.075	0	-	-	5	25	200	50
3	Shell 4	1200	0.1	0	-	-	5	25	200	50
3	Shell 5	1800	0.075	0	-	-	5	25	200	50
3	Shell 6	1800	0.1	0	-	-	5	25	200	50
4	Shell 7	3200	0.1	0	-	-	20	25	200	75
4	Inverse crab 1	8000	0.1	0	-	-	20	25	200	75
4	Inverse crab 2	8000	0.1	0	0.5	90	20	25	200	75
4	Inverse crab 3	6250	0.3	0	-	-	20	25	200	75

To create biomimetic surface topographies, various parameters of the laser can be altered, to influence the outcome of the topography pattern. Table 5.3 show all the variables for the patterns created. For crab based patterns, cross hatch parameters were used, in which passes of the laser were angled from two different directions to “cut out” a peak from the surface material (Figure 5.1). The angle, power, and speed of these laser passes have been altered to effect the depth and pattern of the resulting topography to give the wanted biomimetic features.

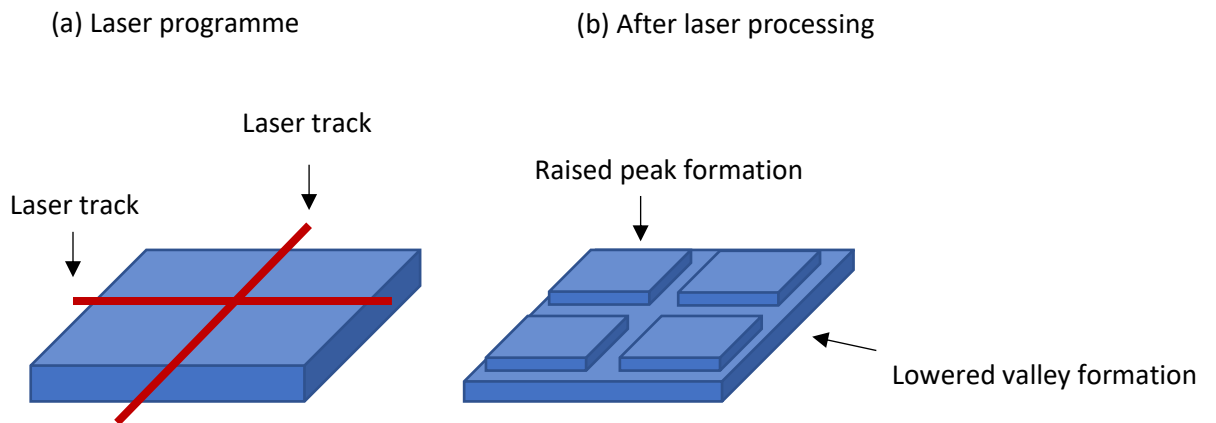


Figure 5.1 A Schematic diagram showing how laser surface texturing can be used to create “peaks” and “valleys” on surfaces.

Crosshatch patterns were mainly used to create crab inspired surfaces, except for Shell 1 pattern in which crosshatch style was used to try and mimic both larger and smaller ridges within the same pattern. For most of the shell patterns, single line laser paths were used to mimic the single line ridge effect found on shells. For the inverse crab patterns, the laser spot was completely separated out by speeding up the laser (see higher speed in table 3) therefore, individual laser spots could be “drilled” into the surface, as a reverse “peak”. This type of approach was inspired by the casting studies that had successfully mimicked crab surfaces (Chen *et al.*, 2010, Scardino and de Nys, 2004).

#### 5.2.1.3 Surface characterization

Once surfaces were created, they were scanned using a 3D microscope (BRUKER) to assess their topography in relation to biomimetic structures; depth and width of surface patterns were recorded.

#### 5.2.2 Antifouling efficacy testing of surfaces

The experiments were submerged during March to June 2017 for a 7 day period, exact date shown in table 5.4. For further details on antifouling testing see section 3.4 (3.4.1 for study site and 3.4.1 for experimental set up).

Biofilm settlement data was collected as outlined in section 3.5 (3.5.1 biofilm settlement, 3.5.2 Biofilm position on patterns). This data was analysed as outlined in section 3.5.2 Statistical analysis.

Table 5.4 Exact dates of experiments

Experiment number	Date submerged	Date removed	Surfaces tested
1	13.03.2017	20.03.2017	Crab 1, Shell 1, Crab2 , Crab 3
2	20.03.2017	27.03.2017	Crab 4, Shell 2, Crab 5
3	10.04.2017	17.04.2017	Shell 3, Shell 4, Shell 5, Shell 6
4	22.06.2017	29.06.2017	Shell 7, Inverse crab 1, Inverse crab 2, Inverse crab 3

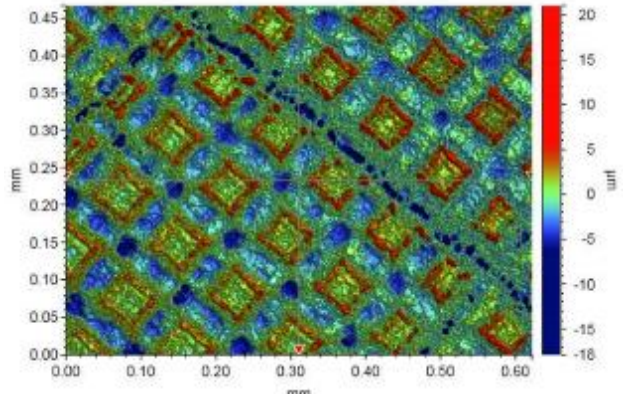
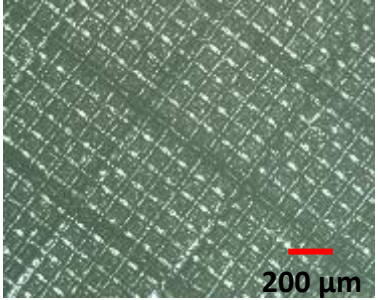
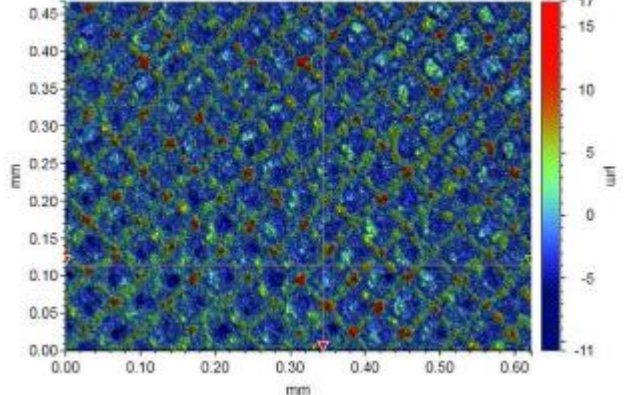
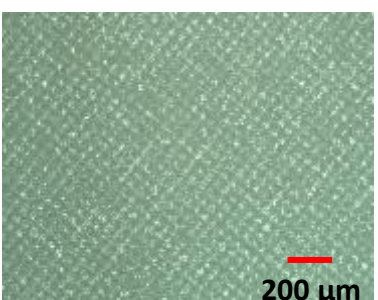
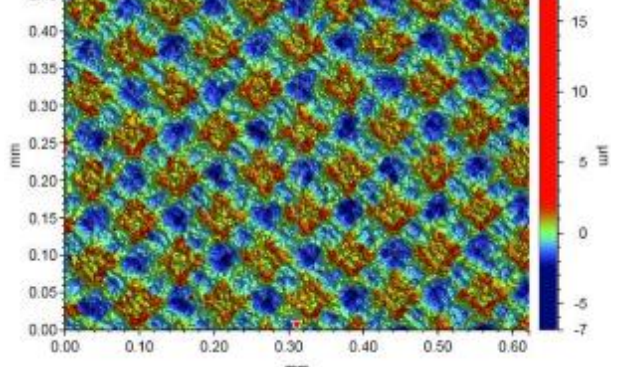
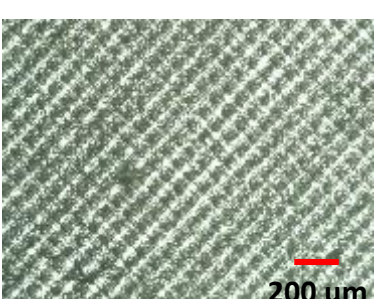
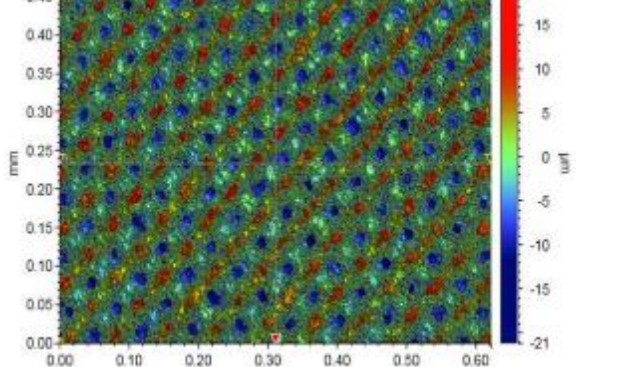
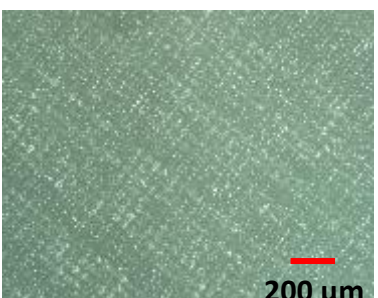
### 5.3 Results

There was not a significant difference in settlement between blocks for all experiments in this chapter (experiment 1,  $F_{(4,24)}=0.474$ ,  $p=0.754$ ; experiment 2,  $F_{(4,19)}=0.750$ ,  $p=0.573$ ; experiment 3,  $F_{(4,24)}=0.422$ ,  $p=0.791$ ; experiment 4,  $F_{(4,24)}=0.481$ ,  $p=0.750$ ), therefore blocks were ignored in further statistical testing.

#### 5.3.1 Surface topography

Biomimetic surfaces were created via laser surface texturing of marine grade stainless steel (316L). Both crab (table 5.5) and shell (table 5.6) based surfaces were able to be created.

Table 5.5 Crab and inverse crab based biomimetic patterns created by laser surface texturing.

Pattern	Topographical (Bruker) image	Microscope image (Zeiss)
Crab 1	 <p>Topographical image of Crab 1 pattern. The x and y axes range from 0.00 to 0.60 mm. The z-axis (height) ranges from -18 to 20 <math>\mu\text{m}</math>. The image shows a regular grid of diamond-shaped features.</p>	 <p>Microscope image of Crab 1 pattern. A red scale bar indicates 200 <math>\mu\text{m}</math>.</p>
Crab 2	 <p>Topographical image of Crab 2 pattern. The x and y axes range from 0.00 to 0.60 mm. The z-axis (height) ranges from -11 to 17 <math>\mu\text{m}</math>. The image shows a dense, irregular texture.</p>	 <p>Microscope image of Crab 2 pattern. A red scale bar indicates 200 <math>\mu\text{m}</math>.</p>
Crab 3	 <p>Topographical image of Crab 3 pattern. The x and y axes range from 0.00 to 0.60 mm. The z-axis (height) ranges from -7 to 18 <math>\mu\text{m}</math>. The image shows a diagonal grid of diamond-shaped features.</p>	 <p>Microscope image of Crab 3 pattern. A red scale bar indicates 200 <math>\mu\text{m}</math>.</p>
Crab 4	 <p>Topographical image of Crab 4 pattern. The x and y axes range from 0.00 to 0.60 mm. The z-axis (height) ranges from -21 to 20 <math>\mu\text{m}</math>. The image shows a dense, irregular texture.</p>	 <p>Microscope image of Crab 4 pattern. A red scale bar indicates 200 <math>\mu\text{m}</math>.</p>

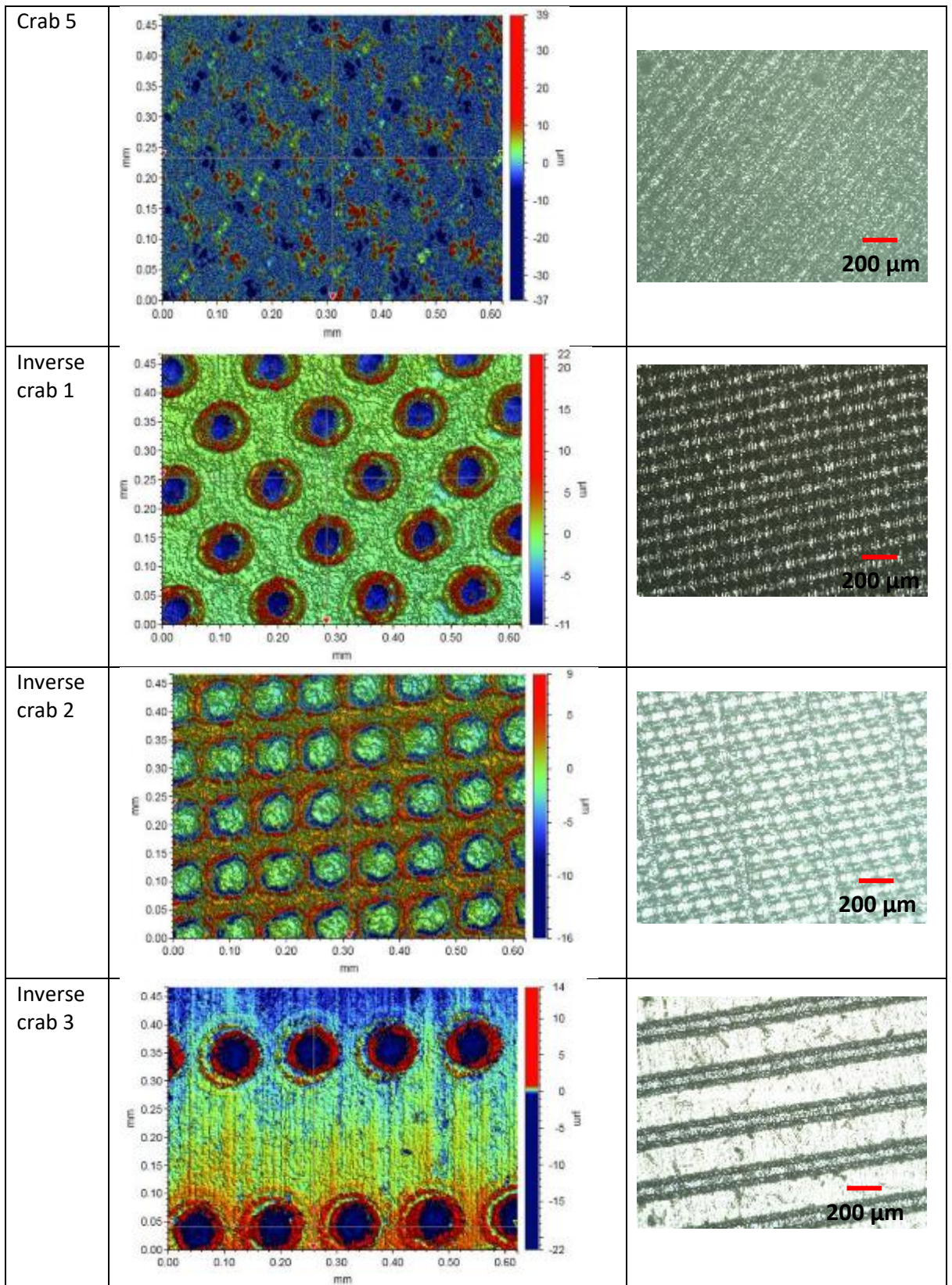
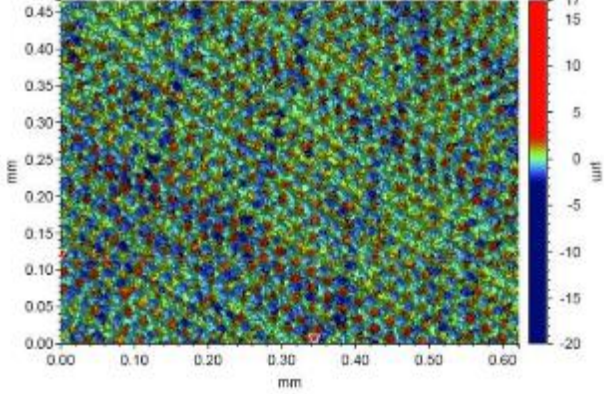
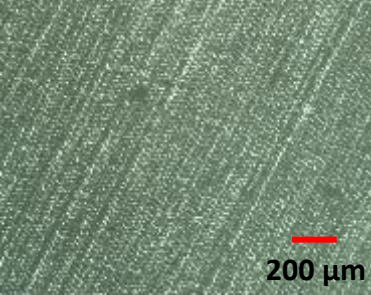
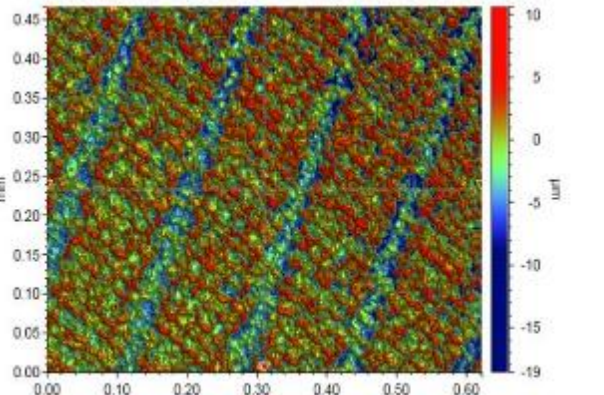
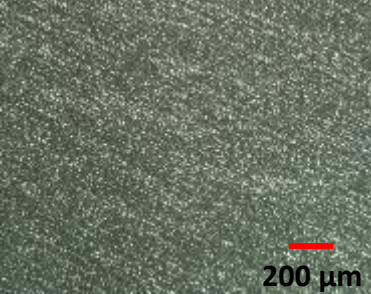
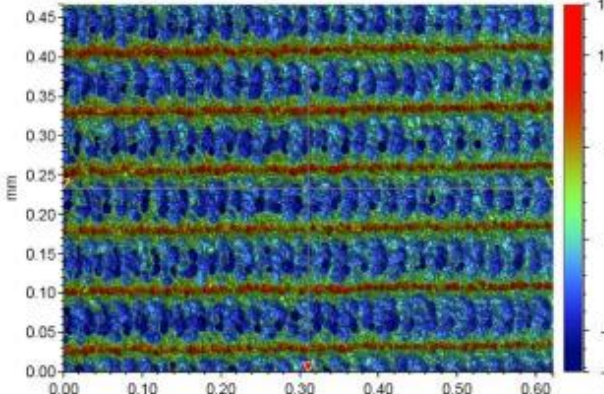
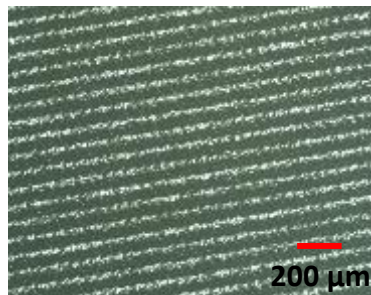
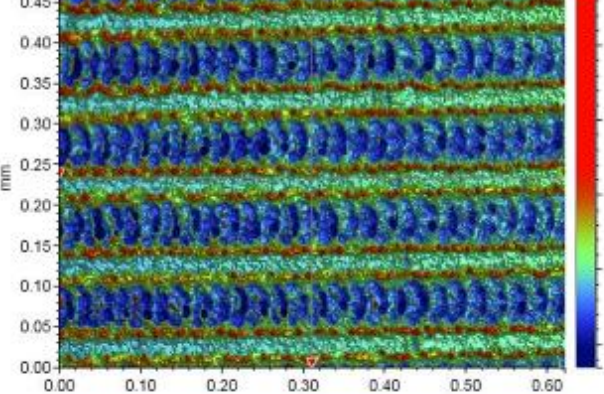
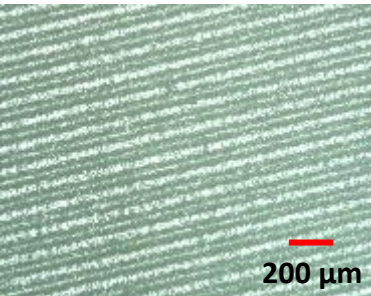
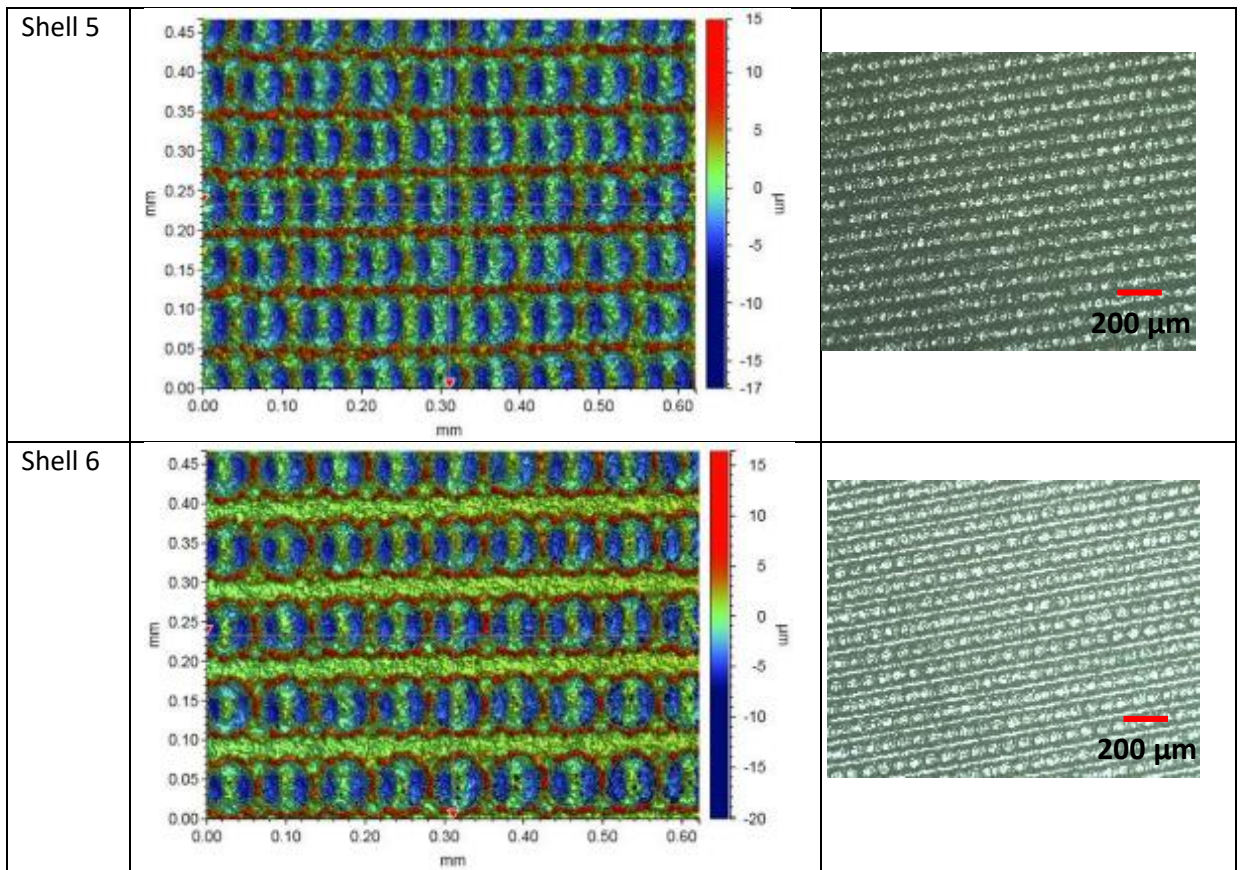


Table 5.6 Shell based biomimetic patterns created by laser surface texturing

Pattern	Topographical (Bruker) image	Microscope image (Zeiss)
Shell 1		
Shell 2		
Shell 3		
Shell 4		



The laser parameters used in this study resulted in the output of 15 biomimetic surfaces; 5 crab surfaces, 3 inverse crab surfaces and 6 shell based surfaces. Bruker images showed surfaces depth and width of laser area ( $\mu\text{m}$ ), which is shown in table 5.7.

Table 5.7 Depth and width of laser processed features of surfaces in this chapter

Surface Name	Depth ( $\mu\text{m}$ )	Width Of Laser Area ( $\mu\text{m}$ )	Experiment
Crab 1	-18	26.2	<b>1</b>
Shell 1	-20	18.6	
Crab 2	-11	34.2	
Crab 3	-7	34.1	
Crab 4	-21	16.5	<b>2</b>
Shell 2	-19	31.4	
Crab 5	-37	34.4	
Shell 3	-7	51.2	<b>3</b>
Shell 4	-7	53.4	
Shell 5	-17	15.6	
Shell 6	-20	16.6	
Shell 7	-14	35.6	<b>4</b>
Inverse Crab 1	-11	39.4	
Inverse Crab 2	-16	19.6	
Inverse Crab 3	-22	54.2	

### 5.3.2 Biofilm settlement

There was a significant difference in the settlement of biofilm across control and biomimetic micro-textured patterns (Experiment 1:  $\chi^2_{(4)} = 18.8$ ,  $p = 0.001$ ; Experiment 2:  $\chi^2_{(3)} = 13.5$ ,  $p = 0.004$ ; Experiment 3:  $\chi^2_{(4)} = 12.432$ ,  $p = 0.014$ ; Experiment 4:  $F_{(23)} = 11.3$ ,  $p < 0.001$ , Figure 5.2). Control samples in experiment 1 had significantly higher settlement of biofilm (median = 3208, LQ = 2612, UQ = 3432) than biomimetic laser textured patterns (Crab 1: median = 84, LQ = 80, UQ = 136,  $p = 0.002$ ; Shell 1: median = 460, LQ = 436, UQ = 488,  $p = 0.003$ ; Crab 2: median = 60, LQ = 36, UQ = 64,  $p = 0.001$ ; Crab 3: median = 100, LQ = 92, UQ = 200,  $p = 0.002$ , figure 5.2a). Post hoc tests did not reveal any significant difference within experiment 2 (median = 6052, LQ = 4440, UQ = 10780; Crab 4: median = 156, LQ = 108, UQ = 224,  $p = 0.092$ ; Shell 2: median = 316, LQ = 212, UQ = 356,  $p = 0.095$ ; Crab 5:

median = 92, LQ = 88, UQ = 180,  $p=0.091$ , figure 5.2b). Control samples in experiment 3 had significantly higher settlement of biofilm (median = 9572, LQ = 3540, UQ = 13080) than biomimetic laser textured patterns (Shell 3: median = 64, LQ = 56, UQ = 68,  $p=0.001$ ; Shell 4: median = 88, LQ = 72, UQ = 108,  $p=0.001$ ; Shell 5: median = 68, LQ = 40, UQ = 84,  $p=0.001$ ; Shell 6: median = 92, LQ = 48, UQ = 152,  $p=0.001$ , figure 5.2c). Control samples in experiment 4 had significantly higher settlement of biofilm (median = 19892, LQ = 12740, UQ = 23924) than biomimetic laser textured patterns (Shell 7: median= 252, LQ= 224, UQ= 344,  $p<0.001$ ; Inverse crab 1: median= 200, LQ= 224, UQ= 208,  $p<0.001$ ; Inverse crab 2: median= 104, LQ= 64, UQ= 204,  $p<0.001$ ; Inverse crab 3: median= 10720, LQ= 6256, UQ= 12820,  $p=0.029$ , figure 5.2d). No significant differences were found between biomimetic patterns except for Shell 1 (median= 460, LQ= 436, UQ= 488) which has significantly higher biofilm settlement than Crab 2 (median= 60, LQ= 36, UQ= 64,  $p=0.006$ ) and Crab 3 (median = 100, LQ = 92, UQ = 200,  $p=0.021$ ).

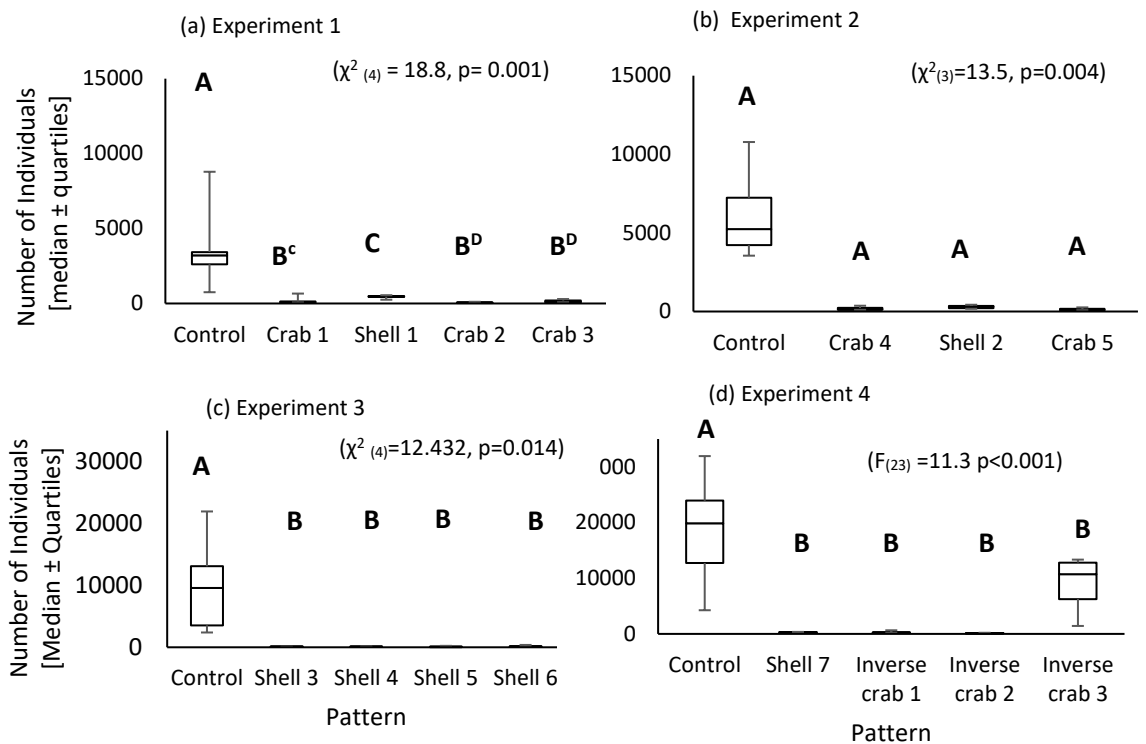


Figure 5.2 The settlement of biofilm [median ± quartiles] settled across biomimetic micro-textured patterns where (a) is experiment 1, (b) is experiment 2, (c) is experiment 3 and (d) is experiment 4. Overall statistical test is displayed on figure, **A, B** and **C** represent significant differences between groups in post hoc tests.

### 5.3.3 Position

PERMANOVA was used to analyse the relationship between settlement and the position of settlement and found there was significant differences in settlement of individuals between patterns in relation to position (Experiment 1, Pseudo F=15.848,  $p=0.0001$ ; Experiment 2, Pseudo F=7.3795,  $p=0.0006$ ; Experiment 4, Pseudo F= 13.436,  $p=0.0001$ ; Figure 5.3*i*). There was not a significant difference in settlement of individuals between patterns in relation to position for shell inspired patterns tested in experiment 3 (Pseudo F=1.48 ,  $p=0.195$ ). For the experiments in which there was a significant difference in the settlement of settlement (experiment 1, and 3), it was found that position 1 and 2 were most important in explaining the variance in the settlement, as the lines on the PCO graphs (Figure 5.3a,c,d) illustrate as the v1 (position 1) and v2 (position 2) are the longest.

Pairwise tests for experiment 1 showed that all patterns were significantly different from each other with significant differences between crab 1 and shell 1 ( $t=5.2596$ ,  $p=0.007$ ), crab 1 and crab 2 ( $t=4.251$ ,  $p=0.012$ ), crab 1 and crab 3 ( $t=3.4802$ ,  $p=0.008$ ), shell 1 and shell 3 ( $t=4.3759$ ,  $p=0.006$ ), shell 1 and crab 3 ( $t=3.4807$ ,  $p=0.009$ ) and crab 2 and crab 3 ( $t=2.6374$ ,  $p=0.02$ ). These significant differences are illustrated on Figure 5.3a as the PCO graph shows crab 1 is strongly linked to position 2 (v2; red circle) and away from the cluster of other surfaces; shell 1, crab 2 and crab 3.

Pairwise tests for experiment 2 showed that there was not a significant difference between crab 4 and shell 2 ( $t=1.7354$ ,  $p=0.0859$ ), but there were significant differences between crab 5 and crab 4 ( $t=3.2909$ ,  $p=0.0076$ ) and crab 5 and crab 4 ( $t=2.9524$ ,  $p=0.0155$ ). These significant differences are illustrated on Figure 5.3b as the PCO graph shows crab 4 and shell 2 are separate to crab 5. The PCO found that crab 4 and shell 2 are aligned within the same direction as position 1. Crab 5 pattern is spread out between position 1 and 2 on the PCO. Position 1 and 2 are most important in explaining the variances as they have the longest lines.

Pairwise tests for experiment 4 showed that there was a not a significant difference shell 7 and inverse crab 1 ( $t=0.458$ ,  $p=0.876$ ), but significant between shell 7 and inverse crab 2 ( $t=1.92$ ,  $p=0.04$ ), shell 7 and inverse crab 3 ( $t=4.47$ ,  $p=0.008$ ), inverse crab 1 and inverse crab 2 ( $t=2.1$ ,  $p=0.017$ ), inverse crab 1 and inverse crab 2 ( $t=4.57$ ,  $p=0.007$ ) and inverse crab 2 and inverse crab 3 ( $t=4.66$ ,  $p=0.01$ ). These significant differences are illustrated on figure 5.3d as the PCO graph shows shell 7 and inverse crab 1, inverse crab 2 and inverse crab 3. Position 2 is most important in explaining the variances as they have the longest line.

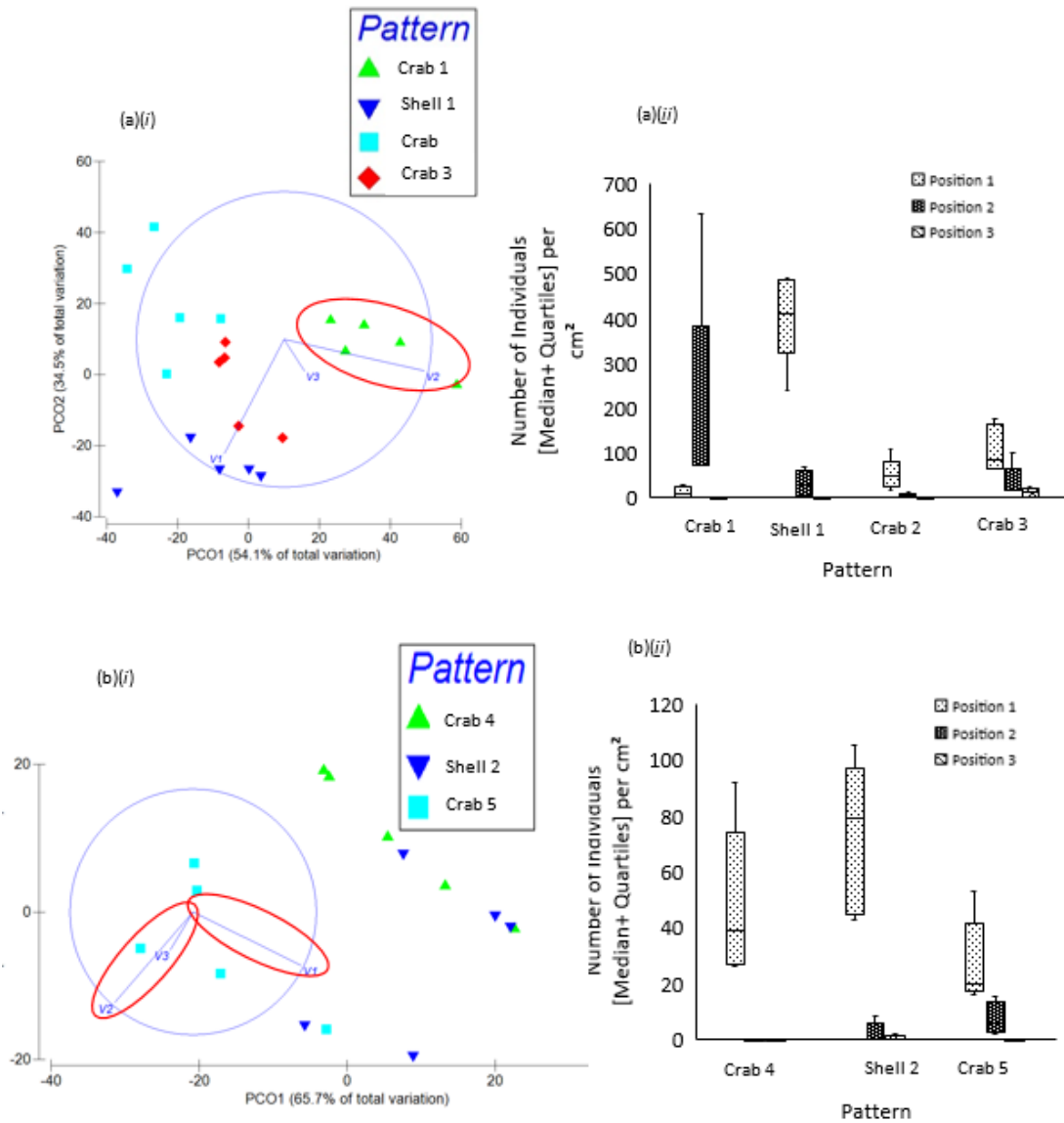


Figure 5.3 (i) Principal Component Ordination for the settlement of biofilm settled in relation to position 1 (v1) position 2 (v2) and position 3 (v3) where (a) is experiment 1, (b) is experiment 2, (c) is experiment 3 and (d) is experiment 4.

(ii) The number of individuals [median  $\pm$  quartiles] settled in all three positions on bio-inspired micro-textured patterns where (a) is experiment 1, (b) is experiment 2, (c) is experiment 3 and (d) is experiment 4.

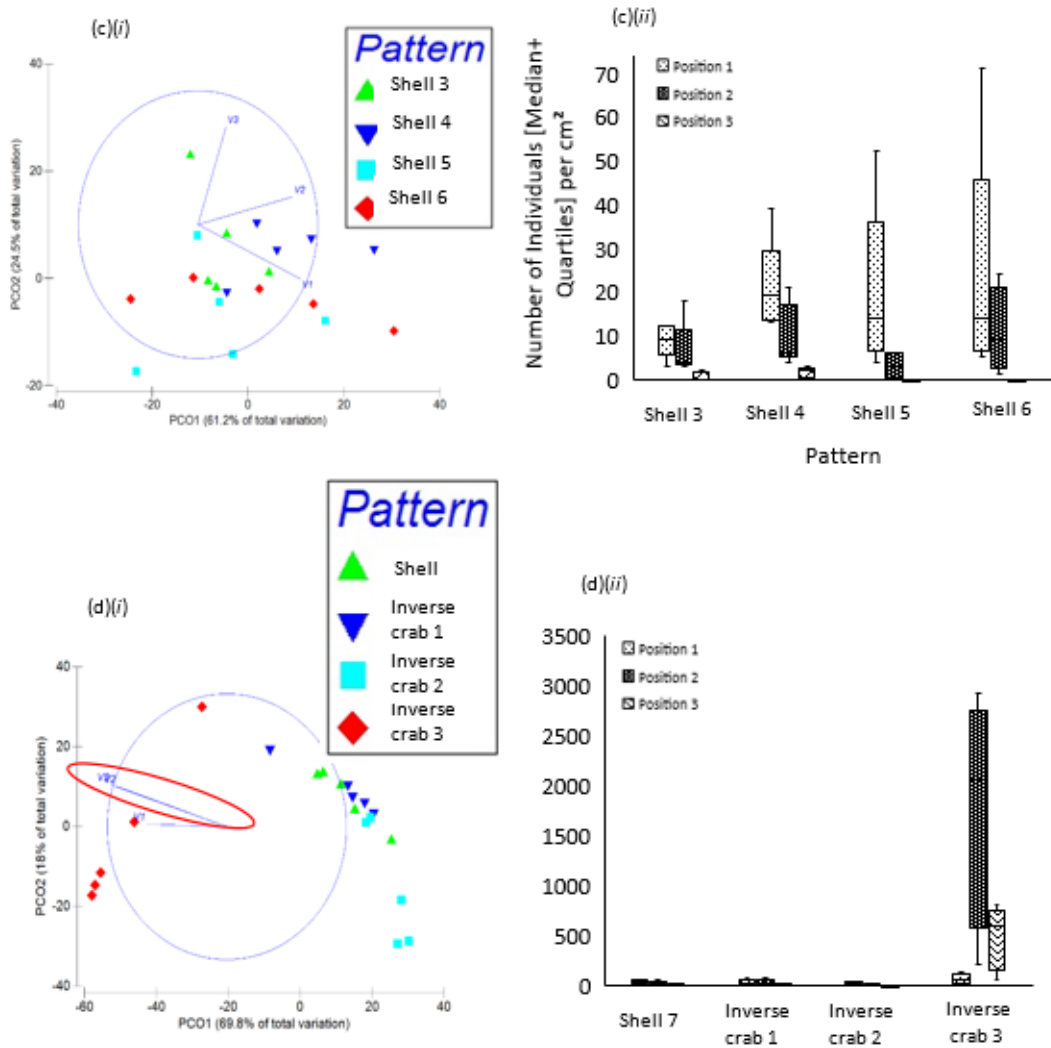


Figure 5.3 (i) Principal Component Ordination for the settlement of biofilm settled in relation to position 1 (v1) position 2 (v2) and position 3 (v3) where (a) is experiment 1, (b) is experiment 2, (c) is experiment 3 and (d) is experiment 4.

(ii) The number of individuals [median  $\pm$  quartiles] settled in all three positions on bio-inspired micro-textured patterns where (a) is experiment 1, (b) is experiment 2, (c) is experiment 3 and (d) is experiment 4.

#### 5.3.4 Position per pattern

Position 1 was most important in contributing to the dissimilarity in biofilm settlement in experiment 1 (Crab 1 and Shell 1; average dissimilarity 62.19%, position 1 contribution, 71.51%; Crab 1 and Crab 2; average dissimilarity 64.63%, position 1 contribution, 30.36%; Crab 1 and Crab 3; average dissimilarity 50.67%, position 1 contribution, 45.31%; Shell 1 and Crab 2; average dissimilarity 51.64%, position 1 contribution, 77.51%; Shell 1 and Crab 3; average dissimilarity 36.54%, position 1 contribution, 65.3%; Crab 2 and Crab 3; average dissimilarity 37.38%, position 1 contribution, 36.77%). There was a significant difference settlement in positions 1 between crab 1, shell 1, crab 1 and crab 3 patterns ( $\chi^2_{(3)} = 16.553$ ,  $p = 0.001$ ). There was significantly more settlement in position 1 on Shell 1 pattern (median = 102, LQ = 102, UQ = 121) than crab 1 (median = 2, LQ = 1, UQ = 5,  $p < 0.01$ ), crab 2 (median = 12, LQ = 9, UQ = 14,  $p < 0.01$ ) and crab 3 (median = 21, LQ = 16, UQ = 37,  $p < 0.01$ ; Figure 5.4a).

Position 1 was most important in contributing to the dissimilarity in biofilm settlement in experiment 2 (Crab 4 and Shell 2; average dissimilarity 21.53%, position 1 contribution, 67.4%; Crab 4 and Crab 5; average dissimilarity 32.08%, position 1 contribution, 44.85%; Shell 2 and Crab 5; average dissimilarity 33.12%, position 1 contribution, 60.93%). There was significant difference settlement in position 1 between crab 4, shell 2, and crab 5 patterns (Position 1;  $\chi^2_{(2)} = 6.140$ ,  $p = 0.046$ ; Crab 4; median = 39, LQ = 27, UQ = 56; Shell 2; median = 79, LQ = 46, UQ = 89; Crab 5; median = 20, LQ = 18, UQ = 30). There was significantly more settlement in position 1 on shell 2 than crab 5 ( $p = 0.029$ ; Figure 5.4b).

Position 1 was most important in contributing to the dissimilarity in biofilm settlement in experiment 3 (Shell 3 and Shell 4; average dissimilarity 23.74%, position 1 contribution, 44.67%; Shell 3 and Shell 5; average dissimilarity 28.9%, position 1

contribution, 45.29%; Shell 3 and Shell 6; average dissimilarity 27.07%, position 1 contribution, 45.42%; Shell 4 and Shell 5; average dissimilarity 30.14%, position 1 contribution, 37.1%; Shell 4 and Shell 6; average dissimilarity 27.62%, position 1 contribution, 41.3%; Shell 5 and Shell 6; average dissimilarity 29.75%, position 1 contribution, 51.82%). There was not significant difference settlement in position 1 between shell 3, shell 4, shell 5 and shell 6 patterns (Position 1;  $\chi^2$  (3) = 5.05,  $p = 0.168$ ; Shell 3; median = 9, LQ = 8, UQ = 12; Shell 4; median = 19, LQ = 14, UQ = 20; Shell 5; median = 14, LQ = 9, UQ = 20; Shell 6; median = 14, LQ = 8, UQ = 20; Figure 5.4c).

Position 2 was most important in contributing to the dissimilarity in biofilm settlement in experiment 4 (Shell 7 and inverse crab 1; average dissimilarity 19.51%, position 2 contribution, 37.39%; Shell 7 and inverse crab 2; average dissimilarity 34.46%, position 2 contribution, 39.88%; Shell 7 and inverse crab 3; average dissimilarity 67.79%, position 2 contribution, 61.72%; Inverse crab 1 and inverse crab 2; average dissimilarity 33.56%, position 2 contribution, 45.31%; Inverse crab 1 and inverse crab 3; average dissimilarity 66.21%, position 2 contribution, 61.08%; Inverse crab 2 and inverse crab 3; average dissimilarity 80.64%, position 2 contribution, 60.59%). There was a significant difference settlement in position 2 between shell 7, Inverse crab 1, Inverse crab 2, and Inverse crab 3 ( $\chi^2$  (3) = 13.674,  $p = 0.003$ ; Shell 7; median = 19, LQ = 12, UQ = 29; Inverse crab 1; median = 21, LQ = 18, UQ = 23; Inverse crab 2; median = 5, LQ = 1, UQ = 16; Inverse crab 3; median = 2044, LQ = 922, UQ = 2573). There was significantly more settlement within position 2 on inverse crab 3, than shell 7 ( $P = 0.001$ ), inverse crab 1 ( $P = 0.001$ ) and inverse crab 2 ( $p = 0.001$ ; Figure 5.4d).

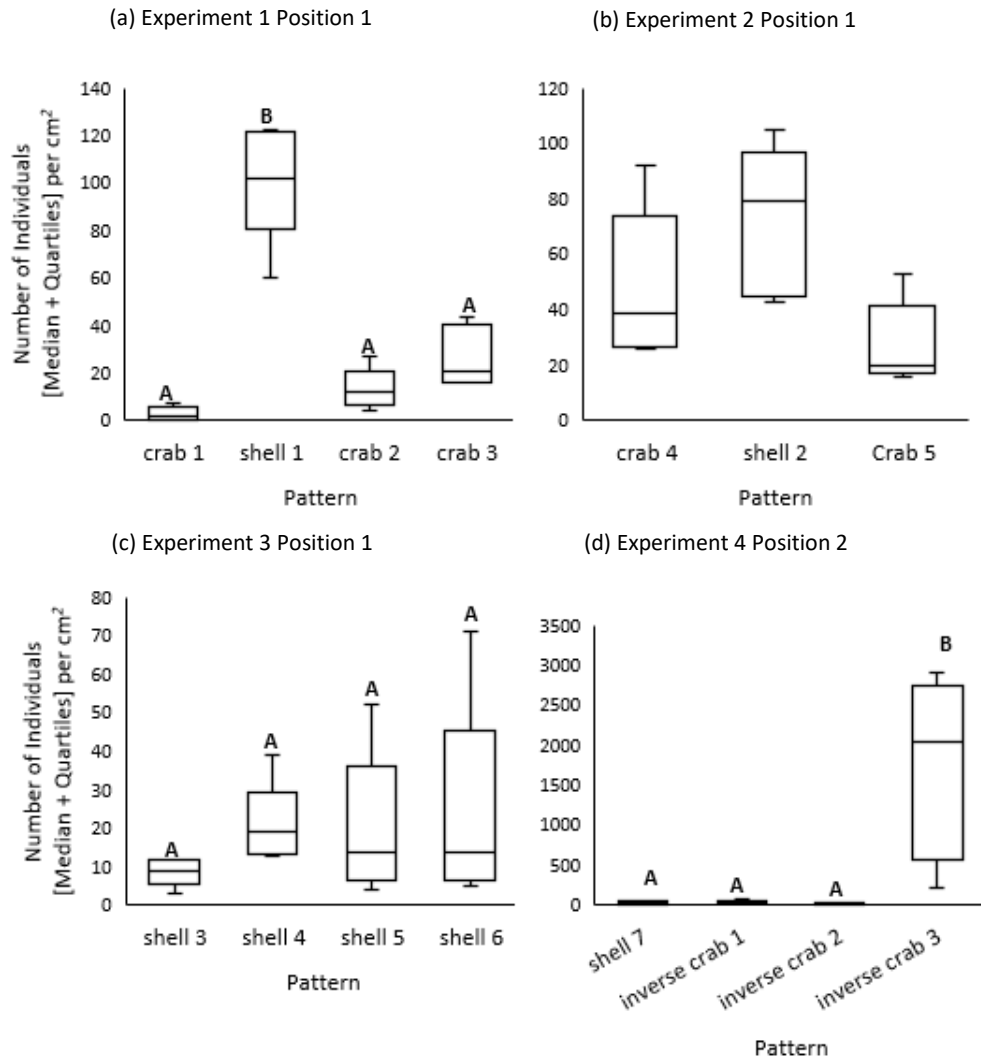


Figure 5.4 The number of individuals [median  $\pm$  quartiles] settled in the most important position on bio-inspired micro-textured patterns where (a) experiment 1, (b) experiment 2, and (c) experiment 3 are position 1, and (d) experiment and are position 2.

## 5.4 Discussion

This study aims to (a) use laser surface texturing create biomimetic crab and shell surfaces on marine grade steel and to (b) determine the effects of crab and shell biomimetic surfaces on the settlement of marine fouling. Biomimetic surfaces were able to be produced directly onto marine grade steel using laser surface texturing. A total of 15 biomimetic surfaces were created in this study; nine crab inspired surfaces and 6 shell inspired surfaces. Settlement of marine biofilm was reduced on all biomimetic surfaces compared to the unprocessed control.

### 5.4.1 Surface topography

Fifteen biomimetic surfaces were produced in this study by using laser surface texturing directly onto marine grade steel. The majority of studies focusing on biomimetic surfaces have concentrated on the use of photolithography as a tool to produce biomimetic surfaces on PMDS substrata (Hoipkemeier-Wilson *et al.*, 2004, Schumacher *et al.*, 2007b, Chung *et al.*, 2007, Carman *et al.*, 2006, Brzozowska *et al.*, 2014a, Sullivan and Regan, 2017, Schumacher *et al.*, 2007a, Schumacher *et al.*, 2008, Magin *et al.*, 2010a). This study is novel in that biomimetic surfaces were created directly onto marine grade (316L) steel using laser surface texturing as a tool. Previous studies used laser surface texturing to create biomimetic surface topographies based on *Mytilus galloprovincialis* and *Tellina plicata* which were processed on PMDS substrata (Scardino *et al.*, 2006b). However, this has not yet been achieved on marine grade steel until this study. Laser surface texturing has been used on other metals for antifouling effects such as Titanium alloy (Cunha *et al.*, 2016), however, this study did not create biomimetic topographies. The creation of biomimetic surfaces directly onto marine grade steel using laser surface texturing in this study is important as it allows for future development of biomimetic surfaces for marine fouling purposes. The use of laser surface texturing as a tool to create biomimetic surfaces

enables these surfaces to not be limited by substrata. This means that the biomimetic surfaces have the potential to be used in more areas across the marine industry, than if they were limited in to the use of PMDS only.

#### 5.4.2 Biofilm settlement

The fifteen biomimetic surfaces were tested for their antifouling potential in the marine environment and all biomimetic surfaces had a reduction in settlement marine biofilm compared to the unprocessed control. This is in agreement with previous biomimetic studies on crab (Brzozowska *et al.*, 2014a) and shell (Scardino *et al.*, 2006b) surfaces that have also found biomimetic surfaces have reduced the settlement of fouling micro-organisms. Inverse crab have also previously been found to have antifouling properties (Chen *et al.*, 2015), therefore inverse crab patterns were investigated in this study. However, unlike previous studies (Brzozowska *et al.*, 2014a, Scardino *et al.*, 2006b, Chen *et al.*, 2015) that have been lab based and tested on singular fouling species, this study has found that the crab, shell and inverse crab biomimetic surfaces are causing a reduction in fouling across the whole biofilm community, as they were tested in the marine environment where multiple species will be attempting to foul.

This study found that all laser processed biomimetic surface have antifouling effects against marine biofilm. This may be because all of the patterns may have worked in a similar way to reduce fouling. Fouling within the laser processed features (position 1) was important for all mixed crab, shell and inverse crab experiments (as shown by the PCO). Therefore, the laser pit and grooves (position 1) of all biomimetic patterns (crab, shell and inverse crab) are acting in a similar way to reduce fouling. The pit and grooves of all the biomimetic patterns grooves disrupt the previously smooth surface, therefore, creating an uneven surface topography, which reduces the attachment point of fouling organisms (Scardino *et al.*, 2008). Previous studies have investigated surfaces of various scales (4–512

$\mu\text{m}$ ) in relation to settlement and attachment points of various fouling species such as the diatom *Amphora* sp., the algae species *Ulva rigida* and *Centroceras clavulatum*, the tube worm *Hydroides elegans* and the bryozoan *Bugula neritina* and it was found that micro-topographical surfaces reduced the attachment points, and therefore reduced the overall fouling settlement of the fouling species (Scardino *et al.*, 2008). This is in agreement with the findings in this study in that position 1 on all biomimetic surfaces in this study possesses features such as pits, grooves and other laser induced surface features that reduce the attachment capabilities of fouling organisms, therefore reducing the overall settlement of marine biofilm. It is important to acknowledge that the laser induced features found in position 1 are limiting the fouling organisms that are larger than the features, as the attachment points will be reduced, and the surface area of the organism in contact with the surface will be less in situations where the texture of the surface is smaller than that of the fouling organism (Scardino *et al.*, 2008, Scardino *et al.*, 2006a).

Although the micro-topographical features found in the position 1 settlement area were important in reducing the overall settlement of marine fouling, it was found in this study that settlement of marine biofilm did still occur in this area. The present studies' finding that settlement still occurred within the grooves and pits of position 1 was popular for fouling organisms is in agreement with other studies in which fouling species *Ulva* preferred to settle within ridges of micro-topographies, next to the walls (Callow *et al.*, 2002, Hoipkemeier-Wilson *et al.*, 2004) and within  $2\ \mu\text{m}$  wide depressions of the sharklet surface (Magin *et al.*, 2010b). Macrofouling species such as *Balanus* sp. and *Polydora* sp have also been found to have a preference for settlement within grooves (Köhler *et al.*, 1999). If the aspect ratio of the fouling organism is smaller than the surface topography, there may be a preference in settling within the grooves and pits, therefore explaining why in this study there was settlement within position 1. The reason for settlement of fouling organisms within position 1 may be because of settling within pits and grooves of a texture

allows for increased number of attachment points between the fouling organism and the surface, therefore this enables a stronger attachment (Scardino *et al.*, 2008) and to protect from shear stress and predation (Bers and Wahl, 2004). This could explain why the micro-fouling organisms in this study are settling in the laser tracks, as it offers protection from the water flow, therefore making them less likely to be washed off from the surface. It also may be that the fouling organisms on the surfaces of this study have multiple methods of attachment, so they are able to overcome unfavourable conditions. This may be due to other attachment structures or the use of flagella to overcome the surface topography. This has been reported for peritrich ciliates (Becker *et al.*, 1998) and has also been reported for bacterial attachment of *Escherichia coli* (Friedlander *et al.*, 2013). Alternative settlement strategies such as flagella may buffer the effects of the unfavourable surface topography, and allow the fouling organism to access grooves and pits of the laser textures surface that are inaccessible to the whole body of the fouling organism (Velic *et al.*, 2019). By using these strategies, the fouling organism is overriding the geometric constraints of the laser textured grooves of biomimetic surface. This may explain why the grooves and pits of position 1 have still had a level of fouling, and are not completely foul free.

All four experiments showed that crab, shell and inverse crab patterns had similar influence on reducing marine biofilm settlement compared to the unprocessed control. As equal levels of settlement occurred across crab, shell and inverse crab biomimetic surfaces, the laser grooves and pits (position 1) created in all biomimetic surfaces must have been similar in size. Previous lab based studies showed reductions in fouling, and found that the fouling organism was 1.4 times the size of the width of the features of the micro-texture (Berntsson *et al.*, 2000, Petronis *et al.*, 2000, Chen *et al.*, 2015). Another study has shown that topography features with dimensions of 50–90% of the target cell diameter were ideal for limiting fouling (Scardino and de Nys, 2011). One study has changed the aspect ratio of the Sharklet™ surface to specifically target barnacle *Balanus amphitrite* cyprids as the

surface has shown previously good antifouling results for a different species. Therefore, in all the successful biomimetic surfaces, the size of the features have been smaller than the size of the fouling organism. The aspect ratio of surface structures to fouling organisms in this study could not be controlled, as the fouling organisms were not known, due to the testing occurring in the marine environment. However, all the surfaces in this study still had antifouling effects. This may be because the laser processed areas (position 1) in the patterns tested in our study has widths of 15-117  $\mu\text{m}$ . Fouling organisms in the biofilm vary in size from bacteria  $<1 \mu\text{m}$ , diatoms and algal spores (3-200  $\mu\text{m}$ ) and tubeworms, bryozoans, ascidians, and barnacle larvae (120–500+  $\mu\text{m}$ ) (Lejars *et al.*, 2012). Therefore, the width scale of all the crab, shell and inverse crab patterns in this study is generally smaller than that of popular fouling organisms. As all the micro-topographical features found within the laser processed areas (position 1) of each pattern were smaller than popular fouling organisms ( $<200\mu\text{m}$ ), this could explain why all biomimetic surfaces had similar levels of reduction of fouling. Features found within position 1 of crab, shell and inverse crab patterns were all of similar size, therefore they may have effected fouling in similar ways. Therefore, this explains why there were similar levels of fouling between the patterns.

In experiment one, Shell 1 pattern was compared against Crab 1, Crab 2 and Crab 3 patterns and it was found that Shell 1 had significantly more fouling than crab patterns (crab 2 and crab 3). This increase in settlement on the shell pattern is due to an increase in settlement within the laser tracks (position 1) on shell based patterns than on crab based patterns. This is in agreement with Hoipkemeier-Wilson's (2004) study that found increased settlement of *Ulva sp.* within the channels, and with very little settlement top of the ridges. The channels within their study are very similar to the shell based patterns within this study. The reason that shell based pattern had more fouling within the laser channels may be due to some fouling organisms being able to sense the energetically most

favourable location to settle (Callow *et al.*, 2002). It may take less energy for fouling organisms to settle within the laser processed channels (position 1) as the organism is in contact with all surfaces of the channel, both walls and the base, therefore the surface area contact is increased to a maximum (Hoipkemeier-Wilson *et al.*, 2004). As it takes less energy to settle here, it became a popular choice for fouling organisms, therefore increasing the level of fouling within shell 1 pattern.

However, shell patterns when tested alone (experiment 3) did not find this increase settlement preference within position 1, in fact they did not show a preference in settlement of fouling, therefore they are susceptible to fouling in all positions. This may be because all the shell-based patterns tested in experiment 3 had very similar micro-topographies so there was no distinct difference between any of the patterns and the control.

Although discussed above all patterns had a similar reduction of levels of fouling, where in which this settlement occurred was different for two main patterns (crab 1 and inverse crab 3). In these patterns, the majority of settlement occurred on position 2. It was found that the flat unprocessed areas within a micro-topographical pattern (position 2) were the most important position in explaining the variance in settlement for crab and inverse crab patterns. The settlement within position 2 may be important in effecting the settlement of marine biofilm as it is the unprocessed flat area between laser processing, therefore it may be the preferred option for fouling organism to settle. Similar results were found in a study by (Rusen *et al.*, 2014) who found that OLN 93 cells preferred to settle on the free space in-between irradiated areas. This may be similar to what occurred in crab 1 pattern, as position 2 had the highest settlement of settlement, meaning that the most settlement occurred on the flat parts of the pattern, where no laser surface texturing had taken place. The reason the flat unprocessed areas (position 2) were important in the settlement of marine biofilm is that fouling species are not limited settling, as they are able

to form multiple attachment points on areas that are smooth (Scardino *et al.*, 2006b). The decrease in overall biofilm from control patterns to biomimetic-textured patterns may be due to the decrease in availability of position 2 space. As fouling organisms may only be able to settle on the pattern where position 2 is available, by limiting the available free space by creating micro-textures on the surface, there is less chance of fouling (Scardino *et al.*, 2006a).

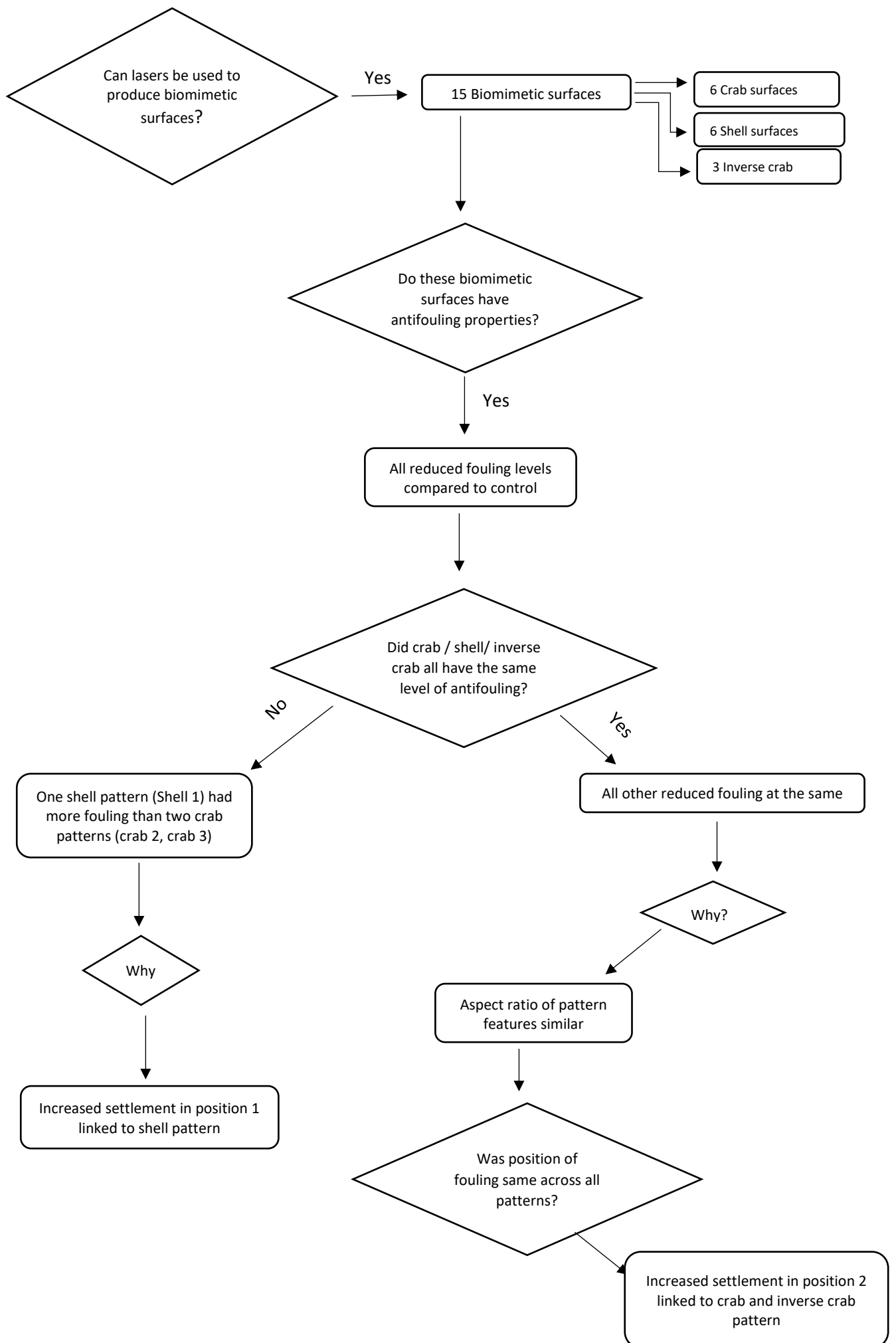


Figure 5.5 Flow chart of this study's findings

This study was a proof of concept study to investigate if (a) laser surface texturing could be used to create biomimetic surfaces directly onto marine grade steel and (b) if these surfaces have antifouling potential. It was found in this study that both aims can be met, as lasers surface texturing was used to bio-mimic crab and shell pattern surfaces directly onto marine steel, and these surfaces were tested and were found to have antifouling properties (Figure 5.5). A surface energy model created by correlating wettability to bio-adhesion had previously lead to the design of other biomimetic surfaces such as Sharklet™ as it predicted that biomimetic micro-textured surfaces would have antifouling effects vs smooth control surfaces (Carman *et al.*, 2006, Ball, 1999, Bechert *et al.*, 2000). This trend predicted by the model that biomimetic micro-textured surfaces would have antifouling effects have been confirmed in this study, along with other studies (Schumacher *et al.*, 2007b, Hoipkemeier-Wilson *et al.*, 2004, Brzozowska *et al.*, 2014b).

A development model showed a key issue with proof of concept studies is how to transfer the concept to marketable products (Lindblad, 2009). Within this study, areas where found in which the patterns could be approved upon before becoming market acceptable products. One of the areas that could be improved is the settlement within position 2. Settlement of fouling in position 2 increased overall biofouling on crab, and inverse crab patterns. If this settlement could be targeted with further studies, it would enable the surfaces to provide better fouling potential and therefore be one step along in going from proof of concept to a marketable product.

Overall, this study has shown that it is possible to create biomimetic antifouling surfaces directly onto marine grade steel using crab and shell surfaces as bio-inspiration. The majority of the biomimetic surfaces has similar reductions in fouling compared to the unprocessed control, and therefore, may be useful in the future as a antifouling technology.

Chapter 6 Biomimicry: Investigating multi-scale multi-feature biomimetic patterns for their antifouling effect.

## 6.1 Introduction

In chapter 5 biomimetic laser textured surfaces were developed and produced demonstrating antifouling efficacy towards marine biofilm. These surface textures were inspired by singular species of crab or mussel. However, multi-scale and multi-feature surface textures have been found to have greater antifouling effects, than single textures alone (Schumacher *et al.*, 2007, Sullivan and Regan, 2017).

The use of multi-scale and multi-feature surfaces for marine antifouling has been limited to very few studies (Schumacher *et al.*, 2007; Efimenko *et al.*, 2009). Multi-scale textures are surfaces that exhibit one type of feature at different scales (e.g. riblets of sharklet are one feature at different lengths; Schumacher *et al.*, 2007). The study (Schumacher *et al.*, 2007b) involving multi-scale textures centre around the creation of Sharket™ which features the same trapezium shape at difference scales, therefore is multi-scale but not multi-feature (Figure 6.1; Schumacher *et al.*, 2007b). Another study created multi-scale uniaxial hierarchically wrinkled surface topographies (uHWST) on PDMS substrate for antifouling efficacy testing in both lab and marine environments (Efimenko *et al.*, 2009) , these surfaces exhibit wrinkles of different sizes, but no other features, so therefore are multi-scale (Figure 6.1).

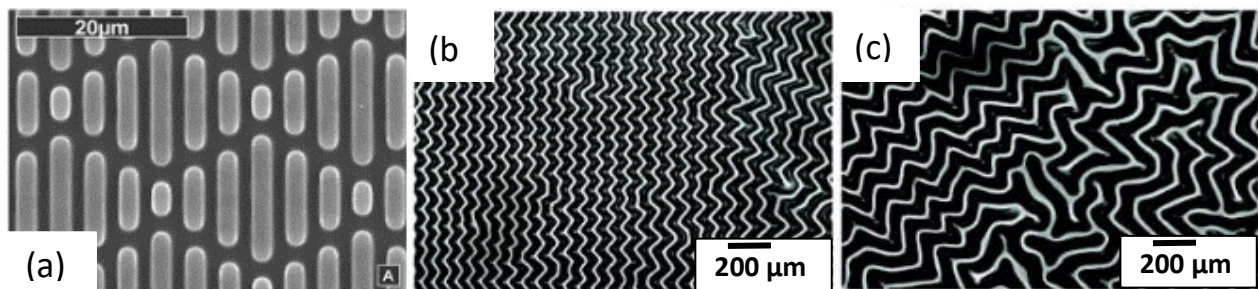


Figure 6.1 Multi-scale textures of (a) Sharklet™ pattern (Schumacher *et al.*, 2007b), and (b) and (c) where both are uHWSST textures at different part of the same sample showing the difference in scale of wrinkles (Source: Efimenko *et al.*, 2009).

However, there are very few other studies on truly multi-scale and multi-feature micro-textured patterns for the marine environment. Multi-feature micro-textures exhibit two or more different features (e.g. different triangles and pillars, Figure 6.2; Schumacher *et al.*, 2007; Sullivan and Regan, 2017). Where they are present (Sullivan and Regan, 2017, Schumacher *et al.*, 2007b), they are created on PDMS substrates using photolithography techniques.

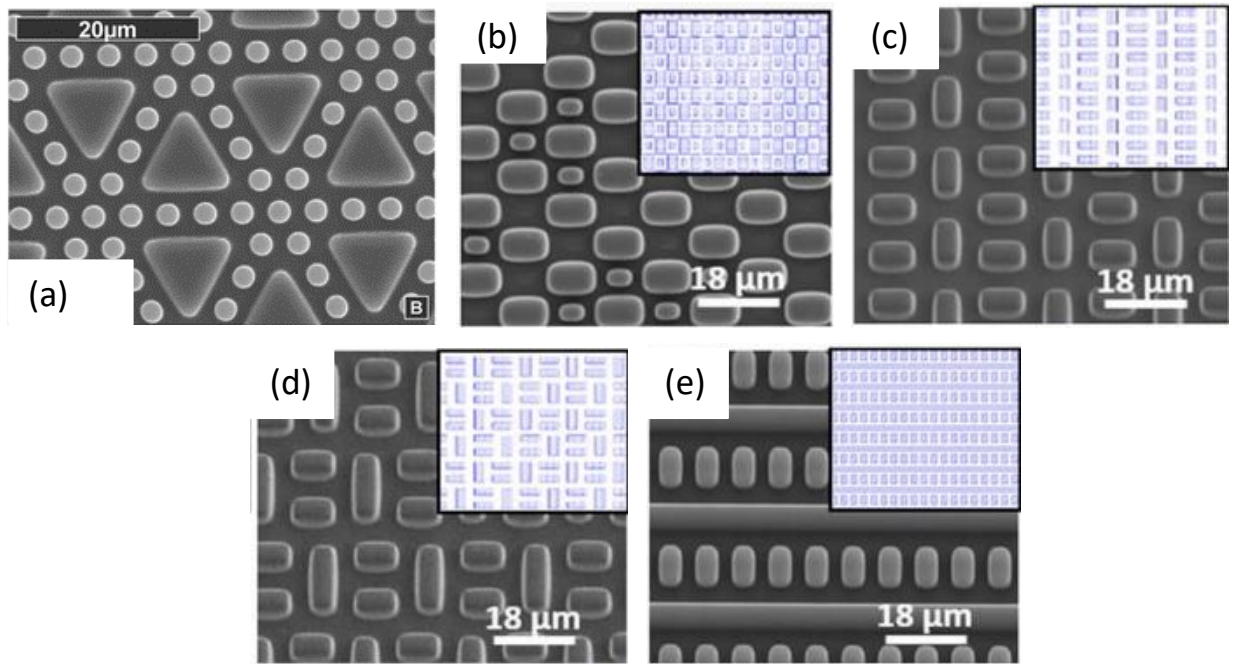


Figure 6.2 Multi-scale and multi-feature textures from (a) Schumacher *et al.*, (2007) and (b-e) (Sullivan and Regan (2017)). All surfaces were created on PDMSe using photolithography techniques.

The previous studies of multi-scale and multi-feature surfaces are all on polymer substrates using various surface texturing techniques. However, the use of multi-scale, multi-feature surface textures as an antifouling technology has not been investigated for stainless steel substrata. Laser surface texturing was demonstrated previously as a tool with which to rapidly and conveniently modify surface topography of stainless steel over various scales without the need for further processing (Engleman *et al.*, 2005, Brown and Arnold, 2010). The process of laser surface texturing with multiple scaling showed to alter wettability of surfaces (Razi *et al.*, 2016), alter lubrication (Segu *et al.*, 2013) and improve bone growth and therefore recovery time for hip replacements (Brown and Arnold, 2010).

The aim of this study was to (a) demonstrate the application of laser surface texturing to create multi-scale and multi-feature biomimetic micro-textured surfaces and to (b) determine the antifouling efficacy of these surfaces.

## 6.2 Methods

The same experimental set up as described in chapter 3 was used to carry out this investigation.

### 6.2.1 Laser set up of combined patterns

To create multi-scale and multi-feature patterns draft-sight™ software was utilised as a drawing tool, which allowed for a larger control of the laser path, as there was freedom to work outside of the X Y axis, and create shapes and diagonal lines for the laser path to follow. Draftsight (Dassault Systèmes SolidWorks Corporation) allows for Drawing eXchange Format (.dxf files) to be created and then imported into the SAMLight laser processing software. A two stage process was implemented for creating combined patterns: (a) a based pattern and (b) an overlay pattern. All base and overlay patterns were inspired by previous bio-inspired patterns tested in chapter 5. Base patterns were processed first onto the metal, and overlay patterns on top, to form a multi-feature, multi-scale combined pattern.

Although in chapter 4 multiple passes demonstrated improved antifouling efficacy compared to a singular pass, multiple passes were also distorting the micro-texture. So in this study a single pass was applied to facilitate a very precise biomimetic micro texture without disruptions from the multiple melt and hardening effects of multiple passes.

#### 6.2.1a Base micro-topography

Base patterns were developed using inspiration from the patterns in chapter 4. Base patterns were laser processed at 100%, 400 speed, 25khz, 200ns, with a single pass.

### 6.2.1b Overlay micro-texture

Overlay patterns were developed using inspiration from the patterns in chapter 4. Overlay patterns were laser processed using 80% power, 200 speed, 25khz, 200ns, with a single pass. Overlay patterns were smaller in diameter and depth than base patterns with the aim of filling the unprocessed areas between base patterns.

### 6.2.1c Multi-feature micro-texture

Multi-feature micro-textures were developed by combining base and overlay patterns for each experiment. The base was first processed onto the steel using 100%, 400 speed, 25khz, 200ns, with a single pass, then the overlay pattern was laser processed using 80% power, 200 speed, 25khz, 200ns, with a single pass.

### 6.2.2 Pattern design

This treatment was a base only micro-topography. Draft-sight features allowing for multiple scales of the same feature, in this case a circle, and allowing for movability and precision of the features. The circular feature was chosen as it was directly inspired by the shore crab.

#### *6.2.1 Experiment 1: Multi-scale circles (M1)*

The objective of this experiment was to utilise the draft-sight software to create a combined pattern using multiple scales of the same circular feature. For experiment 1, data were on the size of the features on shore crabs were collected directly from topographical microscope images using line cross sectional measurements. These data were used to determine the size of the circle features that were used in the laser processing of patterns for experiment 1.

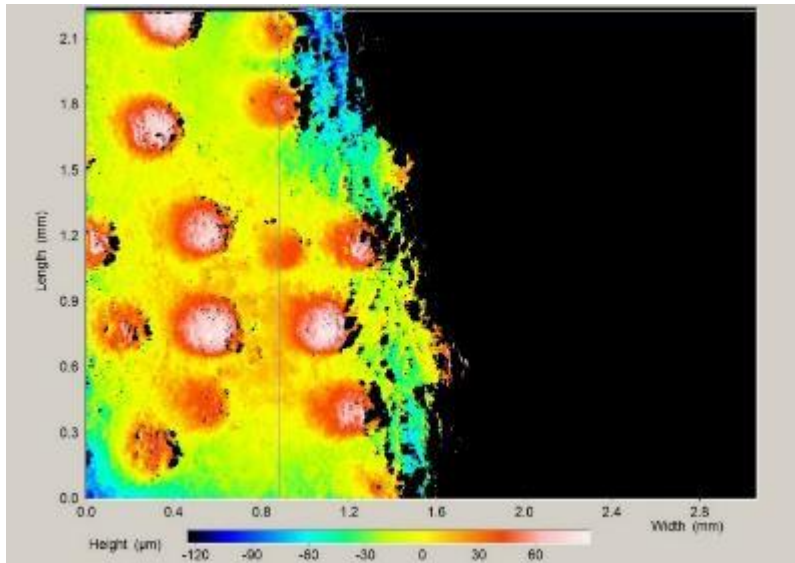


*Figure 6.3 3D micro-topographical scan of shore crab carapace*

From the GFM scans, cross sections of the surface were measured and data were collected on the width of the red circular peaks, as this was a target feature for biomimicry.

From the data collected from the GFM images, four patterns were designed to mimic the shape and scale of the shore crab peaks. The circular feature was constant, but the diameter was changed to three different scales to mimic the range of data collected from the shore crab. The patterns created were: (1) small circles which had a diameter of 230  $\mu\text{m}$ , which was the smallest measurement recorded from GFM images of shore crab; (2) medium circles, which had a diameter of 280  $\mu\text{m}$  that was the average measurement recorded from GFM images of shore crab; and (3) large circles which had a diameter of 360  $\mu\text{m}$ , which was the largest measurement recorded from topographical images of shore crab. In patterns 1 to 3 the circles were in an array. The fourth pattern created for this experiment was a combination of circles used in 1 to 3, but they were distributed freely rather than in an XY array, this is shown in Figure 6.4

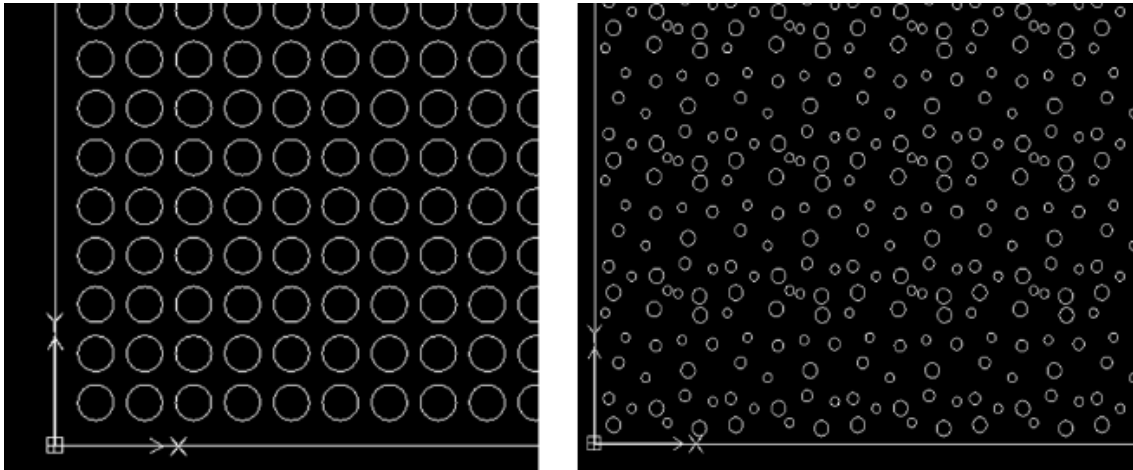


Figure 6.4 Draft sight design for experiment 1, where (a) diameter of circles was changeable for  $230\ \mu\text{m}$  for pattern 1,  $280\ \mu\text{m}$  for pattern 2 and  $360\ \mu\text{m}$  for pattern 3 and (b) where all three sizes were combined to create a combined pattern for pattern 4.

The pattern was drawn in the draft sight software and then imported into Samlight software using a DFX file, the pattern was able to be inverted in the laser process for the first time in the present study. This new method allowed the software to laser process in-between circular features and effectively cut them out from the surface to create raised platforms for the first time (Figure 6.5).

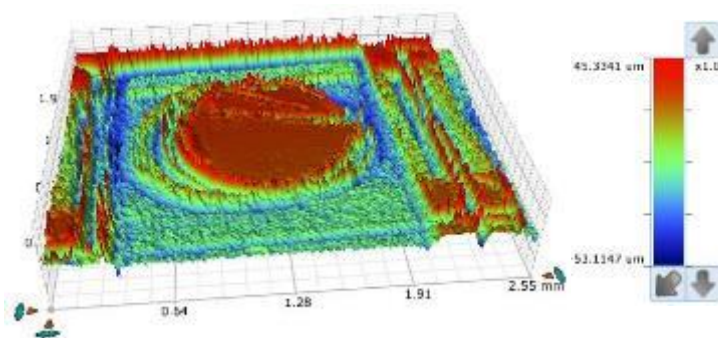


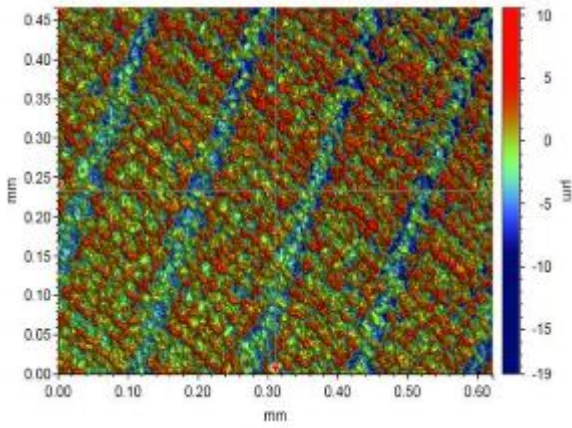
Figure 6.5 A white light interferometer scan of the circular “cut out” feature created by laser texturing of an inverted circular pattern drawn on draftsight (Dassault Systèmes SolidWorks Corporation) and imported into samlight laser software.

### 6.2.2 Experiment 2: Shell base and Crab overlay combination (Multi-feature 2)

The objective of this experiment was to utilise the draft-sight software to combine features of the cockle shell, and crab micro-textures tested in chapter 5 together to create a combined antifouling surface.

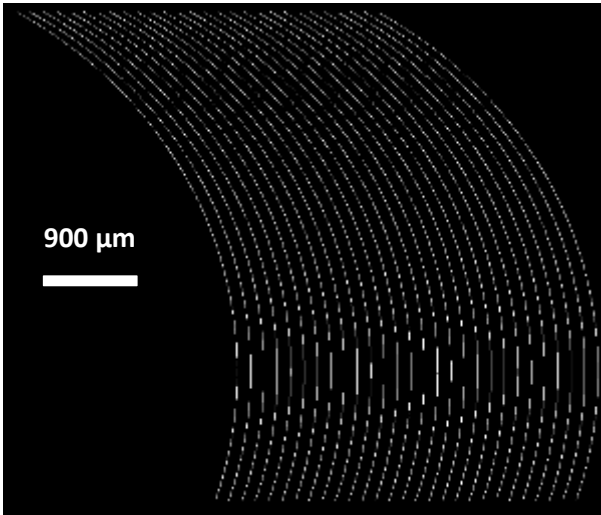
The bio-inspiration for this experiment originated from cockle and crab patterns used in chapter 5 (Figure 6.6). Although cockle shells were used to inspire patterns in Chapter 5 (experiment 3) the draft sight software allows for curvy lines to be drawn for the first time in the present study This novel pattern is based on the curvature of the cockle shell pattern inspired from topographical scan of specimens.

Shell 2 pattern (p.109)

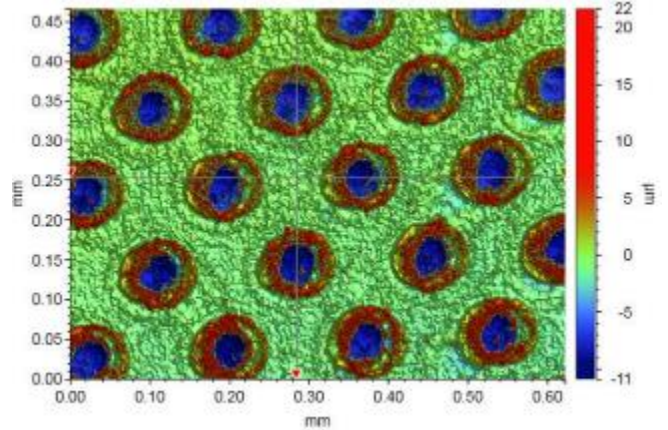


*Introduction of draft sight  
allow for curvy lines*

Base pattern: Curved shell lines



Inverse crab 1 pattern (p. 108)



*Circular features overlay  
between lines*

Combined pattern: Cockle base, crab overlay

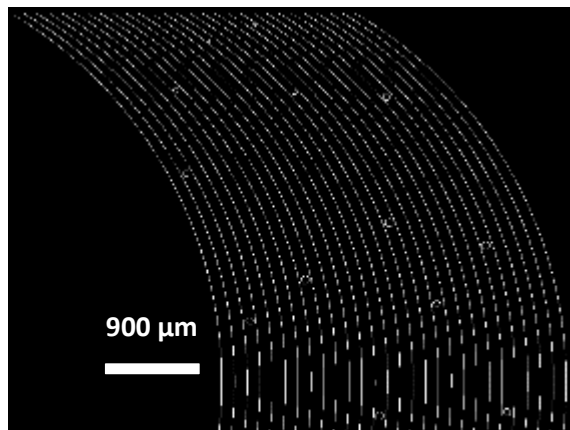


Figure 6.6 Flow chart of how combined pattern was reached for experiment 2 from patterns tested in chapter 4.

All patterns were drawn in draft-sight on a small scale, and then the array feature was used to repeat the pattern to fit the 50x50mm stainless steel coupon (Figure 6.7).

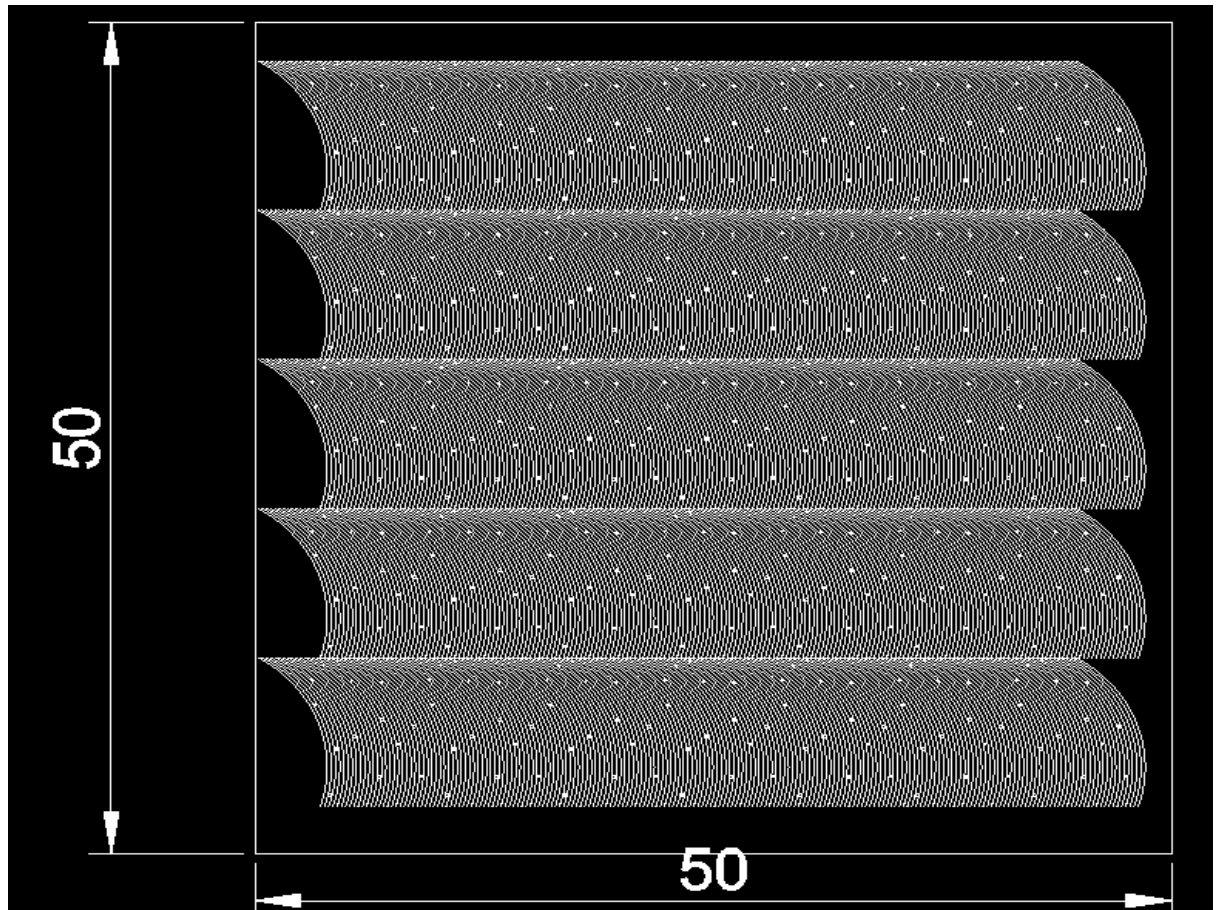


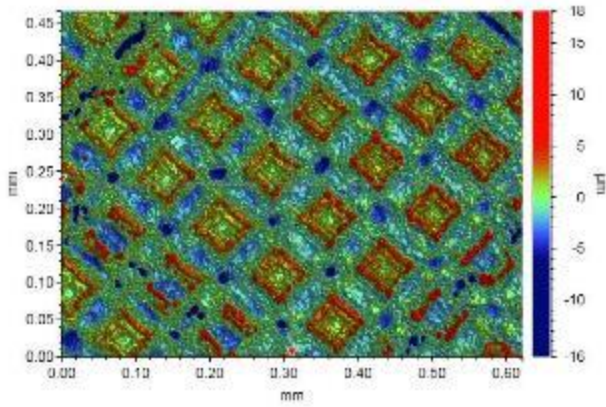
Figure 6.7 Example of pattern scaled up to 50x50mm.

### 6.2.3 Experiment 3: Crab base and shell overlay combination (Multi-feature 3)

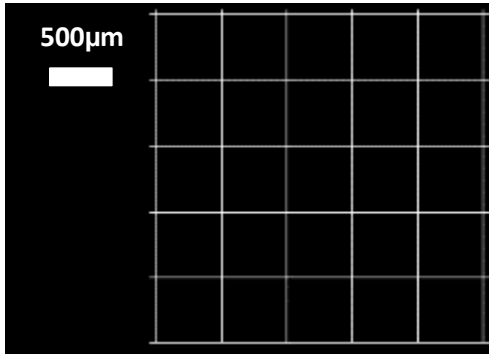
The objective of this experiment was to utilise the draft-sight software to combine features of micro-textures tested in chapter 5 together a combined antifouling surface that has a crab based an shell overlay. The choice of combining layers was to target fouling species of various scales, and to utilise antifouling features seen in different patterns by combining them for a stronger antifouling effect. This pattern was inspired by combining the base layer, which was inspired by the crab hatch with an overlay layer inspired by cockle shell to produce a final combined pattern, a flow diagram of this is shown below

(Figure 6.8). This bio inspiration for this pattern is based on combining crab based features found in crab 1 pattern, and shell 4 pattern (Figure 6.8).

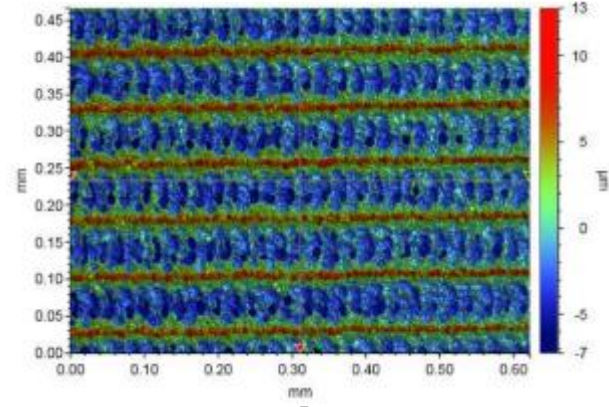
**Crab 1 pattern (p.107)**



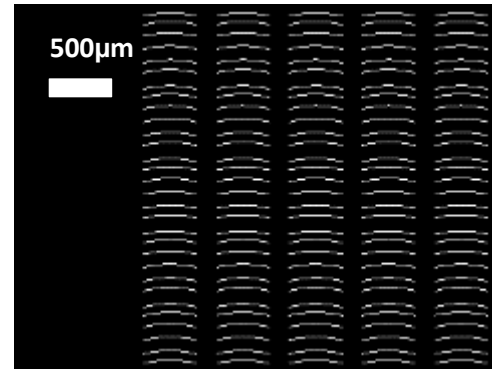
**Base**



**Shell 4 pattern (p.110)**



**Overlay**



**Combined pattern**

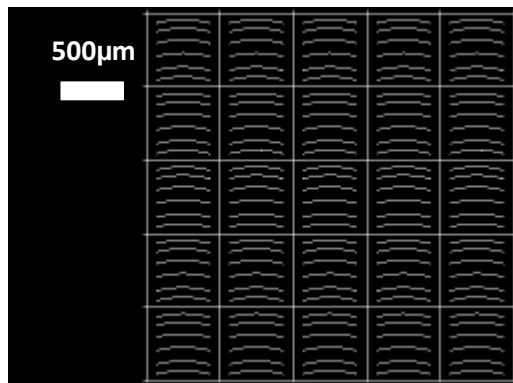


*Figure 6.8 Flow chart of how combined pattern was reached for experiment 3 from patterns tested in chapter 4.*

#### 6.2.4 Experiment 4: Crab based and Crab overlay combination (multi-feature 4)

The objective of this experiment was to utilise the draft-sight software to combine features of micro-textures tested in chapter 5 together to create a combined antifouling surface that had a crab base and crab overlay (Figure 6.9).

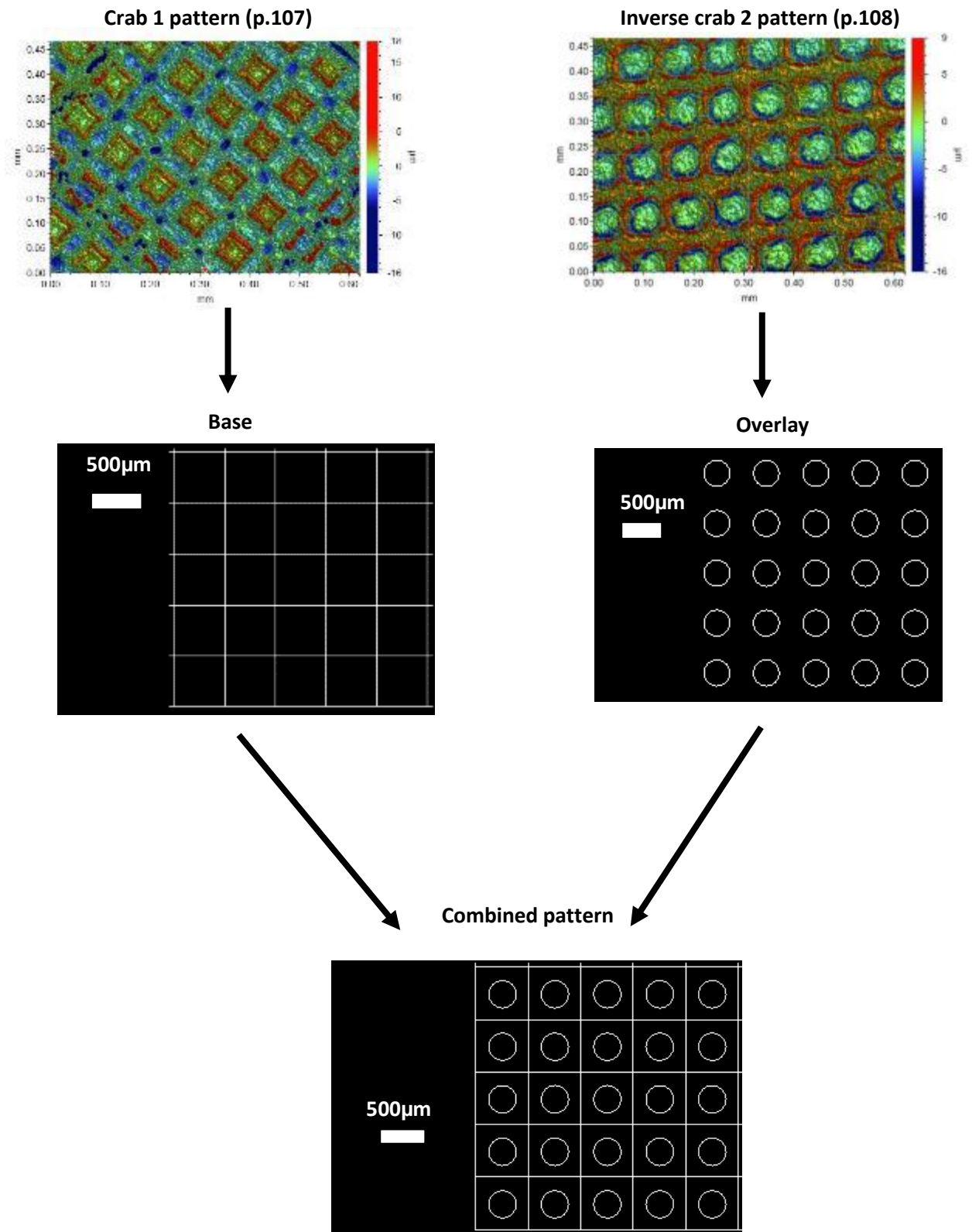


Figure 6.9 A flow chart diagram from crab and shell organism, to topographical scans, to patterns tested in chapter 5, to draft sight designs then to the final pattern tested.

#### 6.2.5 Experiment 5: Circular crab pattern and shell combination (Multi-feature 5)

The objective of this experiment was to utilise the draft-sight software to combine features of micro-textures tested in chapter 5 together to create a combined antifouling surface that was both multi- scale (circular features from experiment 1) and multi-feature (crab based and shell overlay). The final pattern was designed to combine features from experiment 1, 2, 3 and 4 into one final experiment (Figure 6.10).

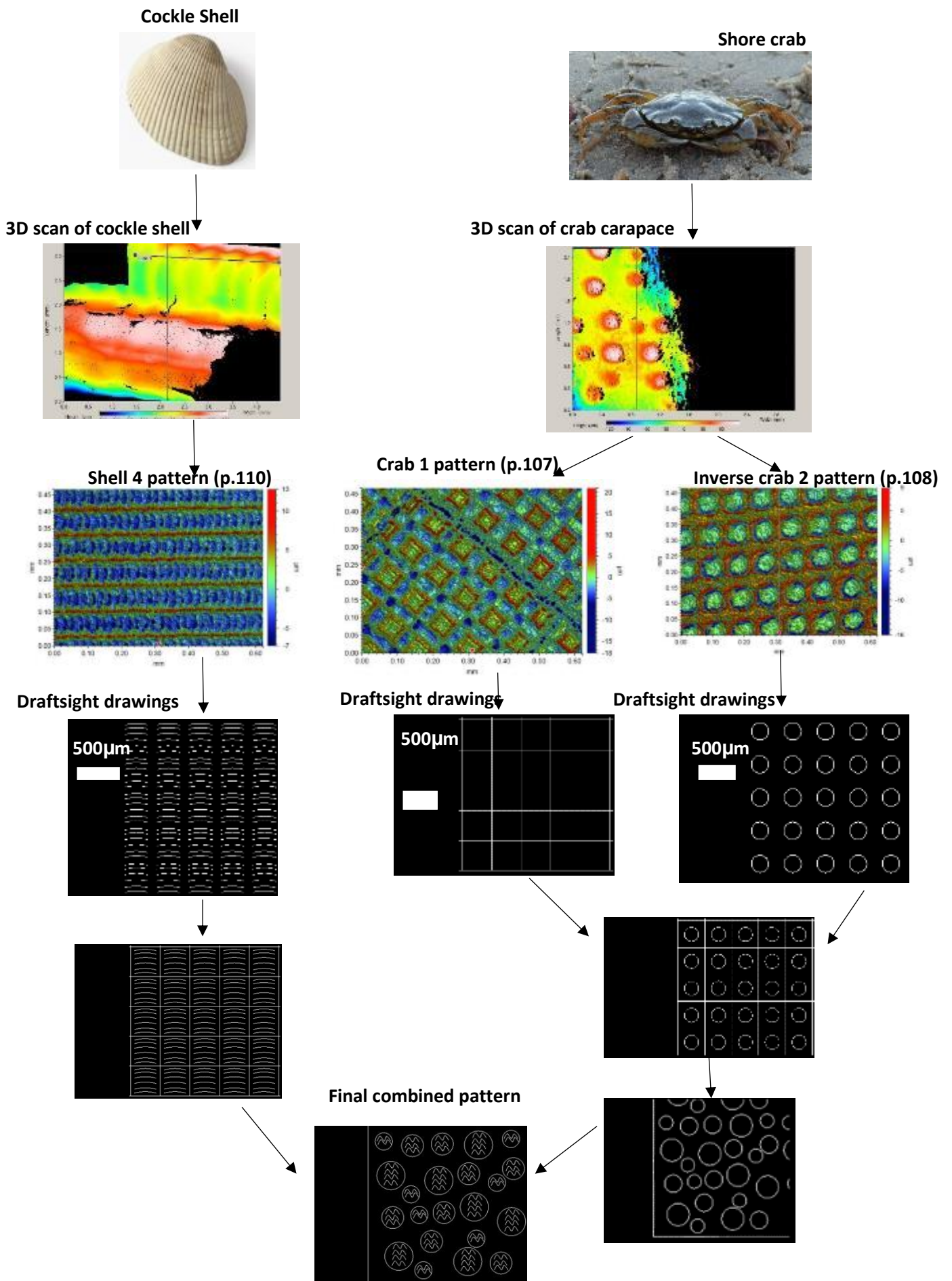


Figure 6.10 A flow chart diagram from crab and shell organism, to topographical scans, to patterns tested in chapter 5, to draft sight designs then to the final pattern tested.

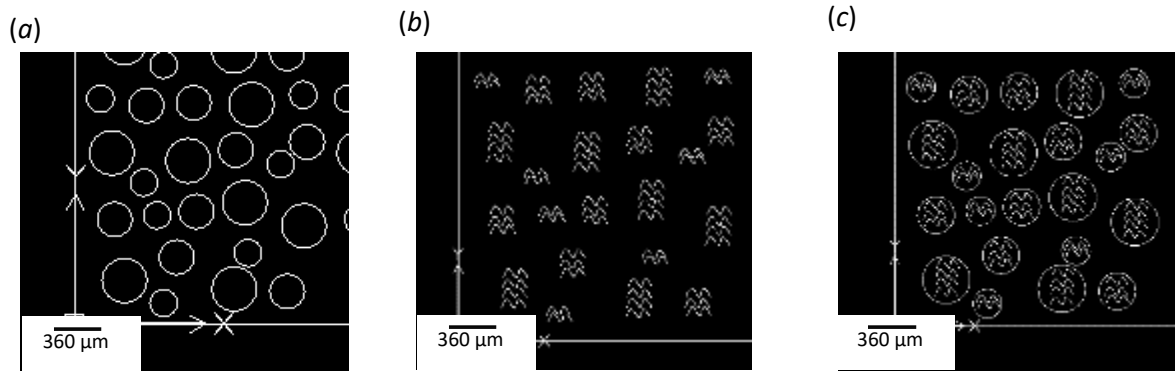


Figure 6.11 Draft sight designs of patterns where (a) is the base pattern inspired by shore crab, (b) is the overlay pattern inspired by cockle shell ridges and (c) is the combined pattern of both of them together.

### 6.2.3 Experimental time and set up to test the Antifouling Efficacy

The experiments were submerged during May to July 2018 for a 7 day period.

Experiment 1 was submerged 14<sup>th</sup> to 21<sup>st</sup> May 2018, Experiment 2, 3 and 4 was submerged 28<sup>th</sup> May to 4<sup>th</sup> June 2018 and experiment 5 was submerged 4<sup>th</sup> to the 11<sup>th</sup> June 2018. For further details on antifouling testing see section 3.4 (3.4.1 for study site and 3.4.1 for experimental set up).

#### 6.2.3.1 Statistical analysis

Biofilm settlement data was collected as outlined in section 3.5 (3.5.1 biofilm settlement, 3.5.2 Biofilm position on patterns). This data was analysed as outlined in section 3.5.2 Statistical analysis. Analysis of similarity (SIMPER; Clarke 1993) was also performed on the position data to identify the position that is most responsible for the dissimilarity in settlement between patterns.

#### 6.2.3.2 Diatom species identification

For species identification purposes, samples of each pattern within experiment 2,3,4 and 5 were selected for the diatom removal process. A whole 50x50mm panel of each pattern was scraped using a soft toothbrush to remove attached algae. Each panel and toothbrush was rinse into a test tube using distilled water. Hydrogen peroxide was added to this test tube, and test tubes were placed in a water bath at 80 degrees for 6 hours to

allow for oxidation to occur so that all organic matter is removed from the sample, and the silica diatom frustule shells are left for identification (Carr *et al.*, 1986).

Once removed from the water bath, the sample was topped up with distilled water and centrifuged at 4000rpm for 10 minutes, then decanted. This rinse process was repeated 4 times until the supernatant water had cleared. This process was to remove hydrogen peroxide from the samples. Diatoms were dried onto microscope cover slips and mounted using Naphrax resin which is of a high refractive order (R.I =1.74) (Hasle and Fryxell, 1970). Cleaned diatoms are colourless and transparent, they have a refractive index (R.I) of 1.44, so mounting in water (R.I. = 1-33) or glycerine jelly (R.I. = 1-41) is not sufficient for revealing the fine structure of the diatoms cells necessary for identification (Peabody, 1977). The cover slip is mounted onto a microscope slide, and heated on a hot plate (200°C) until bubbles cease, creating a permanent microscope slide ready for identification. Microscope slides were placed under Zeiss Axio Imager A2 With DIC (Differential Interference Contrast) and plan apochromat lenses, and diatoms species were identified using Round *et al.*, (1990) and abundance of each species was counted. This was undertaken for a small sample size, therefore, statistics could not be undertaken on the results, but this is discussed in the overall discussion section 7.4.

### 6.3 Results

There was not a significant difference in settlement between blocks for all experiments in this chapter (experiment 1,  $F_{(4,24)}=0.036$ ,  $p=0.997$ ; experiment 2,  $F_{(4,14)}=1.426$ ,  $p=0.295$ ; experiment 3,  $F_{(4,19)}=0.225$ ,  $p=0.902$ ; experiment 4,  $F_{(4,19)}=0.676$ ,  $p=0.619$ ; experiment 5,  $F_{(4,19)}=0.223$ ,  $p=0.921$ ), therefore blocks were ignored in further statistical testing.

#### 6.3.1 Surface Topography

For experiment 1, multiple scales were used (small, medium, large) and then multi-feature (a mix of all three) were created (Table 6.1).

Table 6.1 Topographical and microscope images of surfaces in experiment 1

Pattern	white light interferometer	Microscope
Small circles		
Medium circles		
Large circles		
Multi-feature 1 (m1)		

For experiments 2 to 5 a base pattern was created and an overlay pattern (missing for experiment 2), these patterns were combined to create a multi-feature pattern. The resulting biomimetic patterns and the multi-feature cross over patterns for experiments 2 to 5 are shown in corresponding tables 6.2, 6.3, 6.4 and 6.5.

Table 6.2 Topographical and microscope images of surfaces in experiment 2

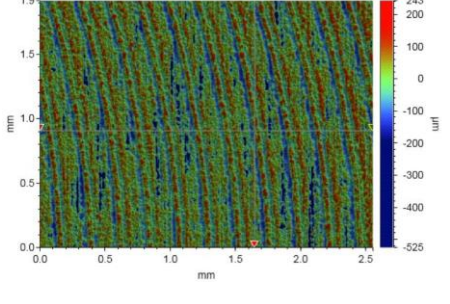
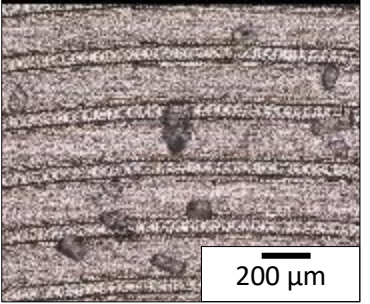
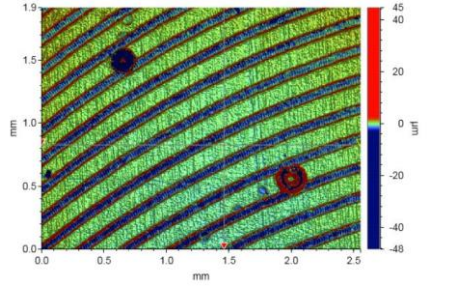
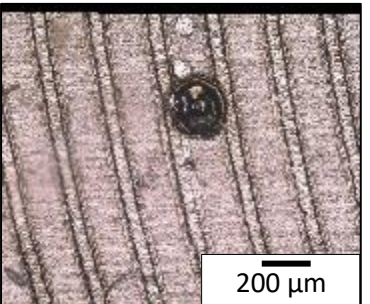
Pattern	White light interferometer	Microscope
Shell base		
Multi-feature 2 (M2)		

Table 6.3 Topographical and microscope images of surfaces in experiment 3

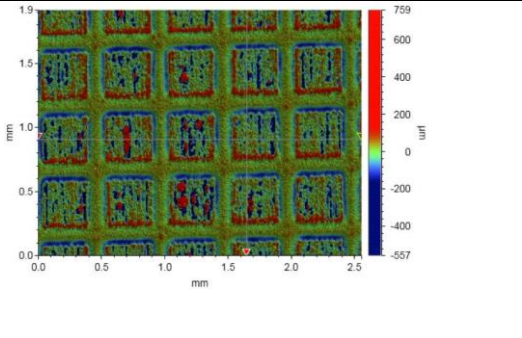
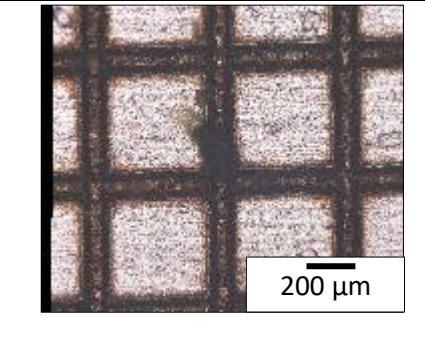
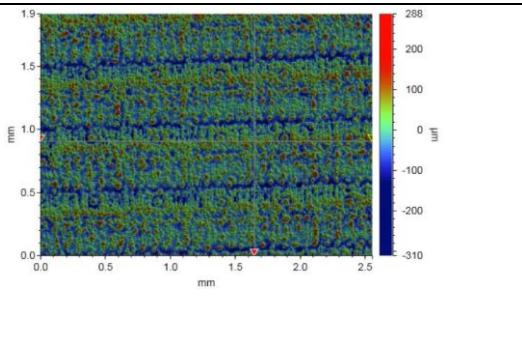
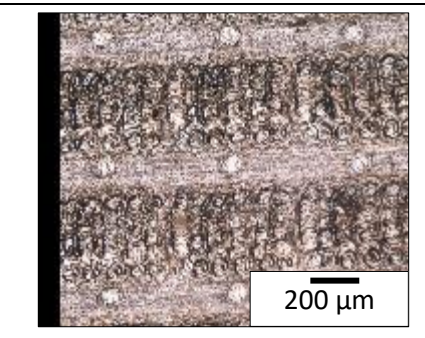
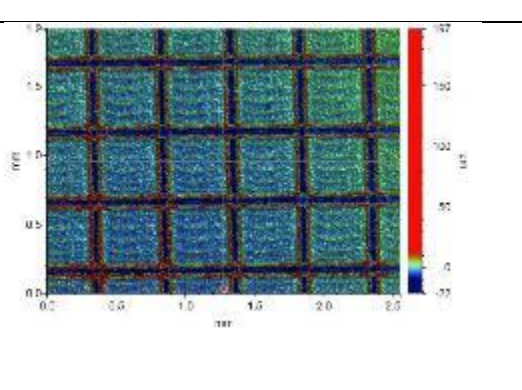
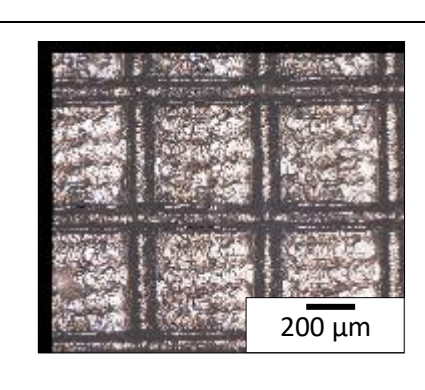
Pattern	Topographical (Bruker)	Microscope (Keyence)
Crab Base	 <p>A topographical map showing a grid pattern. The x and y axes are labeled in mm, ranging from 0.0 to 2.5. A color scale on the right indicates height in μm, ranging from -557 (blue) to 759 (red).</p>	 <p>A grayscale microscope image showing a grid pattern. A scale bar in the bottom right corner indicates 200 μm.</p>
Shell Overlay	 <p>A topographical map showing a grid pattern. The x and y axes are labeled in mm, ranging from 0.0 to 2.5. A color scale on the right indicates height in μm, ranging from -310 (blue) to 288 (red).</p>	 <p>A grayscale microscope image showing a grid pattern. A scale bar in the bottom right corner indicates 200 μm.</p>
Multi-feature 3 (M3)	 <p>A topographical map showing a grid pattern. The x and y axes are labeled in mm, ranging from 0.0 to 2.0. A color scale on the right indicates height in μm, ranging from -77 (blue) to 157 (red).</p>	 <p>A grayscale microscope image showing a grid pattern. A scale bar in the bottom right corner indicates 200 μm.</p>

Table 6.4 Topographical and microscope images of surfaces in experiment 4

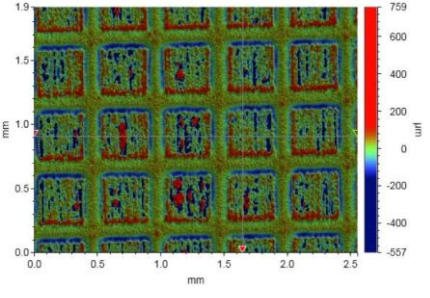
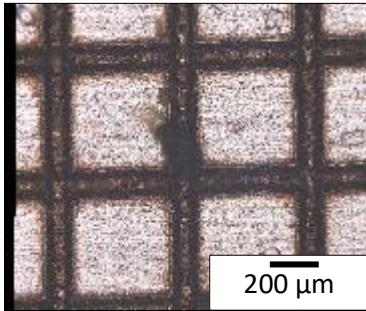
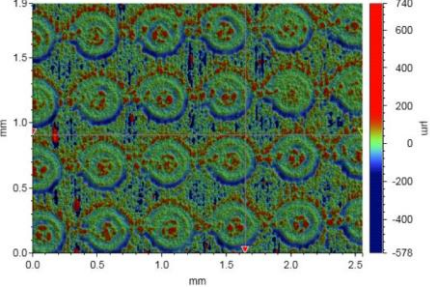
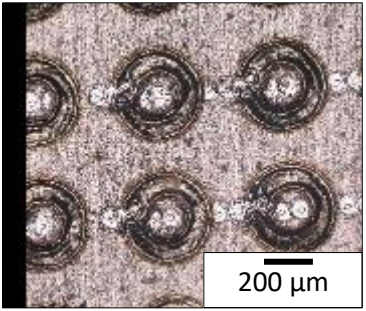
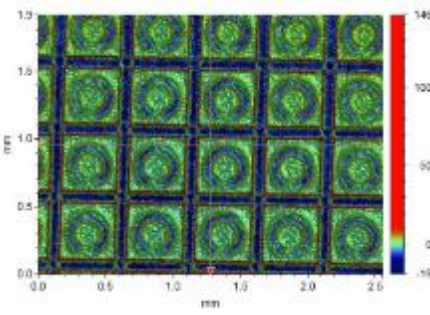
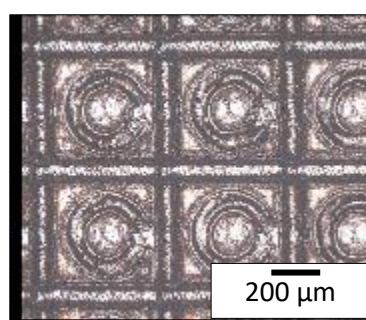
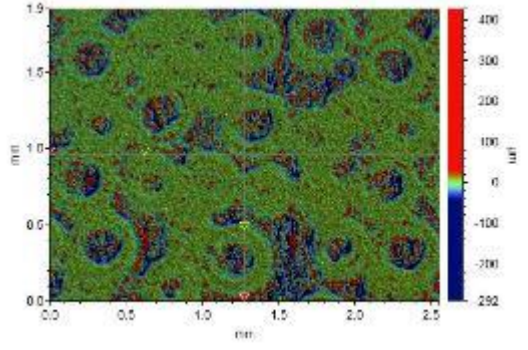
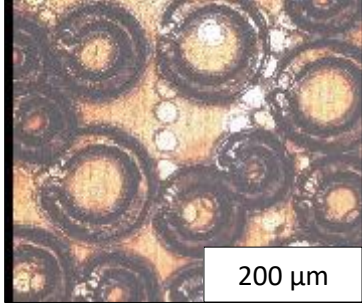
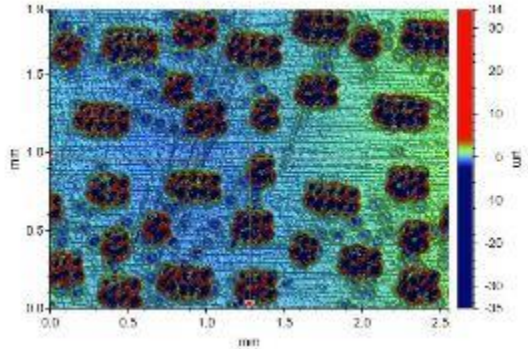
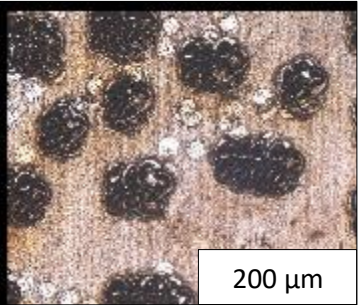
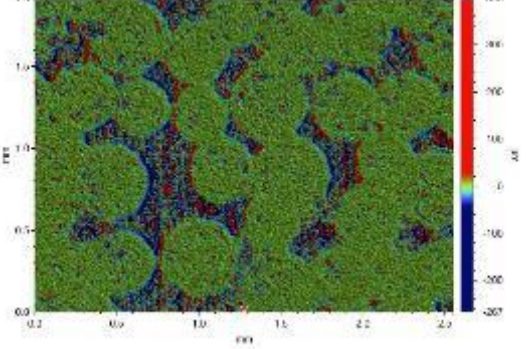
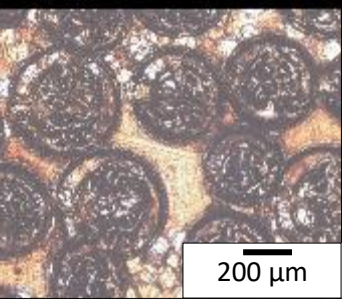
Pattern	Topographical	Microscope (Keyence)
Crab Base		
Crab Overlay		
Multi-feature 4 (M4)		

Table 6.5 Topographical and microscope images of surfaces in experiment 5

Pattern	Bruker	Microscope Image
Circle Crab Base		
Circle Shell Overlay		
Multi-feature 5 (M5)		

### 6.3.2 Biofilm Settlement

There was a significant difference in the abundance of biofilm between control and multi-feature bio-inspired micro-textured patterns (Experiment 1:  $\chi^2_{(4)} = 16.6$ ,  $p = 0.002$ ; Experiment 3:  $\chi^2_{(3)} = 12.851$ ,  $p = 0.005$ ; Experiment 4:  $\chi^2_{(3)} = 10.863$ ,  $p = 0.012$ ; Experiment 5:  $\chi^2_{(3)} = 15.096$ ,  $p = 0.002$ , Figure 6.12). However, there was not a significant difference in the abundance of biofilm between control and multi-feature bio-inspired micro-textured patterns for experiment 2 (Cockle base: median = 753, LQ = 614, UQ = 2084; Multi-scale pattern 2: median = 398, LQ = 248, UQ = 824;  $\chi^2_{(4)} = 3.380$ ,  $p = 0.185$  Figure 6.12b).

Control samples in experiment 1 had significantly higher abundance of biofilm (median = 28860, LQ = 2749, UQ = 3737) than biomimetic laser textured patterns (Small circles: median = 56, LQ = 47, UQ = 78,  $p = 0.003$ ; Medium circles: median = 111, LQ = 110, UQ = 122,  $p = 0.003$ ; Large circles: median = 91, LQ = 64, UQ = 131,  $p = 0.003$ ; Multi-scale pattern 1: median = 113, LQ = 110, UQ = 133,  $p = 0.003$ , Figure 6.12a). There were significant differences between small circles and medium circles ( $p = 0.016$ ), but not between the other patterns (small and large circles,  $p = 0.603$ ; small and multi-scale circles,  $p = 0.263$ ; medium circles and large circles,  $p = 0.881$ ; medium circles and multi-scale circles,  $p = 0.920$ ).

Control samples in experiment 3 did not have higher abundance of biofilm (median = 1431, LQ = 902, UQ = 3224) than base and overlay textured patterns (Crab base: median = 1375, LQ = 1244, UQ = 1921,  $p = 1$ ; Cockle overlay: median = 352, LQ = 243, UQ = 624,  $p = 0.416$ , Figure 6.12c). There was no significant difference between the control (median = 1431, LQ = 902, UQ = 3224) and the multi-feature pattern 3 (median = 215, LQ = 187, UQ = 221,  $p = 0.210$ ).

Control samples in experiment 4 did not have higher abundance of biofilm (median = 1431, LQ = 902, UQ = 3224) than base and overlay textured patterns (Crab base: median =

1375, LQ = 1244, UQ = 1921,  $p=0.9$ ; Crab overlay: median = 1695, LQ =868, UQ = 1731,  $p=0.9$ ). There was no difference in fouling between the control (median = 1431, LQ = 902, UQ = 3224) and the multi-feature pattern 4 (median = 174, LQ = 92, UQ = 191,  $p=0.223$ ).

Control samples in experiment 5 had significantly higher abundance of biofilm (median = 1678, LQ = 1678, UQ = 3033) than biomimetic laser textured patterns (crab circle base: median = 394, LQ = 322, UQ = 490,  $p=0.034$ ; shell overlay: median = 421, LQ =408, UQ = 686,  $p=0.020$ ; Multi-scale pattern 5: median = 152, LQ = 131, UQ = 172,  $p=0.029$ , figure 6.12e). There was also significantly higher settlement differences found in Shell overlay than multi-feature pattern 5 (shell overlay: median = 421, LQ =408, UQ = 686,  $p=0.020$ ; Multi-scale pattern 5: median = 152, LQ = 131, UQ = 172 $p=0.046$ ).

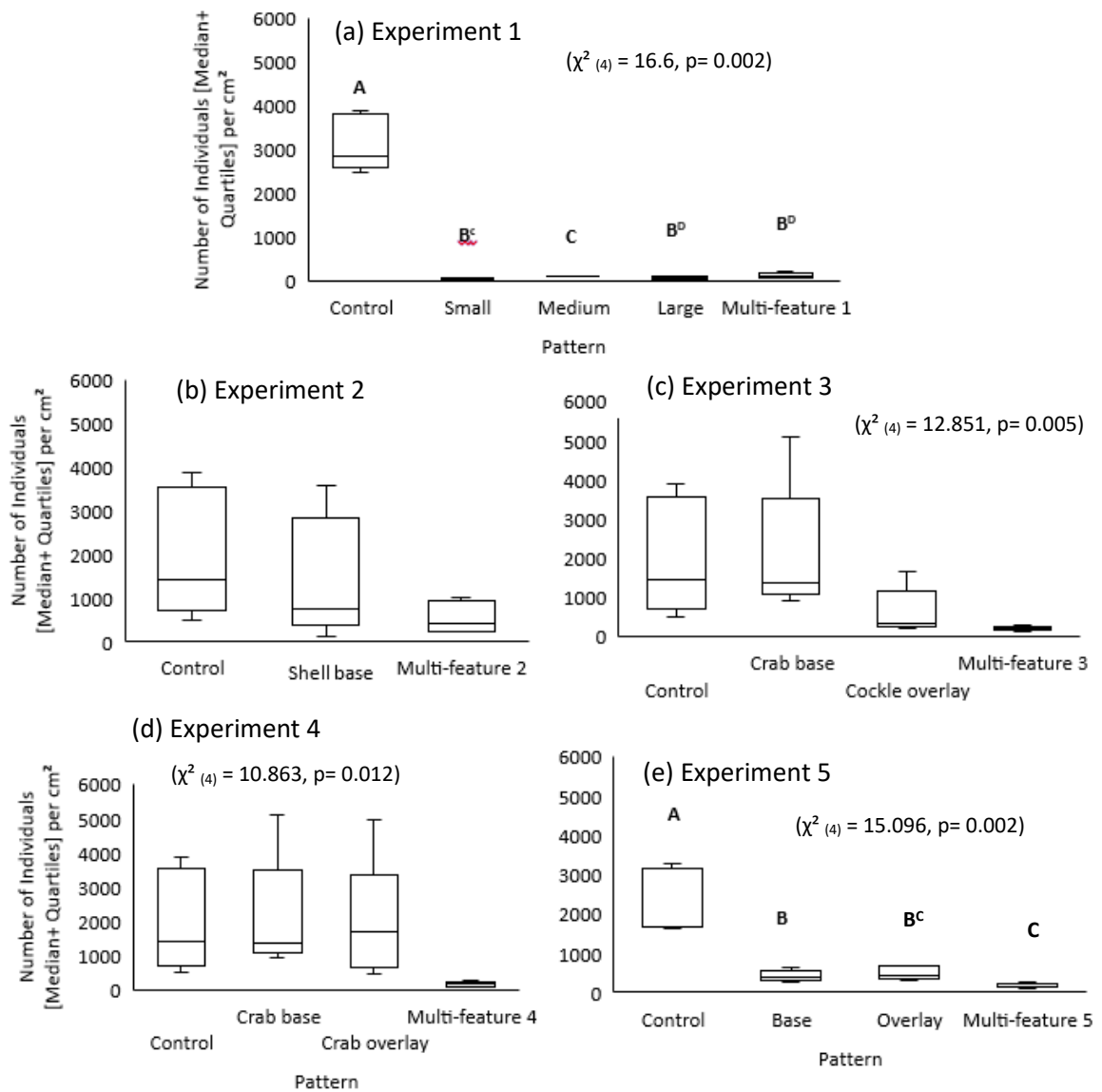


Figure 6.12 Abundance of Biofilm [Median  $\pm$  Quartiles] per cm<sup>2</sup> across the control, base, overlay and multi-feature patterns tested in this chapter where (a) is experiment 1 (b) is experiment 2 (c) is experiment 3 (d) is experiment 4 and (e) is experiment 5. **ABCD** show significant differences from post hoc tests..

### 6.3.3 Position of Biofilm

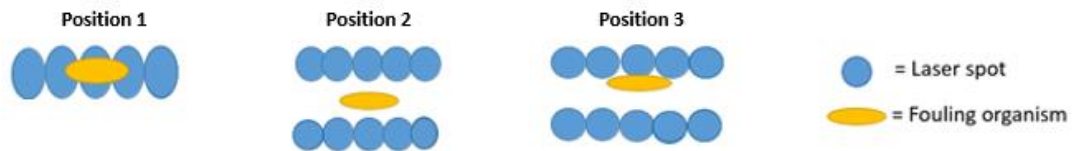


Figure 6.13 A reminder of the definition of positions outlined in methods section 3.5.2.

There was significant differences in abundance of individuals between patterns in relation to position (Experiment 1, Pseudo-F= 6.1657,  $p < 0.001$ ; Experiment 3, Pseudo-F= 8.6014,  $p = 0.002$ ; Experiment 4, Pseudo-F = 13.458,  $p = 0.0011$ ; Experiment 5, Pseudo-F= 9.2562  $p < 0.001$ ; Figure 6.14). There was not a significant differences in abundance of individuals between patterns in relation to position for shell inspired patterns tested in experiment 2 (Pseudo-F= 1.77,  $p = 0.1877$ ).

Pairwise test for experiment 1 showed that all patterns were significantly different from each other (small circles and medium circles,  $t = 2.4623$ ,  $p = 0.0074$ ; small circles and medium circles,  $t = 2.4215$ ,  $p = 0.0068$ ; small circles and large circles,  $t = 2.3375$ ,  $p = 0.0257$ ; medium circles and large circles,  $t = 2.2375$ ,  $p = 0.0153$ ; large circles and multi-feature 1 pattern,  $t = 3.3014$ ,  $p = 0.0086$ ). There was not a significant difference between medium circles and multi-feature 1 pattern ( $t = 1.5298$ ,  $p = 0.1095$ ). These significant differences are illustrated on figure 6.14a as the PCO graph shows position 1 (v1) and position 2 (v2) are most important in explaining the variance of the settlement between patterns.

Pairwise test for experiment 3 showed that all patterns were significantly different from each other (crab base and shell overlay,  $t = 2.3217$ ,  $p = 0.034$ ; crab base and multi-feature 3,  $t = 5.3794$ ,  $p = 0.0087$ ; shell overlay and multi-feature 3,  $t = 1.6763$ ,  $p = 0.0555$ ). The

PCO graph in Figure 6.14c shows position 1, 2 and 3 ( $v_1, v_2, v_3$ ) are important in explaining the variance of the settlement between patterns as lines are a similar length.

Pairwise tests for experiment 4 revealed significant differences in settlement in relation to position between multi-feature 4 pattern and crab base ( $t=5.5837, p=0.0073$ ) and multi-feature 4 pattern and crab overlay ( $t=4.063, p=0.0089$ ). There was not a significant difference between crab base and crab overlay ( $t=0.49, p=0.8168$ ). These significant differences are illustrated on figure 6.14d as the PCO graph in figure 6.14d shows position 1 ( $v_2$ ) and position 2 ( $v_3$ ) are most important in explaining the variance of the settlement between patterns.

Pairwise tests for experiment 5 revealed significant differences in settlement in relation to position between multi-feature pattern 5 and circle crab base ( $t=3.8659, p=0.0096$ ) and multi-feature pattern 5 and circle shell overlay ( $t=3.3006, p=0.0095$ ), and between circle crab base and circle shell overlay ( $t=2.0486, p=0.0141$ ). The PCO graph (figure 6.14e) shows position 2 ( $v_2$ ) was most important in explaining the variation as it is the longest line. Base and overlay seems to be associated with position 2 whereas combined pattern is associated with position 1 and position 3.

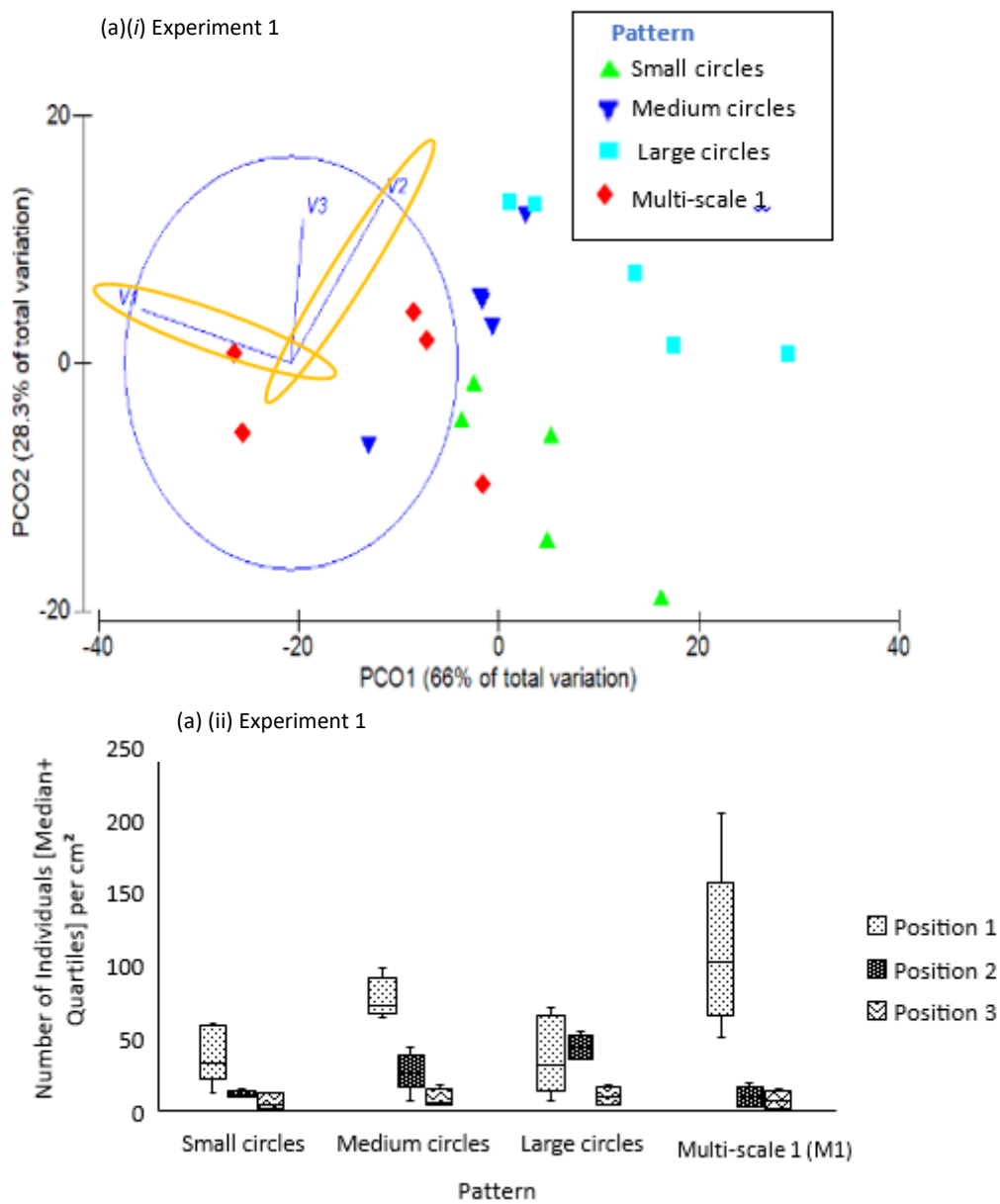


Figure 6.14 (i) Principal Component Ordination for the abundance of biofilm settled in relation to position 1 (v1) position 2 (v2) and position 3 (v3) where (a) is experiment 1, (b) is experiment 2, (c) is experiment 3 and (d) is experiment 4 and (e) is experiment 5.

(ii) The number of individuals [median  $\pm$  quartiles] settled in all three positions on bio-inspired micro-textured patterns where (a) is experiment 1, (b) is experiment 2, (c) is experiment 3, (d) is experiment 4 and (e) is experiment 5

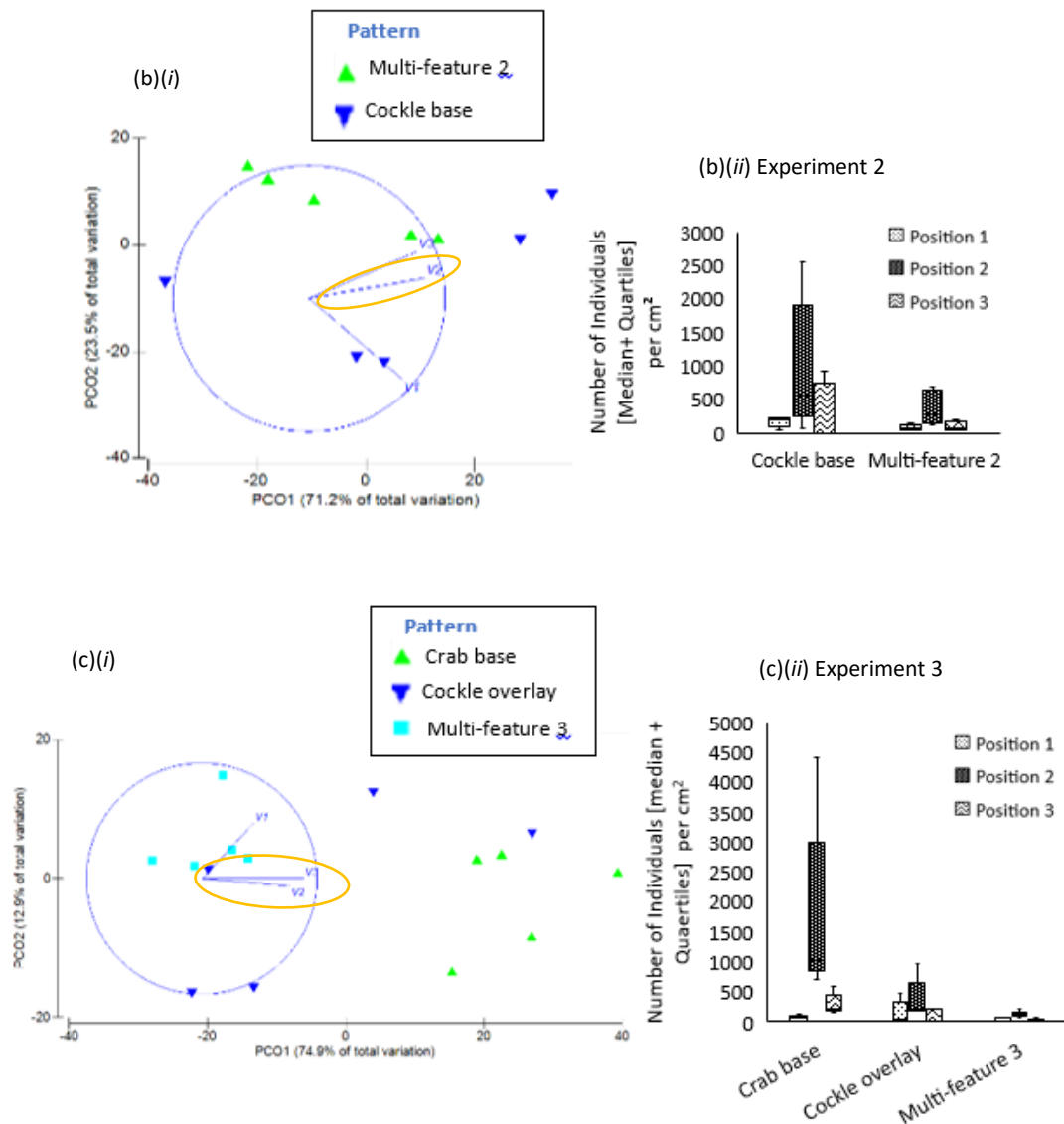


Figure 6.14 (i) Principal Component Ordination for the abundance of biofilm settled in relation to position 1 (v1) position 2 (v2) and position 3 (v3) where (a) is experiment 1, (b) is experiment 2, (c) is experiment 3 and (d) is experiment 4 and (e) is experiment 5.

(ii) The number of individuals [median  $\pm$  quartiles] settled in all three positions on bio-inspired micro-textured patterns where (a) is experiment 1, (b) is experiment 2, (c) is experiment 3, (d) is experiment 4 and (e) is experiment 5

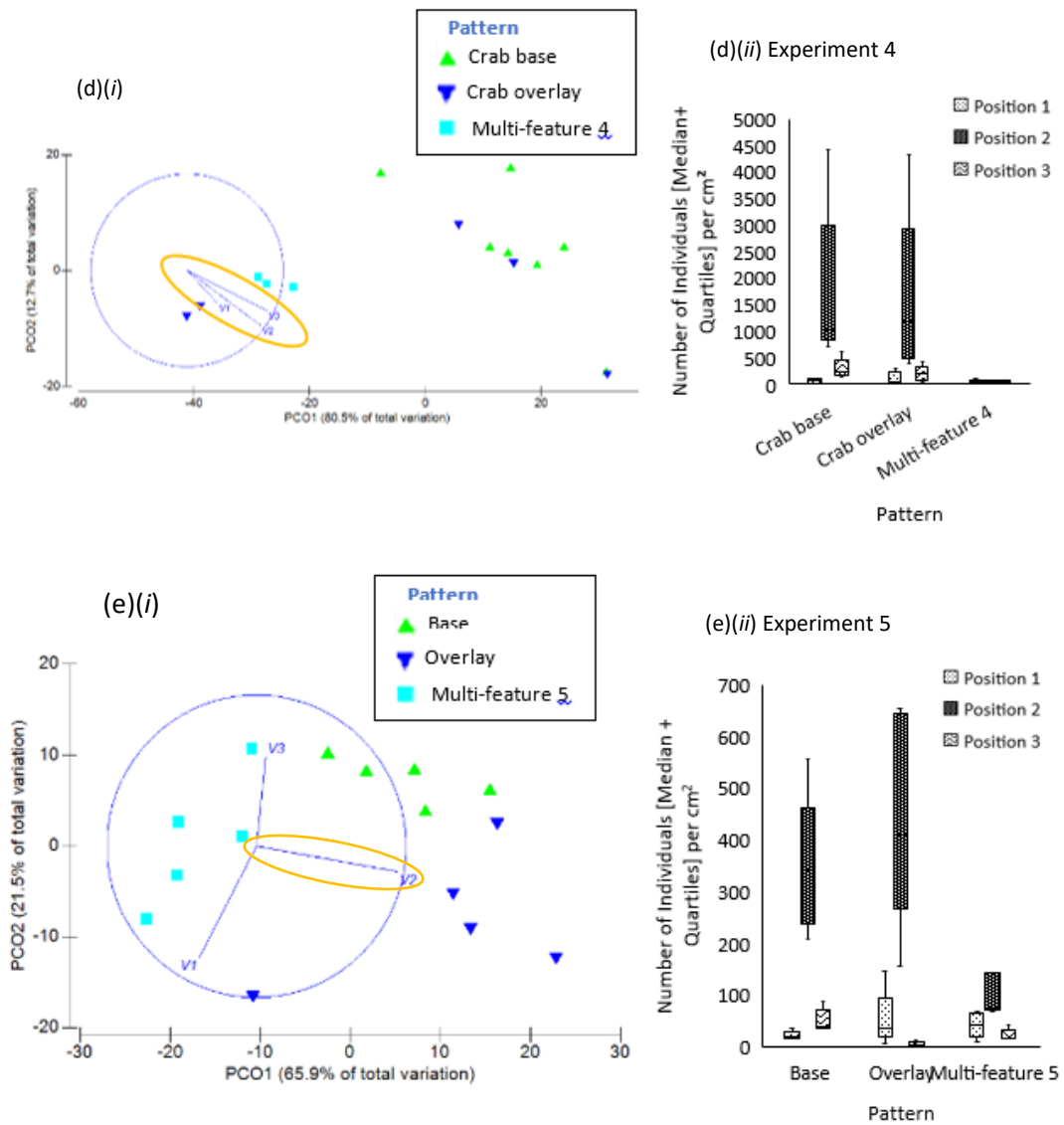


Figure 6.14 (i) Principal Component Ordination for the abundance of biofilm settled in relation to position 1 (v1) position 2 (v2) and position 3 (v3) where (a) is experiment 1, (b) is experiment 2, (c) is experiment 3 and (d) is experiment 4 and (e) is experiment 5.

(ii) The number of individuals [median  $\pm$  quartiles] settled in all three positions on bio-inspired micro-textured patterns where (a) is experiment 1, (b) is experiment 2, (c) is experiment 3, (d) is experiment 4 and (e) is experiment 5

#### 6.3.4 Position per pattern

Position 1 was most important in contributing to the dissimilarity in the small, medium large and combined multi-scale pattern (small and medium circles, average dissimilarity, 20.18%; position 1 contribution, 49%; small and large circles, average dissimilarity, 23.54%; position 1 contribution, 47.8%; large and multiscale, average dissimilarity, 23.09; position 1 contribution, 65.8%; medium and large, average dissimilarity, 18.28%; position 1 contribution, 55.6%; large and multiscale, average dissimilarity, 30.6%; position 1 contribution, 49%). There was a significant difference in settlement of marine biofilm in position 1 between small, medium, large and multi-scale 1 pattern ( $\chi^2_{(2)} = 8.541$ ,  $p = 0.014$ ; small; median = 33, LQ = 32, UQ = 56; medium; median = 73, LQ = 71, UQ = 84; large; median = 32, LQ = 22, UQ = 61; multi-scale 1 patterns; median = 102, LQ = 81, UQ = 109; Figure 6.15a). Multiscale patterns had significantly more settlement within position 1 than small ( $p=0.009$ ) and large circles ( $p=0.023$ ) patterns.

Position 2 was most important in contributing to the dissimilarity in experiment 2 (Multi-feature 2 and crab overlay; average dissimilarity, 36.67%, position 2 contribution, 43.14%;). There was not a significant difference in position 2 between shell base and multi-feature 2 pattern ( $\chi^2_{(1)} = 0.535$ ,  $p = 0.465$ ; shell base; median = 552, LQ = 427, UQ = 1278; multi-feature 2; median = 276, LQ = 137, UQ = 574; Figure 6.15b).

Position 2 was most important in contributing to the dissimilarity in biofilm settlement in experiment 3 (crab base and shell overlay, average dissimilarity 38.42%, position 2 contribution, 55.19%; crab base and multi feature 3; average dissimilarity 47.03% ,position 2 contribution 65.4% ;shell overlay and multi feature 3; average dissimilarity 28.87%; position 2 contribution, 38.79%). There was a significant difference in biofilm settlement in position 2 between crab base, cockle overlay and multi-feature 3 (Position 2;  $\chi^2_{(2)} = 11.520$ ,  $p = 0.003$ ; crab base; median = 1041, LQ = 1003, UQ = 1590; cockle overlay;

median = 226, LQ = 221, UQ = 325; multi-feature 3; median = 22, LQ = 17, UQ = 179; Figure 6.15c). There was significantly less settlement within position 2 on multi-feature 3 pattern compared to crab base pattern ( $p=0.037$ ).

Position 2 was most important in contributing to the dissimilarity in biofilm settlement in experiment 4 (crab base and crab overlay, average dissimilarity 36.55%, position 2 contribution, 65.45%; crab base and multi-feature 4, average dissimilarity, 45.2%, position 2 contribution, 69.87%; crab overlay and multi-feature 4, average dissimilarity, 36.88%, position 2 contribution, 66.69%). There was a significant difference in position 2 between crab base, crab overlay and multi-feature 4 ( $\chi^2_{(2)} = 9.5$ ,  $p = 0.009$ ; Crab base; median = 1041, LQ = 1003, UQ = 1590; crab overlay; median = 1174, LQ = 613, UQ = 1539; multi-feature 4; median = 56, LQ = 26, UQ = 58; Figure 6.15d). There was significantly less settlement within position 2 on multi-feature 4 pattern compared to crab base pattern ( $p=0.04$ ).

Position 2 was most important in contributing to the dissimilarity in biofilm settlement in experiment 5 (base and overlay, average dissimilarity, 22.5%, position 2 contribution, 39.2%; base and multi-feature 5, average dissimilarity, 25.89%, position 2 contribution, 64.43%; overlay and multi-feature 5, average dissimilarity, 33.42%, position 2 contribution, 64.36%). There was a significant difference in position 2 and 3 between base, overlay, and multi-feature 5 patterns ( $\chi^2_{(2)} = 9.98$ ,  $p = 0.007$ ; base; median = 340, LQ = 263, UQ = 366; overlay; median = 409, LQ = 378, UQ = 635; multi-feature 5; median = 74, LQ = 72, UQ = 140; Figure 6.15e). There was significantly less settlement within position 2 on multi-feature 5 pattern compared to crab base pattern ( $p=0.044$ ) and overlay pattern ( $p=0.006$ ).

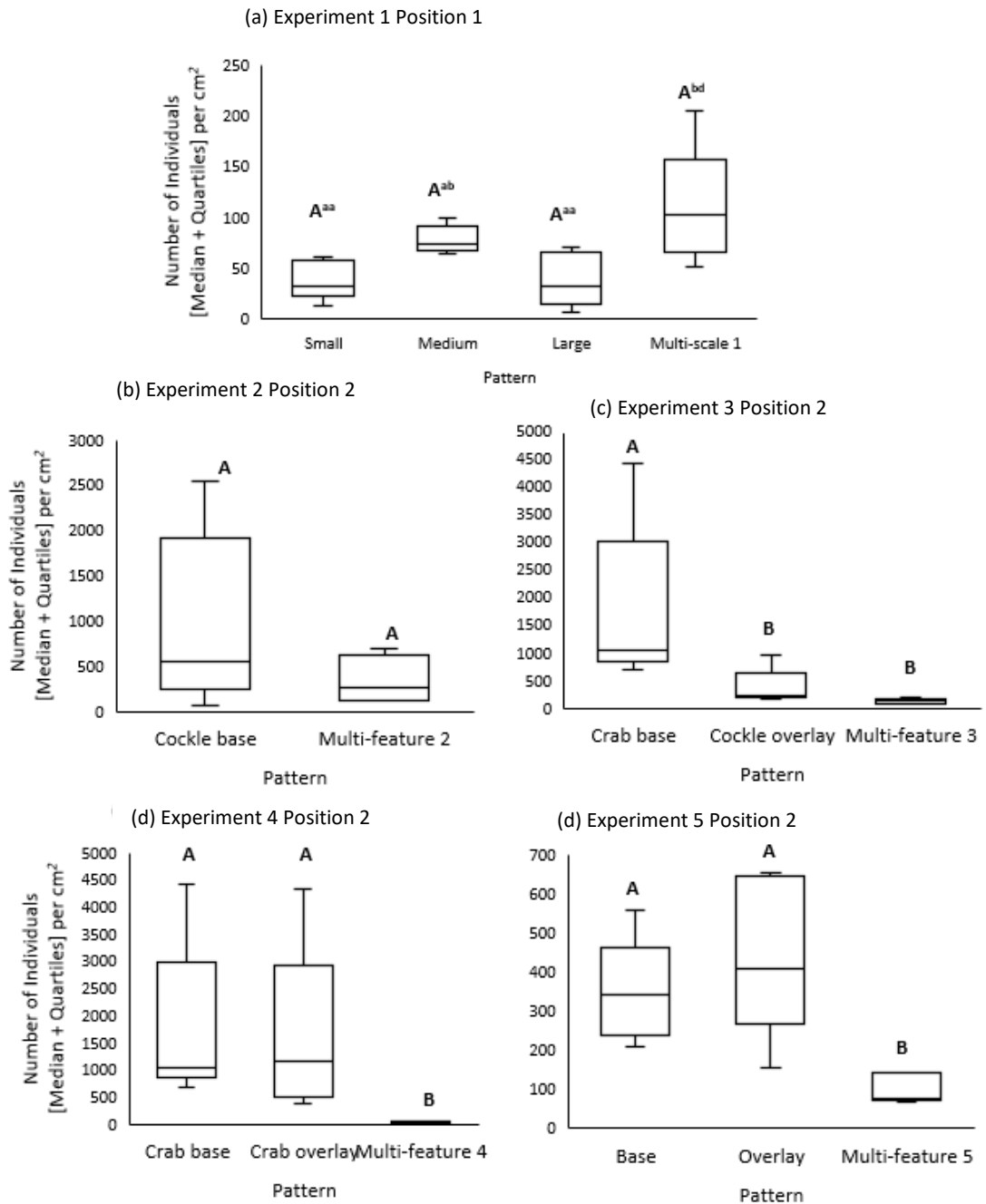


Figure 6.15 The number of individuals [median  $\pm$  quartiles] settled in the most important position on bio-inspired micro-textured patterns where (a) experiment 1 is position 1, and (b) experiment 2 (c) experiment 3 and (d) experiment 4 and (e) is experiment 5 are position 2.

## 6.4 Discussion

The aim of this study was to (a) demonstrate the application of laser surface texturing to create multi-scale and multi-feature biomimetic micro-textured surfaces and to (b) determine the antifouling efficacy of these surfaces. Multi-scale and multi-feature surfaces were able to be created using laser surface texturing. A total of 5 biomimetic, multi-scale, multi-feature surfaces were created in this study; all created from combining patterns inspired by previous surfaces tested in chapter 5. Settlement of marine biofilm was reduced on biomimetic, multi-scale, multi-feature surfaces compared to the unprocessed control.

### 6.4.1 Surface topography

Five biomimetic, multi-scale, multi-feature surfaces biomimetic surfaces were produced in this study by using laser surface texturing directly onto marine grade steel. The previous studies have concentrated on the use of PMDS polymers as a base substratum and the use of either photolithography (Schumacher *et al.*, 2007b) or uniaxial hierarchically wrinkled topographies (Efimenko *et al.*, 2009) as a tool to produce multi-scale, multi-feature surfaces. This study is novel in that biomimetic, multi-scale, multi-feature surfaces were created directly onto marine grade (316L) steel using laser surface texturing as a tool. There are no previous studies on creating biomimetic, multi-scale, multi-feature surface topographies using laser surface texturing directly onto stainless steel for antifouling purposes. The use of laser surface texturing as a tool to create biomimetic surfaces enables these surfaces to not be limited by substratum. This means that the biomimetic, multi-scale, multi-feature surfaces have the potential to be used in more areas across the marine industry, than if they were limited in to the use of PMDS only.

### 6.4.2 Biofilm settlement

#### 6.4.2.1 Multi scale pattern

Laser surface texturing of reverse multi-scale circles reduced the settlement of marine biofilm. Multi-scale and patterns have previously been found to reduce fouling at a greater rate than single scale patterns (Schumacher *et al.*, 2007b). The circular multi-scale patterns (experiment 1) were reverse textured meaning that all of the “free space” between circular features was now laser processed space and the free unprocessed space was at the top of raised sections. As the “free space” was in this series of patterns was on a protruding area, this may have caused the reduction in settlement. It has been previously found that marine fouling organisms prefer to avoid settling on top of protruding areas (Schumacher *et al.*, 2007b, Callow *et al.*, 2002, Hoipkemeier-Wilson *et al.*, 2004). This avoidance of settling on protruded areas may also have been occurring in this study, as settlement within the recessed laser tracks (position 1) was the most important position in reducing the fouling between single and multi-scale patterns in experiment 1.

All scales of the circle pattern reduced fouling, however, the scale of medium circles had the highest level of fouling, therefore the least antifouling potential. This multi-scale differences may have been noticed by the biofilm organisms, as settlement in position varied across the patterns. Medium circles may have had a high level of settlement in position 2, which could be because the aspect ratio of the medium circles was similar to the size of biofilm species, therefore increasing the fouling. Medium circles pattern was ruled out for future experiments as it has higher levels of fouling than others, however the combined multi-scale pattern which featured circles of small, medium and large arranged randomly was selected to influence the final experiment of this study (Multi-feature 5) as it has the most “biomimetic” look as within nature the circles produced on crab shells are a mixture of sizes, and are not distributed in an structured array design.

#### 6.4.2.2 Multi-feature pattern

It was repeatedly found in this study that multi-feature patterns had a greater antifouling potential than that of single scale and single feature patterns. This trend is seen throughout experiments 1, 3, 4 and now 5 therefore is adding to the evidence that multi-scale and multi-feature patterns slow the fouling process down, and therefore increase antifouling efficacy. There has been very little testing of multiscale combined patterns by other research groups (Sullivan and Regan, 2017, Schumacher *et al.*, 2007b; Efimenko *et al.*, 2009), hence the novelty of this research. The previous studies that have measured biofouling on multi-scale and multi-feature surfaces have found a reduction in biofouling on the multi-scale, multi-feature surfaces (Sullivan and Regan, 2017, Schumacher *et al.*, 2007b; Efimenko *et al.*, 2009). Similarly to the present study, Schumacher *et al.*, (2007b) found reduced spore settlement of *Ulva* on combined triangles/pillars patterns, than on pillars base pattern. Schumacher *et al.*, (2007b) found that their multi-scale and multi-feature pattern Sharklet AF™ had the lowest settlement of *Ulva* compared to smooth control, single feature patterns, and multi-feature but single scale patterns. The results in this present study are in agreement with Schumacher *et al.*, (2007b) in that the surfaces that had both multi-scale and multi- feature topographies (in Schumacher *et al.*, (2007b); Sharklet AF™; in present study; Multi-feature 5) had the greatest antifouling efficacy. It may be possible that a reduction in overall fouling is because of the base and overlay patterns working together to affect the positions of settlement for these marine organisms.

The base pattern did not reduce the fouling level for 3 out of 4 experiments. The base patterns were laser processed into the substrate with a more power (%) to leave a deeper impression on the surface, with the aim to make a distinct base pattern. However, although a distinct base pattern was created, the base patterns have not been as successful at antifouling. This may be because settlement within the base pattern was focused on position 2. The base patterns were designed to limit the settlement of larger organisms, as

the base pattern distinctly creates block on the surface which will inhibit settlement of larger organisms by reducing contact points (Scardino *et al.*, 2006, Scardino *et al.*, 2008). However, by having a larger distinct base pattern, smaller fouling organisms which fit within the unprocessed free space of the base pattern were not affected by the surface topography, and were able to foul the base pattern in significant numbers. The settlement of smaller organisms on base patterns could be due to the fact that their attachment was not effect by topography as they were able to form multiple and successful attachment on the unprocessed area (Scardino *et al.*, 2006, Scardino *et al.*, 2008). This enabled high levels fouling on the base patterns (exp 2,3,4). The base pattern may have played a key role in reducing the fouling of larger marine organisms, but enabled fouling of biofilm species (diatoms).

Overlay patterns were more successful at reducing fouling than base patterns as, half of the overlay patterns tested were able to limit the fouling level (exp 3 and exp 5). This may be because they were able to limit the attachment points of these smaller organisms, that were unaffected by the base pattern (Scardino *et al.*, 2006, Scardino *et al.*, 2008). The overlay pattern is laser processed with less power (%), to cause a smaller, but substantial disturbance to the main distinct base pattern. However, when tested alone the overlay pattern was still susceptible to fouling from larger organisms, that may have been able to override the small changes in the topography from the over lay pattern (Becker *et al.*, 1998, Friedlander *et al.*, 2013, Velic *et al.*, 2019). Similarly, to based patterns, overlay patterns had the most amount of settlement within position 2. This may mean that settlement was occurring the free space gaps where the topography of the base pattern would reduce the settlement.

Base and overlay usually had different fouling results, with the overlay pattern having a larger antifouling effect (experiment 3 and 5), however, this was not the case for

experiment 4, where the base and overlay had similar levels of fouling. There are few studies in which have tested singular and combined patterns for antifouling efficacy. When compared with Schumacher *et al.*, (2007b), although they did not have “base” and “overlay” patterns, they tested the single pillars pattern “base” and a combined pillars/triangle pattern, and single pillars “base” pattern had more fouling than combined, however, the triangle “overlay” pattern in which the pillars was combined with was not tested alone, therefore cannot be compared to overlay patterns in the present study. The base and overlay of experiment 4 in the present study had similar levels of fouling. This was an unexpected result and may be because the surface topography of the overlay may have been overridden by fouling species (Becker *et al.*, 1998, Friedlander *et al.*, 2013, Velic *et al.*, 2019). However, this similarity in fouling of base and overlay patterns may have occurred because in experiment 4 both base and overlay patterns were bio-inspired by the crab, therefore, both have similar features, such as lots of free space, and therefore the similarity of the base and overlay patterns meant that the abundance of fouling was similar.

For the majority of experiments (experiment 1,3,4,5), the multi-featured pattern significantly reduce the fouling of the surface. This may be because the base and overlay patterns combined worked in synergy, by combining the large feature found in the base pattern, with the smaller features fouling in the overlay pattern, the multi-scale multi-features patterns were able to reduce fouling. The finding that multi-scale and multi-feature patterns in this study have an improved antifouling efficacy coincides with results on combined patterns for marine antifouling by Schumacher *et al* (2007b) showing that multi-scale and multi-feature patterned surfaces have a greater reduction in fouling than singular patterned surfaces.

However, one experiment within this study did not find that multi-feature, multi-scale patterns reduced fouling (experiment 2). This is in agreement with Sullivan and Regan

(2017) who found that after testing multi-scale and multi-feature patterns a 14 day experimental period that adnate, centric, small raphid, erect and chain-forming diatom species had colonised all exposed surfaces within this time period (Sullivan and Regan, 2017). This may mean that the topography is irrelevant to settlement, no matter the scale, and it is in fact the species present that determine the settlement. It may be that certain species may be present that have mechanisms to overcome the topography and form a biofilm, and then other species that would have been affected by the topography are able to settle, as the cushion of the already formed biofilm is blocking any effects from the topography. This may be why no antifouling effects were seen on the single feature (base) and multi feature 2 pattern in experiment 2. It may also be that the overlay pattern for experiment 2 was sporadic, and not consistent, therefore did not cover the appropriate area, which may have negatively impacted the antifouling results. The lack of antifouling potential of multi-feature pattern in experiment 2 may also be due to the fact that it is the only pattern tested that had a shell base, and as found in chapter 5, shell based patterns were more prone to fouling within position 1, as fouling organisms settle within the grooves (Hoipkemeier-Wilson *et al.*, 2004), therefore any overlay pattern would not have an impact on the fouling in position 1.

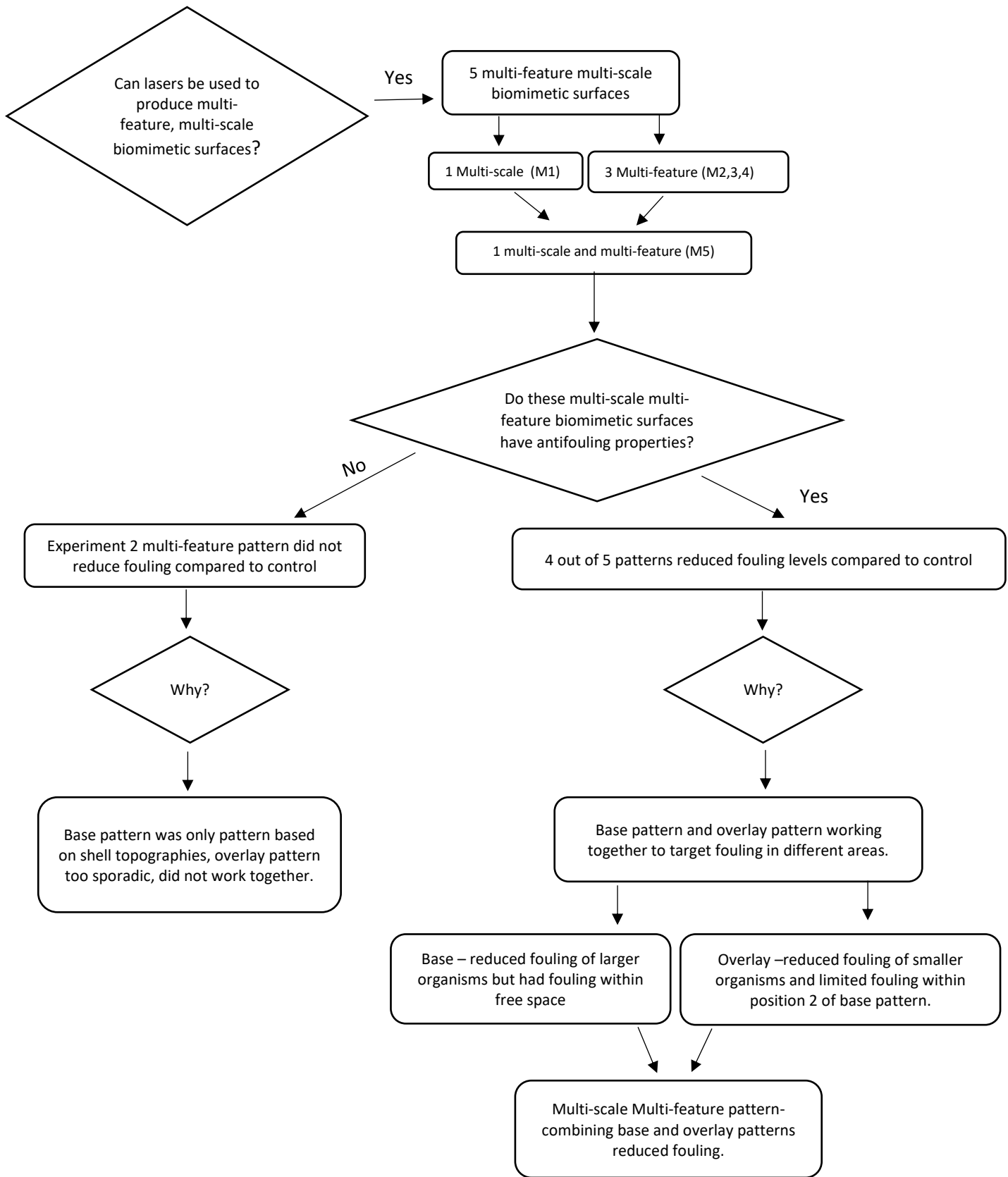


Figure 6.16 Flow chart of this study's key findings

This study was to further the proof of concept study done in earlier chapter 5 in that laser can be used to create biomimetic surface that have antifouling potential. It was repeatedly found that by combining multiple features (base and overlay), the fouling potential of a surface increased, as the best fouling potential came from multi-scale, multi-feature pattern (figure 6.4.2). A previous model surface energy based model had predicted that multi-feature micro-textured surfaces would have antifouling effects vs smooth control surfaces (Carman *et al.*, 2006, Ball, 1999, Bechert *et al.*, 2000). This model led to the design of Sharklet™ which is a multi-scale surface topography and of multi-feature triangles/pillars topography (Schumacher *et al.*, 2007b), and when these surfaces were tested they confirmed the trend predicted by the model in that multi-feature surfaces reduce fouling. This study is in agreement with the previous studies (Schumacher *et al.*, 2007b, Sullivan and Regan, 2017) in that multi-scale and multi-feature surfaces reduced marine biofilm settlement. This study found that the use of multiple sources for bio-inspiration was important, as the pattern that had a crab on crab base and overlay was still antifouling, but better results came from the patterns that had feature from both crab and shell, therefore multi-species inspired biomimetic surface may be the next step in creating an antifouling surface.

Although there is doubt over the longevity of multi-scale micro-textured surfaces as a solution for marine antifouling (Sullivan and Regan, 2017), this study shows there is evidence that multi-scale multi-feature bioinspired micro-textured surfaces slow fouling down over a short term period.

## Chapter 7 Overall Discussion

Overall, the main finding of thesis is that laser surface texturing can be used to create biomimetic surfaces directly onto marine grade steel that have antifouling properties. When compared to previous antifouling studies (Table 7.1), this thesis shows novelty in three main ways (1) the use of laser surface texturing directly onto marine grade stainless steel; (2) antifouling efficacy testing of developed samples in a field environment, and (3) combining features of two marine organisms to develop a multi-scale multi-feature pattern with antifouling properties.

Table 7.1 Previous studies on the development of micro-textures for antifouling purposes with addition of this study.

Substrate	Method of texturing	Fouling organism	Species	Micro-textures reduce biofouling	Lab or Field	Bio-mimetic	Based on	Features	Reference
PDMS	photolithographic techniques	Zoospores	Ulva linza	Yes	Lab	No	straight lines	single	Hoipkemeier-Wilson <i>et al.</i> , (2004)
PDMS	photolithographic techniques	Cyripid	B. amphitrite	Yes	Lab	Yes	Sharklet	single	Schumacher <i>et al</i> (2007)
PDMS	photolithographic techniques	Bacteria	Staphylococcus aureus	Yes	Lab	Yes	Sharklet	single	Chung <i>et al</i> (2007)
PDMS	photolithographic techniques	Zoospores	Ulva	Yes	Lab	Yes	Sharklet and others	Multi	Schumacher <i>et al</i> (2007)
PDMS	photolithographic techniques	Zoospores	Ulva linza	Yes*	Lab	Yes	Sharklet	Single	Carman <i>et al</i> (2006)
PDMS	photolithographic techniques	Diatom	Amphora coffeaeformis	Yes	Lab	Yes	Crab	single	Brzozowska <i>et al</i> (2014)
		Cyripid	Amphibalanus amphitrite	Yes	Lab	Yes	Crab	single	Brzozowska <i>et al</i> (2014)
PDMS	photolithographic techniques	Tube Worms	Unknown	Yes	Field	Yes	<b>Crab</b>	single	Brzozowska <i>et al</i> (2014)
PDMS	photolithographic techniques	Diatoms	Mixture	No	Field	No	targeted to diatoms	Multi	Sullivan <i>et al</i> (2017)
PDMS	photolithographic techniques	Zoospores	Ulva linza	Yes	Lab	Yes	Sharklet	single	Schumacher <i>et al</i> (2008)
PDMS	photolithographic techniques	Zoospores	Ulva	Yes	Lab	Yes	Sharklet	single	Schumacher <i>et al</i> (2007)
PDMS	photolithographic techniques	Bacteria	C. marina	Yes	Lab	Yes	Sharklet triangles and pillars	multi	Magin <i>et al</i> (2010)
PDMS	photolithographic techniques	Diatoms	<i>Navicular incerta</i>	Yes	Lab	Yes	Sharklet	Single	Long (2009)
PDMS	wrinkled surface topographies	Zoospores	Ulva linza	Yes*	Lab	No		Multi	Efimenko <i>et al</i> (2009)
PDMS	wrinkled surface topographies	Diatoms	unknown	Yes	Field	No		Multi	Efimenko <i>et al</i> (2009)
Epoxy resin	Cast directly off marine organism	Range of species**	Range of species**	Yes	Field	Yes	Range of species	single	Bers and Wahl (2004)
Epoxy resin	Cast directly off marine organism	Range of species		Yes	Field	Yes	Mussel	single	Scardino and R. de Nys (2004)
PDMS	Cast directly off marine organism	Diatoms	Closterium and Navicula	Yes	Lab	Yes	lotus leaf, crab shell	Single	Chen <i>et al</i> (2015)
Stainless Steel (4N)	Electro-polishing	Bacteria	S. aureus and P. aeruginosa	Yes	Lab	No		Single	Wu <i>et al</i> (2018)
PDMS	Laser ablation	Diatoms	N. paleacea, N. jeffreyi, . Amphora sp. F. carpentariae	Yes	Lab	Yes	Mussel	single	Scardino <i>et al</i> (2006)
PET	Laser ablation	Osteoprogenitor cells		Yes	Lab	No		single	Duncan <i>et al</i> (2002)
Polycarbonate	Laser ablation	Diatoms, algae	Amphora sp, Ulva rigida, Hydroides	Yes	Lab	No		Single	Scardino <i>et al</i> (2006)
		Tube Worm	elegans						
		Tube Worm	Centroceras clavulatum, Bugula						
		Bryozoa	neritina						

Titanium alloy	Laser ablation	Bacteria	S. aureus	Yes	Lab	No		Single	Cunha <i>et al</i> (2016)
Chitosan	Laser ablation	OLN 93 cell line	oligodendroglia cell	Yes	Lab	Yes	Sponge	Single	(Rusen <i>et al.</i> , 2014)
Stainless Steel	Laser ablation and coating	Unknown		Yes	Field	No		Single	Sun <i>et al</i> (2018)
<b>Stainless Steel</b>	<b>Laser ablation</b>	<b>Diatoms</b>	<b>Diatom community</b>	<b>Yes</b>	<b>Field</b>	<b>Yes</b>	<b>Crab and cockle shells</b>	<b>Multi</b>	<b>This study (Chapter 6)</b>

### 7.1 Laser surface texturing to develop bio-inspired surfaces

Laser surface texturing as a method can achieve the desired result of an antifouling micro-texture produced directly onto marine grade stainless steel (Chapter 4). The majority of previous antifouling studies have used PDMS as a substrate and used techniques such as photolithography (Hoipkemeier-Wilson *et al.*, 2004; Schumacher *et al.*, 2007; Chung *et al.*, 2007; Table 7.1). An advantage of the present study is that it shows that laser surface texturing allows for a wide range of substrates to be used from marine grade stainless steel in this study to PET and PDMS (Table 1; Duncan *et al.*, 2002; Scardino, Harvey and De Nys, 2006b). The present study shows a journey of optimisation to create an enhanced antifouling surface, from basic laser hatches in chapter 4, where surface properties were investigated alongside surface topography, to the complex biomimetic patterns produce in chapter 6. This show how versatile the laser surface texturing process can be, as a whole range of different patterns were created on marine grade stainless steel. By using laser surface texturing, biomimetic surfaces were able to be created on marine grade stainless steel, that are similar to other biomimetic surfaces that have only been created on polymer substrata previously (Figure 7.1).

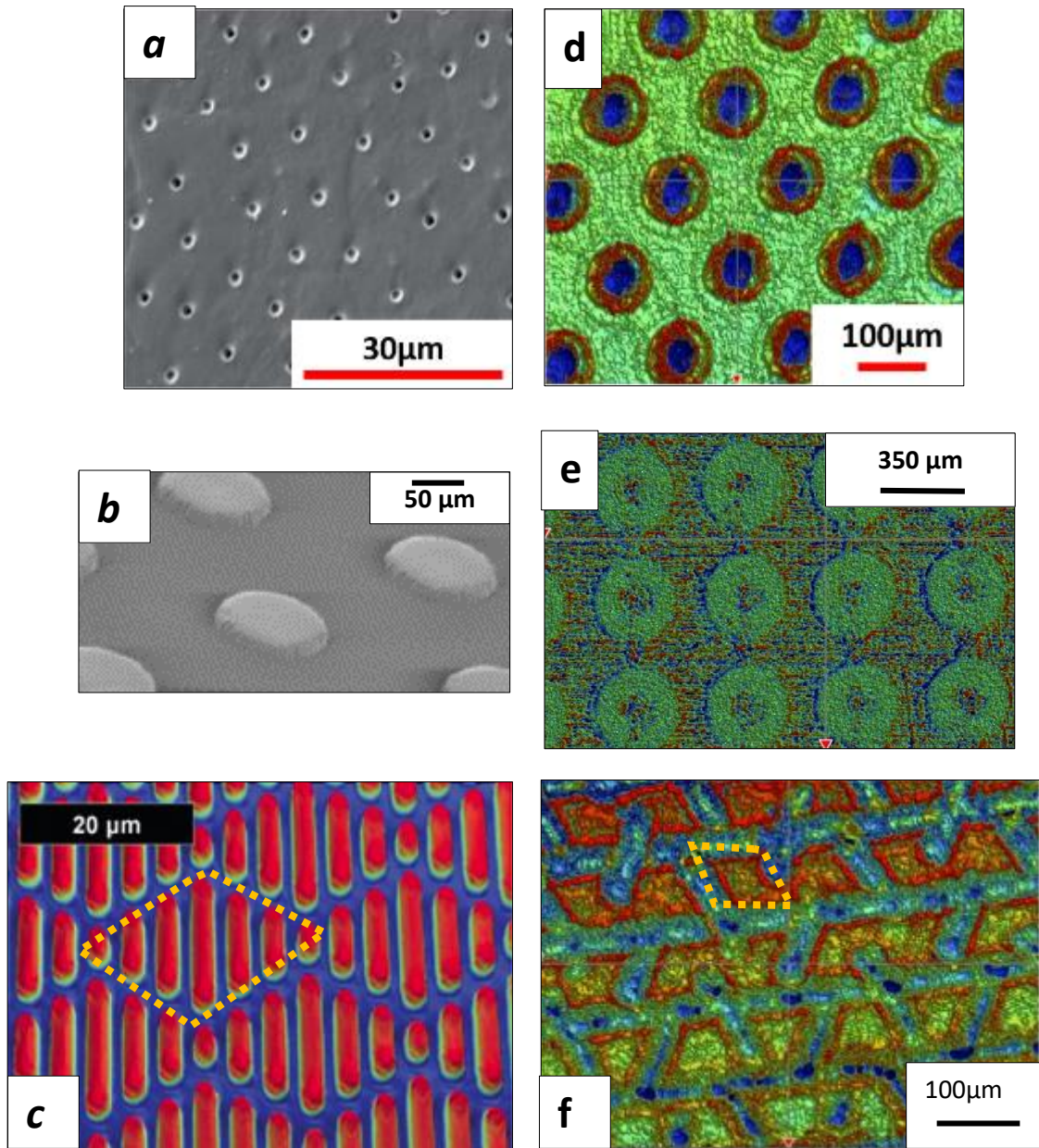


Figure 7.1 Biomimetic surfaces where (a-c) are from previous studies on polymer substrates and (d-f) are replicates created using laser surface texturing. Where, a is a white crab (Chen et al., 2010); b is crab inspired (Brzozowska et al., 2014); c is Sharklet™ pattern inspired by spinner shark (Magin, Cooper and Brennan, 2010); d and e are laser textured crab pattern (this thesis) and f laser textured shark pattern.

Marine grade stainless steel was chosen for the obvious reason that it will not oxidise in the marine environment, therefore it was deemed the best substratum for this investigation. A limitation of this thesis is that only one type of substrate was used. However, different substrate metals will a coating for corrosion resistance in the marine environment such as zinc–magnesium coated steel (Hosking *et al.*, 2007). Therefore, for the micro-textures created in this study to work on a wider variety of materials, they will have to be created on top of the corrosion resistant coating. This may be possible as a previous study has shown it is possible to coat and laser micro-textured a surface at the same time (Boinovich *et al.*, 2018). The steel used as substrate in this thesis may not feature at the interface of marine structural or industrial application as AISI 1020 steel is extensively used for structural work (Venkatesan *et al.*, 2002) . However, the texturing applications developed in this this thesis may be applicable to these alternative substrates.

The patterns that were created on CAD files (Dassault DraftSight files exported in .dxf format) could be easily textured onto plastic surfaces in theory. However, the way in which that a polymer surface melts and re-hardens will be different to the stainless steel in this study and may affect the over outcome pattern. It may be the case that for future work on this the power and the speed of the laser beam may be altered to produce similar effects on other materials. However, as the pattern files are already designed, and stored at .dxf files, the replication of texturing other materials should be a fairly easy next step for this research. Although the use of one sole substrate could be deemed a limitation of this thesis, it also opens up the opportunity to reverse cast other materials such as silicones. As seen throughout this thesis, most other biomimetic surfaces are created on polymer substrates, therefore, a laser processed biomimetic steel surface may be used as a negative to cast off other a biomimetic pattern onto other materials.

## 7.2 Single scale surfaces (crab and shell)

Throughout the experimental chapters of this thesis it was repeatedly found that laser textured biomimetic, surfaces had an antifouling effect on marine biofilm. There are two possible explanations for this, the diatom attachment theory and the air entrapment theory wettability theory.

### 7.2.1 Diatom attachment theory

As discussed in the literature review (Section 1.5), the diatom attachment theory could be a reason to explain why these micro textures may be working to reduce settlement of marine biofilm (Scardino *et al*, 2006). When a surface is flat, diatoms can settle easily on the surface and form multiple attachment points (Figure 7.2). However, when the surface has a micro-texture, one of two things may occur to the diatom. If the surface topography is larger than the scale of the diatom, the diatom may settle comfortably within the crevices, form multiple attachment points, and be protected from hydrostatic forces, or can colonise micro-refuges on surfaces where they are protected from hydrodynamic forces (Granhag *et al*, 2004) and abrasion (Figure 7.2b). However, if the surface topography is smaller than the diatom, the diatom may settle on top of the surface features, and have less surface area of its silica shell in contact with the surface, therefore reducing the amount of attachment points that it can form, leading to weak attachment (Figure 7.2c).

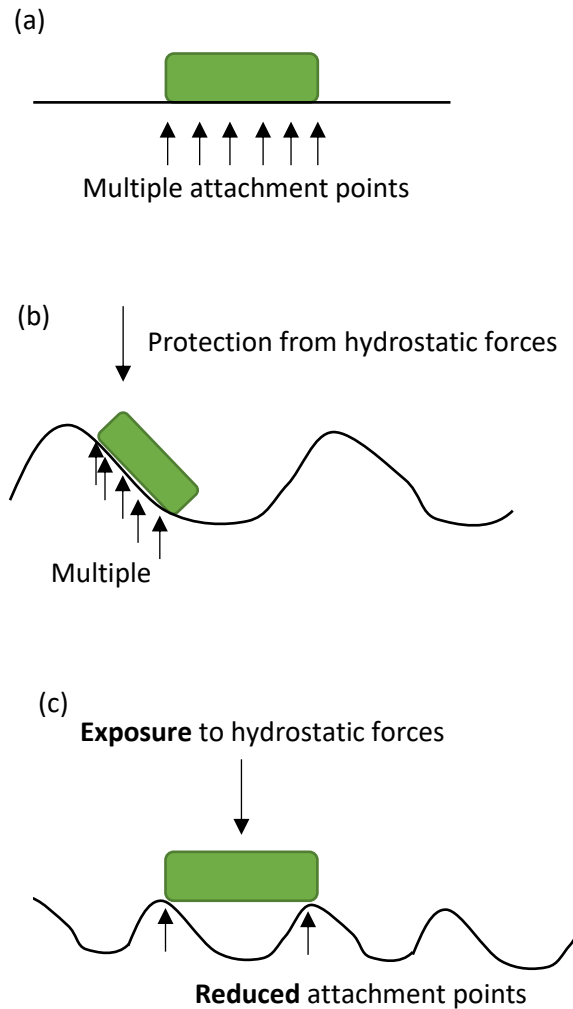


Figure 7.2 A schematic illustration of theoretical attachment points of a diatom; (a) before attachment; (b) attachment on a flat surface; (c) attachment where micro-topography that is larger than organism (micro-refuge) (d) attachment where micro-topography is smaller than the diatom with three points of attachment and (e) attachment where micro-topography is smaller than the diatom with three points of attachment adapted from (Adapted from Scardino *et al*, 2006).

The surfaces created in this thesis may be limiting the attachment points of marine biofilm, and therefore reducing their ability to foul the surface. A reduction in fouling that may have been caused by a reduction in attachment points has been demonstrated with a range of species such as *Ulva linza* (Callow *et al.*, 2002; Hoipkemeier-Wilson *et al.*, 2004;

Carman *et al.*, 2006) multiple species of diatom (Scardino *et al.*, 2006) and for larger fouling species such as barnacle cyprids (Aldred *et al.*, 2010) bryozoan *Buluga neritina* and tube worm *Hydroides elegans* (Scardino *et al.*, 2008). The reduction in attachment points may also be the reason in which marine fouling is being reduced on laser textured biomimetic surfaces in this study.

Laser processed biomimetic surfaces in this thesis reduced the presence of biofilm, and this may be because not only did the micro-topographies limited the attachment points, the micro-topographies also limited the overall contact between the surface area of the fouling organism and the surface texture. The reduced contact between these two areas may have made it more difficult for diatoms to excrete EPS from the raphe directly onto to the surface, therefore EPS may not be able to act as a 'glue' to aid in attachment of diatoms (figure 7.3). EPS acts as a glue to help secure diatoms to the surface, but also allows them a medium to move within, and enable other fouling organisms such as ciliates and zoo-spores to settle on the surface (Singh *et al.*, 2013). Reducing EPS may influence species settlement and may reduce diversity of marine biofilm, as some micro-fouling species may not be able to settle without EPS, although this has only been shown for macrofoulers such as *Hydroides elegans* (Huggett, Nedved and Hadfield, 2009), *Mytilus galloprovincialis* (Bao *et al.*, 2007), *Mytilus edulis* (Toupoint *et al.*, 2012) and *Mytilus coruscus* (Wang *et al.*, 2012). However, if the lack of EPS on the surface limits the settlement of further biofilm species, this may have been a contributing factor to the reduction in marine biofilm settlement. This reduction in species diversity may effect biofilm growth, and productivity leading to less marine biofilm settlement.

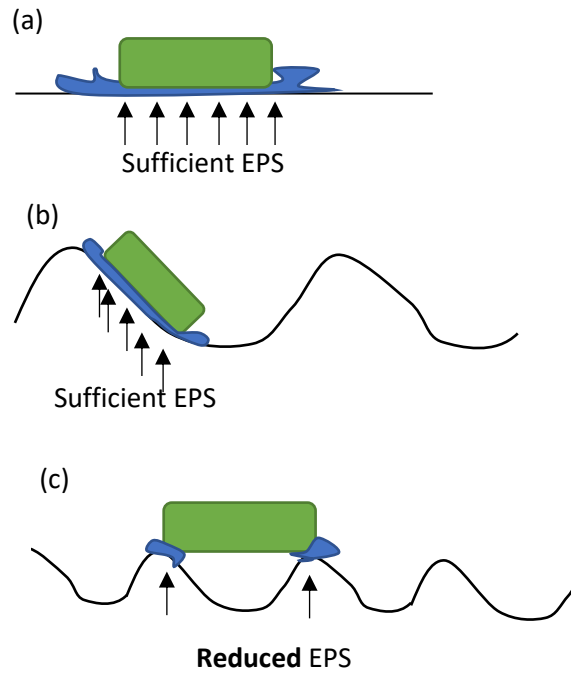


Figure 7.3 A schematic diagram showing the reduction of EPS use as a “glue” for aiding diatom settlement.

Biofilm development may have been interrupted if there was a gap between the diatom frustule and the surface as attachment points and EPS production may not be optimum. The reduction in fouling may have also been aided by the movement of water, as the cavity (eg. pit or groove) of the micro-textured surface may have filled with water in submersion, and may be enabling hydrostatic forces to remove the marine biofilm (figure 7.4).

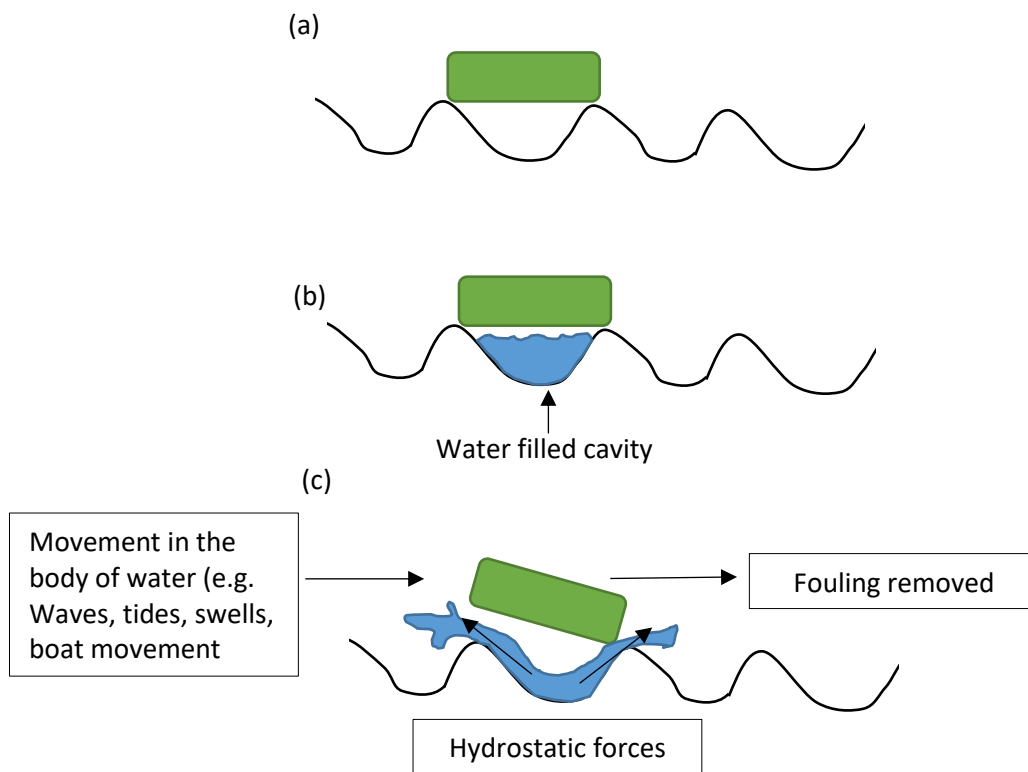


Figure 7.4 A Schematic diagram of laser textured surfaces showing potential effects of hydrostatic forces on diatom settlement.

However, this theory of hydrostatic forces acting within a cavity may not be completely accepted by some authors due to the surface already being fully submerged. However, the role of these hydrostatic forces may come into play when the antifouling surface textures is at the interface between water and air, such as when a tide is retreating, or waves are crashing and retreating. In these two instances, the water within the filled cavity may aid in biofilm removal.

### 7.2.2 Air entrapment theory

It is generally agreed that roughness and wettability of a surface are interlinked (Kubiak *et al.*, 2011; Ta *et al.*, 2015; Bizi-Bandoki *et al.*, 2011). The roughness and contact angle of the laser-textured surfaces was investigated in chapter 4, and showed a relationship between roughness, contact angle and fouling. A study by Wu *et al.*, (2013) investigated the use of super-hydrophobic surfaces in relation to diatom *amphora coffeaeformis* settlement and proposed that trapped air bubbles may on super-hydrophobic surfaces may be the cause of the reduction in fouling (Figure 7.5). As discussed in section 1.8.4 , this air entrapment theory may not be completely accepted by some authours due to the likelihood of entrapped air when submerged. In Wu *et al* (2013) investigation in-situ small-angle x-ray scattering was used to measure the percentage interface that remains dry on superhydrophobic surfaces immersed in diatom culture media and it was found that surfaces exhibited a degree of resilience against wetting, therefore, providing evidence that air entrapment is occurring on these surfaces, which may be leading to the antifouling effects.

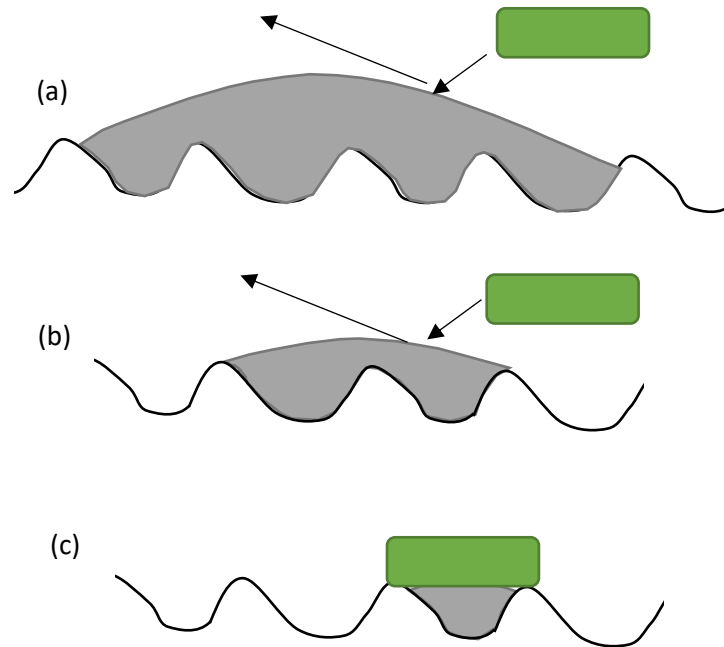


Figure 7.5 A Schematic diagram demonstrating the effects of air pocket size on diatom attachment where (a) the air pocket is much larger than the diatom, (b) the air pocket is similar size to the diatom and (c) the air pocket is smaller than the diatom (adapted from (Wu *et al.*, 2013).

It may be that on the laser textured biomimetic surfaces a combination of both methods are working together to limiting the fouling of biofilm. The air pockets may act in a similar way by limiting the attachment point of the fouling organism (Wu *et al.*, 2013), therefore reducing overall biofilm settlement. It has been previously found that a reduction in contact surface area between fluid and surface will limit the probability of marine fouling settlement (Zhang *et al.*, 2005).

In this case, the air bubbles may have reduced the contact surface area between the waterbody and the textured surface, and this in in turn may have led to a reduction in

the abundance of marine fouling. It has been suggested that the high contact angles seen on micro-textured surfaces may be due to the large air pockets, and the size of the air pockets can be fine-tuned by surface roughness (Wu *et al.*, 2013). Therefore, roughness and wettability may be affecting the settlement of marine biofilm by the creation of large air pockets between at the interface of the surface.

The reduction of cells with increasing roughness has been repeatedly found throughout the literature, and has shown similar trends to that found in this thesis. A study on the marine fouling organism *Ulva sp.* also found a decreasing linear relationship between engineered roughness index and the settlement of *Ulva sp.* spores (Schumacher *et al.*, 2007b). A decreasing exponential relationship between biofilm settlement roughness has also been found when analysing data roughness and settlement data from electro-polished stainless steel when tested with two different bacteria species (Figure 7.6).

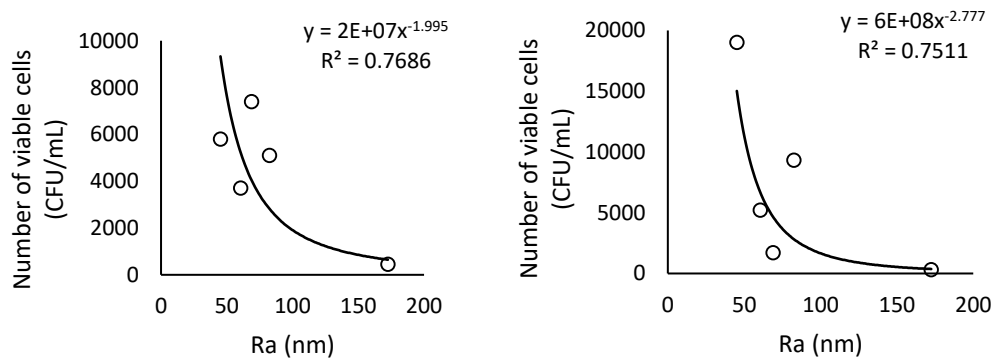


Figure 7.6 The relationship between roughness (Ra, nm) of stainless steel and settlement of viable cells (CFU/mL) for two bacteria species; (a) *S. aureus* and (b) *P. aeruginosa* (adapted from Wu (2018)).

This trend between roughness and settlement spans across different surface texturing methods, as it is not just found in laser-processed stainless steel surfaces (this thesis) but also on electro polished stainless steel surfaces (Wu *et al.*, 2018) and photolithography textured silicone (Schumacher *et al.*, 2007b). This means that different

methods of surface modification could be used for antifouling effects, depending on what is best use with the substrate. The modification of roughness of surfaces for antifouling surfaces could be used for a whole range of industries e.g. maritime (marine antifouling) and food manufacture (Wu *et al.*, 2018) to reduce biofilm development.

### 7.3 Multi- scale, Multi-feature patterns

Multi-scale, multi- feature patterns were able to further reduce marine fouling in the majority of experiments (4 out of 5). This may have been because the base and overlay patterns effecting the positions of settlement for these marine organisms. The base pattern may limit the fouling of large diatoms by reducing their attachment points (Figure 7.7) and the same may be occurring on the overlay pattern for smaller diatoms, therefore making combined pattern the best protection against fouling

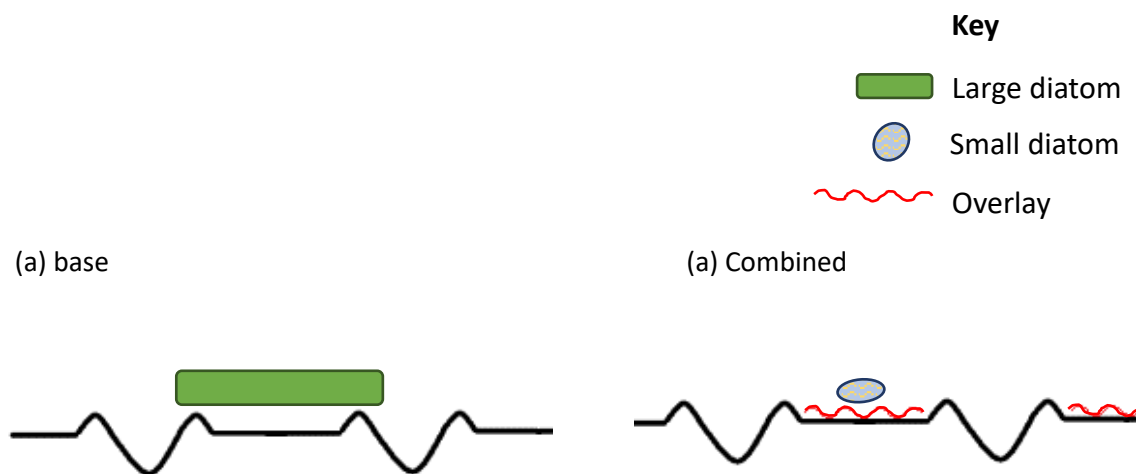
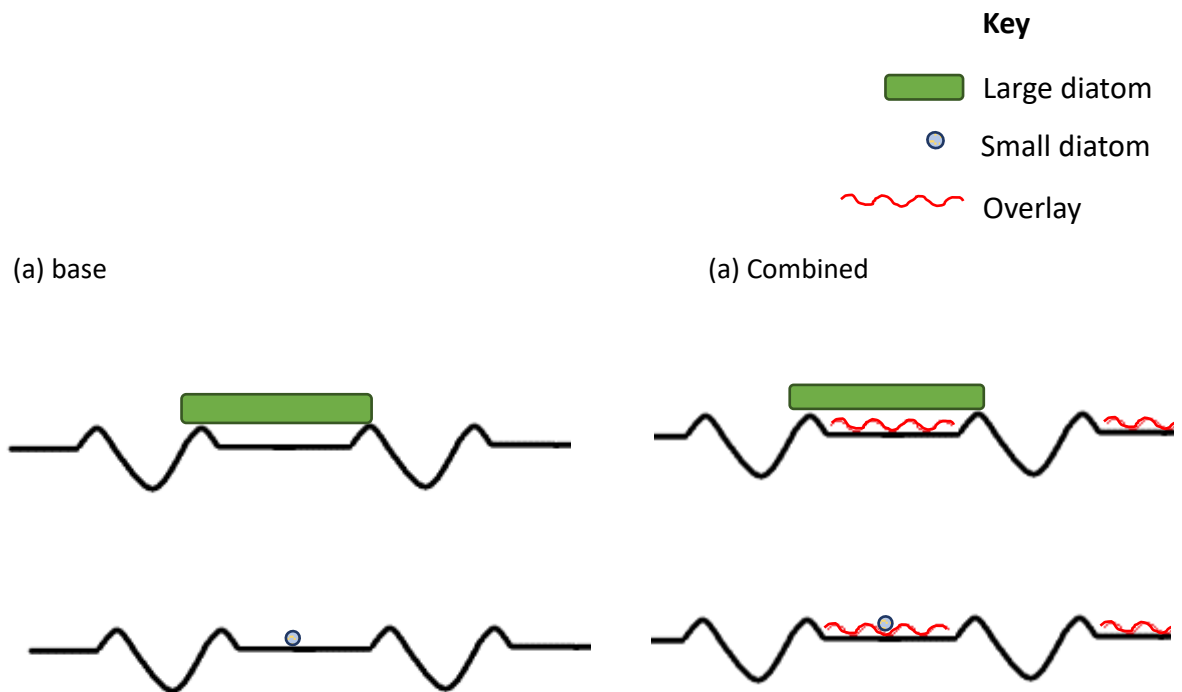


Figure 7.7 Schematic diagram showing possible interactions between (a) base and (b) combined patterns on different sized diatoms, where base and combined pattern both limit the attachment points of fouling organism.

In chapter 6, the shell based multi-feature pattern did not have a reduction in fouling, therefore it could be argued that multi-feature patterns do not have antifouling

potential. However, this increase in fouling was thought to have arisen from the large gaps between the base pattern, enabling increased settlement within the free space (position 2). This was found in another study, where the wide flat unprocessed space between features increased fouling (Carman *et al.*, 2006). The availability of “free space” (position 2) appears to be a key in influencing the levels of settlement.

High levels of settlement within the free space on the base and overlay patterns can be expected, as these patterns were of different scales. The base was a larger scale than the overlay pattern, therefore the base pattern may have been reducing larger organisms, and the overlay pattern may have been reducing smaller organisms. However, within the “free space” of the base pattern smaller organisms may have been able to settle, increasing the settlement within position 2 (Figure 7.8). This is similar to results found by (Sullivan and Regan, 2017) as they found that the majority of settled cells on their multi-scale multi-feature patterns were small and motile, adnate or centric diatoms.



*Figure 7.8 Schematic diagram showing possible effects of (a) base and (b) combined patterns on different sized diatoms, where base and combined pattern may not limit the attachment points of smaller fouling organisms.*

The overlay pattern was designed to target settlement within the free space (position 2) as its role was to limit the free space available for settlement. However, in the process, the overlay pattern may have encouraged smaller species to settle within the micro-pits. The overlay pattern may even result in a stronger adhesion for smaller diatoms as the sides of the pit may provide a wall to attach against as well as a horizontal surface. This is in agreement with results by (Sullivan and Regan, 2017) as they found that smaller diatoms are settling in higher numbers than larger diatoms on multi-scale, multi-feature topographies.

#### 7.4 Longevity of textures

Although the results in this thesis found that laser processed biomimetic surface have antifouling properties against marine biofilm, there is doubt over how long they may be effective (Sullivan and Regan, 2017). This thesis is evidence in that micro-textures can slow down the fouling process on a short term basis. Although this thesis found micro-textures provided antifouling efficacy on a short term basis, it is inevitable that over time, the surfaces will become fouled as space is a limiting factor in the marine environment (Connell and Keough, 1985). Biomimetic surface may be overruled by fouling in the long term, as the marine species in which they are based on use behaviour mechanism to avoid fouling, as well as the micro-textured structure, therefore, this combination provides fouling protection in the marine environment, not just the structures alone (Becker and Wahl, 1996). Crab micro-topographies were used as a biomimetic influence throughout this thesis, however, many crab species also use behavioural mechanisms such as bury in the sediment to avoid colonization (Glynn, 1970; Barnes and Bagenal, 1951; Mori and Zunino, 1987; Svavarsson and Davidsdottir, 1994) and moulting to remove fouling (Barnes and Bagenal, 1951). It has been identified that the most important behaviours to keep fouling rates low on crab species are burying, hiding, nocturnal activity and emersion (Becker and Wahl, 1996). Therefore, although the crab inspired micro-topographies have shown anti-fouling results in the short term, long term they may be overridden as in the natural world crabs used a combination of fouling textures and behavioural mechanism to avoid fouling. In the long term, the biofouling succession process outlined in (Section 1.1) will happen resulting in a macro-fouling community (Wahl, 1989).

It has been suggested that due to the diversity in size ranges of fouling diatoms and their diversity in shape, the sole development of micro-textured surface for antifouling efficacy would be difficult to achieve (Sullivan and Regan, 2017).

Table 7.2a Species list of diatoms found on surfaces

Diatom species	Control	Shell base	Multi-feature 2	Crab base	Shell overlay	Multi-feature 3	Crab overlay	Multi-feature 4
<b>Rhabdonema minutum</b>	✓	✓	✓	✓	✓	✓	✓	-
<b>Synedra fasciculata</b>	✓	✓	✓	✓	✓	✓	✓	✓
<b>Tryblionella apiculata</b>	✓	✓	✓	✓	✓	✓	✓	✓
<b>Tryblionella hungarica</b>	✓	✓	✓	✓	-	-	✓	✓
<b>Parlibellus delognei</b>	✓	✓	✓	-	-	✓	✓	✓
<b>Melosira moniliformis</b>	✓	✓	✓	✓	✓	✓	✓	✓
<b>Cocconeis</b>	✓	✓	✓	-	✓	✓	✓	✓
<b>Amphora</b>	✓	✓	✓	✓	✓	✓	✓	✓
<b>Diplonies</b>	-	✓	✓	-	-	✓	✓	-
<b>Haslea spicula</b>	-	-	-	✓	-	-	-	-
<b>Parabellus Berkeleyi</b>	-	-	✓	-	✓	✓	-	-
<b>Licmophora paradoxia</b>	-	✓	-	-	-	✓	✓	✓
<b>Achnanthes</b>	✓	-	-	-	✓	✓	✓	-
<b>Amphora coffeaeformis</b>	-	-	-	-	-	-	✓	-
<b>Achnanthes longipes</b>	-	-	-	-	-	-	✓	-
<b>Amphora Ventricosa</b>	-	-	✓	-	-	-	-	-

Table 7.2b Species list of diatoms found on surfaces

Diatom species	Control	Circle crab base	Circle shell overlay	Multi-feature 5
<b>Rhabdonema minutum</b>	✓	-	✓	✓
<b>Synedra fasciculata</b>	✓	✓	✓	✓
<b>Tryblionella apiculata</b>	✓	✓	✓	✓
<b>Tryblionella hungerica</b>	✓	✓	✓	-
<b>Parlibellus delognei</b>	-	✓	-	-
<b>Melosira moniliformis</b>	✓	-	✓	-
<b>Cocconeis</b>	✓	-	✓	✓
<b>Amphora</b>	✓	-	✓	-
<b>Diplonies</b>	-	-	-	-
<b>Haslea</b>	-	-	-	-
<b>Haslea spicula</b>	-	-	-	-
<b>Parabellus Berkeleyi</b>	✓	-	✓	✓
<b>Achnanthes</b>	✓	-	-	-

The diversity of sizes and shape of diatoms may be detrimental to the antifouling properties of the surfaces tested in this study. Over all the surfaces, 23 different diatom species were found on the surfaces (Table 7.2a and Table 7.2b). However, the diatom species present in a water body show seasonal and spatial variations (Lange *et al.*, 1985; Snell *et al.*, 2019; Nohe *et al.*, 2020; Moerdijk-Poortvliet *et al.*, 2018; Kókai *et al.*, 2019; McIntire and Moore, 1977). The seasonal change of temperature is a primary driver in the changes in diatom assemblages. Therefore, the antifouling potential of surfaces may alter with seasonality or with location. It is generally agreed that biodiversity is greatest in the tropics (Brown, 2014), therefore, testing biomimetic surfaces in tropical regions may reduce the antifouling efficacy, as there is a wider diversity of fouling species. However, this may not be the case, as diatoms appear to be an exception to the rule of latitudinal diversity gradient, as diatoms possess an extraordinary dispersal capacity due to large population densities and small sizes (Passy, 2010). Diatom species have been known to utilize a range of dispersal vectors such as ground water run off, hurricanes, and migrating fauna (Finlay 2002). Therefore, as diatom species ranges are relieved from geographical restrictions, it may be that seasonal changes will have more of an impact in antifouling efficacy of surfaces than spatial changes.

It has been suggested that with extended exposure in the marine environment, micro-topographical surfaces may be overridden, and the texture becomes obsolete (Sullivan and Regan, 2017). A way in which this could potentially happen to the surfaces tested in this study is by the dominance of chain building species on the panel. Although not reported in chapter 6, the cluster species *Synedra fasciculata* was a dominant species in the biofilm community (Figure 7.9). Other species found within the diatom assemblage on this study were chain building species *Melosira sp.* and tube dwelling species *Parlibellus delognei*. Both species are common fouling species; *Melosira* has previously been recorded as a fouling species in Langstone Harbour, South Coast of England (Pyne *et al.*, 1986) and

all over the UK (Crawford, 1977); and *Parlibellus delognei* has been previous recorded fouling in-service cruise ship hulls (Hunsucker *et al.*, 2014).

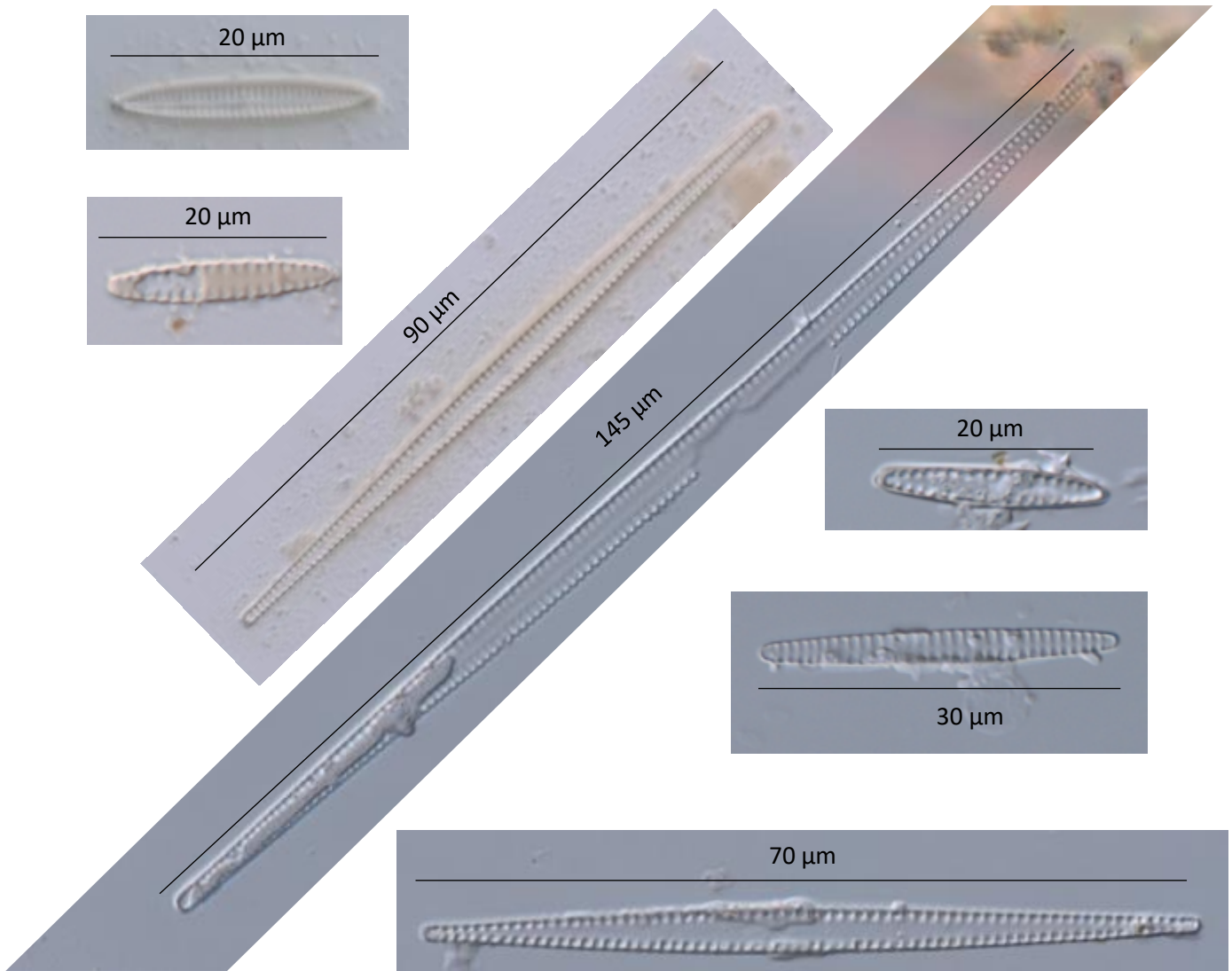


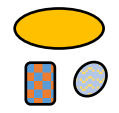
Figure 7.9 Dominant species *Synedra fasciculata* of various sizes found on multi-scale and multi-feature surfaces throughout this study.

Dominant species are important as they can be ecosystem engineers and alter the conditions of the niche to boost community richness (Jones *et al.*, 1994; Wright *et al.*, 2002). As *Synedra fasciculata* was a dominant species found on surfaces within chapter 6, it may be affecting the settlement of biofilm. *Synedra fasciculata* is a marine diatom first described by Kützing (1844) and is known to grow in bundles and clusters (Stearn, 1973). *Synedra fasciculata* has previously been found to be a dominant species on non-toxic panels in Canada (Prince Edward Island; Bacon and Taylor, 1976), and panels immersed in Langstone Harbour, South Coast of England (Pyne *et al.*, 1986) showing that the diatom is a common species widely distributed within the global water bodies.

*Synedra fasciculata* recorded in this study range from 20 µm to 145 µm (Figure 7.4.2). Therefore, they may have been a dominant species as they were able to occupy both small niches created by the overlay texture, and large niches created by the base pattern. *Synedra fasciculata* has been known to form three dimensional colonises. When these colonises have been analysed it has been found that singular cells of other diatom species are present, as they are able to embed into the extra cellular polymeric substance (EPS) that holds the clusters together (Ferreira and Seeliger, 1985). It is these types of colonises that may override the surface topography, and encourage biofilm settlement.

### Key

 Chain building diatom

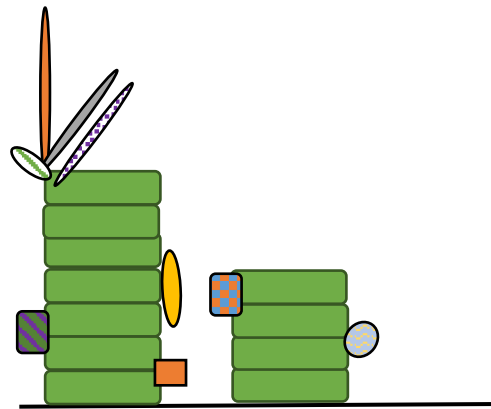
 Others – each colour individual species

 Surface

(a)



(b)



#### Non-chain building

Lower species richness

Higher diversity/ evenness

Each species have 25% abundance

#### Chain building

Higher species richness

Lower diversity / evenness

Chain building have 90% abundance, other species 1-2%

Figure 7.10 Schematic diagram showing possible species richness, diversity and interaction when the dominant species is (a) non-chain building and (b) chain building diatoms.

Both this study, and a previous study by Sullivan and Regan (2017), are in agreement that colonial forming diatom species play a role in enabling settlement on micro-textured surfaces. In this study *Synedra fasciculata* was found to be the dominant cluster building species with a frustule length of 20-145  $\mu\text{m}$ , chain building species (*Melosira*) and mucilage tube dwellers (*Parlibellus delognei*) were also present in the biofilm community on many of the patterns in this study (see table 7.2). Whereas in Sullivan and Regan (2017) the chain-forming species was identified as *Neosynedra* with frustule sizes between 50–100  $\mu\text{m}$ . They found that chain-forming diatoms were able to bridge multiple surface features at once, therefore increasing their attachment points, rather than surfaces limiting it. Therefore, designing surfaces that limit the chain forming type of diatom may be the future for reducing marine fouling.

*Synedra fasciculata* may be the dominant species as it has a size range of 20-145  $\mu\text{m}$ , therefore was able to settle in a wider range of places. Other common species within the diatom assemblage found in this study were chain forming species *Melosira sp.*, and mucilage tube dwellers *Parlibellus delognei*. When chain and cluster forming diatom settle within a free space, one single cell is able to settle, and form multiple attachment points (Figure 7.2; Scardino *et al.*, 2006a). By secreting EPS attachment can become stronger, and then diatoms can reproduce to form chains. By building chains, there is a removal of competition for space on the panel, and they are able to reproduce exponentially, which may be why they are dominant across the panels (Figure 7.11).

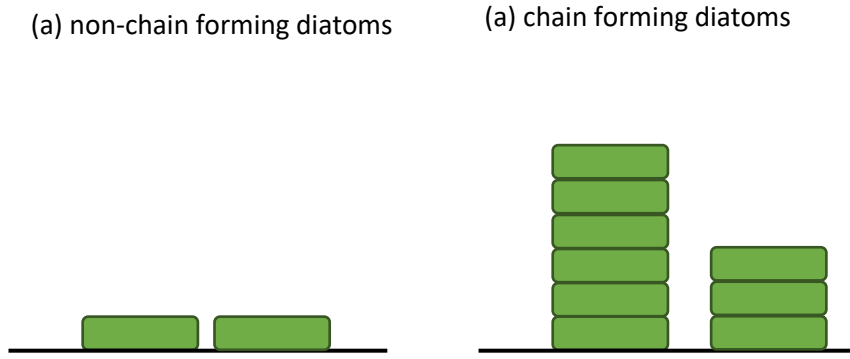


Figure 7.11 Schematic diagram showing attachment strategies of (a) non-chain forming diatoms and (b) chain forming diatoms.

It has been discussed previously, that the micro-textured surfaces are causing a reduction in attachment points, which is leading to a reduction in fouling of the surface. This effect may be amplified when the dominant species are chain forming diatoms. This could be because the whole chain could become unstable when settled within the laser processed area (Figure 7.12).

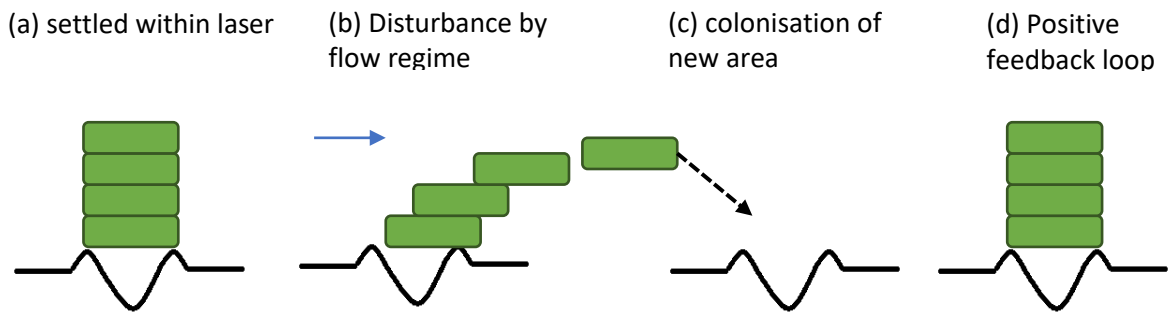


Figure 7.12 Schematic diagram showing chain forming diatoms in a positive feedback loop where (a) they settle on the micro textured surface and produce chains, (b) sections of the chain are dislodged and land on other areas of the micro-texture, and (c) settlement and chain building of dispersed chain forming diatoms, as feedback loop starts again.

If chain forming diatoms settle on micro-textures, it could make their chains less stable as attachment points reduced on the “base” individual. There will be less of a stronghold on the chain to the surface at the point of attachment. The diatom chain may still grow, but as it gets longer, it will become more prone to the flow regimes of the water around the micro-textured surface, and a small disturbance may be enough to knock the chain off, and break it up into clusters or individual diatom cells. Once a chain has broken up, some may be transported back into the water column, however, other may settle on the surface a small distance from where they originated in a chain. These diatoms go on to colonise a new area and form their own chain. This positive feedback loop may be the reason why chain building diatom are dominant species on combined patterns. This feedback loop would enable a low but constant abundance of chain building diatoms on combined patterns, and this is exactly what we found within the species analysis (Section 6.3.8). This type of positive feedback loop has been described in the literature as a way of biofilm dispersal (Lewandowski, 2000). However, it would be plausible that the micro-textured surface encourages and accelerates detachment and re-colonisation, as the settlement on the surface is unstable and delicate. It is also plausible that once streamers of chains building diatoms are established, they may break off in small groups of diatoms encased in EPS called mucilage aggregates. These aggregates may contain both chain-building and other species of diatom, and they may attach to a surface as one entity (Figure 7.13).

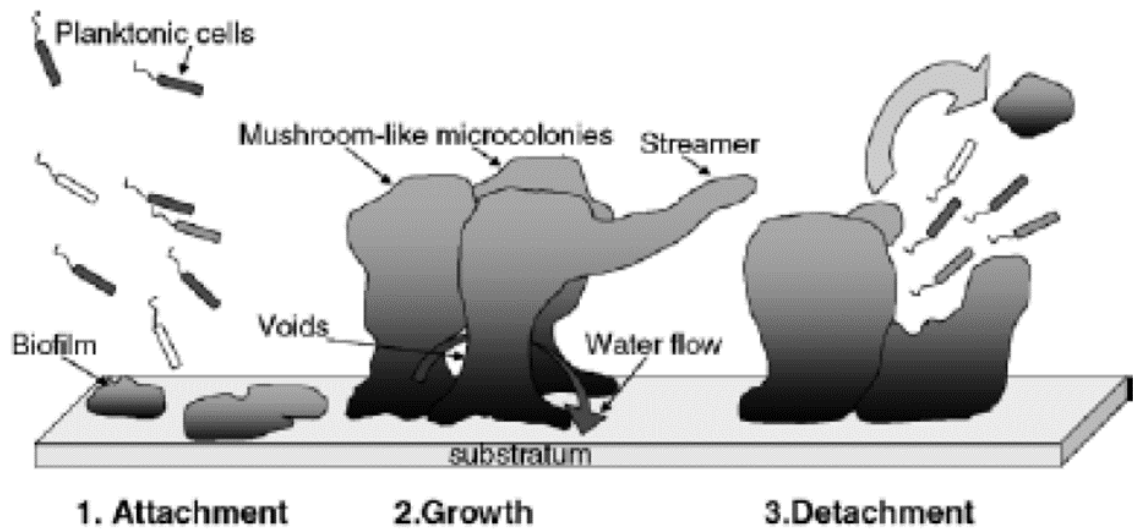


Figure 7.13 The cycle of a biofilm; attachment, growth, detachment (Lewandowski, 2000).

First descriptions of biofilm development have led us to believe that diatoms will settle in neat individual cells, and then form attachment points, produce EPS and multiply to produce a biofilm. However, diatoms may not settle in individual cells, as diatoms can group together and become encased in EPS to form mucilage aggregates. These mucilage aggregates are present in water bodies (Alldredge and Silver, 1988; Alldredge and Crocker, 1995) and they may be larger than the micro-textured surface. If mucilage aggregates come into contact with the surface, they may be able to attach as: (a) they are already encased in sticky mucus, so stick to the surface, and (b) the size of their combined entity may larger than the antifouling texture, and therefore it may not have any effect (Figure 7.14).

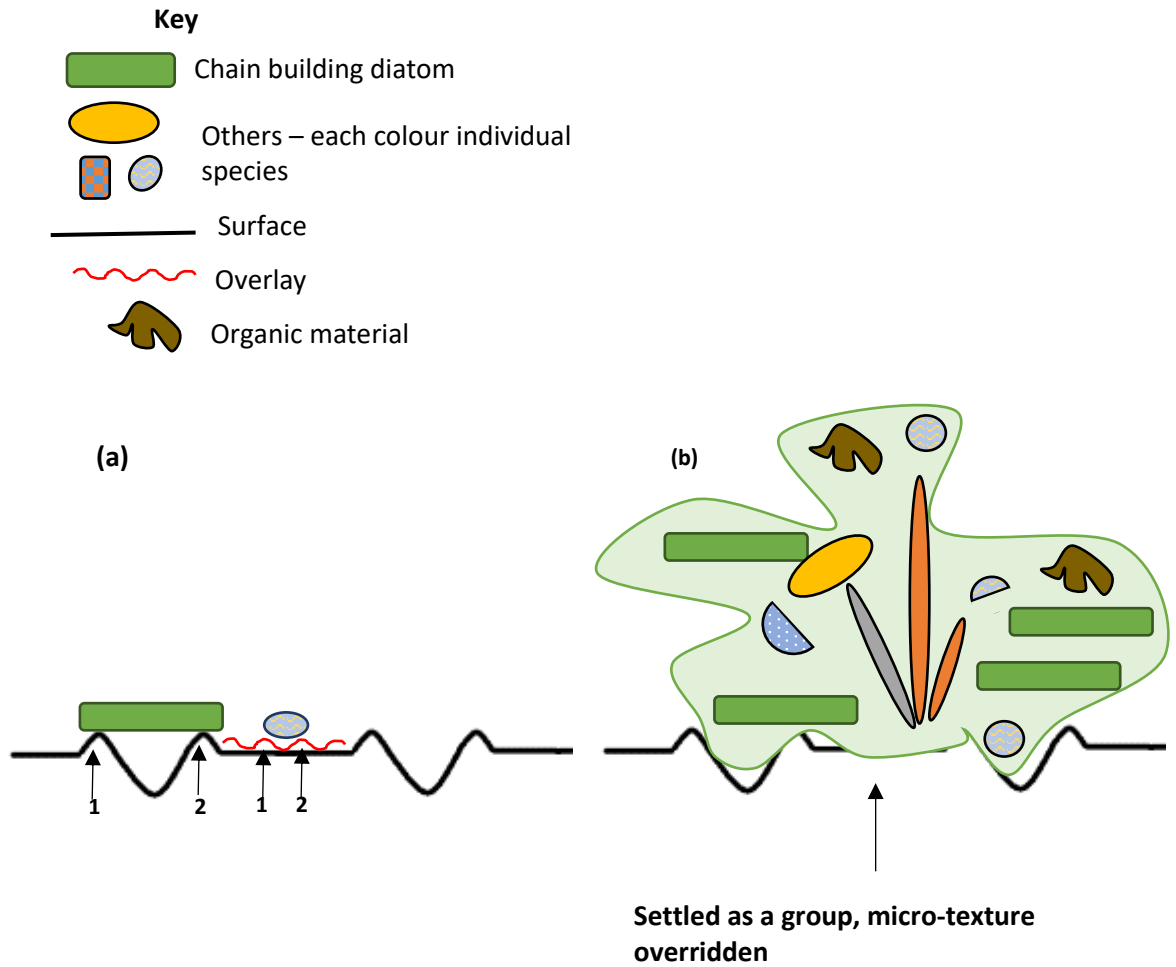


Figure 7.14 Schematic diagram showing settlement mechanisms of (a) single diatoms of different sizes and (b) mucilage aggregates.

This study found mucilage aggregates present on the samples after a 7 day period, and they may play a role in overriding surface textures and therefore encouraging biofilm settlement. This is similar to results found by Sullivan and Regan (2017) study on multi-feature micro-textured surfaces in the marine environment found that mucilage aggregates were commonly found on textured surfaces in this study after a 7 day period. The chance of colonisation as a group of diatoms, compared to a single cell may be higher. Mucilage aggregates within both this study and Sullivan and Regan (2017) study were generally

comprised of bacterial cells, and damaged and intact frustules of benthic and planktonic diatom species. Within this study where possible, identification of diatoms was undertaken, however, it was not reported if certain species were grouped in mucilage aggregates. It has been suggested that planktonic diatom species may cause the start of forming an aggregate suggesting that they provide the mucus base, and that benthic species such as *Navicula*, *Amphora* or *Cocconeis* encounter and attach to the aggregates within the water column (Sullivan and Regan, 2017). Aggregates may play a role in transportation of the primary colonising cells to a newly submerged surface. Settlement of groups of diatoms rather than individual species may be mitigating the effect of surface topography, and it may be why some surfaces, such as the surfaces used in Chapter 6 of this study, do not have an antifouling effect. Once aggregates colonise a surface, their presence may significantly affect the hydrodynamic flow of the surface, contributing to increased settlement as areas may be blocked from currents due to protruding aggregates.

The role of settlement of groups may also indicate why the same species are found repeatedly on the slides (Table 7.2a and 7.2b), as the chance of colonisation within an aggregate may be higher than single diatom cells alone. Micro-textures may have an effect against single cell diatoms, however, the antifouling effect may be overridden when settlement within groups. This also may be why chain and cluster building diatoms were a dominant species on panels within this study, as they form mucilage aggregates which may break off and re-colonise surfaces as described in Figure 7.13.

Overall, reducing settlement may not be as simple as reducing attachment points, as it may be that diatom cells attach and settle within mucus group which may over-ride any micro-texture present on the surface. It is also known that diatoms have the innate ability to quickly release from a surface (Cohn and Weitzell Jr, 1996) and that the formation

of mucilage aggregates is standard procedure and may not be a reaction to the surface features on a substratum (Cohn and Weitzell Jr, 1996). From the results of this study, and the study by Sullivan and Regan (2017) it is possible to suggest that single cell diatoms are the primary colonisers and may be the most important in the first 7 days, which is why there was a reduction in settlement on micro-textures in this study. However, as the period of immersion increases, it is likely that colonisation by mucilage aggregates increases, and therefore reduces the antifouling efficacy of the surfaces. To test this theory, longer immersion of surfaces in the marine environment would be required so that the longevity of the antifouling efficacy can be tested (Sullivan and Regan, 2017).

#### 7.5 Lab vs. Field based studies

These surfaces tested in this thesis have a real world antifouling effect as they were tested *in situ* in the marine environment. The majority of papers referenced within previous chapters rely on lab-based assays (Hoipkemeier-Wilson *et al.*, 2004; Schumacher *et al.*, 2007a; Schumacher *et al.*, 2008; Table 7.1) whereas this thesis is an example of biomimetic surfaces on marine grade steel working directly in the natural environment. This highlights the novelty of the thesis as very few studies have tested biomimetic antifouling surfaces in the marine environment. The studies that have tested micro-textured in the marine environment are in agreement with this thesis in that a reduction in fouling was found on micro-textured surfaces (Efimenko *et al.*, 2009; Brzozowska *et al.*, 2014). As testing of micro-textures in the field has very few studies compared to lab based environments, these studies are crucial in providing real world data, which will be useful in deciding the next steps of biomimetic antifouling applications. This thesis provides real world data that biomimetic surfaces have an antifouling effect outside of lab-based scenarios, and therefore it may be possible to scale up this type of work to commercialisation. The commercialisation of biomimetic surfaces has already occurred for the Sharklet™ pattern, as it is used in catheter tubes to reduce the settlement of bacteria

that produce catheter-associated urinary tract infection (CAUTI; Reddy *et al.*, 2011; May *et al.*, 2015). However, there is currently no available biomimetic antifouling micro-texture for the marine environment. This thesis aims to bridge this gap, as it shows that a marine anti-fouling micro-texture has been developed directly onto marine grade steel exposed within maritime industries without the use of any extra polymers or coatings. The areas in which this texture may be applicable in the future where steel is exposed in the marine environment are on scientific instruments (Davis *et al.*, 1997), where coatings or added chemical may interfere with data recordings, therefore, short term no toxic antifouling solutions would be beneficial.

#### 7.6 Antifouling textures without additional chemicals.

Other studies on laser surface texturing on steel for an antifouling effect have required further processing by the addition of silicone coatings (Sun *et al.*, 2018), however, this thesis is the first to show that laser surface texturing can be used to directly create a biomimetic antifouling surface without the addition of further chemicals. The creation of an antifouling surface with the lack of additional chemicals could have potentially a massive impact on the health of the oceans if made commercially available, as currently anti-fouling paints use chemicals that may have negative effects on the ocean. Historically TBT was used, and this had negative effects on marine life (as discussed in section 1.3.1). However, since the ban on TBT, the active ingredient used in antifouling paint, alternative booster biocides have been used in antifouling paint. Of 18 booster biocides produce, nine of them are approved for use in UK waters (Voulvoulis, Scrimshaw and Lester, 2002). However, these booster biocides are toxic to a large range of aquatic life outlined in a review by (Konstantinou and Albanis, 2004). There is also concern at the rapid rate that new chemicals are being produced into the antifouling market, it is unknown how these chemical will effect the ocean in the long term (Voulvoulis, Scrimshaw and Lester, 1999). One of the biocides, Diuron, has been found to reversibly affect photosynthesis of

seagrasses (Macinnis-Ng and Ralph, 2003) by inhibiting the photosynthetic electron flow within photosystem II (Miles, 1990; Falkowski and Raven, 1997). Not only does this effect the marine life, but by inhibiting photosynthesis there is the potential to effect ocean processes such as carbon sequestration. The sequestration of carbon into the ocean is an ecosystem service that we currently rely upon to store and sink carbon dioxide out of the atmosphere, to reduce global warming (Sun, 2011). Diatoms are a keystone functional group in the carbon cycle, and if this delicate carbon balance was disrupted by the effect of booster biocides on photosynthesis, there may be implications for climate change. Therefore, although TBT has been banned, the alternative booster biocides are not an ideal replacement as they too can have negative effects on the ocean and have already been found within the sediment (Konstantinou and Albanis, 2004). This highlights the importance of this thesis, as it has repeatedly shown that the laser surface texturing of biomimetic antifouling surfaces can produce antifouling results without the use of additional chemicals, which are repeatedly being found to be detrimental to the marine environment. If scaled up, this research has the potential to offer a non-toxic alternative to the antifouling industry.

#### 7.7 Limitations of this study

Although this thesis has shown to potential use of marine anti-fouling micro-textures directly onto marine steel, there are limitations in the study in that they have only been tested in UK waters, therefore it is unknown if they will work in other areas, where different diatom species may be dominant. It is well established that abiotic factors such as light availability, depths and temperature effect the diatoms present on the surface (Patrick, 1971; Pyne, Fletcher and Jones, 1986b; Munda, 2005; Yang *et al.*, 2015). However, the experiments undertaken in this thesis have shown that the laser textured biomimetic surfaces were able to work in all seasons, as the settlement on the control samples increased with season, but the biofouling efficacy remained. This is shown in chapter 5 as

settlement within control samples increased from 3200 in early spring (experiment 1), to 20000 in summer months (experiment 4), however, the surfaces still provided antifouling results.

Previous studies have shown that species composition changes through the seasons, as some species such as *Synedra fasciculata* were found to be dominant throughout May and June, however, when water temperatures became warmer and exceeded 10°C there was a shift in the community and it was no longer dominant species (Bacon and Taylor, 1976). *Synedra fasciculata* was also a dominant diatom on the panels within this thesis (Chapter 6) and therefore it is likely that the species composition of our panels changed seasonally, however, the antifouling efficacy remained. Therefore, it is likely that the antifouling effects have not been effected by the change community composition, and that the antifouling protection is working against a larger range of species, both in the communities where *Synedria* are dominant, and on other communities where *Synedra fasciculata* is not dominant, and different species may be present. As experiments were carried out all year round, the surfaces is not overpowered by higher growth rates in spring and summer months.

Another possible limitation of this thesis is that all patterns were tested at 1m depth. It is known that species communities change with depth (Pyne *et al.*, 1986) and often there is clear zonation of distinct communities with depth. Therefore, it could be argued that as this study has only tested panels at shallow depth, they may not be effective in deeper parts of the ocean as there will be different species present. However, within deep ocean environments the fouling pressure is decreased this is reflected in studies that show, the corrosion levels are reduced as there is less microbial induced corrosion in the deep ocean (Venkatesan *et al.*, 2002). Although the surfaces in this thesis were only tested at a shallow depth, they were tested where the fouling pressure is greatest (Wahl, 1989). Fouling pressure decreases as depth increases, this is due to photosynthesis being a limiting

factor of biofilm growth (Brouns & Heijs 1986). The growth fouling diatoms is fuelled by photosynthesis, and photosynthesis only occurs in the euphotic zone of the ocean (Ryther, 1956). Therefore, although only tested in shallow depth, they may be more beneficial in deeper waters, as fouling pressure is reduced, therefore they may have a greater antifouling efficacy.

Overall, this thesis is in agreement with many other studies (Table 7.1) in that biomimetic surfaces reduce the settlement of marine fouling organisms. It was found that by designing multi-scale and multi-feature patterns that took inspiration from two marine organisms, can increase the antifouling efficacy. So far, in the literature, only one other study has combined patterns, and therefore there is still plenty of opportunities to develop new patterns that may have antifouling effects inspired by marine organisms. The main reason in explaining this reduction is the diatom attachment theory (Scardino *et al.*, 2006a; Scardino *et al.*, 2008) as the micro-textures are reducing the number of attachment points and therefore the surface is having an antifouling effect. There is sufficient evidence within this thesis, and among other studies, that the micro-textures are significantly reducing the settlement of diatoms and other micro-fouling species. Therefore, as there is a lack of biofilm, this may affect settlement of macrofouling species. A study has shown that the biofilm density and presence of particular diatom species significantly affected the settlement of *Bugula neritina* larvae (Dahms *et al.*, 2004). Similarly, it was found that larval settlement success of *Haliotis rufescens* differed significantly between mucus substrate, diatom substrate and  $\gamma$ -aminobutyric acid substrate (Slattery, 1992) and that diatoms may significantly contribute to the recruitment of larval settlement onto substrates in *Hydroides elegans* (Harder *et al.*, 2002). As these studies show, diatoms are a precursor to the macrofouling species settlement, as increases in biofilm coverage leads to increases in further settlement (Harder *et al.*, 2002; Joint *et al.*, 2002; Callow and Callow, 2006). Therefore, with a reduction in biofilm settlement, further macrofouling settlement

may be reduced. This means that as the biomimetic laser textured surfaces tested in this thesis may not only be directly effecting the biofilm, but may indirectly be effecting the macrofoulers ability to settle, by removing the presence of diatom species. If this type of surface presented in this thesis becomes commercial, the ability to limit not only microfoulers, but also macrofoulers will be a great advantage as macrofoulers such as mussels, cockles and tubeworms can cause more damage to structures and increase the drag of ships due to the weight of their calcareous shells (Townsin, 2003). If this type of surface were available commercially, it would help reduce the problem invasive species, as ship fouling is one of the main ways invasive species are moved around the globe, for example the zebra mussel which was first recorded in London docks in 1824, after being transported from the Baltic region, but is now widespread across the whole of the UK and Ireland (Aldridge, Elliott and Moggridge, 2004).

In the majority of micro-texture antifouling studies, the surfaces are found to limit and reduce fouling. However, in some studies such as (Carman *et al.*, 2006) and (Sullivan and Regan, 2017) the certain surface combinations have been found to promote the attachment of cells, this usually occurs where the cell is similar in size to the topography so can fit in-between the micro-texture. It could be argued that if micro-textured surfaces can exhibit control of marine diatom cells, by effecting their settlement, that micro-textures could be used to promote the settlement of marine organisms. Studies have shown that some micro-textures can increase the settlement of spores of the green alga *Ulva linza* (Xiao *et al.*, 2013) and the mussel *Mytilus galloprovincialis* (Carl *et al.*, 2012). This could be useful for coral reef restoration projects such as Biorock projects in which steel structures are sunken and provided with an electric current to enhance the promotion of corals in areas that have suffered mass coral death due to bleaching and erosion (Wells *et al.*, 2010; Goreau and Prong, 2017). By texturing the surface of this steel structure, it may add to their effect of increasing the coral settlement and a quicker restoration of the reef habitat.

## 7.8 Conclusion

The overall aim of this study was to develop a biomimetic pattern using laser surface texturing directly onto marine grade steel that has antifouling properties. The reasons in which why laser textured biomimetic surfaces would be an advantage such as providing an eco-friendly antifouling solution for the maritime industry, improving the health of the oceans, and lower costs for fouling within industry were discussed in Chapter 1. This thesis was a proof of concept study that met this aim by investigating three objectives; if the method of laser surface texturing could have an antifouling effect (chapter 4); if biomimetic antifouling patterns could be produced using laser surface texturing (chapter 5) and if combining patterns to create multi-scale and multi-feature patterns would enhance the antifouling potential of the patterns (chapter 6; Figure 7.15).

Aim: to develop a biomimetic pattern using laser surface texturing directly onto marine grade steel that has antifouling properties

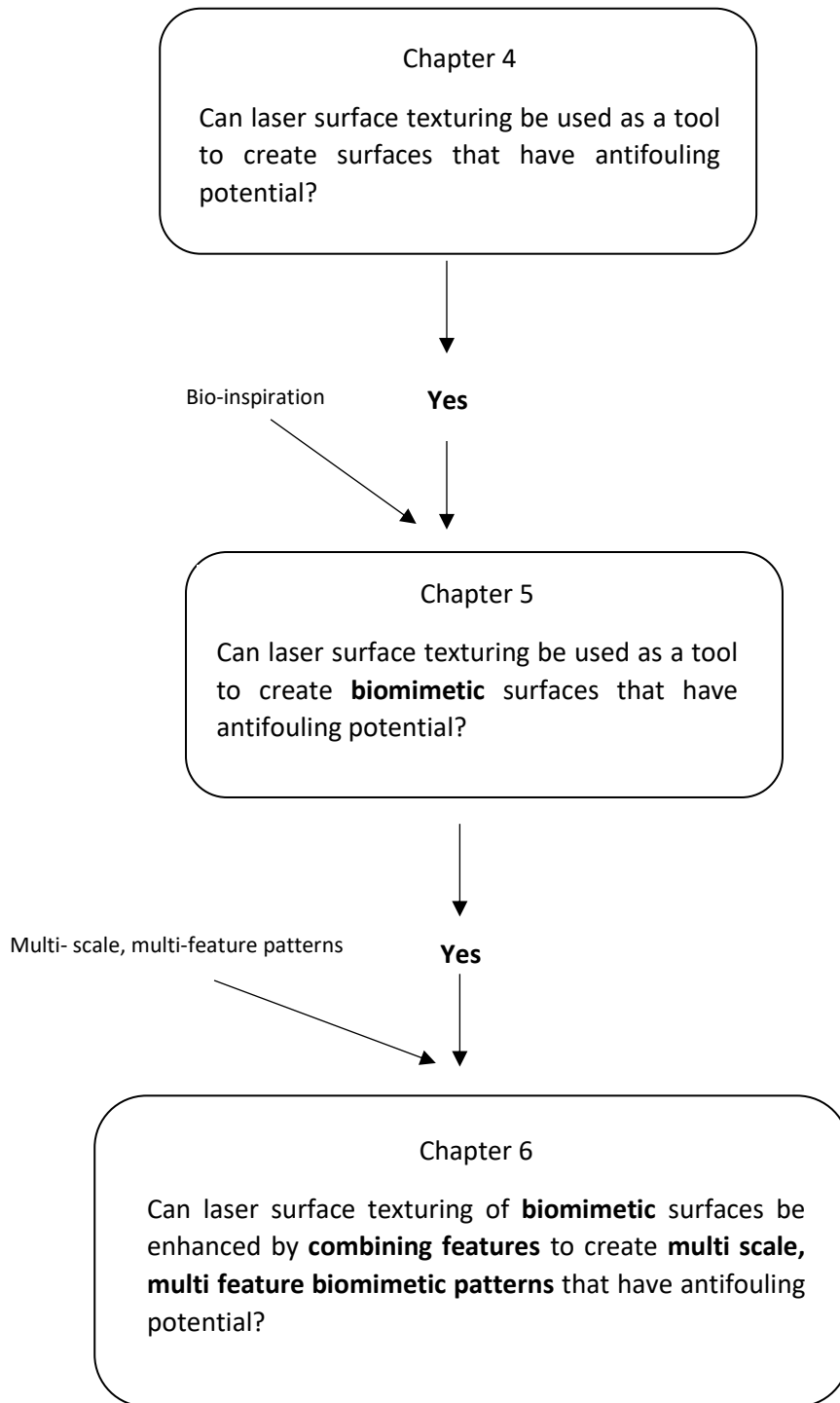


Figure 7.15 Evolution of experimental chapters to meet overall aim of thesis.

The experimental data has repeatedly shown that the biomimetic laser textured surfaces are having an antifouling effect, in which combined features from multiple marine organisms to create multi-scale and multi-feature patterns improve the antifouling efficacy. This thesis is in agreement with others (Schumacher *et al.*, 2007b; Efimenko *et al.*, 2009; Sullivan and Regan, 2017) in that the use of multi-scale, and multi-feature surface textures is the way forward in increasing antifouling efficacy of micro-textured surfaces. The experimental work carried out within this thesis was all field based, reinforcing the fact that this has real world applications.

Alongside the importance of multi-scale and multi-feature surfaces is the importance of aspect ratio of fouling organism to the size of the surface pattern (and / or texture). This is less important than the multi-scale and multi-feature aspect as when tested in the marine environment as the dimensions of the fouling organisms are unknown. There is also the role of roughness and contact angle of the surface within the micro-textures which play a role in the antifouling efficacy. Overall, the importance of a micro-textured surface having multi-scale and multi-feature micro-texture is highest, as this is what will have the created antifouling efficacy against a wide range of fouling organisms (Figure 7.16).

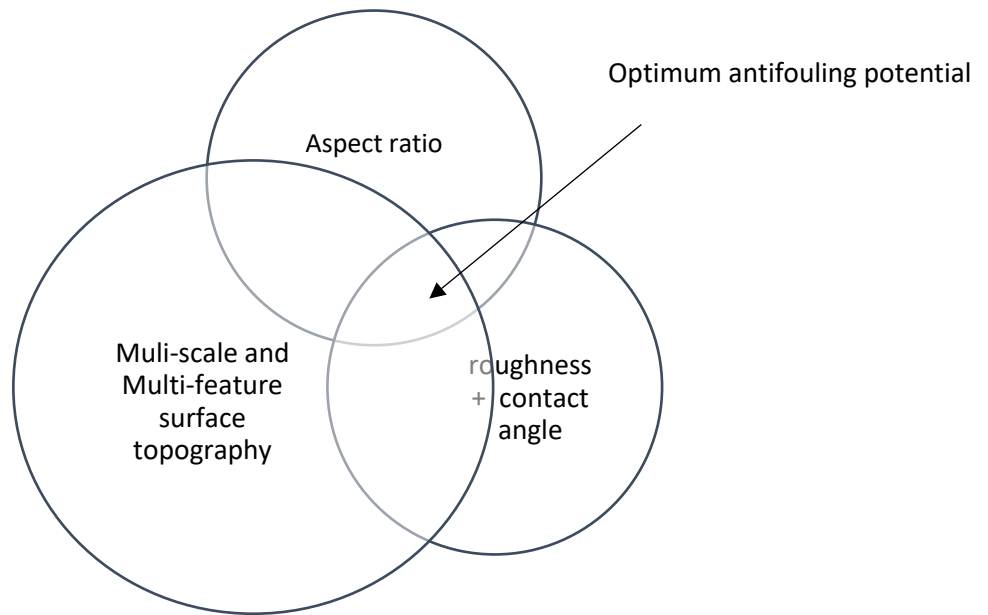


Figure 7.16 Interlinking relationships between multi-feature and multi-scale topography, roughness and contact angle, and aspect ratio of fouling organisms that lead to the optimum antifouling potential of a surface.

## Chapter 8 Future work

Ideally, the end goal for this type of technology would be to be used on areas of metal that are exposed on a short term basis in ocean environments. An area of interest for this technology could be ocean instruments that are often deployed for long periods to collect data on ecological processes as they are prone to fouling, which can effect components such as light sources, fluorometers, and sensors (Davis *et al.*, 1997). Without antifouling protection, ocean instruments can be limited in deployment to several weeks (Davis *et al.*, 1997). In the past, bronze rings containing tributyltin oxide have been used to limit fouling of ocean instruments (Butman and Folger, 1979) although this is no longer the case after the TBT ban. Divers have also been used to periodically clean the ocean instruments while in situ (Martini and Strahle, 1993), however, instruments may be drifting with currents, or in remote or rugged regions, therefore the use of divers for biofouling maintenance is not practical. Therefore, the use of biomimetic laser textures surfaces may

be an idea solution to the problem, as texturing could be used on instruments before deployment to extend the deployment lifespan.

Another area of metal that are exposed on a short term basis in ocean environments are bronze ship propellers. It has been found that propeller blade surfaces which are often polished metals such as manganese bronze have no anti-fouling protection (Townsin, 2003). The lack of fouling protection may be because when the propeller is turning, there is very little chance of biofilm settlement. However, once in the harbour and static in a water body for a couple of days the biofouling process will occur, and a biofilm will develop on the propeller. This is where there the micro-textured surfaces would be beneficial, as they will be able to limit the biofilm development over a short term period while the propeller is static. This application may be achievable as there is already research into laser texturing of bronze substrates to increase micro-hardness (Tang *et al.*, 2006) therefore micro-texturing using laser may be able to combine increasing the micro-hardness and providing antifouling. Within the maritime industry there are many other surface areas at the interface of a hard substrate and water in which fouling occurs such as; on aquaculture infrastructure, oil rig infrastructure, and inside pipelines on heat exchangers.

The main challenge that faces this work going forward is to do with scaling up the project. As the work in this thesis was carried out on 50x50mm coupons, therefore laser surface texturing was quick, efficient and of reasonable price. The development of portable hand held laser devices may be an option in solving the logistical problems that occur in scaling up this research (Wolf *et al.*, 2009).

Inevitably, there will be a trade off between price to produce the surface (laser costs) and price of what currently available, as most companies are likely to choose the cheapest option. However, this may change as we as a society become more aware of the

necessity to protect our oceans, companies may become more conscious and factor eco-friendly options into their budget. As this technology is non-toxic and chemical free, it may prevail as more and more chemicals are being banned from used in the ocean.

A limitation of the biomimetic side of the project was that the availability of the biological specimens was limited to that of what would be found locally, and what was stored within LJMU archives. There was also difficulty in scanning specimens as GFM and Bruker machines are generally designed for use within material science where samples are of regular shapes, therefore scanning for a surface on the curvature of a shell became an issue. For future work, a larger range of biological species could be investigated prior to the pattern design stage. As discussed in the literature review, the appearance of micro-textures across a whole range of species, whereas this thesis mainly focuses on crab and bi-valve species. Future work could be done incorporating more of the feature, such as pyramid type shapes, wavy lines (shown in section 1.4.2 Table 4) into the draft sight designs. A process in which removes the uncertainty about the depth of laser surface texturing would also enhance this project as then patterns could be planned in 3D not just 2D as they are currently in this thesis. It was possible to mimic other creatures using the laser surface texturing process such as the spinner shark, recreating a Sharklet™ like pattern directly onto marine grade steel (Figure 8.1), however, due the constraints of the laser surface texturing program (SamLight), the pattern was not able to be scaled down to the microscale.

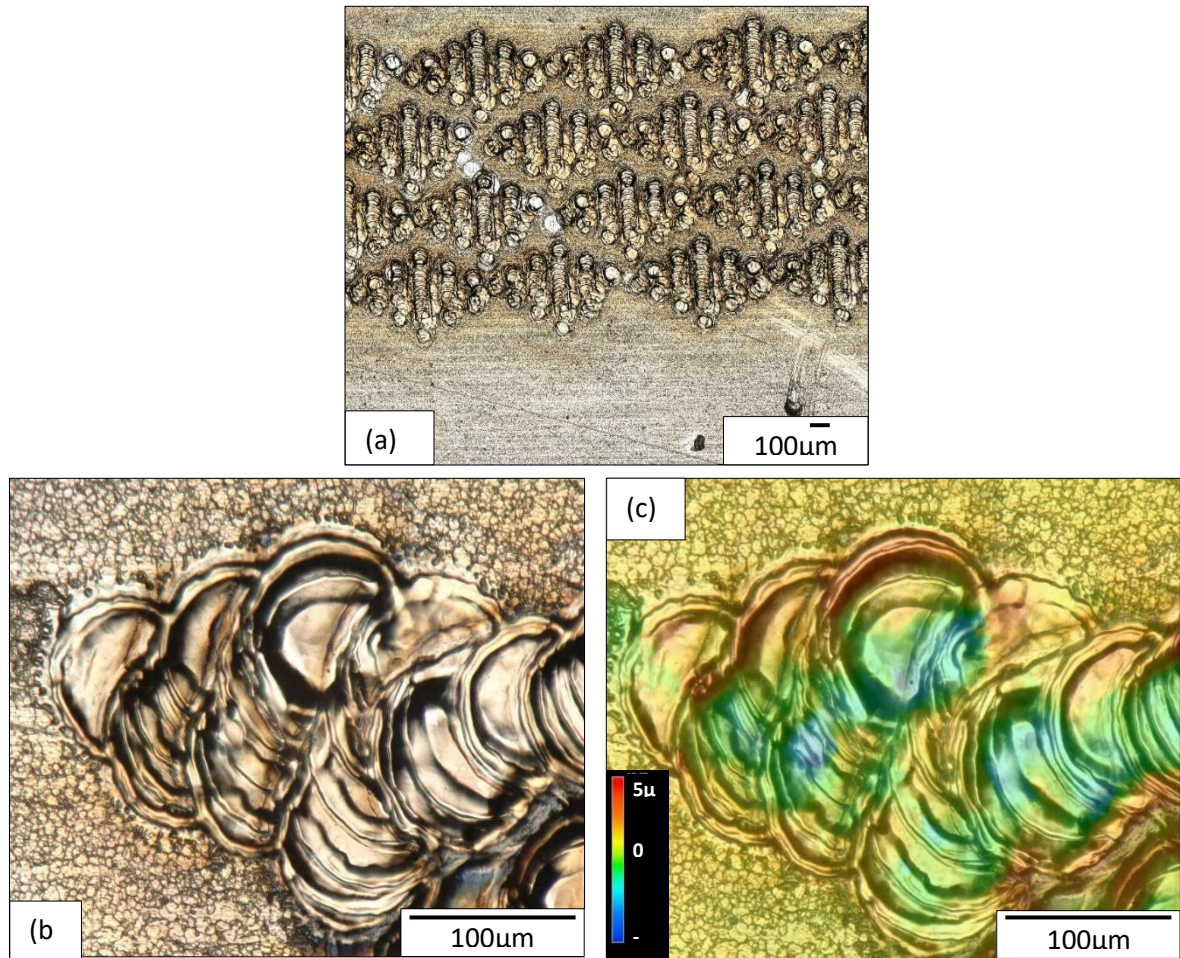


*Figure 8.1 Spinner shark inspired laser surface textured pattern directly onto marine grade steel using processes outlined in methods section and chapter 6 where (a) is at x100 magnification, (b) at x1000 magnification and (c) a 3D*

## References

Airoidi, L. (1998) Roles of disturbance, sediment stress, and substratum retention on spatial dominance in algal turf. *Ecology*, 79 (8), 2759-2770.

Aldred, N., Scardino, A., Cavaco, A., de Nys, R. and Clare, A.S. (2010) Attachment strength is a key factor in the selection of surfaces by barnacle cyprids (*Balanus amphitrite*) during settlement. *Biofouling*, 26 (3), 287-299.

Aldridge, D.C., Elliott, P. and Moggridge, G.D. (2004) The recent and rapid spread of the zebra mussel (*Dreissena polymorpha*) in Great Britain. *Biological Conservation*, 119 (2), 253-261.

Allredge, A.L. and Crocker, K.M. (1995) Why do sinking mucilage aggregates accumulate in the water column? *Science of the Total Environment*, 165 (1-3), 15-22.

Allredge, A.L. and Silver, M.W. (1988) Characteristics, dynamics and significance of marine snow. *Progress in oceanography*, 20 (1), 41-82.

Allen, J. (1993) Can biological filtration be used improve water quality? Studies in the Albert Dock Complex, Liverpool. *Urban waterside regeneration: problems and prospects*, 377-385.

Allen, J., Hawkins, S., Russell, G. and White, K. (1992) Eutrophication and urban renewal: problems and perspectives for the management of disused docks. In: (ed.) *Marine Coastal Eutrophication*. Elsevier. pp. 1283-1295.

Allen, J.R. and Hawkins, S.J. (1993) Pelagic—benthic Interactions in an enclosed coastal ecosystem: The impact of *Mytilus edulis* populations on water quality in the South Docks, Liverpool. In: (ed.) *Bivalve Filter Feeders*. Springer. pp. 515-516.

Anselme, K. (2000) Osteoblast adhesion on biomaterials. *Biomaterials*, 21 (7), 667-681.

Arnold, J. and Bailey, G. (2000) Surface finishes on stainless steel reduce bacterial attachment and early biofilm formation: scanning electron and atomic force microscopy study. *Poultry science*, 79 (12), 1839-1845.

Atalah, J., Otto, S.A., Anderson, M.J., Costello, M.J., Lenz, M. and Wahl, M. (2007) Temporal variance of disturbance did not affect diversity and structure of a marine fouling community in north-eastern New Zealand. *Marine Biology*, 153 (2), 199-211.

Aymerich, M., Nieto, D., Álvarez, E. and Flores-Arias, M. (2017) Laser surface microstructuring of biocompatible materials using a microlens array and the Talbot effect: evaluation of the cell adhesion. *Materials*, 10 (2), 214.

Bachmann, R. and Edyvean, R. (2005) Biofouling: an historic and contemporary review of its causes, consequences and control in drinking water distribution systems. *Biofilms*, 2 (3), 197-227.

Bacon, G. and Taylor, A. (1976) *Succession and stratification in benthic diatom communities colonizing plastic collectors in a Prince Edward Island estuary*. Walter de Gruyter, Berlin/New York.

Ball, P. (1999) Engineering shark skin and other solutions. *Nature*, 400 (6744), 507.

Bao, W.-Y., Satuito, C.G., Yang, J.-L. and Kitamura, H. (2007) Larval settlement and metamorphosis of the mussel *Mytilus galloprovincialis* in response to biofilms. *Marine Biology*, 150 (4), 565-574.

Barbosa, J.P., Fleury, B.G., da Gama, B.A., Teixeira, V.L. and Pereira, R.C. (2007) Natural products as antifoulants in the Brazilian brown alga *Dictyota pfaaffii* (Phaeophyta, Dictyotales). *Biochemical Systematics and Ecology*, 35 (8), 549-553.

Barnes, H. and Bagenal, T. (1951) Observations on *Nephrops norvegicus* (L.) and on an epizoic population of *Balanus crenatus* Brug. *Journal of the Marine Biological Association of the United Kingdom*, 30 (2), 369-380.

Bechert, D., Bruse, M. and Hage, W. (2000) Experiments with three-dimensional riblets as an idealized model of shark skin. *Experiments in fluids*, 28 (5), 403-412.

Becker, K., Siriratanachai, S. and Hormchong, T. (1998a) Influence of initial substratum surface tension on marine micro- and macro-fouling in the Gulf of Thailand. *Helgoländer Meeresuntersuchungen*, 51 (4), 445-461.

Becker, K., Siriratanachai, S. and Hormchong, T. (1998b) Influence of initial substratum surface tension on marine micro- and macro-fouling in the Gulf of Thailand. *Helgoländer Meeresuntersuchungen*, 51 (4), 445.

Becker, K. and Wahl, M. (1991) Influence of substratum surface tension on biofouling of artificial substrata in Kiel Bay (Western Baltic): in situ studies. *Biofouling*, 4 (4), 275-291.

Becker, K. and Wahl, M. (1996) Behaviour patterns as natural antifouling mechanisms of tropical marine crabs. *Journal of Experimental Marine Biology and Ecology*, 203 (2), 245-258.

Beech, I.B. (2003) Biocorrosion: Role of sulfate reducing bacteria. *Encyclopedia of Environmental Microbiology*.

Beech, I.B. and Sunner, J. (2004) Biocorrosion: towards understanding interactions between biofilms and metals. *Current opinion in Biotechnology*, 15 (3), 181-186.

Benyus, J.M. (1997) *Biomimicry: Innovation inspired by nature*. Morrow New York.

Berntsson, K.M., Jonsson, P.R., Lejhall, M. and Gatenholm, P. (2000) Analysis of behavioural rejection of micro-textured surfaces and implications for recruitment by the barnacle *Balanus improvisus*. *Journal of Experimental Marine Biology and Ecology*, 251 (1), 59-83.

Bers, A.V., Díaz, E.R., da Gama, B.A.P., Vieira-Silva, F., Dobretsov, S., Valdivia, N., Thiel, M., Scardino, A.J., McQuaid, C.D., Sudgen, H.E., Thomason, J.C. and Wahl, M. (2010) Relevance of mytilid shell microtopographies for fouling defence – a global comparison. *Biofouling*, 26 (3), 367-377.

Bers, A.V. and Wahl, M. (2004) The influence of natural surface microtopographies on fouling. *Biofouling*, 20 (1), 43-51.

Bhushan, B., Nosonovsky, M. and Chae Jung, Y. (2007) Towards optimization of patterned superhydrophobic surfaces. *Journal of the Royal Society Interface*, 4 (15), 643-648.

Bico, J., Thiele, U. and Quéré, D. (2002) Wetting of textured surfaces. *Colloids and Surfaces A: Physicochemical and Engineering Aspects*, 206 (1-3), 41-46.

Bixler, G.D. and Bhushan, B. (2013) Shark skin inspired low-drag microstructured surfaces in closed channel flow. *Journal of colloid and interface science*, 393, 384-396.

Bixler, G.D., Theiss, A., Bhushan, B. and Lee, S.C. (2014) Anti-fouling properties of microstructured surfaces bio-inspired by rice leaves and butterfly wings. *Journal of colloid and interface science*, 419, 114-133.

Bizi-Bandoki, P., Benayoun, S., Valette, S., Beaugiraud, B. and Audouard, E. (2011) Modifications of roughness and wettability properties of metals induced by femtosecond laser treatment. *Applied Surface Science*, 257 (12), 5213-5218.

Bobzin, S.C. and Faulkner, D.J. (1992) Chemistry and chemical ecology of the Bahamian sponge *Aplysilla glacialis*. *Journal of chemical ecology*, 18 (3), 309-332.

Bodammer, J.E. and Sawyer, T.K. (1981) Aufwuchs Protozoa and Bacteria on the Gills of the Rock Crab, *Cancer irroratus* Say: A Survey by Light and Electron Microscopy 1: Protozoa And Bacteria On Crab Gills. *The Journal of Protozoology*, 28 (1), 35-46.

- Boinovich, L.B., Emelyanenko, K.A., Domantovsky, A.G. and Emelyanenko, A.M. (2018) Laser tailoring the surface chemistry and morphology for wear, scale and corrosion resistant superhydrophobic coatings. *Langmuir*, 34 (24), 7059-7066.
- Bormashenko, E. (2008) Why does the Cassie–Baxter equation apply? *Colloids and Surfaces A: Physicochemical and Engineering Aspects*, 324 (1-3), 47-50.
- Brady Jr, R.F. and Singer, I.L. (2000) Mechanical factors favoring release from fouling release coatings. *Biofouling*, 15 (1-3), 73-81.
- Braun, D., Greiner, C., Schneider, J. and Gumbsch, P. (2014) Efficiency of laser surface texturing in the reduction of friction under mixed lubrication. *Tribology international*, 77, 142-147.
- Bronzino, J.D. and Park, J.B. (2002) *Biomaterials: principles and applications*. crc press.
- Brown, M.S. and Arnold, C.B. (2010) Fundamentals of laser-material interaction and application to multiscale surface modification. In: (ed.) *Laser precision microfabrication*. Springer. pp. 91-120.
- Brown, J.H. (2014) Why are there so many species in the tropics? *Journal of biogeography*, 41 (1), 8-22.
- Brunette, D. (1988) The effects of implant surface topography on the behavior of cells. *International Journal of Oral & Maxillofacial Implants*, 3 (4).
- Brzozowska, A.M., Parra-Velandia, F.J., Quintana, R., Xiaoying, Z., Lee, S.S., Chin-Sing, L., Jańczewski, D., Teo, S.L.-M. and Vancso, J.G. (2014a) Biomimicking micropatterned surfaces and their effect on marine biofouling. *Langmuir*, 30 (30), 9165-9175.
- Brzozowska, A.M., Parra-Velandia, F.J., Quintana, R., Xiaoying, Z., Lee, S.S.C., Chin-Sing, L., Jańczewski, D., Teo, S.L.M. and Vancso, J.G. (2014b) Biomimicking Micropatterned Surfaces and Their Effect on Marine Biofouling. *Langmuir*, 30 (30), 9165-9175.
- Butler, A.J., Canning-Clode, J., Coutts, A.D., Cowie, P.R., Dobretsov, S., Durr, S., Faimali, M., Lewis, J.A., Page, H.M. and Pratten, J. (2010) Techniques for the quantification of biofouling. *Biofouling; Durr, S., Thomason, J., Eds.; Wiley-Blackwell: Chichester, UK*, 319-332.
- Burja, A.M. and Hill, R.T. (2001) Microbial symbionts of the Australian Great Barrier reef sponge, *Candidaspongia flabellata*. *Hydrobiologia*, 461 (1-3), 41-47.

- Buskens, P., Wouters, M., Rentrop, C. and Vroon, Z. (2013) A brief review of environmentally benign antifouling and foul-release coatings for marine applications. *Journal of Coatings Technology and Research*, 10 (1), 29-36.
- Busscher, H., Van Pelt, A., De Boer, P., De Jong, H. and Arends, J. (1984) The effect of surface roughening of polymers on measured contact angles of liquids. *Colloids and Surfaces*, 9 (4), 319-331.
- Butman, B. and Folger, D.W. (1979) An instrument system for long-term sediment transport studies on the continental shelf. *Journal of Geophysical Research: Oceans*, 84 (C3), 1215-1220.
- Caley, M., Carr, M., Hixon, M., Hughes, T., Jones, G. and Menge, B. (1996) Recruitment and the local dynamics of open marine populations. *Annual Review of Ecology and Systematics*, 27 (1), 477-500.
- Callow, J. and Callow, M. (2006a) Antifouling compounds. *Biofilms*, 141-170.
- Callow, J. and Callow, M. (2006b) Biofilms. In: (ed.) *Antifouling Compounds*. Springer. pp. 141-169.
- Callow, J.A. and Callow, M.E. (2006c) Biofilms. In: Fusetani, N. and Clare, A. S. (ed.) *Antifouling Compounds*. Berlin, Heidelberg: Springer Berlin Heidelberg. pp. 141-169.
- Callow, M., Callow, J., Pickett-Heaps, J. and Wetherbee, R. (1998) Primary adhesion of Enteromorpha (Chlorophyta, Ulvales) propagules: Quantitative settlement studies and video microscopy. *Oceanographic Literature Review*, 7 (45), 1195.
- Callow, M.E., Callow, J.A., Pickett-Heaps, J.D. and Wetherbee, R. (1997) PRIMARY ADHESION OF ENTEROMORPHA (CHLOROPHYTA, ULVALES) PROPAGULES: QUANTITATIVE SETTLEMENT STUDIES AND VIDEO MICROSCOPY 1. *Journal of Phycology*, 33 (6), 938-947.
- Callow, M.E., Jennings, A.R., Brennan, A., Seegert, C., Gibson, A., Wilson, L., Feinberg, A., Baney, R. and Callow, J. (2002) Microtopographic cues for settlement of zoospores of the green fouling alga Enteromorpha. *Biofouling*, 18 (3), 229-236.
- Campbell, A.H., Meritt, D.W., Franklin, R.B., Boone, E.L., Nicely, C.T. and Brown, B.L. (2011) Effects of age and composition of field-produced biofilms on oyster larval setting. *Biofouling*, 27 (3), 255-265.
- Carl, C., Poole, A., Sexton, B.A., Glenn, F., Vucko, M.J., Williams, M., Whalan, S. and De Nys, R. (2012) Enhancing the settlement and attachment strength of pediveligers of *Mytilus galloprovincialis* by changing surface wettability and microtopography. *Biofouling*, 28 (2), 175-186.

Carman, M.L., Estes, T.G., Feinberg, A.W., Schumacher, J.F., Wilkerson, W., Wilson, L.H., Callow, M.E., Callow, J.A. and Brennan, A.B. (2006) Engineered antifouling microtopographies—correlating wettability with cell attachment. *Biofouling*, 22 (1), 11-21.

Carr, J.M., Hergenrader, G.L. and Troelstrup Jr, N.H. (1986) A simple, inexpensive method for cleaning diatoms. *Transactions of the American Microscopical Society*, 152-157.

Cassie, A. (1948) Contact angles. *Discussions of the Faraday society*, 3, 11-16.

Cassie, A. and Baxter, S. (1944) Wettability of porous surfaces. *Transactions of the Faraday society*, 40, 546-551.

Chambers, L.D., Stokes, K.R., Walsh, F.C. and Wood, R.J. (2006) Modern approaches to marine antifouling coatings. *Surface and Coatings Technology*, 201 (6), 3642-3652.

Chaudhury, M.K., Finlay, J.A., Chung, J.Y., Callow, M.E. and Callow, J.A. (2005) The influence of elastic modulus and thickness on the release of the soft-fouling green alga *Ulva linza* (syn. *Enteromorpha linza*) from poly (dimethylsiloxane)(PDMS) model networks. *Biofouling*, 21 (1), 41-48.

Che, L.M., Le Campion-Alsumard, T., Boury-Esnault, N., Payri, C., Golubic, S. and Bézac, C. (1996) Biodegradation of shells of the black pearl oyster, *Pinctada margaritifera* var. *cumingii*, by microborers and sponges of French Polynesia. *Marine Biology*, 126 (3), 509-519.

Chen, G., Kwee, T., Tan, K., Choo, Y. and Hong, M. (2010) Laser cleaning of steel for paint removal. *Applied Physics A*, 101 (2), 249-253.

Chen, Z., Zhao, W., Xu, J., Mo, M., Peng, S., Zeng, Z., Wu, X. and Xue, Q. (2015) Designing environmentally benign modified silica resin coatings with biomimetic textures for antibiofouling. *RSC Advances*, 5 (46), 36874-36881.

Cheng, Y.-T. and Rodak, D.E. (2005) Is the lotus leaf superhydrophobic? *Applied Physics Letters*, 86 (14), 144101.

Choi, W., Tuteja, A., Mabry, J.M., Cohen, R.E. and McKinley, G.H. (2009) A modified Cassie–Baxter relationship to explain contact angle hysteresis and anisotropy on non-wetting textured surfaces. *Journal of colloid and interface science*, 339 (1), 208-216.

Chung, K.K., Schumacher, J.F., Sampson, E.M., Burne, R.A., Antonelli, P.J. and Brennan, A.B. (2007) Impact of engineered surface microtopography on biofilm formation of *Staphylococcus aureus*. *Biointerphases*, 2 (2), 89-94.

Clements, F.E. (1928) *Plant succession and indicators* [online]

Cohn, S.A. and Weitzell Jr, R.E. (1996) ECOLOGICAL CONSIDERATIONS OF DIATOM CELL MOTILITY. I. CHARACTERIZATION OF MOTILITY AND ADHESION IN FOUR DIATOM SPECIES 1. *Journal of Phycology*, 32 (6), 928-939.

Coleman, D. C., O'donnell, M. J., Shore, A. C. & Russell, R. J. 2009. Biofilm problems in dental unit water systems and its practical control. *Journal of Applied Microbiology*, 106, 1424-1437

Connell, J.H. (1985) Disturbance and patch dynamics of subtidal marine animals on hard substrata. *Natural Disturbance and Patch Dynamics*, 125-151.

Cooksey, K.E. (1981) Requirement for calcium in adhesion of a fouling diatom to glass. *Appl. Environ. Microbiol.*, 41 (6), 1378-1382.

Costerton, J.W., Lewandowski, Z., Caldwell, D.E., Korber, D.R. and Lappin-Scott, H.M. (1995) Microbial biofilms. *Annual Reviews in Microbiology*, 49 (1), 711-745.

Crawford, R.M. (1977) The taxonomy and classification of the diatom genus *Melosira* C. Ag. II. *M. moniliformis* (Müll.) C. Ag. *Phycologia*, 16 (3), 277-285.

Cunha, A., Elie, A.-M., Plawinski, L., Serro, A.P., Botelho do Rego, A.M., Almeida, A., Urdaci, M.C., Durrieu, M.-C. and Vilar, R. (2016a) Femtosecond laser surface texturing of titanium as a method to reduce the adhesion of *Staphylococcus aureus* and biofilm formation. *Applied Surface Science*, 360, 485-493.

Cunha, A., Elie, A.-M., Plawinski, L., Serro, A.P., do Rego, A.M.B., Almeida, A., Urdaci, M.C., Durrieu, M.-C. and Vilar, R. (2016b) Femtosecond laser surface texturing of titanium as a method to reduce the adhesion of *Staphylococcus aureus* and biofilm formation. *Applied Surface Science*, 360, 485-493.

Cunha, A., Serro, A.P., Oliveira, V., Almeida, A., Vilar, R. and Durrieu, M.-C. (2013) Wetting behaviour of femtosecond laser textured Ti-6Al-4V surfaces. *Applied Surface Science*, 265, 688-696.

Curtis, A. and Wilkinson, C. (1997) Topographical control of cells. *Biomaterials*, 18 (24), 1573-1583.

Dahlström, M., Jonsson, H., Jonsson, P.R. and Elwing, H. (2004) Surface wettability as a determinant in the settlement of the barnacle *Balanus improvisus* (Darwin). *Journal of Experimental Marine Biology and Ecology*, 305 (2), 223-232.

Dahms, H.-U., Dobretsov, S. and Qian, P.-Y. (2004) The effect of bacterial and diatom biofilms on the settlement of the bryozoan *Bugula neritina*. *Journal of Experimental Marine Biology and Ecology*, 313 (1), 191-209.

Davis, R., Moore, C., Zaneveld, J. and Napp, J. (1997) Reducing the effects of fouling on chlorophyll estimates derived from long-term deployments of optical instruments. *Journal of Geophysical Research: Oceans*, 102 (C3), 5851-5855.

Dayton, P.K. (1971) Competition, disturbance, and community organization: the provision and subsequent utilization of space in a rocky intertidal community. *Ecological Monographs*, 41 (4), 351-389.

De Nys, R. and Guenther, J. (2009) The impact and control of biofouling in marine finfish aquaculture. In: (ed.) *Advances in marine antifouling coatings and technologies*. Elsevier. pp. 177-221.

De Romero, M., Duque, Z., De Rinco, O., Perez, O. and Araujo, I. (2003) Study of the cathodic depolarization theory with hydrogen permeation and the bacteria *Desulfovibrio desulfuricans*. *Revista De Metalurgia*, 182-187.

De Romero, M., Duque, Z., De Rincon, O., Pérez, O., Araujo, I. and Briceno, B. (2002) Microbiological corrosion: hydrogen permeation and sulfate-reducing bacteria. *Corrosion*, 58 (5), 429-435.

Den Braber, E., De Ruijter, J., Ginsel, L., Von Recum, A. and Jansen, J. (1998) Orientation of ECM protein deposition, fibroblast cytoskeleton, and attachment complex components on silicone microgrooved surfaces. *Journal of Biomedical Materials Research: An Official Journal of The Society for Biomaterials, The Japanese Society for Biomaterials, and the Australian Society for Biomaterials*, 40 (2), 291-300.

Di Pippo, F., Di Gregorio, L., Congestri, R., Tandoi, V. and Rossetti, S. (2018) Biofilm growth and control in cooling water industrial systems. *FEMS microbiology ecology*, 94 (5), fiy044.

Dobretsov, S., Dahms, H.-U. and Qian, P.-Y. (2006) Inhibition of biofouling by marine microorganisms and their metabolites. *Biofouling*, 22 (1), 43-54.

Dobretsov, S. (2010) Marine biofilms. *Biofouling*, 123-136.

Dougherty, J. and Russell, M.P. (2005) The association between the coquina clam *Donax fossor* Say and its epibiotic hydroid *Lovenella gracilis* Clarke. *Journal of Shellfish Research*, 24 (1), 35-46.

Drelich, J. (2013) Guidelines to measurements of reproducible contact angles using a sessile-drop technique. *Surface innovations*, 1 (4), 248-254.

- Duncan, A., Weisbuch, F., Rouais, F., Lazare, S. and Baquey, C. (2002a) Laser microfabricated model surfaces for controlled cell growth. *Biosensors and Bioelectronics*, 17 (5), 413-426.
- Duncan, A.C., Weisbuch, F., Rouais, F., Lazare, S. and Baquey, C. (2002b) Laser microfabricated model surfaces for controlled cell growth. *Biosensors and Bioelectronics*, 17 (5), 413-426.
- Dunn, A., Wasley, T.J., Li, J., Kay, R.W., Stringer, J., Smith, P.J., Esenturk, E., Connaughton, C. and Shephard, J.D. (2016) Laser textured superhydrophobic surfaces and their applications for homogeneous spot deposition. *Applied Surface Science*, 365, 153-159.
- Dupont, A., Caminat, P., Bournot, P. and Gauchon, J. (1995) Enhancement of material ablation using 248, 308, 532, 1064 nm laser pulse with a water film on the treated surface. *Journal of Applied Physics*, 78 (3), 2022-2028.
- Dürr, S. and Watson, D.I. (2010) Biofouling and antifouling in aquaculture. *Biofouling*, 267-287.
- Edgar, L. (1983) Mucilage secretions of moving diatoms. *Protoplasma*, 118 (1), 44-48.
- Edgar, L.A. and Pickett-Heaps, J.D. (1983) The mechanism of diatom locomotion. I. An ultrastructural study of the motility apparatus. *Proceedings of the Royal Society of London. Series B. Biological Sciences*, 218 (1212), 331-343.
- Edgar, L.A. and Pickett-Heaps, J.D. (1984) VALVE MORPHOGENESIS IN THE PENNATE DIATOM NAVICULA CUSPIDATA 1. *Journal of Phycology*, 20 (1), 47-61.
- Edgar, L.A. and Zavortink, M. (1983) The mechanism of diatom locomotion. II. Identification of actin. *Proceedings of the Royal Society of London. Series B. Biological Sciences*, 218 (1212), 345-348.
- Efimenko, K., Finlay, J., Callow, M.E., Callow, J.A. and Genzer, J. (2009) Development and testing of hierarchically wrinkled coatings for marine antifouling. *ACS applied materials & interfaces*, 1 (5), 1031-1040.
- Ekin, A. and Webster, D.C. (2007) Combinatorial and High-Throughput Screening of the Effect of Siloxane Composition on the Surface Properties of Crosslinked Siloxane–Polyurethane Coatings. *Journal of combinatorial chemistry*, 9 (1), 178-188.
- Engleman, P.G., Dahotre, N.B., Kurella, A., Samant, A. and Blue, C.A. (2005) The application of laser-induced multi-scale surface texturing. *Jom*, 57 (12), 46-50.

Ensikat, H.J., Ditsche-Kuru, P., Neinhuis, C. and Barthlott, W. (2011) Superhydrophobicity in perfection: the outstanding properties of the lotus leaf. *Beilstein journal of nanotechnology*, 2 (1), 152-161.

Erbil, H.Y. and Cansoy, C.E. (2009) Range of applicability of the Wenzel and Cassie– Baxter equations for superhydrophobic surfaces. *Langmuir*, 25 (24), 14135-14145.

Estes, T.G. (2005) *Studies of directed adhesion of bio-organisms on functionalized polydimethylsiloxane elastomer*. University of Florida Gainesville, FL.

Etsion, I. and Sher, E. (2009) Improving fuel efficiency with laser surface textured piston rings. *Tribology international*, 42 (4), 542-547.

Faimali, M., Garaventa, F., Terlizzi, A., Chiantore, M. and Cattaneo-Vietti, R. (2004) The interplay of substrate nature and biofilm formation in regulating *Balanus amphitrite* Darwin, 1854 larval settlement. *Journal of Experimental Marine Biology and Ecology*, 306 (1), 37-50.

Falkowski, P. and Raven, J. (1997) *Aquatic Photosynthesis* Blackwell Science. Malden, Massachusetts.

Feeley, T.J., Green, L., Murphy, J.T., Hoffmann, J. and Carney, B.A. (2005) Department of Energy/Office of fossil energy's power plant water management R&D program. *US department of energy*.

Feng, L., Zhang, Y., Xi, J., Zhu, Y., Wang, N., Xia, F. and Jiang, L. (2008) Petal effect: a superhydrophobic state with high adhesive force. *Langmuir*, 24 (8), 4114-4119.

Ferreira, S. and Seeliger, U. (1985) The colonization process of algal epiphytes on *Ruppia maritima* L. *Botanica marina*, 28 (6), 245-250.

Field, A. (2013) *Discovering statistics using IBM SPSS statistics*. sage.

Finlay, B.J. (2002) Global dispersal of free-living microbial eukaryote species. *Science*, 296 (5570), 1061-1063.

Fish, K., Osborn, A. and Boxall, J. (2017) Biofilm structures (EPS and bacterial communities) in drinking water distribution systems are conditioned by hydraulics and influence discolouration. *Science of the Total Environment*, 593, 571-580.

Flemming, H.-C., Neu, T.R. and Wozniak, D.J. (2007) The EPS matrix: the "house of biofilm cells". *Journal of bacteriology*, 189 (22), 7945-7947.

- Flemming, H.-C., Wingender, J., Griebe, T. and Mayer, C. (2000a) Physico-chemical properties of biofilms. *Biofilms: recent advances in their study and control*, 19-34.
- Flemming, H.-C., Wingender, J., Griegbe, T. and Mayer, C. (2000b) Physico-chemical properties of biofilms. *Biofilms: recent advances in their study and control*. Amsterdam: Harwood Academic Publishers, 19-34.
- Flemming, R., Murphy, C.J., Abrams, G., Goodman, S. and Nealey, P. (1999) Effects of synthetic micro- and nano-structured surfaces on cell behavior. *Biomaterials*, 20 (6), 573-588.
- Forrest, B.M. and Atalah, J. (2017) Significant impact from blue mussel *Mytilus galloprovincialis* biofouling on aquaculture production of green-lipped mussels in New Zealand. *Aquaculture Environment Interactions*, 9, 115-126.
- Friedlander, R.S., Vlamakis, H., Kim, P., Khan, M., Kolter, R. and Aizenberg, J. (2013) Bacterial flagella explore microscale hummocks and hollows to increase adhesion. *Proceedings of the National Academy of Sciences*, 110 (14), 5624-5629.
- Fusetani, N. (2011) Antifouling marine natural products. *Natural product reports*, 28 (2), 400-410.
- Gao, L. and McCarthy, T.J. (2006) The "lotus effect" explained: two reasons why two length scales of topography are important. *Langmuir*, 22 (7), 2966-2967.
- Gattass, R.R. and Mazur, E. (2008) Femtosecond laser micromachining in transparent materials. *Nature photonics*, 2 (4), 219.
- Geesey, G. (1982) Microbial exopolymers: ecological and economic considerations. *Am Soc Microbiol News*, 48, 9-14.
- Geist, J. and Hawkins, S.J. (2016) Habitat recovery and restoration in aquatic ecosystems: current progress and future challenges. *Aquatic Conservation: Marine and Freshwater Ecosystems*, 26 (5), 942-962.
- Glynn, P.W. (1970) Growth of algal epiphytes on a tropical marine isopod. *Journal of Experimental Marine Biology and Ecology*, 5 (1), 88-93.
- Gordon, R. (1987) A retaliatory role for algal projectiles, with implications for the mechanochemistry of diatom gliding motility. *Journal of theoretical biology*, 126 (4), 419-436.

Goreau, T. and Prong, P. (2017) Biorock electric reefs grow back severely eroded beaches in months. *Journal of Marine Science and Engineering*, 5 (4), 48.

Gower, M.C. (2000) Industrial applications of laser micromachining. *Optics Express*, 7 (2), 56-67.

Greiner, C. and Schäfer, M. (2015) Bio-inspired scale-like surface textures and their tribological properties. *Bioinspiration & biomimetics*, 10 (4), 044001.

Grossart, H.-P. and Tang, K.W. (2010) www. aquaticmicrobial. net. *Communicative & integrative biology*, 3 (6), 491-494.

Grossart, H.P. (2010) Ecological consequences of bacterioplankton lifestyles: changes in concepts are needed. *Environmental Microbiology Reports*, 2 (6), 706-714.

Han, P., Kim, J., Ehmann, K.F. and Cao, J. (2013) Laser surface texturing of medical needles for friction control. *International Journal of Mechatronics and Manufacturing Systems* 1, 6 (3), 215-228.

Hadfield, M.G. (1986) Settlement and recruitment of marine invertebrates: a perspective and some proposals. *Bulletin of Marine Science*, 39 (2), 418-425.

Hao, L., Lawrence, J., Phua, Y., Chian, K., Lim, G. and Zheng, H. (2005) Enhanced human osteoblast cell adhesion and proliferation on 316 LS stainless steel by means of CO<sub>2</sub> laser surface treatment. *Journal of Biomedical Materials Research Part B: Applied Biomaterials: An Official Journal of The Society for Biomaterials, The Japanese Society for Biomaterials, and The Australian Society for Biomaterials and the Korean Society for Biomaterials*, 73 (1), 148-156.

Harder, T., Lam, C. and Qian, P.-Y. (2002) Induction of larval settlement in the polychaete *Hydroides elegans* by marine biofilms: an investigation of monospecific diatom films as settlement cues. *Marine Ecology Progress Series*, 229, 105-112.

Hasle, G.R. and Fryxell, G.A. (1970) Diatoms: cleaning and mounting for light and electron microscopy. *Transactions of the American Microscopical Society*, 469-474.

Hasse, J. (1974) Utilization of rabbitfishes (Siganidae) in tropical oyster culture. *The Progressive Fish-Culturist*, 36 (3), 160-162.

Hastings, A. (1980) Disturbance, coexistence, history, and competition for space. *Theoretical population biology*, 18 (3), 363-373.

Hawkins, S., Allen, J. and Bray, S. (1999) Restoration of temperate marine and coastal ecosystems: nudging nature. *Aquatic Conservation: Marine and Freshwater Ecosystems*, 9 (1), 23-46.

Hawkins, S., Allen, J., Fielding, N., Wilkinson, S. and Wallace, I. (1999) Liverpool Bay and the estuaries: human impact, recent recovery and restoration. *Ecology and Landscape Development: a History of the Mersey Basin*. Conference Proceedings of Conference.

Hawkins, S. and Southward, A. (1992) The Torrey Canyon oil spill: recovery of rocky shore communities. *Restoring the Nations Marine Environment*, (ed. GW Thorpe), 583-631.

Haygood, M.G. and Davidson, S.K. (1997) Small-subunit rRNA genes and in situ hybridization with oligonucleotides specific for the bacterial symbionts in the larvae of the bryozoan *Bugula neritina* and proposal of "Candidatus endobugula sertula". *Appl. Environ. Microbiol.*, 63 (11), 4612-4616.

Hellio, C., Maréchal, J.-P., Da Gama, B., Pereira, R. and Clare, A. (2009) Natural marine products with antifouling activities. In: (ed.) *Advances in marine antifouling coatings and technologies*. Elsevier. pp. 572-622.

Hellio, C., Pons, A.M., Beaupoil, C., Bourgougnon, N. and Le Gal, Y. (2002) Antibacterial, antifungal and cytotoxic activities of extracts from fish epidermis and epidermal mucus. *International Journal of Antimicrobial Agents*, 20 (3), 214-219.

Henderson, P. (2010) Fouling and antifouling in other industries—power stations, desalination plants—drinking water supplies and sensors. *Biofouling*, 288-305.

Hentschel, U., Fieseler, L., Wehrl, M., Gernert, C., Steinert, M., Hacker, J. and Horn, M. (2003) Microbial diversity of marine sponges. In: (ed.) *Sponges (Porifera)*. Springer. pp. 59-88.

Hoagland, K.D., Rosowski, J.R., Gretz, M.R. and Roemer, S.C. (1993) Diatom extracellular polymeric substances: function, fine structure, chemistry, and physiology. *Journal of Phycology*, 29 (5), 537-566.

Hoipkemeier-Wilson, L., Schumacher, J.F., Carman, M.L., Gibson, A.L., Feinberg, A.W., Callow, M.E., Finlay, J.A., Callow, J.A. and Brennan, A.B. (2004) Antifouling potential of lubricious, micro-engineered, PDMS elastomers against zoospores of the green fouling alga *Ulva* (Enteromorpha). *Biofouling*, 20 (1), 53-63.

Höller, U., Wright, A.D., Matthee, G.F., König, G.M., Draeger, S., Hans-Jürgen, A. and Schulz, B. (2000) Fungi from marine sponges: diversity, biological activity and secondary metabolites. *Mycological Research*, 104 (11), 1354-1365.

Hosking, N., Ström, M., Shipway, P. and Rudd, C. (2007) Corrosion resistance of zinc-magnesium coated steel. *Corrosion science*, 49 (9), 3669-3695.

Huggett, M.J., Nedved, B.T. and Hadfield, M.G. (2009) Effects of initial surface wettability on biofilm formation and subsequent settlement of *Hydroides elegans*. *Biofouling*, 25 (5), 387-399.

Huggett, M.J., Williamson, J.E., de Nys, R., Kjelleberg, S. and Steinberg, P.D. (2006) Larval settlement of the common Australian sea urchin *Heliocidaris erythrogramma* in response to bacteria from the surface of coralline algae. *Oecologia*, 149 (4), 604-619.

Hultgren, K.M. and Stachowicz, J.J. (2011) Camouflage in decorator crabs: integrating ecological, behavioural and evolutionary approaches. In: (ed.) *Animal camouflage: mechanisms and function*. Cambridge University Press. pp. 212-236.

Hunsucker, K.Z., Koka, A., Lund, G. and Swain, G. (2014) Diatom community structure on in-service cruise ship hulls. *Biofouling*, 30 (9), 1133-1140.

Hurlbert, S.H. (1984) Pseudoreplication and the design of ecological field experiments. *Ecological Monographs*, 54 (2), 187-211.

Joint, I., Tait, K., Callow, M.E., Callow, J.A., Milton, D., Williams, P. and Cámara, M. (2002) Cell-to-cell communication across the prokaryote-eukaryote boundary. *Science*, 298 (5596), 1207-1207.

Jones, C.G., Lawton, J.H. and Shachak, M. (1994) Organisms as ecosystem engineers. In: (ed.) *Ecosystem management*. Springer. pp. 130-147.

Jopp, J., Gröll, H. and Yerushalmi-Rozen, R. (2004) Wetting behavior of water droplets on hydrophobic microtextures of comparable size. *Langmuir*, 20 (23), 10015-10019.

Kaehler, S. (1999) Incidence and distribution of phototrophic shell-degrading endoliths of the brown mussel *Perna perna*. *Marine Biology*, 135 (3), 505-514.

Kaehler, S. and McQuaid, C. (1999) Lethal and sub-lethal effects of phototrophic endoliths attacking the shell of the intertidal mussel *Perna perna*. *Marine Biology*, 135 (3), 497-503.

- Kinzler, K., Gehrke, T., Telegdi, J. and Sand, W. (2003) Bioleaching—a result of interfacial processes caused by extracellular polymeric substances (EPS). *Hydrometallurgy*, 71 (1-2), 83-88.
- Kirschner, C.M. and Brennan, A.B. (2012) Bio-inspired antifouling strategies. *Annual review of materials research*, 42, 211-229.
- Kiss, K. and Genkal, S. (1993) Winter blooms of centric diatoms in the River Danube and in its side-arms near Budapest (Hungary). *Twelfth International Diatom Symposium of Conference*.
- Kókai, Z., Borics, G., Bácsi, I., Lukács, Á., Tóthmérész, B., Csépes, E., Török, P. and Viktória, B. (2019) Water usage and seasonality as primary drivers of benthic diatom assemblages in a lowland reservoir. *Ecological Indicators*, 106, 105443.
- Köhler, J., Hansen, P. and Wahl, M. (1999) Colonization patterns at the substratum-water interface: How does surface microtopography influence recruitment patterns of sessile organisms? *Biofouling*, 14 (3), 237-248.
- Konstantinou, I. and Albanis, T. (2004) Worldwide occurrence and effects of antifouling paint booster biocides in the aquatic environment: a review. *Environment international*, 30 (2), 235-248.
- Kubiak, K., Wilson, M., Mathia, T. and Carval, P. (2011) Wettability versus roughness of engineering surfaces. *Wear*, 271 (3-4), 523-528.
- Kützing, F.T. (1844). Die Kieselschaligen Bacillarien oder Diatomeen. pp. [i-vii], [1]-152, pls 1-30. Nordhausen: zu finden bei W. Köhne.
- Kurella, A. and Dahotre, N.B. (2005) Surface modification for bioimplants: the role of laser surface engineering. *Journal of biomaterials applications*, 20 (1), 5-50.
- Kuwa, M. (1984) Fouling organisms on floating cage of wire netting and the removal by *Oplegnathus* sp. cultured with other marine fish. *Bulletin of the Japanese Society of Scientific Fisheries*.
- Lachnit, T., Blümel, M., Imhoff, J.F. and Wahl, M. (2009) Specific epibacterial communities on macroalgae: phylogeny matters more than habitat. *Aquatic Biology*, 5 (2), 181-186.
- Lange, K.B., de Ciencias Naturales, C.-M.A., Rivadavia, B. and Gallardo, A. (1985) Spatial and seasonal variations of diatom assemblages. *Oceanol. Acta*, 8 (3), 361-369.

- Lafuma, A. and Quéré, D. (2003) Superhydrophobic states. *Nature materials*, 2 (7), 457.
- Lane, A. & Willemsen, P. (2004) Collaborative effort looks into biofouling. *Fish Farming International*, September, 34-35.
- Lawes, J.C., Neilan, B.A., Brown, M.V., Clark, G.F. and Johnston, E.L. (2016) Elevated nutrients change bacterial community composition and connectivity: high throughput sequencing of young marine biofilms. *Biofouling*, 32 (1), 57-69.
- Lee, S., Yang, D. and Nikumb, S. (2008) Femtosecond laser micromilling of Si wafers. *Applied Surface Science*, 254 (10), 2996-3005.
- Lejars, M.n., Margaiilan, A. and Bressy, C. (2012) Fouling release coatings: a nontoxic alternative to biocidal antifouling coatings. *Chemical reviews*, 112 (8), 4347-4390.
- Liu, Y. and Choi, C.-H. (2013) Condensation-induced wetting state and contact angle hysteresis on superhydrophobic lotus leaves. *Colloid and Polymer Science*, 291 (2), 437-445.
- Li, B.-j., Li, H., Huang, L.-j., Ren, N.-f. and Kong, X. (2016) Femtosecond pulsed laser textured titanium surfaces with stable superhydrophilicity and superhydrophobicity. *Applied Surface Science*, 389, 585-593.
- Li, J. and Ananthasuresh, G. (2001) A quality study on the excimer laser micromachining of electro-thermal-compliant micro devices. *Journal of Micromechanics and microengineering*, 11 (1), 38.
- Lindblad, L.M. (2009) Developing new marine antifouling substances: learning from the pharmaceutical industry. In: (ed.) *Advances in marine antifouling coatings and technologies*. Elsevier. pp. 263-274.
- Liu, K. and Jiang, L. (2011) Bio-inspired design of multiscale structures for function integration. *Nano Today*, 6 (2), 155-175.
- Lurie-Luke, E. (2014) Product and technology innovation: What can biomimicry inspire? *Biotechnology Advances*, 32 (8), 1494-1505.
- Ma, M. and Hill, R.M. (2006) Superhydrophobic surfaces. *Current opinion in colloid & interface science*, 11 (4), 193-202.
- MacArthur, R.H. and Wilson, E.O. (2001) *The theory of island biogeography*. Princeton university press.

- Macinnis-Ng, C.M. and Ralph, P.J. (2003) Short-term response and recovery of *Zostera capricorni* photosynthesis after herbicide exposure. *Aquatic Botany*, 76 (1), 1-15.
- Magin, C.M., Cooper, S.P. and Brennan, A.B. (2010) Non-toxic antifouling strategies. *Materials today*, 13 (4), 36-44.
- Magin, C.M., Long, C.J., Cooper, S.P., Ista, L.K., López, G.P. and Brennan, A.B. (2010) Engineered antifouling microtopographies: the role of Reynolds number in a model that predicts attachment of zoospores of *Ulva* and cells of *Cobetia marina*. *Biofouling*, 26 (6), 719-727.
- Maiman, T. (1960) Optical and microwave-optical experiments in ruby. *Physical review letters*, 4 (11), 564.
- Majewska, R., Gambi, M.C., Totti, C.M. and De Stefano, M. (2013a) Epiphytic diatom communities of Terra Nova Bay, Ross Sea, Antarctica: structural analysis and relations to algal host. *Antarctic Science*, 25 (4), 501-513.
- Majewska, R., Gambi, M.C., Totti, C.M., Pennesi, C. and De Stefano, M. (2013b) Growth form analysis of epiphytic diatom communities of Terra Nova Bay (Ross Sea, Antarctica). *Polar biology*, 36 (1), 73-86.
- Manov, D.V., Chang, G.C. and Dickey, T.D. (2004) Methods for reducing biofouling of moored optical sensors. *Journal of Atmospheric and Oceanic Technology*, 21 (6), 958-968.
- Marmur, A. (2003) Wetting on hydrophobic rough surfaces: to be heterogeneous or not to be? *Langmuir*, 19 (20), 8343-8348.
- Marshall, K., STOUT, R. and Mitchell, R. (1971a) Mechanism of the initial events in the sorption of marine bacteria to surfaces. *Microbiology*, 68 (3), 337-348.
- Marshall, K., STOUT, R. and Mitchell, R. (1971b) Mechanism of the initial events in the sorption of marine bacteria to surfaces. *Journal of General Microbiology*, 68 (3), 337-348.
- Marszalek, D.S., Gerchakov, S.M. and Udey, L.R. (1979) Influence of substrate composition on marine microfouling. *Appl. Environ. Microbiol.*, 38 (5), 987-995.
- Martini, M. and Strahle, W. (1993) Multi-sensor system for coastal environments. *SEA TECHNOLOGY*, 34, 49-49.

Masuda, M., Abe, T., Sato, S., Suzuki, T. and Suzuki, M. (1997) DIVERSITY OF HALOGENATED SECONDARY METABOLITES IN THE RED ALGA LAURENCIA NIPPONICA (RHODOMELACEAE, CERAMIALES) 1, 2. *Journal of Phycology*, 33 (2), 196-208.

May, R.M., Magin, C.M., Mann, E.E., Drinker, M.C., Fraser, J.C., Siedlecki, C.A., Brennan, A.B. and Reddy, S.T. (2015) An engineered micropattern to reduce bacterial colonization, platelet adhesion and fibrin sheath formation for improved biocompatibility of central venous catheters. *Clinical and translational medicine*, 4 (1), 9.

McCook, L. and Chapman, A. (1997) Patterns and variations in natural succession following massive ice-scour of a rocky intertidal seashore. *Journal of Experimental Marine Biology and Ecology*, 214 (1-2), 121-147.

McIntire, C. and Moore, W.W. (1977) Marine littoral diatoms: ecological considerations. *The biology of diatoms*, 13, 333-371

McGhee, G.R., Müller, G.B. and Schäfer, K. (2011) *Convergent evolution: limited forms most beautiful*. MIT Press.

Menge, B.A. and Sutherland, J.P. (1987) Community regulation: variation in disturbance, competition, and predation in relation to environmental stress and recruitment. *The American Naturalist*, 130 (5), 730-757.

Medlin, L., Crawford, R. and Andersen, R. (1986) Histochemical and ultrastructural evidence for the function of the labiate process in the movement of centric diatoms. *British Phycological Journal*, 21 (3), 297-301.

Messenger, H. (1991) *LASER SYSTEM WILL AUTOMATE PAINT STRIPPING*. PENNWELL PUBL CO 5TH FLOOR TEN TARA BOULEVARD, NASHUA, NH 03062-2801.

Meurant, G. (2012) *The ecology of natural disturbance and patch dynamics*. Academic press.

Miles, D. (1990) The role of chlorophyll fluorescence as a bioassay for assessment of toxicity in plants. In: (ed.) *Plants for toxicity assessment*. ASTM International.

Mouchtouri, V.A., Goutziana, G., Kremastinou, J. and Hadjichristodoulou, C. (2010a) Legionella species colonization in cooling towers: risk factors and assessment of control measures. *American journal of infection control*, 38 (1), 50-55.

Mouchtouri, V.A., Goutziana, G., Kremastinou, J. and Hadjichristodoulou, C. (2010b) Legionella species colonization in cooling towers: Risk factors and assessment of control measures. *American Journal of Infection Control*, 38 (1), 50-55.

Moerdijk-Poortvliet, T.C., van Breugel, P., Sabbe, K., Beauchard, O., Stal, L.J. and Boschker, H.T. (2018) Seasonal changes in the biochemical fate of carbon fixed by benthic diatoms in intertidal sediments. *Limnology and Oceanography*, 63 (2), 550-569.

Mori, M. and Zunino, P. (1987) Aspects of the biology of *Liocarcinus depurator* (L.) in the Ligurian Sea. *Investigacion Pesquera* (Spain).

Munda, I.M. (2005) Seasonal fouling by diatoms on artificial substrata at different depths near Piran (Gulf of Trieste, Northern Adriatic). *Acta Adriatica: international journal of Marine Sciences*, 46 (2), 137-157.

Nayak, B.K., Iyengar, V.V. and Gupta, M.C. (2011) Efficient light trapping in silicon solar cells by ultrafast-laser-induced self-assembled micro/nano structures. *Progress in Photovoltaics: Research and Applications*, 19 (6), 631-639.

Nendza, M. (2007) Hazard assessment of silicone oils (polydimethylsiloxanes, PDMS) used in antifouling-/foul-release-products in the marine environment. *Marine Pollution Bulletin*, 54 (8), 1190-1196.

Nohe, A., Goffin, A., Tyberghein, L., Lagring, R., De Cauwer, K., Vyverman, W. and Sabbe, K. (2020) Marked changes in diatom and dinoflagellate biomass, composition and seasonality in the Belgian Part of the North Sea between the 1970s and 2000s. *Science of The Total Environment*, 136316

O'Toole, G., Kaplan, H.B. and Kolter, R. (2000) Biofilm formation as microbial development. *Annual Reviews in Microbiology*, 54 (1), 49-79.

Page, H.M., Dugan, J.E. and Piltz, F. (2010) Fouling and antifouling in oil and other offshore industries. *Biofouling*, 252-266.

Passy, S.I. (2010) A distinct latitudinal gradient of diatom diversity is linked to resource supply. *Ecology*, 91 (1), 36-41.

Park, J.B. and Bronzino, J.D. (2002) *Biomaterials: principles and applications*. crc press.

Patil, J. and Anil, A. (2000) Epibiotic community of the horseshoe crab *Tachypleus gigas*. *Marine Biology*, 136 (4), 699-713.

Patrick, R. (1971) The effects of increasing light and temperature on the structure of diatom communities. *Limnology and Oceanography*, 16 (2), 405-421.

Peabody, A. (1977) Diatoms in forensic science. *Journal of the Forensic Science Society*, 17 (2), 81-87.

Petronis, Š., Berntsson, K., Gold, J. and Gatenholm, P. (2000) Design and microstructuring of PDMS surfaces for improved marine biofouling resistance. *Journal of Biomaterials Science, Polymer Edition*, 11 (10), 1051-1072.

Pickett-Heaps, J., Hill, D.R. and Blaze, K.L. (1991) ACTIVE GLIDING MOTILITY IN AN ARAPHID MARINE DIATOM, ARDISSONEA (FORMERLY SYNEDRA) CRYSTALLINA 1. *Journal of Phycology*, 27 (6), 718-725.

Pickett-Heaps, J.D., Hill, D.R. and Wetherbee, R. (1986) CELLULAR MOVEMENT IN THE CENTRIC DIATOM ODONTELLA SINENIS 1. *Journal of Phycology*, 22 (3), 334-339.

Pickett, S.T. and White, P. (2013) *The Ecology of Natural Disturbance and Patch Dynamics*. Elsevier.

Platt, W.J. and Connell, J.H. (2003) Natural disturbances and directional replacement of species. *Ecological Monographs*, 73 (4), 507-522.

Poulsen, N.C., Spector, I., Spurck, T.P., Schultz, T.F. and Wetherbee, R. (1999) Diatom gliding is the result of an actin-myosin motility system. *Cell motility and the cytoskeleton*, 44 (1), 23-33.

Prajitno, D., Maulana, A. and Syarif, D. (2016) Effect of surface roughness on contact angle measurement of nanofluid on surface of stainless steel 304 by sessile drop method. *Journal of Physics: Conference Series of Conference*.

Prescott, R.C. (1990) Sources of predatory mortality in the bay scallop *Argopecten irradians* (Lamarck): interactions with seagrass and epibiotic coverage. *Journal of Experimental Marine Biology and Ecology*, 144 (1), 63-83.

Pyne, S., Fletcher, R. and Jones, E. (1986a) Diatom Communities on Non-Toxic Substrata and Two Conventional Antifouling Surfaces Immersed in Langstone Harbour, South Coast of England. In: (ed.) *Studies in Environmental Science*. Elsevier. pp. 101-113.

Pyne, S., Fletcher, R.L. and Jones, E.B.G. (1986b) Chapter 7 Diatom Communities on Non-Toxic Substrata and Two Conventional Antifouling Surfaces Immersed in Langstone Harbour, South Coast of England. In: Evans, L. V. and Hoagland, K. D. (ed.) *Studies in Environmental Science*. Elsevier. pp. 101-113.

Qian, P.-Y., Lau, S.C., Dahms, H.-U., Dobretsov, S. and Harder, T. (2007) Marine biofilms as mediators of colonization by marine macroorganisms: implications for antifouling and aquaculture. *Marine Biotechnology*, 9 (4), 399-410.

Railkin, A.I. (2003) *Marine biofouling: colonization processes and defenses*. CRC press.

Rasband, W. (2007) ImageJ, US National Institutes of Health. [http://rsb.info.nih.gov/ij/\(1997-2007\)](http://rsb.info.nih.gov/ij/(1997-2007)).

Ratner, B.D., Hoffman, A.S., Schoen, F.J. and Lemons, J.E. (2004) *Biomaterials science: an introduction to materials in medicine*. Elsevier.

Razi, S., Madanipour, K. and Mollabashi, M. (2016) Laser surface texturing of 316L stainless steel in air and water: A method for increasing hydrophilicity via direct creation of microstructures. *Optics & Laser Technology*, 80, 237-246.

Ready, J.F. (1997) *Industrial applications of lasers*. Elsevier.

Reddy, S.T., Chung, K.K., McDaniel, C.J., Darouiche, R.O., Landman, J. and Brennan, A.B. (2011) Micropatterned surfaces for reducing the risk of catheter-associated urinary tract infection: an in vitro study on the effect of sharklet micropatterned surfaces to inhibit bacterial colonization and migration of uropathogenic *Escherichia coli*. *Journal of endourology*, 25 (9), 1547-1552.

Reyssat, M., Pépin, A., Marty, F., Chen, Y. and Quéré, D. (2006) Bouncing transitions on microtextured materials. *EPL (Europhysics Letters)*, 74 (2), 306.

Ries, L. and Sisk, T.D. (2004) A predictive model of edge effects. *Ecology*, 85 (11), 2917-2926.

Rode, A.V., Freeman, D., Baldwin, K., Wain, A., Uteza, O. and Delaporte, P. (2008) Scanning the laser beam for ultrafast pulse laser cleaning of paint. *Applied Physics A*, 93 (1), 135-139.

Rohwerder, T., Gehrke, T., Kinzler, K. and Sand, W. (2003) Bioleaching review part A. *Applied microbiology and biotechnology*, 63 (3), 239-248.

Rosowski, J.R. (1980) VALVE AND BAND MORPHOLOGY OF SOME FRESHWATER DIATOMS. II. INTEGRATION OF VALVES AND BANDS IN NAVICULA CONFERVACEA VAR. CONFERVACEA 1 2. *Journal of Phycology*, 16 (1), 88-101.

Round, F., Crawford, R. and Mann, D. (1990a) *The diatoms Biology and morphology of the genera* Cambridge University Press. Cambridge.

Round, F.E., Crawford, R.M. and Mann, D.G. (1990b) *Diatoms: biology and morphology of the genera*. Cambridge university press.

Rusen, L., Cazan, M., Mustaciosu, C., Filipescu, M., Sandel, S., Zamfirescu, M., Dinca, V. and Dinescu, M. (2014) Tailored topography control of biopolymer surfaces by ultrafast lasers for cell–substrate studies. *Applied Surface Science*, 302, 256-261.

Russell, G. and Veltkamp, C. (1984) Epiphyte survival on skin-shedding macrophytes. *Marine ecology progress series. Oldendorf*, 18 (1), 149-153.

Russell, G., Hawkins, S., Evans, L., Jones, H. and Holmes, G. (1983) Restoration of a disused dock basin as a habitat for marine benthos and fish. *Journal of Applied Ecology*, 43-58.

Ryther, J.H. (1956) The Measurement of Primary Production<sup>1</sup>. *Limnology and Oceanography*, 1 (2), 72-84.

Sabater, S., Guasch, H., Romaní, A. and Muñoz, I. (2002) The effect of biological factors on the efficiency of river biofilms in improving water quality. *Hydrobiologia*, 469 (1-3), 149-156.

Sand, W. (2003) Microbial life in geothermal waters. *Geothermics*, 32 (4-6), 655-667.

Scardino, A. (2009) Surface modification approaches to control marine biofouling. In: (ed.) *Advances in marine antifouling coatings and technologies*. Elsevier. pp. 664-692.

Scardino, A. and de Nys, R. (2004) Fouling deterrence on the bivalve shell *Mytilus galloprovincialis*: a physical phenomenon? *Biofouling*, 20 (4-5), 249-257.

Scardino, A., De Nys, R., Ison, O., O'Connor, W. and Steinberg, P. (2003) Microtopography and antifouling properties of the shell surface of the bivalve molluscs *Mytilus galloprovincialis* and *Pinctada imbricata*. *Biofouling*, 19 (S1), 221-230.

Scardino, A., Guenther, J. and De Nys, R. (2008) Attachment point theory revisited: the fouling response to a microtextured matrix. *Biofouling*, 24 (1), 45-53.

Scardino, A., Harvey, E. and De Nys, R. (2006a) Testing attachment point theory: diatom attachment on microtextured polyimide biomimics. *Biofouling*, 22 (1), 55-60.

Scardino, A., Hudleston, D., Peng, Z., Paul, N.A. and De Nys, R. (2009) Biomimetic characterisation of key surface parameters for the development of fouling resistant materials. *Biofouling*, 25 (1), 83-93.

Scardino, A.J. and de Nys, R. (2011) Mini review: biomimetic models and bioinspired surfaces for fouling control. *Biofouling*, 27 (1), 73-86.

Scardino, A.J., Harvey, E. and De Nys, R. (2006b) Testing attachment point theory: diatom attachment on microtextured polyimide biomimics. *Biofouling*, 22 (1), 55-60.

Scarlett, A., Donkin, M., Fileman, T. and Donkin, P. (1997) Occurrence of the marine antifouling agent Irgarol 1051 within the Plymouth Sound locality: implications for the green macroalga *Enteromorpha intestinalis*. *Marine Pollution Bulletin*, 34 (8), 645-651.

Scarlett, A., Donkin, P., Fileman, T. and Morris, R. (1999) Occurrence of the antifouling herbicide, Irgarol 1051, within coastal-water seagrasses from Queensland, Australia. *Marine Pollution Bulletin*, 38 (8), 687-691.

Schultz, M., Bendick, J., Holm, E. and Hertel, W. (2011) Economic impact of biofouling on a naval surface ship. *Biofouling*, 27 (1), 87-98.

Schultz, M.P. (2007) Effects of coating roughness and biofouling on ship resistance and powering. *Biofouling*, 23 (5), 331-341.

Schumacher, J.F., Aldred, N., Callow, M.E., Finlay, J.A., Callow, J.A., Clare, A.S. and Brennan, A.B. (2007a) Species-specific engineered antifouling topographies: correlations between the settlement of algal zoospores and barnacle cyprids. *Biofouling*, 23 (5), 307-317.

Schumacher, J.F., Carman, M.L., Estes, T.G., Feinberg, A.W., Wilson, L.H., Callow, M.E., Callow, J.A., Finlay, J.A. and Brennan, A.B. (2007b) Engineered antifouling microtopographies—effect of feature size, geometry, and roughness on settlement of zoospores of the green alga *Ulva*. *Biofouling*, 23 (1), 55-62.

Schumacher, J.F., Long, C.J., Callow, M.E., Finlay, J.A., Callow, J.A. and Brennan, A.B. (2008) Engineered nanoforce gradients for inhibition of settlement (attachment) of swimming algal spores. *Langmuir*, 24 (9), 4931-4937.

Schuster, J.M., Schvezov, C.E. and Rosenberger, M.R. (2015) Influence of experimental variables on the measure of contact angle in metals using the Sessile Drop Method. *Procedia Materials Science*, 8, 742-751.

Sciti, D., Trucchi, D., Bellucci, A., Orlando, S., Zoli, L. and Sani, E. (2017) Effect of surface texturing by femtosecond laser on tantalum carbide ceramics for solar receiver applications. *Solar Energy Materials and Solar Cells*, 161, 1-6.

Segu, D.Z., Choi, S.G., hyouk Choi, J. and Kim, S.S. (2013) The effect of multi-scale laser textured surface on lubrication regime. *Applied Surface Science*, 270, 58-63.

Semaltianos, N., Perrie, W., Vishnyakov, V., Murray, R., Williams, C., Edwardson, S., Dearden, G., French, P., Sharp, M. and Logothetidis, S. (2008) Nanoparticle formation by the debris produced by femtosecond laser ablation of silicon in ambient air. *Materials Letters*, 62 (14), 2165-2170.

Singh, R.P., Shukla, M.K., Mishra, A., Reddy, C. and Jha, B. (2013) Bacterial extracellular polymeric substances and their effect on settlement of zoospore of *Ulva fasciata*. *Colloids and Surfaces B: Biointerfaces*, 103, 223-230.

Singh, S.P., Li, Y., Be'er, A., Oren, Y., Tour, J.M. and Arnusch, C.J. (2017) Laser-induced graphene layers and electrodes prevents microbial fouling and exerts antimicrobial action. *ACS Applied Materials & Interfaces*, 9 (21), 18238-18247.

Sharp, K.H., Eam, B., Faulkner, D.J. and Haygood, M.G. (2007) Vertical transmission of diverse microbes in the tropical sponge *Corticium* sp. *Appl. Environ. Microbiol.*, 73 (2), 622-629.

Slattery, M. (1992) Larval settlement and juvenile survival in the red abalone (*Haliotis rufescens*), an examination of inductive cues and substrate selection. *Aquaculture*, 102 (1), 143-153.

Smith, W. (1856). A synopsis of the British Diatomaceae; with remarks on their structure, functions and distribution; and instructions for collecting and preserving specimens. Vol. 2 pp. [i-vi] - xxix, 1-107, pls 32-60, 61-62, A-E. London: John van Voorst.

Smol, J.P. and Stoermer, E.F. (2010) *The diatoms: applications for the environmental and earth sciences*. Cambridge University Press.

Snell, M., Barker, P.A., Surridge, B.W.J., Benskin, C.M.H., Barber, N., Reaney, S., Tych, W., Mindham, D., Large, A. and Burke, S. (2019) Strong and recurring seasonality revealed within stream diatom assemblages. *Scientific reports*, 9 (1), 1-7.

Sommer, S., Ekin, A., Webster, D.C., Stafslie, S.J., Daniels, J., VanderWal, L.J., Thompson, S.E., Callow, M.E. and Callow, J.A. (2010) A preliminary study on the properties and fouling-release performance of siloxane-polyurethane coatings prepared from poly(dimethylsiloxane)(PDMS) macromers. *Biofouling*, 26 (8), 961-972.

Sousa, W.P. (1984) The role of disturbance in natural communities. *Annual Review of Ecology and Systematics*, 15 (1), 353-391.

Stern, D.L. (2013) The genetic causes of convergent evolution. *Nature Reviews Genetics*, 14, 751.

Sullivan, T. and Regan, F. (2017) Marine diatom settlement on microtextured materials in static field trials. *Journal of materials science*, 52 (10), 5846-5856.

Sun, J. (2011) Marine phytoplankton and biological carbon sink. *Acta Ecologica Sinica*, 31 (18), 5372-5378.

Sun, K., Yang, H., Xue, W., He, A., Zhu, D., Liu, W., Adeyemi, K. and Cao, Y. (2018) Anti-biofouling superhydrophobic surface fabricated by picosecond laser texturing of stainless steel. *Applied Surface Science*, 436, 263-267.

Svavarsson, J. and Davíðsdóttir, B. (1994) Foraminiferan (Protozoa) epizoites on Arctic isopods (Crustacea) as indicators of isopod behaviour? *Marine Biology*, 118 (2), 239-246.

Ta, D.V., Dunn, A., Wasley, T.J., Kay, R.W., Stringer, J., Smith, P.J., Connaughton, C. and Shephard, J.D. (2015) Nanosecond laser textured superhydrophobic metallic surfaces and their chemical sensing applications. *Applied Surface Science*, 357, 248-254.

Tan, J. and Saltzman, W.M. (2004) Biomaterials with hierarchically defined micro-and nanoscale structure. *Biomaterials*, 25 (17), 3593-3601.

Tang, C., Cheng, F. and Man, H. (2006) Laser surface alloying of a marine propeller bronze using aluminium powder: Part I: Microstructural analysis and cavitation erosion study. *Surface and Coatings Technology*, 200 (8), 2602-2609.

Teo, S.L.-M. and Ryland, J.S. (1995) Potential antifouling mechanisms using toxic chemicals in some British ascidians. *Journal of Experimental Marine Biology and Ecology*, 188 (1), 49-62.

Thakur, N.L., Anil, A.C. and Müller, W.E. (2004) Culturable epibacteria of the marine sponge *Ircinia fusca*: temporal variations and their possible role in the epibacterial defense of the host. *Aquatic microbial ecology*, 37 (3), 295-304

Thieltges, D.W. and Buschbaum, C. (2007) Vicious circle in the intertidal: facilitation between barnacle epibionts, a shell boring polychaete and trematode parasites in the periwinkle *Littorina littorea*. *Journal of Experimental Marine Biology and Ecology*, 340 (1), 90-95.

Toupoint, N., Gilmore-Solomon, L., Bourque, F., Myrand, B., Pernet, F., Olivier, F. and Tremblay, R. (2012) Match/mismatch between the *Mytilus edulis* larval supply and seston quality: effect on recruitment. *Ecology*, 93 (8), 1922-1934.

Townsin, R. (2003) The ship hull fouling penalty. *Biofouling*, 19 (S1), 9-15.

Trdan, U., Hočvar, M. and Gregorčič, P. (2017) Transition from superhydrophilic to superhydrophobic state of laser textured stainless steel surface and its effect on corrosion resistance. *Corrosion science*, 123, 21-26.

Turner, M.G., Baker, W.L., Peterson, C.J. and Peet, R.K. (1998) Factors influencing succession: lessons from large, infrequent natural disturbances. *Ecosystems*, 1 (6), 511-523.

Underwood, A. (1998) Grazing and disturbance: an experimental analysis of patchiness in recovery from a severe storm by the intertidal alga *Hormosira banksii* on rocky shores in New South Wales. *Journal of Experimental Marine Biology and Ecology*, 231 (2), 291-306.

Van Kooten, T., Schakenraad, J., Van der Mei, H. and Busscher, H. (1992) Influence of substratum wettability on the strength of adhesion of human fibroblasts. *Biomaterials*, 13 (13), 897-904.

Vandevivere, P. and Kirchman, D.L. (1993a) Attachment stimulates exopolysaccharide synthesis by a bacterium. *Applied and Environmental Microbiology*, 59 (10), 3280-3286.

Vandevivere, P. and Kirchman, D.L. (1993b) Attachment stimulates exopolysaccharide synthesis by a bacterium. *Appl. Environ. Microbiol.*, 59 (10), 3280-3286.

Velasquez, T., Han, P., Cao, J. and Ehmann, K.F. (2013) Feasibility of laser surface texturing for friction reduction in surgical blades. *ASME 2013 International Manufacturing Science and Engineering Conference collocated with the 41st North American Manufacturing Research Conference of Conference*.

Velic, A., Mathew, A., Hines, P. and Yarlagadda, P.K. (2019) Control of bacterial attachment by fracture topography. *Journal of the mechanical behavior of biomedical materials*, 91, 416-424.

Venkatesan, R., Venkatasamy, M., Bhaskaran, T., Dwarakadasa, E. and Ravindran, M. (2002) Corrosion of ferrous alloys in deep sea environments. *British Corrosion Journal*, 37 (4), 257-266.

Venugopalan, V.P. (2018) Industrial Seawater Cooling Systems under Threat from the Invasive Green Mussel *Perna viridis*. *ASEAN Journal on Science and Technology for Development*, 35 (1-2), 65-69.

Videla, H. (2018) *Manual of biocorrosion*. Routledge.

Videla, H.A. (1996) *Manual of biocorrosion*. CRC Press.

Videla, H.A. and Characklis, W.G. (1992a) Biofouling and microbially influenced corrosion. *International Biodeterioration & Biodegradation*, 29 (3-4), 195-212.

Videla, H.A. and Characklis, W.G. (1992b) Biofouling and microbially influenced corrosion. *International Biodeterioration & Biodegradation*, 29 (3-4), 195-212.

Voulvoulis, N., Scrimshaw, M. and Lester, J. (1999) Alternative antifouling biocides. *Applied organometallic chemistry*, 13 (3), 135-143.

Voulvoulis, N., Scrimshaw, M.D. and Lester, J.N. (2002) Comparative environmental assessment of biocides used in antifouling paints. *Chemosphere*, 47 (7), 789-795.

Vucko, M., Poole, A., Carl, C., Sexton, B., Glenn, F., Whalan, S. and De Nys, R. (2014) Using textured PDMS to prevent settlement and enhance release of marine fouling organisms. *Biofouling*, 30 (1), 1-16.

Wahl, M. (1989) Marine epibiosis. I. Fouling and antifouling: some basic aspects. *Marine ecology progress series*, 58, 175-189.

Wahl, M., Kröger, K. and Lenz, M. (1998) Non-toxic protection against epibiosis. *Biofouling*, 12 (1-3), 205-226.

Wahl, M. (2008) Ecological modulation of environmental stress: interactions between ultraviolet radiation, epibiotic snail embryos, plants and herbivores. *Journal of animal ecology*, 549-557.

Wahl, M., Goecke, F., Labes, A., Dobretsov, S. and Weinberger, F. (2012) The Second Skin: Ecological Role of Epibiotic Biofilms on Marine Organisms. *Frontiers in Microbiology*, 3 (292).

Wahl, M., Hay, M. and Enderlein, P. (1997) Effects of epibiosis on consumer-prey interactions. *Hydrobiologia*, 355 (1-2-3), 49-59.

Wang, C., Bao, W.-Y., Gu, Z.-Q., Li, Y.-F., Liang, X., Ling, Y., Cai, S.-L., Shen, H.-D. and Yang, J.-L. (2012) Larval settlement and metamorphosis of the mussel *Mytilus coruscus* in response to natural biofilms. *Biofouling*, 28 (3), 249-256.

Wang, N., Butler, J.P. and Ingber, D.E. (1993) Mechanotransduction across the cell surface and through the cytoskeleton. *science*, 260 (5111), 1124-1127.

Wang, X., Wu, L.Y., Shao, Q. and Zheng, H. (2009) Laser micro structuring on a Si substrate for improving surface hydrophobicity. *Journal of Micromechanics and Microengineering*, 19 (8), 085025.

Ward, M.D. and Hammer, D.A. (1993) A theoretical analysis for the effect of focal contact formation on cell-substrate attachment strength. *Biophysical Journal*, 64 (3), 936-959.

Webster, N.S. and Taylor, M.W. (2012) Marine sponges and their microbial symbionts: love and other relationships. *Environmental microbiology*, 14 (2), 335-346.

Wells, L., Perez, F., Hibbert, M., Clerveaux, L., Johnson, J. and Goreau, T.J. (2010) Effect of severe hurricanes on Biorock coral reef restoration projects in Grand Turk, Turks and Caicos Islands. *Revista de biología tropical*, 141-149.

Wenzel, R.N. (1936) Resistance of solid surfaces to wetting by water. *Industrial & Engineering Chemistry*, 28 (8), 988-994.

Wetherbee, R., Lind, J.L., Burke, J. and Quatrano, R.S. (1998) Minireview—the first kiss: establishment and control of initial adhesion by raphid diatoms. *Journal of Phycology*, 34 (1), 9-15.

Willemsen, P. (2005) Biofouling in European aquaculture: is there an easy solution. *European Aquaculture Society Special Publ*, 35, 82-87.

Wilkinson, S.B., Zheng, W., Allen, J.R., Fielding, N.J., Wanstall, V.C., Russell, G. and Hawkins, S.J. (1996) Water quality improvements in Liverpool docks: the role of filter feeders in algal and nutrient dynamics. *Marine ecology*, 17 (1-3), 197-211.

Witt, V., Wild, C., Anthony, K.R., Diaz-Pulido, G. and Uthicke, S. (2011) Effects of ocean acidification on microbial community composition of, and oxygen fluxes through, biofilms from the Great Barrier Reef. *Environmental Microbiology*, 13 (11), 2976-2989.

Wolf, K., Krincher, R. and Ermalovich, J. (2009) Laser strip: a portable hand-held laser stripping device for reducing VOC, toxic and particulate emissions. *Institute for Research and Technical Assistance, IRTA, USA*.

Wong, M., Eulenberger, J., Schenk, R. and Hunziker, E. (1995) Effect of surface topology on the osseointegration of implant materials in trabecular bone. *Journal of biomedical materials research*, 29 (12), 1567-1575.

Woollacott, R. (1981) Association of bacteria with bryozoan larvae. *Marine Biology*, 65 (2), 155-158.

Wright, J.P., Jones, C.G. and Flecker, A.S. (2002) An ecosystem engineer, the beaver, increases species richness at the landscape scale. *Oecologia*, 132 (1), 96-101.

Wu, A.H., Nakanishi, K., Cho, K. and Lamb, R. (2013) Diatom attachment inhibition: limiting surface accessibility through air entrapment. *Biointerphases*, 8 (1), 5.

Wu, S., Altenried, S., Zogg, A., Zuber, F., Maniura-Weber, K. and Ren, Q. (2018) Role of the Surface Nanoscale Roughness of Stainless Steel on Bacterial Adhesion and Microcolony Formation. *ACS Omega*, 3 (6), 6456-6464.

Xiao, L., Thompson, S.E., Röhrig, M., Callow, M.E., Callow, J.A., Grunze, M. and Rosenhahn, A. (2013) Hot embossed microtopographic gradients reveal morphological cues that guide the settlement of zoospores. *Langmuir*, 29 (4), 1093-1099.

Yang, C., Wang, J., Yu, Y., Liu, S. and Xia, C. (2015) Seasonal variations in fouling diatom communities on the Yantai coast. *Chinese Journal of Oceanology and Limnology*, 33 (2), 439-446.

Zhang, H., Lamb, R. and Lewis, J. (2005) Engineering nanoscale roughness on hydrophobic surface—preliminary assessment of fouling behaviour. *Science and Technology of Advanced Materials*, 6 (3-4), 236-239.

Zupančič, M., Može, M., Gregorčič, P. and Golobič, I. (2017) Nanosecond laser texturing of uniformly and non-uniformly wettable micro structured metal surfaces for enhanced boiling heat transfer. *Applied Surface Science*, 399, 480-490.

